Characterisation of acid sulfate soils in south-west Victoria, Australia

Submitted by

Fiona Glover

B. Env. Science (Hons)

A thesis submitted in total fulfilment of the

requirements for the degree of

Doctor of Philosophy

School of Life Sciences

Faculty of Science, Technology and Engineering

La Trobe University

Bundoora, Victoria, 3086

Australia

December 2014

Table of Contents

List of Figures

List of Tables

Abstract

Acid sulfate soils (ASS) are an important environmental concern. Acidity from the oxidation of these sediments can be flushed into waterways following rainfall events, causing ecological and infrastructure degradation. Until recently, the distribution of ASS was believed to be predominantly coastal, but ASS are now recognised in inland environments. While knowledge of ASS has been growing, little of the published literature has been conducted on a regional scale, and this gap has been highlighted across many areas of Australia, including within the Corangamite Catchment Management Authority (CMA). Four sites were investigated on the Basalt Plains, where drainage patterns have been disrupted by lava flows: two sites are swamps and two sites are smaller depressions. The two swamps are waterlogged for longer periods of time than the smaller depressions; sufficient evaporation within the upper layer of the swamps allows precipitation of carbonate minerals, providing a buffering capacity in excess of any potential acidity generated by the sulfide minerals. The depressions contain no carbonate minerals, but only have very low levels of sulfides, and therefore will not undergo a large acidification. In the Otway Ranges, five sites were investigated: three occur in 'peat swamps' and two within the altered floodplain of the Barwon River. The three sites that occur in 'peat' swamps are currently oxidising due to seasonal fluctuation in the watertable and alteration of nearby creeks. There is a large potential for further oxidation, and analysis of the surface water at one of the 'peat' swamp sites (Boundary Creek) shows acid is leaching from the swamp. No carbonate minerals were found, and the sites have no ability to neutralise the acidity in-situ. The two remaining sites on the altered floodplain of the Barwon River have

only low levels of sulfides, and are unlikely to undergo acidification. Mapping of ASS is therefore important in determining areas potentially at risk. The Basalt Plains were excluded from the mapping due to the large buffering capacity within the sediments. Mapping of the Otway Ranges was conducted using LIDAR topography, geology and ecological vegetation maps (EVCs). Areas with slope angles of 0-4° extracted from the LIDAR overestimated the potential areas for ASS to occur, and were constrained by using the pre-existing EVC mapping overlaid on the LIDAR topography. The GIS mapping matched known ASS sites, indicating that the method developed for mapping these areas remotely is accurate.

Statement of Authorship

Except where reference is made in the text of the thesis, this thesis contains no material published elsewhere or extracted in whole or in part from a thesis submitted for the award of any other degree or diploma.

No other person's work has been used without due acknowledgment in the main text of the thesis.

CRS and AVS analysis was conducted by Graham Lancaster on the bulk of the samples analysed, carbon dating of the sediment (section 5.3.2) was conducted by Beta Analytic and trace element analysis of the water in Boundary Creek (section 5.1.3) was sampled and analysed by the Colac Otway Shire. XRF analysis was conducted by Alex Fink, and carbon analysis was run by Gary Clark.

This thesis has not been submitted for the award of any degree or diploma in any other tertiary institution.

19 December, 2014

Acknowledgements

I gratefully acknowledge the help, funding and guidance from the Corangamite Inland Acid Sulphate Soils Steering Committee, and the members from Colac Otway Shire, Southern Rural Water, Corangamite Catchment Management Authority (CCMA), Barwon Water, and the Department of Environment and Primary Industries. Without the help from these organisations, this project would not have been possible.

I would also like to thank my supervisor, Associate Professor John Webb, for his support and guidance during this project, and throughout my many years at La Trobe University. I would also like to thank Dr Sue White for all her help, guidance, the many coffees she bought me, and for her final proof reading of this thesis.

For their help with analysis, I would like to thank Graham Lancaster for his help with CRS and AVS analysis, Beta Analytic for the carbon dates and Alex Fink for his help with XRD and XRF analysis.

Finally, I wish to thank my family and friends for their invaluable support, chats over coffee, help driving to places unknown, and understanding of the time and effort this project has taken. In particular, I would like to thank my parents for their encouragement and generosity, and to Sharon, Karen and Eidann, who motivated me when I needed it and believed I could finish, even when I did not.

Glossary

AASS	Actual acid sulfate soil
AHD	Australian height datum; height above mean average sea level
ANC	Acid neutralising capacity
ASS	Acid sulfate soils
AVS	Acid volatile sulfur; sometimes also noted as S_{AV}
CMA	Catchment Management Authority
CRS	Chromium reducible sulfur; sometimes also noted as S_{CR}
DEM	Digital Elevation Model
DSE	Department of Sustainability and Environment (Victorian Government)
EC	Electrical conductivity
EVC	Ecological Vegetation Classes
LIDAR	A type of laser remote sensing technique for mapping the Earth's surface
LOI	Loss on Ignition
PASS	Potential acid sulfate soil
SRW	Southern Rural Water
TAA	Titratable actual acidity
TPA	Titratable peroxide acidity
TSA	Titratable sulfidic acidity
USGS	United States Geological Survey
WSPA	Water supply protection area
XRD	X-ray diffraction
XRF	X-ray fluorescence

Chapter 1

Introduction

Within Australia and globally, acid sulfate soils (ASS) are a serious environmental issue, and can lead to fish kills, severe ecological degradation and the corrosion of infrastructure (Gardner et al. 2000; Glover 2008; Sammut 2000; Demas et al. 2004). ASS have been estimated to occur across 12-13 million hectares of land worldwide (Andriesse and van Mensvoort 2006), across parts of the USA, such as Virginia and Maryland, Canada, Uganda, Great Britain, Denmark, Zimbabwe, Germany, Sweden, Finland, the Netherlands, South and Southeast Asia, West Africa, the north-eastern coast of South America and Australia. Of these, 10 million hectares cover geologically recent coastal plains, mainly in the tropics, and consist of highly pyritic material that will acidify on aeration. Sulfide-rich sediments can also occur in other environments, such as under thick layers of peat (such as in Indonesia and Malaysia), under non-pyritic alluvial sediments, and in older sediments (Pleistocene, Tertiary or older), often originally deposited in tidal environments (Pons et al. 1982; Andriesse and van Mensvoort 2006; Brinkman and Pons 1973; Orndorff et al. 2008; Fanning et al. 2004; Demas et al. 2004; Fanning et al. 2010).

Until relatively recently, the distribution of ASS was believed to be predominantly coastal, reflecting the extensive development of modern-day coastal zones and exposure of these sediments (Fitzpatrick and Shand 2008; Gardner et al. 2000; Sammut 2000; Rabenhorst et al. 2006). As a result, sulfidic sediments in low-lying coastal areas have been well studied (Andriesse and van Mensvoort 2006; Dent 1986; Sammut 2000; Fanning 1993). However,

the presence of ASS in inland wetlands has been recognised (Bibi et al. 2011; Hall et al. 2006; Lamontagne et al. 2006). Within Australia, development of our current understanding of inland ASS only began post-1990, particularly with the extensive drying of wetland and river systems during the extreme drought conditions of 2006-2009 (Fitzpatrick et al. 2008b; Fitzpatrick and Shand 2008).

Inland ASS form under a wide range of environmental conditions, from freshwater systems to highly salinised areas (Glover 2008; Hall et al. 2006; Lamontagne et al. 2003; Glover et al. 2011; Wallace et al. 2008a). Major occurrences have been documented in freshwater river and wetland systems (such as the Murray River and Lower Lakes), artificially drained landscapes such as the WA wheat belt, the Yass Valley in New South Wales, south-eastern Queensland and upland landscapes, such as the Mount Lofty Ranges in South Australia and the Dundas Tablelands in Victoria (Degens et al. 2008; Fawcett et al. 2008; Fitzpatrick et al. 2008b; Glover 2008; Hall et al. 2006; Pyper and Davidson 2001; Glover et al. 2011; Wallace et al. 2008b; Wallace et al. 2008a). It is estimated that in Australia, ASS cover 215,000 km^2, of which 58,000 km^2 is defined as coastal and 157,000 km^2 are inland ASS (Fitzpatrick et al. 2008a). As a result, the documentation and mapping of inland ASS across Australia has been considerably expanded (Fitzpatrick et al. 2008b), and this thesis forms part of that effort.

For the purpose of this thesis, the wetland sediments will be referred to as ASS, following the generally accepted usage of “acid sulfate soils” to refer to any near surface sulfide-containing soil or sediment. This thesis makes no attempt to classify the soil types present, as it is not a soil science thesis. Instead, the soil/sediment descriptions will be based on acidity, mineralogy and elemental analysis.

1.1 Acid Sulfate Soils (ASS)

ASS are defined as soils and surface sediments that either contain iron sulfide minerals or have been affected by sulfide oxidation (Ahern and McElnea 1999; Dent 1986; Powell and Ahern 1999; Fanning and Fanning 1989; Fanning and Muckel 2004). The most common sulfide mineral in ASS is pyrite (FeS_2), although other sulfides, including marcasite (FeS_2; a dimorph of pyrite) and iron monosulfides (such as amorphous sulfides (FeS_{amorph}), mackinawite (Fe_9S_8) and greigite (Fe_3S_4)), can occur in lesser amounts (Bush et al. 2004b; Moses et al. 1987; Ward 2004; Smith 2004; Evans et al. 2000; Rabenhorst and Fanning 2006; Rickard 2012).

1.1.1 Formation of ASS

Iron sulfide minerals are one of the end products of sulfate reduction, which occurs as a natural process in lakes, rivers, wetlands and oceans (Fitzpatrick et al. 2008b; Fanning et al. 2010). However, the amount of iron sulfide accumulation in a specific environment is dependent on multiple factors, including the level of dissolved sulfate (SO_4^{2-}), a source of iron (generally Fe^{3+} from iron oxide/hydroxide minerals and clays) and amount of organic matter (Melville et al. 1993; Sammut 2000; Rabenhorst et al. 2006; Fanning 1993; Rickard 2012). Environments that contain waterlogged, anaerobic conditions rich in organic matter are ideal for sulfide formation (assuming that iron and sulfate sources are present), in particular for the catalysing bacteria, with warmer temperatures providing a more favourable environment for bacterial growth, and therefore a greater potential to form iron sulfides (Madigan and Martinko 2006; Powell and Ahern 1999; Rabenhorst and Fanning 2006; Rabenhorst et al. 2006). A common source of sulfate is seawater, however

in more sulfate-limited inland environments, sulfate can be sourced from rainfall, surface water or groundwater (Fitzpatrick et al. 2008b; Rabenhorst et al. 2006; Wallace et al. 2008a); 10-20% of the salinity in rainfall, surface water and groundwater is contributed by sulfate (Lamontagne et al. 2003).

The first step in the formation of low temperature (< 100°C) iron sulfide minerals is the bacterial reduction of sulfate (Konhauser 2007). In anaerobic conditions, bacteria such as *Desulfovibrio* and *Desulfotomaculum* species can reduce sulfate to hydrogen sulfide in the presence of organic matter (Madigan and Martinko 2006; Janzen and Ellert 1998; Fanning et al. 2012):

$$CH_3COO^- + 3H^+ + SO_4^{2-} \rightarrow 2CO_2 + H_2S + 2H_2O \quad (1)$$

Organic matter + sulfate → carbon dioxide + hydrogen sulfide + water

The hydrogen sulfide can then react further with iron present in the soil to form amorphous iron monosulfide (FeS_{amorph}), which forms rapidly and has been shown to be a disordered form of mackinawite (Konhauser 2007; Rickard 1995; Rickard 2006). For simplicity, the slight non-stoichiometry of disordered mackinawite (caused by the substitution of other metals, such as copper) is mostly ignored within the literature, and the reaction is generally written as (Wilkin & Barnes; Rickard 2006):

$$Fe^{2+} + HS^- \rightarrow FeS + H^+ \quad (2)$$

Ferrous iron + hydrogen sulfide → iron monosulfides + acidity

Within the literature, mackinawite is commonly written as FeS, however a more general reaction that accounts for the variable stoichiometry can be written as (Wilkin and Barnes 1997):

$$(1+x)Fe^{2+} + HS^- + xH_2(g) \rightarrow Fe_{(1+x)}S + (1+2x)H^+ \quad (3)$$

Iron + hydrogen sulfide + hydrogen gas → mackinawite + acidity

Disordered mackinawite converts over time to crystalline (tetragonal) mackinawite (FeS_m); this can take up to two years (Rickard 1995; Wolthers et al. 2005). Ordered mackinawite can then react with many of the sulfur intermediate species (such as elemental sulfur or thiosulfate) to form greigite (Fe_3S_4) (Konhauser 2007):

$$3FeS + S^0 \rightarrow Fe_3S_4 \quad (4)$$

Mackinawite + elemental sulfur → greigite

Iron monosulfides are an important component in the cycling of iron and sulfur within ASS (Berner 1970; Smith 2004), and act as intermediates in the process of pyrite or marcasite formation, as they form much faster that the disulfide minerals (Berner 1970; Dent 1986; Konhauser 2007; Smith 2004; Schoonen and Barnes 1991):

$$FeS_{(s)} + H_2S_{(aq)} \rightarrow FeS_2 + H_{2(g)} \quad (5)$$

Iron monosulfide + hydrogen sulfide → pyrite + hydrogen gas

$$FeS_{(s)} + HS^- + H_2O \rightarrow FeS_2 + H_{2(g)} + OH^- \quad (6)$$

Iron monosulfide + hydrogen sulfide ion → pyrite + hydrogen gas + hydroxide ion

$$FeS_{(s)} + S_n^{2-} \rightarrow FeS_2 + S_{n-1}^{2-} \quad (7)$$

Iron monosulfide + polysulfide → pyrite + polysulfide

$$FeS_{(s)} + S_2O_3^{2-} \rightarrow FeS_2 + SO_3^{2-} \quad (8)$$

Iron monosulfide + thiosulfate → pyrite + sulfite

Marcasite is less abundant than pyrite in sulfidic sediments due to its meta-stable crystal structure under prolonged and strongly reducing conditions. Marcasite forms under acidic (pH < 4) conditions, and is considered an important intermediate in the formation of pyrite under those conditions (Lennie et al. 1997; Schoonen and Barnes 1991; Bush et al. 2004b).

Significant rates of pyrite formation generally require the soil to have high levels of iron monosulfides (Konhauser 2007); the natural rate of pyrite formation is around one hundred years to form ten kilograms per cubic metre of sediment (Dent 1986). Therefore, geologically, the formation of ASS is a virtually instantaneous process and is also rapid compared with most processes of soil formation (Brinkman and Pons 1973).

1.1.2 Oxidation of Iron Sulfides in ASS

As long as sediments or soils containing pyrite and other iron sulfides remain under reducing conditions, they are subject to little change aside from the ongoing sulfide mineral transformation and recrystallization (Brinkman and Pons 1973; Ward 2004; Schoonen and Barnes 1991). Most of the harmful effects associated with ASS are caused by the formation of sulfuric acid (H_2SO_4), which is released due to oxidation of the sulfide minerals when exposed to the atmosphere (Dent and Pons 1993; Fitzpatrick et al. 2008b; Rabenhorst and Fanning 2006; Fanning 1993). Oxidising ASS are in rapid flux, whereby the acid forming

from oxidation during one year can leach from the system and a similar quantity reform, so that the sediments can have a similar low pH from one year to the next, despite the reserves of potential acidity decreasing (Brinkman and Pons 1973).

Oxidation can be caused by seasonal lowering of the watertable, the wetting and drying cycles of wetlands, tidal variation in low lying coastal areas or through human activity such as excavation, drainage or disturbance. This can lead to severe acidification, deoxygenation and the release of heavy metals (Bowman 1993; Dent 1986; Fitzpatrick and Shand 2008; Sammut et al. 1996; Simpson et al. 2008; Fanning et al. 2004). Draining of river or wetland/lake systems can be particularly important, as the sulfidic material may not have had contact with the atmosphere for a considerable period of time, leading to a build-up of sulfide minerals within the sediments (Glover 2008; Simpson et al. 2008).

As pyrite is the typical iron sulfide mineral found in coastal ASS, the process of pyrite oxidation has been studied extensively (Ahern and McElnea 1999; Baker and Banfield 2003; Gardner et al. 2000; Powell and Ahern 1999). Pyrite oxidation, once initiated, can be autocatalytic (cyclic) (Gardner et al. 2000), with the ferric iron (Fe^{3+}) released propagating the sulfide oxidation by reacting with pyrite itself (Baker and Banfield 2003; Singer and Stumm 1970):

$$FeS_2 + \tfrac{7}{2}O_2 + H_2O \rightarrow Fe^{2+} + SO_4^{2-} + 2H^+ \quad (9)$$

$$Fe^{2+} + \tfrac{1}{4}O_2 + H^+ \rightarrow Fe^{3+} + \tfrac{1}{2}H_2O \quad (10)$$

$$Fe^{3+} + 3H_2O \rightarrow Fe(OH)_3(s) + 3H^+$$

$$FeS_2 + 14Fe^{3+} + 8H_2O \rightarrow 15Fe^{2+} + 2SO_4^{2-} + 16H^+ \quad (11)$$

Pyrite oxidation is affected by many factors, including particle size, temperature, microbial activity and oxygen concentration (Evangelou and Zhang 1995; Singer and Stumm 1970). Oxygen and ferric iron (Fe^{3+}) have been shown to be the main oxidants of pyrite in the natural system (Moses and Herman 1991; Moses et al. 1987), with the rate of pyrite oxidation generally highest at low pH (< 4) where several of the rate-limiting steps are catalysed by bacteria (Dent 1986; Evangelou and Zhang 1995). However, the initial acidification during ASS oxidation has been attributed to oxidation of the more reactive iron monosulfides and elemental sulfur rather than pyrite (Hart 1963), as oxidation of iron monosulfides (generalised formula FeS) is more rapid than that of pyrite. The oxidation of iron monosulfides releases sulfate into solution and results in the production of acidity and a ferrous iron (Fe^{2+}) intermediate (Aller 1980):

$$4FeS + 8O_2 \rightarrow 4Fe^{2+} + 4SO_4^{2-} \quad (12)$$

Iron monosulfides + oxygen → ferrous iron + sulfate

$$4Fe^{2+} + O_2 + 10H_2O \rightarrow 8H^+ + 4Fe(OH)_3 \quad (13)$$

Ferrous iron + oxygen + water → acidity + iron hydroxide

The oxidation of iron monosulfides (reactions 12 & 13) can take place at high pH (Aller 1980) and generates around 2 moles of acid for each mole of oxidised iron monosulfides, compared to the 4 moles released for pyrite (Lamontagne et al. 2004). Abiotic oxidation of both pyrite and iron monosulfides can occur but is very slow (Arkensteyn 1980; White et al. 1997), with bacterially catalysed reactions being the more dominant oxidative process (Watkinson and Bolan 1998). Biotic oxidation is generally caused by autotrophic bacteria

(Gardner et al. 2000; Watkinson and Bolan 1998); *Thiobacilli* are commonly responsible (Baker and Banfield 2003; Powell and Ahern 1999) and have been considered the main catalysts of reduced sulfur oxidation in Australian soils (Vitolins and Swaby 1969).

Biotic and abiotic oxidation of both pyrite and iron monosulfides occurs in stages (Hicks et al. 1999). Intermediates, such as K-jarosite ($KFe_3(OH)_6(SO_4)_2$), form from incomplete oxidation or hydrolysis of iron (McElnea et al. 2002b; Fanning et al. 2010). Other intermediates, such as elemental sulfur (S°) and thiosulfate ($S_2O_3^{2-}$) can also form (Madigan and Martinko 2006; Watkinson and Bolan 1998).

Oxidised ASS can have a pH of < 4 (Powell and Ahern 1999; Brinkman and Pons 1973; Fitzpatrick and Shand 2008; Demas et al. 2004); the acidity allows dissolution of iron, aluminium and sometimes manganese from the soil (Sammut 2000; Fanning et al. 2010; Fanning and Muckel 2004). The iron is released from the iron sulfides, and aluminium is released by the breakdown of clay minerals (Melville et al. 1993). The aluminium and iron can enter groundwater and surface water, and this can be damaging to plant and aquatic life (Bowman 1993; Fitzpatrick and Shand 2008; Fitzpatrick et al. 2008a; Demas et al. 2004). At the low pH, heavy metals such as lead, cobalt, arsenic, chromium, cadmium and copper are also mobilised, or released from the sulfides, allowing them to move through soil and potentially contaminate both surface and groundwater (Bowman 1993; Fitzpatrick and Shand 2008; Glover 2008; Sammut 2000; Fitzpatrick et al. 2008a). Rainfall can also flush sulfide oxidation products from the soil, leading to pulses of contaminated water flowing into streams and rivers (Fitzpatrick et al. 2008a; Demas et al. 2004; Fanning et al. 2004).

1.1.3 Buffering Capacity of ASS

As the majority of environmental effects from the oxidation of ASS are due to the generation of sulfuric acid, the buffering capacity of ASS becomes an important consideration (Fanning and Muckel 2004; Orndorff et al. 2008; Wallace et al. 2008b; Wallace et al. 2008a). The buffering or neutralising capacity of a soil or sediment is defined as its ability to resist chances in pH (its capacity to neutralise acidity) (Ahern and McElnea 1999; Dear et al. 2002). Most commonly, this buffering capacity is due to carbonates such as limestone ($CaCO_3$) and dolomite ($CaCO_3.MgCO_3$) (Wallace et al. 2008b), according to the following reaction:

$$CaCO_3 + H^+ \rightarrow Ca^{2+} + HCO_3^- \quad (14)$$

Calcium carbonate + acidity → calcium ion + bicarbonate

$$CaMg(CO_3)_2 + 2H^+ \rightarrow Ca^{2+} + Mg^{2+} + 2HCO_3^- \quad (15)$$

Calcium magnesium carbonate + acidity → calcium ion + magnesium ion + bicarbonate

However, buffering capacity can also come from the cation exchange capacity (CEC) of clays in the soil and alkalinity in the pore waters (such as seawater and some river waters) (Bowman 1993; Dear et al. 2002; Dent and Bowman 1993). Neutralisation due to the CEC, whereby hydrogen ions (H^+) exchange onto the clay minerals, has much less of an affect than neutralisation due to carbonates (Brady and Weil 2002). Buffering capacity can also come from reactions with organic matter within the soil (Gardner et al. 2000).

1.1.4 Freshwater ASS Environments

While freshwater environments require the same basic conditions as their coastal equivalents to form ASS (a source of sulfate and iron, organic matter and anaerobic conditions), the timescale of development can be considerably longer (Fitzpatrick and Shand 2008; Lamontagne et al. 2003). Salinisation of these environments since European settlement in Australia has impacted the development of ASS, with salinity contributing higher levels of sulfate to these riverine environments. The prolonged waterlogging resulting from the removal of the wetting and drying conditions due to human alteration has also increased sulfide formation (Fitzpatrick et al. 1996; Glover 2008; Lamontagne et al. 2003; Pyper and Davidson 2001; Sammut et al. 1996).

The most common freshwater environments for ASS are wetlands; however, ASS can also occur near seepages and springs (Campbell 1983; Fitzpatrick et al. 1996; Fitzpatrick and Shand 2008; Hall et al. 2006; Lamontagne et al. 2003). A common inland wetland environment containing sulfide minerals is freshwater, poorly drained *Melaleuca* or tea-tree peat swamps, which are found across Eastern Asia and Australia (Brinkman and Pons 1973; Sammut et al. 1996).

1.1.4.1 Peat Swamps

Freshwater peatlands or peat swamps are defined as organic wetlands characterised by a living plant layer and thick accumulations of organic material, where organic matter production is in excess of decomposition (Grover et al. 2005; Warburton et al. 2004; Vile and Novak 2006). The permanent waterlogging and therefore anaerobic conditions, along with the presence of both inorganic and organic sulfur and large amounts of organic

matter, provide ideal environments for the accumulation of iron sulfides and the formation of ASS. Organic sulfur originates from the decomposing plant material, while inorganic sulfur can come from either atmospheric deposition (rainfall) or surface and groundwater sources (Vile and Novak 2006). Peat swamps typically have carbon-14 ages of between 200 and 20,000 years, allowing adequate time for the development of pyrite and marcasite (Bush et al. 2004b; Clymo 1983).

Peat is defined as a biogenic deposit composed of partially decayed organic matter that has accumulated under saturated conditions, which is one of the reasons peat formation is often favoured in cool climates and waterlogged conditions (Charman 2002; Grover et al. 2005). When saturated, peat consists of about 90-95% water and about 5-10% solid material. The organic content of the solid fraction is very high, often up to 95% (Warburton et al. 2004). Water is an important factor in understanding how peatlands function, particularly changes in the composition of the soil or sediment which spends most of its time in a waterlogged state (Charman 2002; Ingram 1983).

Within the Australasian region, peatlands range from blanket bogs on subarctic islands such as the Auckland Islands and south-western New Zealand, the buttongrass moorlands of Tasmania, to widespread topogenic swamps (occurring in valleys) in high rainfall parts of eastern Australia and New Zealand (Whinam and Hope 2005). The climate of mainland Australia does not favour the development of permanent peatlands, except for comparatively small alpine areas and areas of high rainfall (Campbell, 1983). As a result, the definition of 'peatlands' in Australia has been expanded to include terrestrial sediments in which organic matter exceeds 20% dry weight, and with a depth generally greater than 0.3 m (Whinam and Hope 2005).

1.1.5 Previous ASS Mapping

ASS mapping was collated as part of the Australian Soil Resource Information System (ASRIS), which was designed as an integrated system for managing all types of soil data and information. ARSIS was developed and is maintained through the Australian Collaborative Land Evaluation Program (ACLEP), which is a partnership between the Commonwealth Scientific and Industrial Research Organisation (CSIRO), the Australian Government Department of Agriculture, Fisheries and Forestry, and the state and territory agencies responsible for land resource assessment (CSIRO 2012).

As part of ARSIS, a national dataset of available ASS mapping inferred from surrogate datasets was put together, known as the Atlas of Australian Acid Sulfate Soils. The mapping was classified with a nationally consistent legend that includes risk assessment criteria and correlations between Australian and International Soil Classification Systems. The 'inland' component of the mapping was compiled with a provisional ASS classification inferred from national and state soils, hydrography and landscape coverages. The base scale is 1:2.5 million for Victoria, overlayed with a 1:250k hydrography. The composite data layer was sourced from the best available data, with polygons depicted at varying scales and classified with varying levels of confidence (Fitzpatrick et al. 2011).

Coastal ASS mapping has also been conducted in Victoria at a 1:100,000 scale, as part of *Victorian Coastal Acid Sulfate Soils Strategy*. The mapping approach identified areas of higher sea level during the mid-Holocene (about 10,000 years ago), which resulted in the laying down of sediments that contained iron sulfides, usually in the form of pyrite. This geomorphologic mapping was correlated with data derived from comprehensive testing of

mapped areas, and the on-ground investigation was concentrated on priority areas where pressure for land development is high and where coastal acid sulfate soils (CASS) issues are known to have occurred (DSE 2009).

1.2 Classification of ASS

Until recently, ASS were generally classified into one of two types: actual acid sulfate soils (AASS) or potential acid sulfate soils (PASS). PASS are defined either as soils that "contain pyrite that has not been oxidised" (Bowman 1993, p. 97) or soils in which the amount of pyrite or other iron sulfide exceeds the natural buffering capacity of the soil (Bowman 1993; Dent 1986; Gardner et al. 2000). These soils have the potential for the pyrite to oxidise to sulfuric acid (Sammut 2000), but oxidation has not occurred because the soils are under reducing conditions (Smith et al. 2003). In comparison, AASS are soils where the iron sulfides have oxidised due to exposure to the atmosphere, generating acidity and therefore decreasing the pH of the soil (Bowman 1993). For AASS to occur the amount of acidity generated must be greater than the buffering capacity of the soil or sediment (Melville et al. 1993) or the rate of acid production must be faster than the rate of neutralisation (Dent and Bowman 1993), although the latter factor depends on the amount of rainfall and its seasonal variation, evapotranspiration, soil permeability and the leaching rate during and after oxidation (Brinkman and Pons 1973).

Several variations to the classification scheme have been proposed. Brinkman & Pons (1973) proposed an additional category of pseudo-acid sulfate soil, which are soils that show the products of sulfide oxidation without a pH decrease to below 4. Fanning (2006) discussed the addition of postactive ASS, described as ASS where oxidation has already

occurred and the sulfides have weathered from the soil and the soil is no longer acidic. Sullivan et al. (2010) proposed a new classification of hypersulfidic and hyposulfidic soils. Hypersulfidic soil is a "sulfidic soil material that is capable of severe acidification as a result of oxidation of contained sulfides" (Sullivan et al. 2010, p.5), in that the soil either has a field pH of 4 or below, or experiences a substantial pH drop to 4 or below after incubation in the laboratory (designed to replicate the conditions of oxidation). This definition does not identify whether acidity is already present, and so encompasses the terms AASS and PASS. Hyposulfidic soil is defined as "sulfidic soil material that is not capable of severe acidification as a result of oxidation of contained sulfides" (Sullivan et al. 2010, p.5), i.e. a hyposulfidic soil would not show a significant pH drop during incubation, but may show indications of acidity at the sites where it is exposed.

An alternate classification scheme using six categories has been proposed for this project (Figure 1.1). The terms **AASS** and **PASS** are retained, along with **post-active ASS** from Fanning (2006) and three new terms are added: **buffered sulfidic soil (BSS)** (soils with a buffering capacity that exceeds the amount of potential acid generated), **low-risk ASS** (soils which contain sulfides, but which if oxidised, will not show significant acidification), and **non-sulfidic soils** for soils that do not contain any sulfides. In addition, the definition of PASS has been refined to any ASS that contains potential to generate a significant amount of acidity, but is not currently oxidising.

It should be noted that the variability within a soil or sediment means that any classification should only be applied to individual sections of the profile; it is possible, for instance, to have a soil classified as AASS within the upper part of the profile and as a PASS at depth. Therefore, each sampled part of the sediment or soil profile should be classified separately.

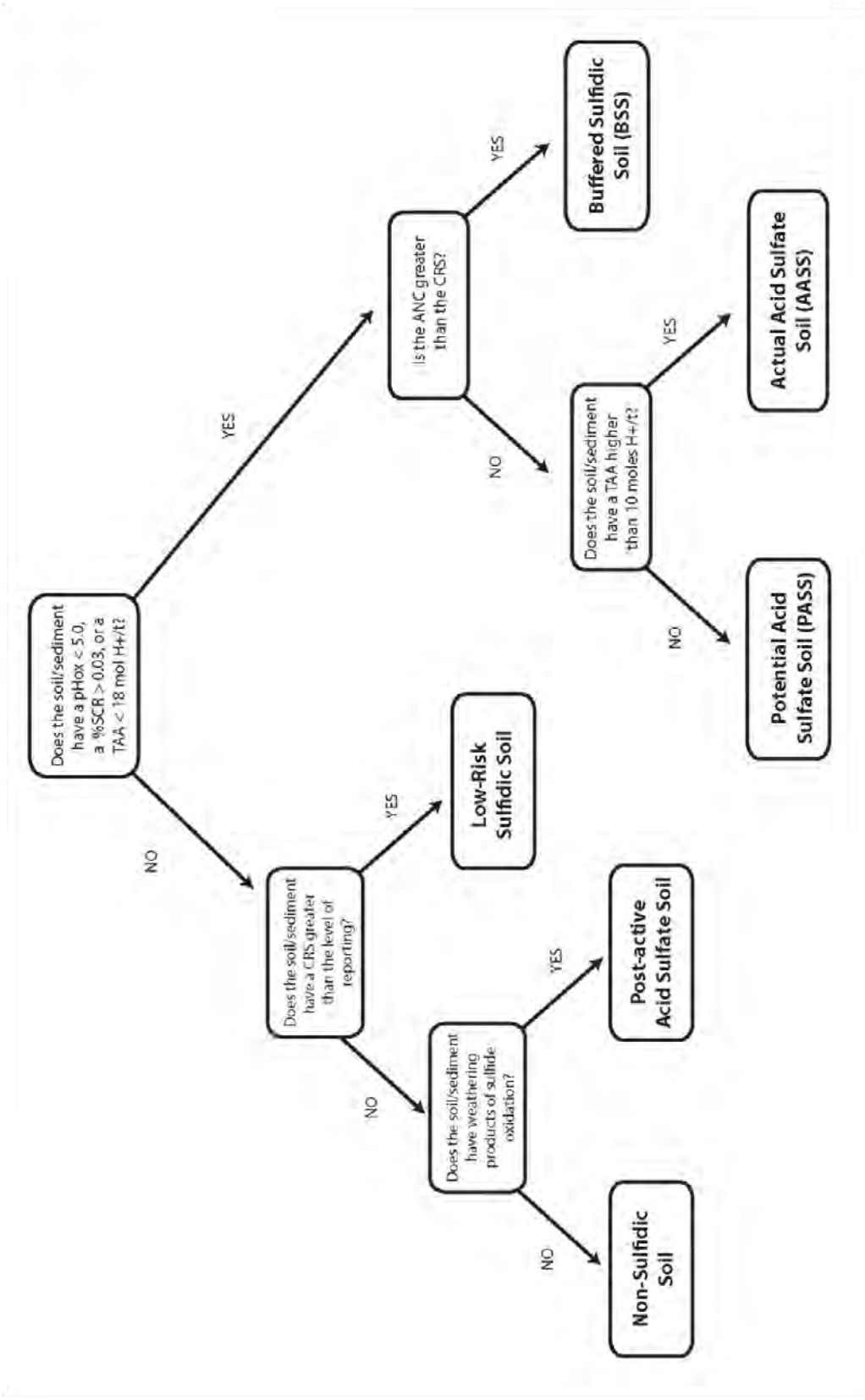

Figure 1.1 Classification Scheme (thresholds taken from (EPA 2009))

1.3 Aims of thesis

While knowledge of inland ASS is growing, much of the published literature has been conducted on a site-specific basis (Glover 2008; Fitzpatrick et al. 2008a; Sammut et al. 1996), or on the process of pyrite formation (Berner 1970; Berner 1984; Schoonen and Barnes 1991) and sulfide oxidation (Moses and Herman 1991; Moses et al. 1987; Smith 2004; Evangelou and Zhang 1995). In particular, inland ASS have been little studied on a regional scale, with most of the research focusing on the Murray River (Baldwin et al. 2007; Hall et al. 2006; Lamontagne et al. 2004; Wallace et al. 2005a). This gap in mapping has been highlighted across many areas of Australia, including the Corangamite Basin in Victoria (Fitzpatrick and Shand 2008). The inland ASS also found within freshwater environments are still poorly understood compared to areas associated with salinisation (Fitzpatrick and Shand 2008; Glover 2008; Hall et al. 2006; Lamontagne et al. 2003).

This thesis has the overall aim of providing a method to predict the distribution of inland ASS that may occur over a regional scale. The Corangamite Catchment Management Authority (CMA) region was selected to gain a better understanding of inland ASS and their environments of formation, particularly as management plans for areas within the region have begun stating the potential of ASS as an environmental risk that requires management and planning (SRW 2010).

To undertake this aim, a variety of freshwater environments containing inland ASS conditions were studied. The investigation used geochemical and sedimentary analytical techniques to quantify the potential release of acid into the environment based on a series

of field sites, before GIS and mapping techniques were used to isolate areas of potential and actual ASS throughout the Corangamite area.

1.4 Thesis Outline

This thesis:

- Defines the background and context of the issue of inland ASS soils within Australia and the world, including knowledge gaps and common issues (Chapter 1)
- Outlines the methodology used to define and quantify the potential and actual acidity and other geochemical and sedimentary factors of inland ASS, including limitations and comparisons (Chapter 2)
- Discusses the regional geological, geomorphological, climatic and hydrological setting of the Eastern Otway Basin and justifies the choice of study areas within it (Chapter 3)
- Describes and discusses the inland ASS found within the Basalt Plains region of the study area (Chapter 4)
- Describes and discusses the inland ASS found within the Otway Ranges and foothills of the study area (Chapter 5)
- Outlines the methodology developed for mapping the types of inland ASS found within the Corangamite CMA region and describes and discusses the areas mapped (Chapter 6)
- Places the factors involved in forming inland ASS described from both areas into a regional landscape (Chapters 4, 5, 6 and 7)

Chapter 2

Methods

When analysing ASS, emphasis is placed on two aspects: determining the existing acidity within the sediment that may be exported (including contributions from dissolved iron and aluminium), and the potential acidity in the form of reduced inorganic sulfur (pyrite and other iron sulfide minerals) that may be oxidised. Since environments containing inland ASS are diverse and dynamic, and the oxidation states of sulfur range from -2 to +6, the quantification of acidity through laboratory analysis can be difficult (McElnea et al. 2002; Ahern et al. 2004). This chapter describes the methods used in this study to analyse the potential and existing acidity of the sampled ASS, characterise the composition of the sediment, and assess its physical properties. Standard methods have been used, based on those in *Acid Sulfate Soils Laboratory Guidelines 2.1* (Ahern et al. 2004), unless otherwise stated.

2.1 Sediment Collection and Handling

The occurrence of inland ASS varies according to location within the landscape and depth of the sediment (Ahern et al. 2004). As a result, the selection of sites within the study area was based on assessments of the vegetation and the geomorphic and geological setting, using available geological and wetland mapping, LIDAR topography, local knowledge and field investigation. Prior to sampling, all sites were described in field notes and photographed. Sediment cores were collected using a 1.0 m stainless steel gouge auger to the depth of the underlying the ASS layer, either determined by a colour change or

increased difficulty in sample collection. Samples were collected from each visible layer within the profile, or at every 0.2 m depth when layers were not seen. The depth of each sample within the profile was recorded, along with the thickness of the soil profile and any layers within the profile.

At the time of sampling, a sub-sample from each depth in the core was placed into a small plastic sample container and enough deionised water was added to turn the soil into a paste. The field pH (pH_F) was then recorded using a calibrated pH meter. For each of the same subsamples, a small amount of soil was oxidised with 30% hydrogen peroxide (H_2O_2). After the reaction subsided, the pH_{FOX} was measured and recorded.

After collection, samples were immediately placed in air-tight polyethylene bags and double-bagged to minimise contact with the atmosphere and avoid moisture loss. During transport back to the laboratory, samples were kept cold in an ice-filled esky to reduce the possibility of oxidation until the samples could be frozen.

2.1.1 Boundary Creek

At the Boundary Creek site a different sampling methodology was used. Much of the site was inaccessible for the early part of the study due to the ongoing fire risk, so rather than coring, sampling was conducted along the east-west fire trench dug along the southern edge of the swamp. Samples were collected at 0.5 m intervals through the profile exposed in the trench wall to a depth of 2.0 m at three locations: upstream, central and downstream (Figure 5.2). At the time of sampling, the trenches were dry, indicating oxidation was already occurring.

At the downstream (north-eastern) end of the fire trench, a core was drilled using a rotary drill to a depth of 4.5 m below the base of the trench (until the weathered bedrock was reached). Sampling from the trench and core followed the same protocols as used at the other sites. During drilling and sampling, the height of the water level in the trench was recorded.

2.1.2 Water Sample Collection and Preparation

If surface water was present at the site, samples were taken from the deepest and/or fastest moving locations, using a sampling container attached to a long pole. Samples were then placed into acid washed plastic containers and kept cold for transport back to the laboratory. At each sample point, field measurements of temperature, pH, redox, electrical conductivity (EC) and dissolved oxygen were recorded. Upon reaching the laboratory, all samples were filtered through 0.45 µm cellulose filters using a vacuum pump, with one of the samples for each site acidified to pH 2-3 using 69% (w/v) nitric acid (HNO_3).

2.2 ASS Sample Preparation and Storage

Prior to laboratory analysis, ASS samples were removed from the freezer, allowed to thaw, and a subsample placed on a watch glass and dried in an oven at 80-90˚C for approximately 48 hours in order to kill bacteria and remove water to minimise further oxidation of pyrite (Ahern et al. 1996). After drying, coarse material, such as gravel, was removed using a 2 mm sieve. If required for the analytical technique, samples were ground in a mortar and pestle. For analytical techniques requiring wet samples (such as acid volatile sulphur; section 2.3.5), samples were removed from the freezer and allowed to partially thaw until

a representative sample could be taken, and the bulk of the sample was returned to the freezer.

2.3 Soil Acidity Measurements

2.3.1 Titratable Actual Acidity (TAA)

Within ASS, existing acidity can be separated into 'actual' and 'retained' acidity. The 'actual' acidity of an ASS is largely soluble and exchangeable, and can be measured in the laboratory by titration against sodium hydroxide (NaOH) (Ahern et al. 2004). This method is referred to as Titratable Actual Acidity (TAA), and is used to quantify the acidity in the soil before oxidation of any sulfidic material present. This method was previously termed Total Actual Acidity (TAA) (Dent and Bowman 1996), but as it does not analyse for acidity from insoluble minerals (such as jarosite; the 'retained' acidity), it therefore underestimates total acidity (McElnea et al. 2002). The TAA method used within this study was first outlined in Dent & Bowman (1993) and modified by Ahern *et al.* (1996) and Santomartino (2000). However, no analysis for retained acidity was performed on the samples in this thesis, as no jarosite was found to be present during XRD analysis.

For each sample, approximately 2.5 g of dried soil was weighed and recorded (m), and placed in a 100 mL plastic beaker to which 50 mL (V_1) of 1 M KCl was added. The suspension was mixed with a stirring bead for an hour, before it was sealed with laboratory film and left to stand overnight (approximately 12-16 hours). After standing, each sample was mixed with the stirring bead for ten minutes and then centrifuged at 700 rpm for an additional ten minutes, before 25 mL (V_2) of supernatant was transferred into a 100 mL plastic beaker. The pH of the solution was measured using a calibrated pH probe. If the

pH was below 5.5, the solution was titrated with 0.05 M (**C**) NaOH to an endpoint of pH 5.5 and the volume of titre (**T**) recorded in mL. The titratable actual acidity (TAA) was then calculated (as moles of H^+ per tonne) using the following equation:

$$TAA = (\frac{V_1}{V_2}) \times (T \times C) \times (\frac{1000}{m}) \quad (16)$$

2.3.2 Titratable Peroxide Acidity (TPA)

The Titratable Peroxide Acidity (TPA) method measures the net acidity of a sample, both the acidity already present in the soil, and the additional acidity released by oxidation of any sulfide minerals by 30% hydrogen peroxide, after this acidity has reacted with any acid-neutralising (buffering) capacity present within the sample (Ahern et al. 2004). To measure the TPA, approximately 2.0 g of dried sample was weighed and recorded (**m**) and placed in a 150 mL beaker with the 50 mL level accurately marked on the side. Initially, a 10 mL aliquot of 30% analytical grade hydrogen peroxide (H_2O_2) was added to the beaker and swirled to mix it with the sample. The solution was left for 30 minutes to allow oxidation to occur. Deionised water was added until the total volume was 45-50 mL; during this process the solution was mixed to ensure it remained as homogeneous as possible. The suspension was heated on a hotplate to a temperature of between 80 and 90˚C for another 30 minutes. During the heating, the suspension was mixed once every ten minutes to keep it homogenised, and the volume of the solution was kept constant by the addition of deionised water.

Once the sample had been heated for a maximum of 30 minutes, the beaker was removed from the hotplate and allowed to return to room temperature. A second 10 mL aliquot of

30% hydrogen peroxide was added and allowed to react for a further 10 minutes. The sample was returned to the hotplate for another 30 minutes, periodically mixed and kept at a constant volume as previously. Once the sample had again returned to room temperature, the pH of the solution was measured using a calibrated probe. If the pH was greater than 6.5, a carbonate modification step was performed on the sample before continuing (see section 2.3.2.1. for details). If the pH was below 2.0, the entire procedure was performed again, this time with only 1.0 g of dried sediment. If the pH was between 2.0 and 6.5, the peroxide decomposition step was carried out. To decompose the peroxide, 1.0 mL of 6.30 x 10^{-3} M $CuCl_2.2H_2O$ was added and the solution returned to the hotplate for a maximum of 30 minutes or until any noticeable reaction had stopped. The volume was again kept constant by the addition of deionised water.

After the solution had cooled to room temperature, 30 mL of ~2.66 M KCl was added to the beaker and mixed, giving the entire solution a total volume of approximately 80 mL. The pH was measured again and if below 5.5, the solution was titrated to pH 5.5 using 0.05 M (C_1) NaOH and the volume of titre (V_1) recorded in mL. To ensure all the iron in solution was converted to iron III (Fe^{3+}) and therefore precipitated as $Fe(OH)_3$ during the titration, 1.0 mL of 30% H_2O_2 was added to the solution; the pH of this aliquot of H_2O_2 was adjusted to 5.5. The pH was measured again and the sample titrated with 0.05 M NaOH to a pH of 6.5 and the titre (V_2) recorded in mL.

During this process, two solution blanks were oxidised and titrated using the same procedure as the samples without the addition of dried sediment. If the pH of the sample blanks was below 5.5 prior to the final oxidation step, the blanks were also titrated to 5.5 using 0.05 M NaOH, and the titre (V_3) recorded in mL. Following the final oxidation step, a

second titration was performed on the blanks to a pH of 6.5 and the titre (V_4) recorded in mL. If any of the samples underwent the carbonate modification step, one of the sample blanks was also put through this process. Titratable peroxide acidity (in units of moles of H^+ per tonne) can then be calculated using the follow equation:

$$TPA = [(V_1 + V_2 - V_3 - V_4) \times C_1] \times (\frac{1000}{m}) \quad (17)$$

2.3.2.1 The Carbonate Modification Step

ASS may contain carbonate minerals that can react with any acidity produced by sulfide oxidation, and this results in the ASS having an acid-neutralising (or buffering) capacity (ANC). The ANC may exceed any acid-generating potential of the soil, and is then termed excess acid neutralising capacity (ANC_E). Measurement of ANC_E is determined by titration with hydrochloric acid (HCl) to a pH of 4 (McElnea et al. 2002a; McElnea et al. 2002b; Ahern et al. 2004; Holdgate et al. 2001), as a carbonate modification step within the TPA method.

For those ASS samples with a pH above 6.5 prior to the peroxide decomposition step during TPA analysis, a carbonate modification step must be performed. After the addition of the second 10 mL aliquot of 30% H_2O_2, the sample is removed from the hotplate and allowed to cool to room temperature. Then, using 0.5 M (C_2) HCl, the sample is titrated to pH 4.0 and the titre volume (V_5) is recorded in mL. The solution blank is not titrated using HCl, as it does not contain any carbonate.

After the titration, 25 mL of 30% H_2O_2 is added to the suspension and the beaker is returned to the hotplate, and swirled every ten minutes for a maximum of one hour or until the reaction has ceased. Once the carbonate modification is completed, the samples can

undergo the peroxide decomposition step. If the sample needs to be transferred to a larger beaker during the process, the sample can be washed out using a maximum of 5.0 mL of deionised water. If the total volume of the sample is greater than 50 mL after the carbonate modification step, the volume was reduced on the hotplate to 50 mL. The excess acid neutralising capacity (ANC_E) can be calculated (in moles of H^+ per tonne) from the equation:

$$ANC_E = [V_5 \times C_2 \times (\frac{1000}{m_1})] - [(V_1 + V_2 - V_3 - V_4) \times C_1] \times (\frac{1000}{m_1}) \quad (18)$$

If the net result of this equation is positive, the sample has an intrinsic excess acid neutralising capacity and the TPA is reported as zero. However, if the net result is negative, then ANC_E is reported as zero and the absolute value is reported as TPA.

2.3.3 Titratable Sulfidic Acidity (TSA)

As TPA measures the acidity produced by sulfide oxidation as well as any acidity present in the soil (TAA), the Titratable Sulfidic Acidity (TSA) is used to accurately evaluate the potential acidity contained within ASS. TSA is the acidity due to the complete oxidation of all the sulfidic compounds in the soil by 30% hydrogen peroxide (H_2O_2), and is calculated from the difference in TPA and TAA results (in moles of H^+ per tonne):

$$TSA = TPA - TAA \quad (19)$$

2.3.4 Chromium Reducible Sulfur (CRS)

Chromium Reducible Sulfur (CRS) analysis is regarded as the most reliable and direct measure of reduced inorganic sulfur present as disulfide (S_2^{2-}) e.g. in pyrite (FeS_2); this

method also analyses for elemental sulfur but not for acid volatile monosulfides (AVS). The CRS method is applicable over the wide range of values encountered in ASS, because it is not subject to significant interferences from the sulfur in either organic matter or sulfate minerals such as gypsum. The use of a chromium reduction method to measure reduced inorganic sulfur was first proposed by Zhabina and Volkov (1978), and has since been widely used (Morse and Cornwell 1987; Canfield et al. 1986; Sullivan et al. 1999; Burton et al. 2008). The chromium reduction method is based on the reduction of inorganic sulfur to H_2S by a hot acidic chromium(II) chloride ($CrCl_2$) solution; the evolved hydrogen sulfide (H_2S) is trapped in a zinc acetate solution as ZnS and can be quantified by iodometric titration. Initial CRS analyses for this project were conducted by the author using the method as stated within *Acid Sulfate Soil Laboratory Methods Guidelines* (Ahern et al. 1998), with all other analyses being carried out by the Environmental Analysis Laboratory (EAL), using the same method.

For a chromium reducible sulfur (CRS) determination, between 0.475 g and 0.525 g of dried soil was accurately weighed out and recorded (m). The soil was placed in a double-neck, round-bottomed digestion flask set up in a fume hood, along with 2.0 g of analytical grade chromium powder and 10 mL of 95% ethanol, and swirled. A solution blank was also made up and subjected to the same procedure as the samples. The digestion flask was placed on the heating mantle and connected to the condenser (Figure 2.1). The pressure-equalising funnel was attached and a Pasteur pipette was attached to the top of the condenser and inserted into a 100 mL Erlenmeyer flask containing 40 mL of 0.5 M zinc acetate solution.

After the water to the condenser was turned on, 60 mL of 6 M HCl was added to the glass dispenser in the pressure-equalising funnel. Nitrogen gas (N_2) was connected to the pressure-equalising funnel, and once a bubble rate of approximately three bubbles per second was obtained in the zinc acetate solution, the system was purged for approximately three minutes. The 6 M HCl was slowly released from the dispenser and after two minutes the heating mantle was turned on and the mixture brought up to a gentle boil. The solution was allowed to digest for 20 minutes, before the Erlenmeyer flask was removed and the Pasteur pipette washed with distilled water into the flask.

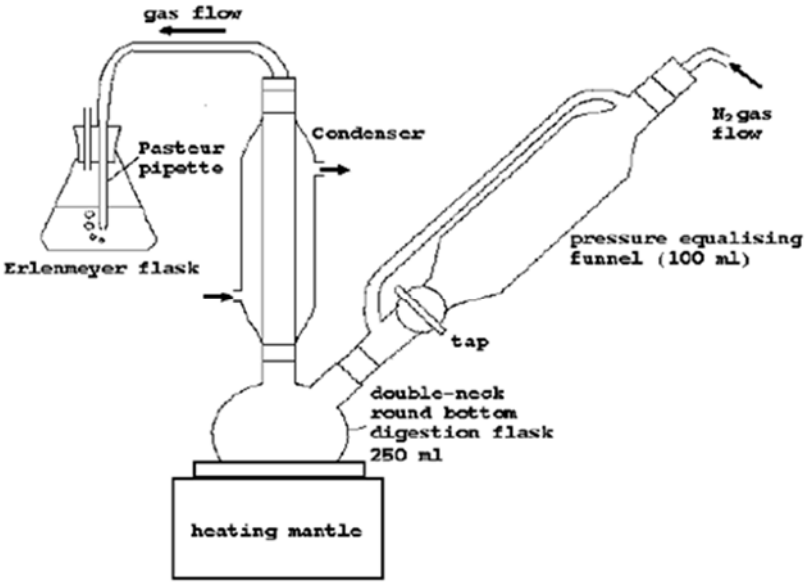

Figure 2.1 Apparatus used in Chromium Reducible Sulfur (CRS) method (Ahern et al. 2004)

After the digestion, 20 mL of 6 M HCl and 1 mL of starch indicator were added to the zinc acetate solution, before being gently mixed with a magnetic stirrer, before the zinc acetate solution was titrated against an iodine solution to a permanent blue end-point. The volume

of titrant (**A**) was recorded in mL. The blank was also titrated and the titre (**B**) was recorded in mL. The concentration (**C**) is the calculated molarity (in M) of the iodine solution determined by titration with standard 0.025M $Na_2S_2O_3$, which was performed at the beginning of each sample run. The volume (in mL) of sodium thiosulfate (**D**) and iodine solution (**E**) was recorded, and the calculation performed as below:

$$C = \frac{0.025 \times D}{E} \tag{20}$$

The concentration of chromium reducible sulfur (wt %) was then calculated:

$$CRS = \frac{(A - B) \times C \times 3.2066}{m} \tag{21}$$

2.3.4.1 Converting %S to moles H^+/t

To convert percentage sulfur, such as CRS values, into moles of H^+/t for comparison, the following calculation is used:

$$S\,(mol H^+ / t) = \frac{A}{B} \times 2 \times 10{,}000 \tag{22}$$

Where **A** is the %S as grams of sulfur per 100 g of oven dry soil, and **B** is the molar mass of sulfur (32.066 g/mole).

2.3.5 Acid Volatile Sulfur (AVS)

ASS may contain substantial quantities of monosulfides (Chapter 1), which are far more reactive that pyrite, and may represent a serious environmental threat (Burton et al. 2006; Bush et al. 2004a). These minerals, along with any dissolved sulfide (H_2S and HS^-) in sediment pore water, are known as acid volatile sulfur (AVS). AVS analytical methods are

based on the volatilisation of monosulfide to hydrogen sulfide (H_2S) by hydrochloric acid (HCl) – the H_2S is carried by a nitrogen gas flow into a trapping solution, where it is precipitated as a metal sulfide and quantified by iodometric titration, potentiometric titration, colorimetric spectrophotometry, or gravimetrically. Morse & Cornwell (1987) found that cold 6N HCl best discriminated acid volatile sulfur from pyrite, but recovered only 75% AVS due to interference from ferric iron (Fe^{3+}); as a result, AVS concentrations extracted using HCl need to be corrected for this (Morse and Cornwell 1987; Ahern et al. 1998).

Initial AVS analyses for this project were conducting using the method as stated within *Acid Sulfate Soil Laboratory Methods Guidelines* (Ahern et al. 1998), with subsequent analyses being carried out by the Environmental Analysis Laboratory (EAL) using the same method. Into a digestion flask, 5.0 g of wet sample was weighed (m) and added, followed by 10 mL of ethanol solution, before the stopper was attached, ensuring an air-tight seal. The digestion flask was placed inside a fume hood and a Pasteur pipette was connected to the digestion flask (Figure 2.2) and inserted into a 50 mL beaker containing 30 mL of 3% zinc acetate and 25% ammonium hydroxide trapping solution.

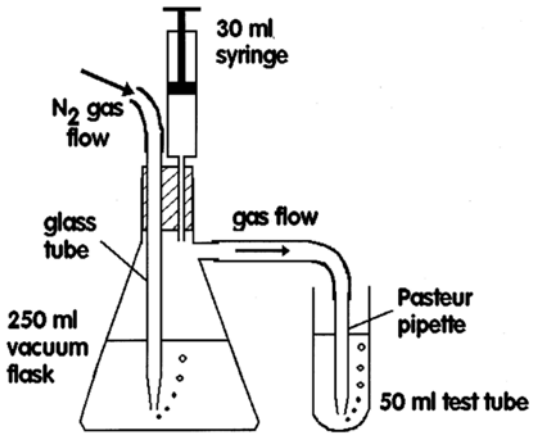

Figure 2.2 Apparatus used in AVS method (Ahern et al. 1998)

Nitrogen gas (N_2) was connected and a bubble rate of approximately three bubbles per second was obtained in the trapping solution, before being allowed to purge the system for approximately three minutes. Once the system was purged, 20 mL of 12N HCl was added into the digestion flask and swirled 2-3 times to agitate. The digestion was left for 1 hour, with the solution agitated every 10 minutes.

After digestion, the Pasteur pipette was washed with distilled water into the flask to capture all ZnS. The solution was then transferred into a 100 mL Erlenmeyer flask and 1 mL of starch indicator was added, followed by 20 mL of 6 M HCL. The trapping solution was titrated against a standardised iodine solution to a permanent blue end-point and the volume of titrant (**A**) recorded in mL. The blank was also titrated and the titre (**B**) was recorded in mL. The concentration (**C**) is the calculated molarity (in M) of the iodine solution determined by titration with standard 0.025M $Na_2S_2O_3$, which was performed at the beginning of each sample run. The concentration of acid volatile sulfur (wt %) is given by the following equation:

$$AVS = \frac{(A - B) \times C \times 1600 \times 1.33}{m} \quad (23)$$

2.4 Limitations of Analytical Methods

The quantification of the various sources of acidity within ASS can be very difficult and prone to interference from a variety of sources due, in part, to the indirect nature of some methods (McElnea et al. 2002). In particular, methods involving peroxide digestion are vulnerable to inaccuracies. For instance, samples that have a TPA result of zero may have no pyrite, or a larger amount of carbonate than pyrite (stochiometrically); the TPA method

alone cannot distinguish between these possibilities (Ahern et al. 2004). However, the main reason for the inaccuracies with peroxide digestion methods is the underlying assumption that the pyrite is completely oxidised according to the following stoichiometry (Ward et al. 2002; McElnea et al. 2002):

$$FeS_2 + {}^{15}\!/_{2}\, H_2O_2 \rightarrow Fe(OH)_3 + 2H_2SO_4 + 4H_2O \qquad (24)$$

Pyrite + hydrogen peroxide → iron hydroxide + sulfuric acid + water

This oxidation reaction may be complicated by the addition of sulfate from the dissolution of sulfate minerals and/or the oxidation of organic sulfur (Ahern et al. 1998; Ahern et al. 2004; Sullivan et al. 1999), and by the formation of sulfur compounds that are not extractable by 1M KCl (such as jarosite) (Ahern et al. 1998; Ward et al. 2002). These interferences may result in errors that are an order of magnitude greater than some of the threshold criteria (such as 0.03 %S for sands) that are currently used to identify ASS in Australia (Sullivan et al. 1999; EPA 2009).

Conversely, the oxidation of organic matter within the sediment can release organic acids, leading to an overestimation of potential acidity. This is complicated by the rate of release, as within natural systems, organic matter is oxidised slowly, compared to the rapid rate of oxidation by hydrogen peroxide (Sullivan et al. 1999). In highly organic ASS, peroxide digestion methods can also release hydrolysable metal ions that contribute additional acidity to the measurements, and therefore an overestimation of potential acidity (Ahern et al. 2004; McElnea et al. 2002a; McElnea et al. 2002b).

In comparison, the CRS method has been shown to be specific to reduced inorganic sulfur compounds and is unaffected by either organic sulfur or sulfates such as gypsum (Morse and Cornwell 1987; Canfield et al. 1986). However, as the CRS method measures a combination of iron disulfides and elemental sulfur, specific pretreatments must be undertaken if the CRS method is to be used to quantify only disulfide minerals (pyrite) (Sullivan et al. 1999).

For an ASS that has not undergone oxidation and contains negligible buffering capacity and organic matter, the TSA (as derived from the TPA and peroxide digestion) is comparable to the potential sulfidic acidity predicted from the CRS measurement (Ahern et al. 2004; Ward et al. 2002; McElnea et al. 2002). However, the CRS method by itself cannot quantify the existing acidity or buffering capacity of an ASS, and must therefore be combined with other methods (such as TAA and ANC determinations) to provide accurate information for managing ASS (Ahern et al. 2004).

2.5 Physical Characteristics

2.5.1 Soil Texture and Grain Size

Soil texture and physical characteristics are important when assessing ASS, as they can govern the buffering capacity of the soil and affect oxidation rates (Ahern et al. 2004), and EPA thresholds for risk assessment of ASS have been determined using soil texture for small disturbances (1-1000 tonnes) (EPA 2009). In this study, extensive field notes were taken during sample collection, including soil description and colour, and laser diffraction grain size analysis was performed by a Malvern Mastersizer 2000 after the dried sediment was sieved to remove particles of greater than 2 mm. A small amount of sediment was

suspended in distilled water, using a stirring speed of 750 rpm, and cycled through a laser beam to measure the particle size; the output was then analysed in Microsoft Excel.

2.6 Elemental and Mineralogical Analysis

2.6.1 X-ray Diffraction (XRD)

Identification of the mineral composition of ASS is important, particularly for carbonate and sulfide minerals. X-Ray Diffraction (XRD) was performed on samples that had been dried and ground, using a Siemens D5000 Power X-ray Diffractometer equipped with copper tube and graphite monochrometer. Samples were measured over 0-70° 2Θ for 8 hours and the resulting scan was analysed using EVA version 2.0 (Bruker AXS, USA) for peak identification. The phases were quantified by Reitveld analysis using the Siroquant programme version 3.0 (Sietronics, Australia).

2.6.2 X-ray Fluorescence (XRF)

Major and trace elemental analysis was carried out with a Siemens 303 X-Ray Fluorescence (XRF) instrument using a rhodium X-ray tube and an analytical power of 50 kV and 50 mA. For analysis of the major elements, the sample was dried, ground and weighed accurately to 0.75000 g, before being placed in a clean glass vial and 6.75000 g of X-ray Flux Pty Ltd 66% Lithium tetraborate: 34% Lithium metaborate flux added, after the flux was dried at 400°C for four hours and cooled in a desiccator. The soil and flux were mixed completely, before being fused at 1050°C in platinum crucibles and then cooled into glass disks. For trace element analysis, 10 g of sample was dried and weighed, before being placed in a

clean glass vial. The sample was then placed into a small container, before being pressed into a pellet at a pressure of 5 tonne (6000 psi) for one minute.

2.6.2.1 Loss on Ignition (LOI)

The weight of volatiles, such as water and carbon dioxide released from organic carbon and carbonates, was analysed by loss on ignition (LOI). Each soil sample was accurately weighed to 0.2 g (m_1), before being heated at 1000°C for 45 minutes. The samples were then allowed to cool in a desiccator and reweighed (m_2). LOI is calculated by the change in mass:

$$\mathrm{LOI}(\%) = \left(\frac{m_1 - m_2}{m_1} \right) \times 100 \qquad (25)$$

2.6.3 Carbon, Nitrogen and Hydrogen analysis

The organic matter content of an acid sulfate soil can range from minor amounts in some sands to extremely high levels in peats, and is an important factor in assessing ASS. Traditionally, it has been assumed that 58% (by weight) of soil organic matter is organic carbon, but this usually only occurs in highly stable humus, and organic carbon typically comprises 50% of soil organic matter (Brady and Weil 2002).

Total carbon levels were measured using Perkin Elmer 2400 Series II CHNS/O analyser. Between 0.01 g and 0.03 g of each sample was weighed to the fourth decimal place, before being added to a small foil sample container. The foil container was then folded and rolled to exclude as much air as possible. Samples were then combusted in a pure oxygen

environment, with the resultant combustion gases measured in an automated fashion, and the weight percentage of carbon recorded.

2.7 Surface Water Analysis

To assess the water quality at all sites, major element analysis was completed in the laboratory on all water samples collected.

2.7.1 Alkalinity Titrations

To assess the buffering capacity of the surface waters, the alkalinity was analysed through a laboratory titration, where 20 mL of sample (**A**) was titrated with standardised 0.1 M HCl (**C**) to a pH of 4.5. The volume of titre (**T**) was recorded, following the method of Rayment & Higginson (1992). The process was repeated until three replicates ± 0.05 mL of each other were produced. The total alkalinity (in mg/L as $CaCO_3$) was then calculated using the following equation:

$$\text{Alkalinity} = \frac{T \times C \times 50040}{A} \quad (26)$$

To convert to mg/L HCO_3^-, the alkalinity was multiplied by a conversion factor of 1.219.

2.7.2 Major Element Analysis

All major element analyses were carried out at La Trobe University. All samples were diluted to the working range of the required instrument, using a range of calibrated pipettes that were checked for accuracy by weighing various volumes of distilled water. All standard solutions were prepared from National Institute of Science and Technology (NIST) certified standards and from this calibration the concentrations were determined.

Sodium (Na^+) and potassium (K^+) were determined using a Sherwood Model 410 Flame Photometer, with a working range of 0-30 mg/L. The instrument sensitivity was ± 0.1 mg/L, and it was calibrated using five standards made up on the day of the analysis. Total iron, calcium, copper, magnesium, zinc and aluminium were analysed using a GBC Quantima Inductively Coupled Plasma–Optical Emission Spectrometer located in the Chemistry Department at La Trobe University. Multi-element standards were made up on the day of the analysis, with the working range of magnesium, iron and calcium as 5-50 mg/L and the working range of copper, zinc and aluminium 2.5-25 mg/L. Chloride (Cl^-), bromide (Br^-) and sulfate (SO_4^{2-}) were analysed on a Phenomenex A300 anion peak Ion Chromatograph with a 1.7 mM $NaHCO_3$/1.8 mM Na_2CO_3 eluent, 25 mM H_2SO_4 regenerate solution, and flow rate of 1.5 mL/min. The samples were diluted to fit the working ranges of 0-200 mg/L for chloride, 0-50 mg/L for sulfate and 0-150 mg/L for bromide.

Chapter 3

Regional Setting

3.1 Study Location

The Corangamite Catchment Management Authority (CMA) area lies approximately 150 km west of Melbourne (Figure 3.1) and covers 13,340 km^2 of south-western Victoria, including 175 km^2 of coastal fringe and 280 km of coastline. The boundary of the region stretches from Ballarat in the north to Geelong in the east, and extends along the coast to Peterborough, including the Otway Ranges (DSE 2008). The major towns in the study area include Geelong to the east and Ballarat to the north, with Colac located approximately in the centre of the region. Other towns include Port Campbell, Anglesea, Cressy and Lorne (Figure 3.1). The region is well known for its coastline and the tourist attraction of the Great Ocean Road, which stretches west from Lorne to near Port Campbell, as well as the historic gold mining region around Ballarat, and the Basalt Plains in the centre of the CMA, which are flanked to the north by the Central Highlands and the Otway Ranges to the south (CCMA 2003).

While the Corangamite CMA has been studied extensively for salinity (De Deckker 2003; Dahlhaus et al. 2008; Hose et al. 2008; Nicholson et al. 2006) and hydrogeology (Barton et al. 2006; Petrides and Cartwright 2006; Dahlhaus 2002), little has been done to investigate any inland ASS found within the region. As noted in Chapter 1, wetlands provide an ideal environment for the formation of ASS. Many wetlands occur across the Corangamite CMA (Figure 3.1), including eleven which are internationally-recognised Ramsar sites. In total,

the region contains over 1,500 wetlands covering an area of 650 km^2. Most wetlands are small, with 74% being less than 0.1 km^2 in size. Nine wetlands are greater than 10 km^2, including Lake Corangamite, which is the largest permanent inland lake in Australia (Williams 1995; Sheldon 2005). As the loss of anaerobic conditions in the wetland sediments can lead to the oxidation of any sulfide minerals present and result in acidification (see Chapter 1), it is important to assess the location, distribution and characteristics of these wetlands to gain an understanding of the potential ASS threat they represent across the region.

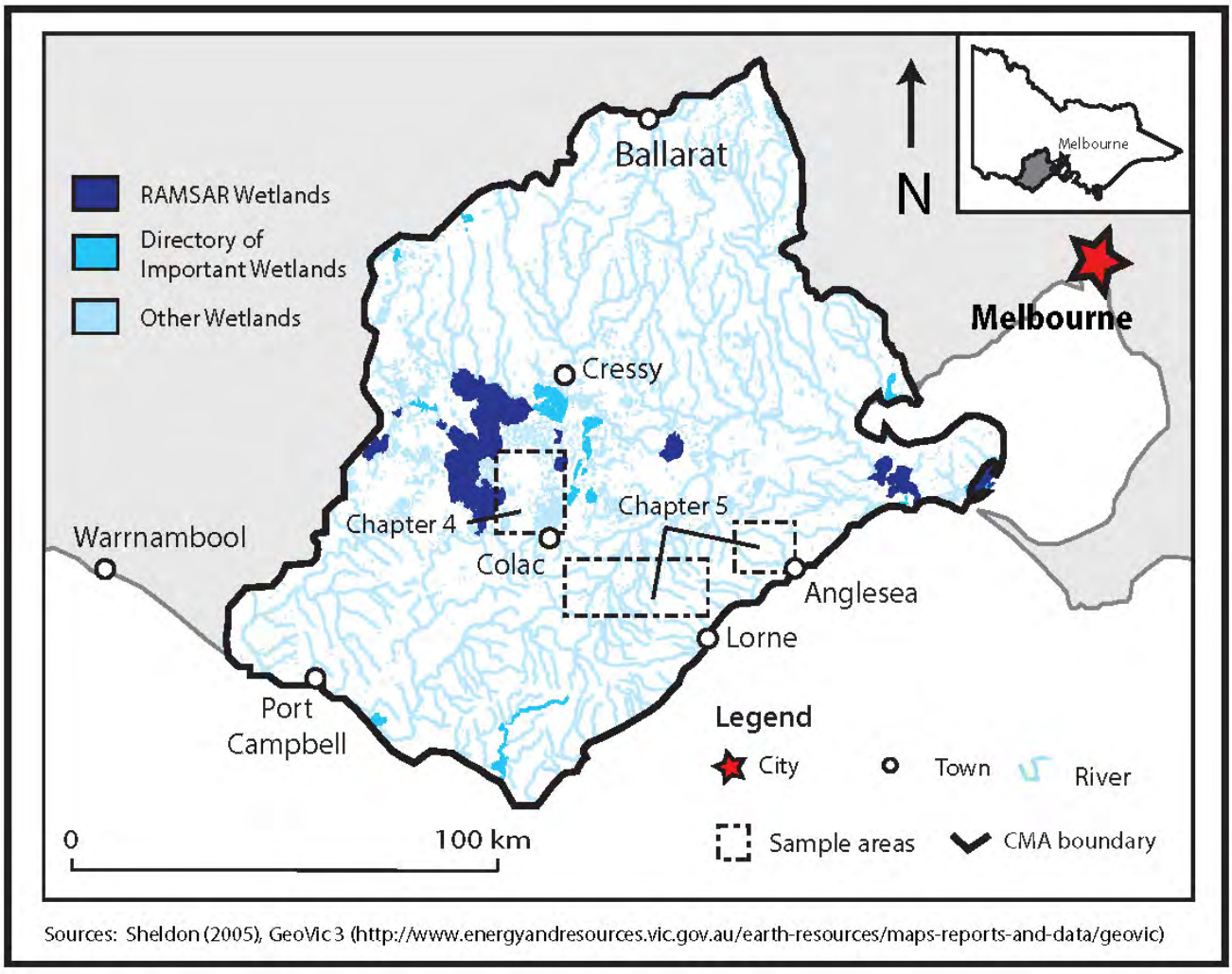

Figure 3.1 Location of study area and study sites

3.2 Regional Geology

3.2.1 Palaeozoic Basement

The Palaeozoic sedimentary and volcanic rocks of the Lachlan Fold Belt (LFB) and the Delamerian Fold Belt (DFB) compose the bedrock that underlies most of south-eastern Australia, including the study area (Crawford et al. 2003; Fergusson 2003; Foster and Gray 2000). The LFB and DFB were originally part of a Palaeozoic orogenic system that extended along the margin of Gondwana (Fergusson 2003; Foster and Gray 2000). The LFB comprises three distinct sub-provinces (eastern, central and western), which have differences in rock type, metamorphic grade and structural history (Foster and Gray 2000; Gray and Foster 1997). Generally the LFB is considered to be dominated by deep water, quartz-rich turbidites and calcalkaline volcanic rocks, that overlie mafic ocean crust and are intruded by numerous granitic plutons (Gray and Foster 1997; Korsch et al. 2002; Foster and Gray 2000; Fergusson 2003). The sub-provinces have been divided into fault-bounded structural zones, and the northern extent of the Corangamite CMA region lies within two of these structural zones of the western sub-province of the LFB: the Stawell Zone and the Bendigo-Ballarat Zone (Figure 3.2a), separated by the steeply west-dipping Avoca Fault (Morand et al. 1995). The Stawell and Bendigo-Ballarat Zones contain Cambrian to Ordovician, largely unfossiliferous, deep marine quartz-mica turbidites and occasional black shales of the St Arnaud Group and the Castlemaine Group (Crawford et al. 2003; Foster and Gray 2000; Department of Agriculture 1999; Cayley and McDonald 1995), deposited as part of a submarine fan system that was derived from the newly uplifted DFB to the west (Fergusson 2003; Cayley and McDonald 1995).

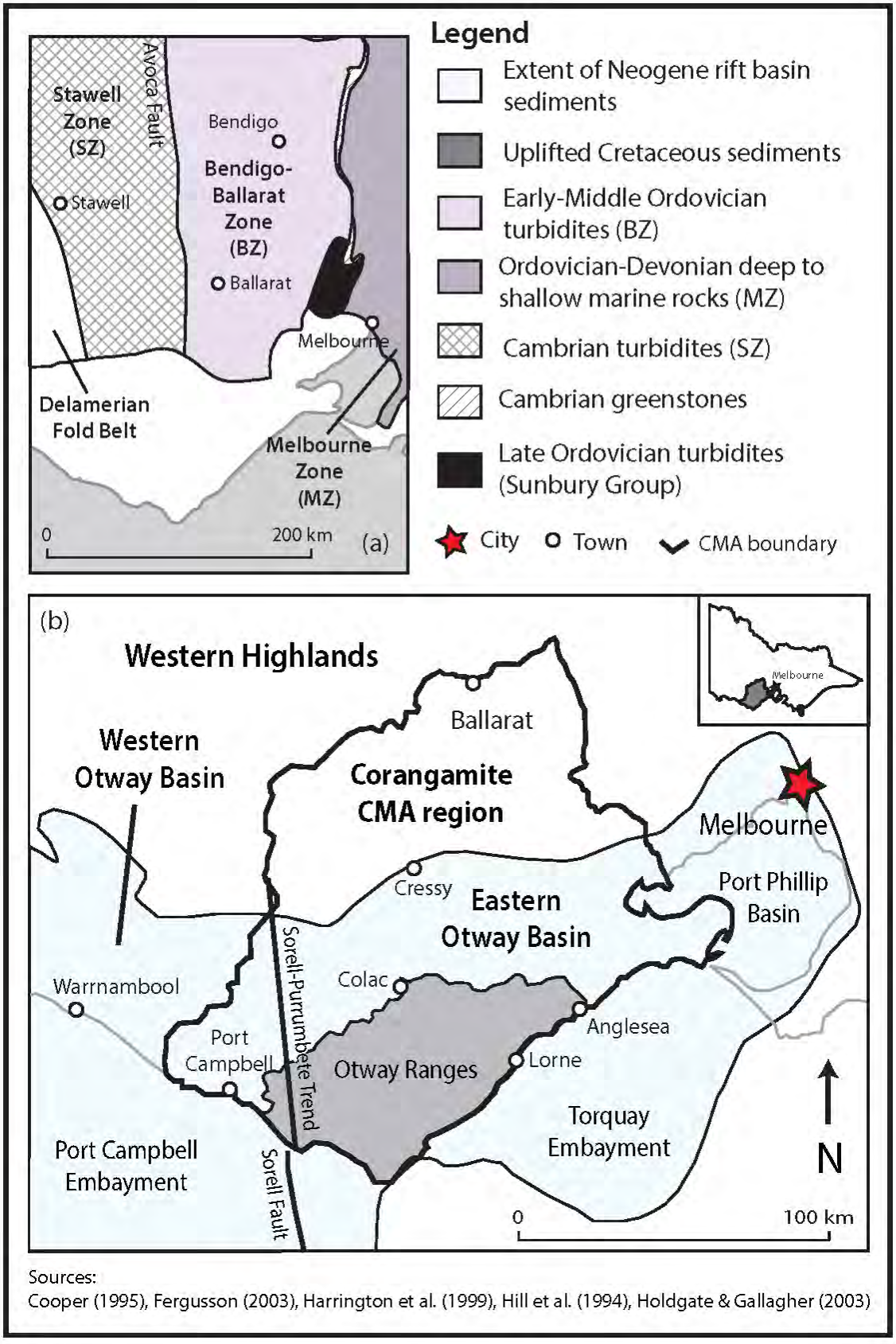

Figure 3.2a and b Structural setting of the Corangamite CMA

During the Devonian, moderately shallow-level granite plutons intruded the western sub-province of the LFB and metamorphosed the surrounding sediments of the St Arnaud Group and the Castlemaine Group to hornfels (Department of Agriculture 1999). The plutons are mainly post deformational or very shallow level subvolcanic, and are associated with caldera-collapse rhyolites and ash flows (Foster and Gray 2000; Morand et al. 1995).

3.2.2 Mesozoic Rifting – the Otway Basin

During the Mesozoic breakup of Australia and Antarctica, a series of extensional basins formed as part of a failed rift system along the southern margin of Australia. The continental rifting spread eastwards from Western Australia, extending all the way to Victoria and the Otway Basin (Cooper 1995; Duddy 2003a; GSV 1995). The eastern Otway Basin comprises the onshore Otway Ranges and Colac Trough and the offshore Torquay Embayment (Figure 3.2b; Cooper 1995), and includes the southern half of the Corangamite CMA. It has a different history to the western Otway Basin, as it contains NE-striking, NW-dipping faults instead of the NW-SE faults found in the rest of the basin, and has a different thermal and burial history (Duddy 2003b; Hill et al. 1994; Miller et al. 2002a; Cooper 1995; House et al. 1999).

The initial Late Jurassic to Early Cretaceous phase of the two-stage rifting of the Otway Basin deposited the Otway Group (Figure 3.3; Constantine 2001; Cooper 1995; Duddy 2003a), which consists of the non-marine volcanogenic Casterton Formation, Crayfish Subgroup and Eumeralla Formation (in stratigraphic order) (Duddy 2003b). The sandstone and shale with minor interbedded coal and olivine basalt of the Casterton Formation were deposited in relatively deep lakes, most likely related to initial rifting (Constantine 2001;

Duddy 2003b; Tosolini et al. 2002). Rifting then escalated in the Early Cretaceous, and the Crayfish Subgroup was deposited in a series of rapidly subsiding half-grabens (Duddy 2003b; Jensen-Schmidt et al. 2002; Cooper 1995) as a thick sequence of fluvial quartz-rich sandstones and mudstones derived largely from the erosion of the Palaeozoic basement on the basin margin (Duddy 2003b; Struckmeyer and Felton 1990). The overlying thick succession of volcanogenic sediments of the Eumeralla Formation was deposited across the southern margin of Australia in the Early Cretaceous (Constantine 2001; Duddy 2003b; Jensen-Schmidt et al. 2002). Faulting during the initial stages of Eumeralla Formation deposition suggests continued extension during this time (Jensen-Schmidt et al. 2002; Miller et al. 2002a; Cooper 1995; Bryan et al. 1997).

There was a period of uplift and block faulting during the mid-Cretaceous (around 95 Ma) (Duddy 2003a; Cooper 1995; Lavin 1997), resulting in the inversion of the north-east trending Early Cretaceous grabens (Cooper 1995; Lavin 1997) and the partial inversion of the Otway Ranges (Miller et al. 2002b; Dickinson et al. 2002; Lavin 1997; House et al. 1999; Hill et al. 1997; Douglas 1977), which did not form a significant topographic high during this period.

A renewed phase of extension at the beginning of the Late Cretaceous, coinciding with the onset of Tasman rifting, resulted in the deposition of the Sherbrook Group in marginal and near-shore marine environments west of the Otway Ranges (which had been uplifted in the mid-Cretaceous; Cooper 1995; Lavin 1997); this unit decreases in thickness to the north-east (GSV 1995).

3.2.3 Neogene Geology

3.2.3.1 Palaeocene to Miocene Spreading

A thick sequence of Late Eocene to Miocene marine siliclastic and carbonate sediments was deposited in the Otway Basin during the Neogene due to the progressive spreading of the Southern Ocean. The Otway Basin was exposed to the full force of the Southern Ocean swells for most of this period of time (Holdgate and Gallagher 2003; Cooper 1995). The oldest Neogene unit is the Palaeocene to Middle Eocene siliclastic Wangerrip Group (Holdgate and Gallagher 2003), which disconformably overlies the Late Cretaceous Sherbrook Group in central areas and unconformably overlies the Early Cretaceous Otway Group on the basin margins (GSV 1995; Holdgate and Gallagher 2003). It was deposited during a basin-wide marine transgression, and comprises, in stratigraphic order, the restricted shallow marine Pebble Point Formation, the clastic-dominated deltaic Dilwyn Formation (Miyazaki et al. 1990), and the grey muddy siltstones and lesser sandstones of the Burrungule Member (Holdgate and Gallagher 2003; Boult et al. 2002). In the northeast of the Otway Basin, the marine Wangerrip Group grades laterally into the non-marine Eastern View Formation, which consists of brown coals, claystones and sandstones that were deposited in high-energy braided stream and swamp environments from the Palaeocene to Early Eocene (GSV 1995). The Eastern View Formation outcrops on the northern flank of the Otway Ranges and near Anglesea (Figure 3.3), where it is up to 500m thick and is folded into the Anglesea Syncline and partially exposed and dissected by the tributaries of the Anglesea River. Like the Wangerrip Group along the basin margins, the Eastern View Formation unconformably overlies the Otway Group (Holdgate and Gallagher 2003).

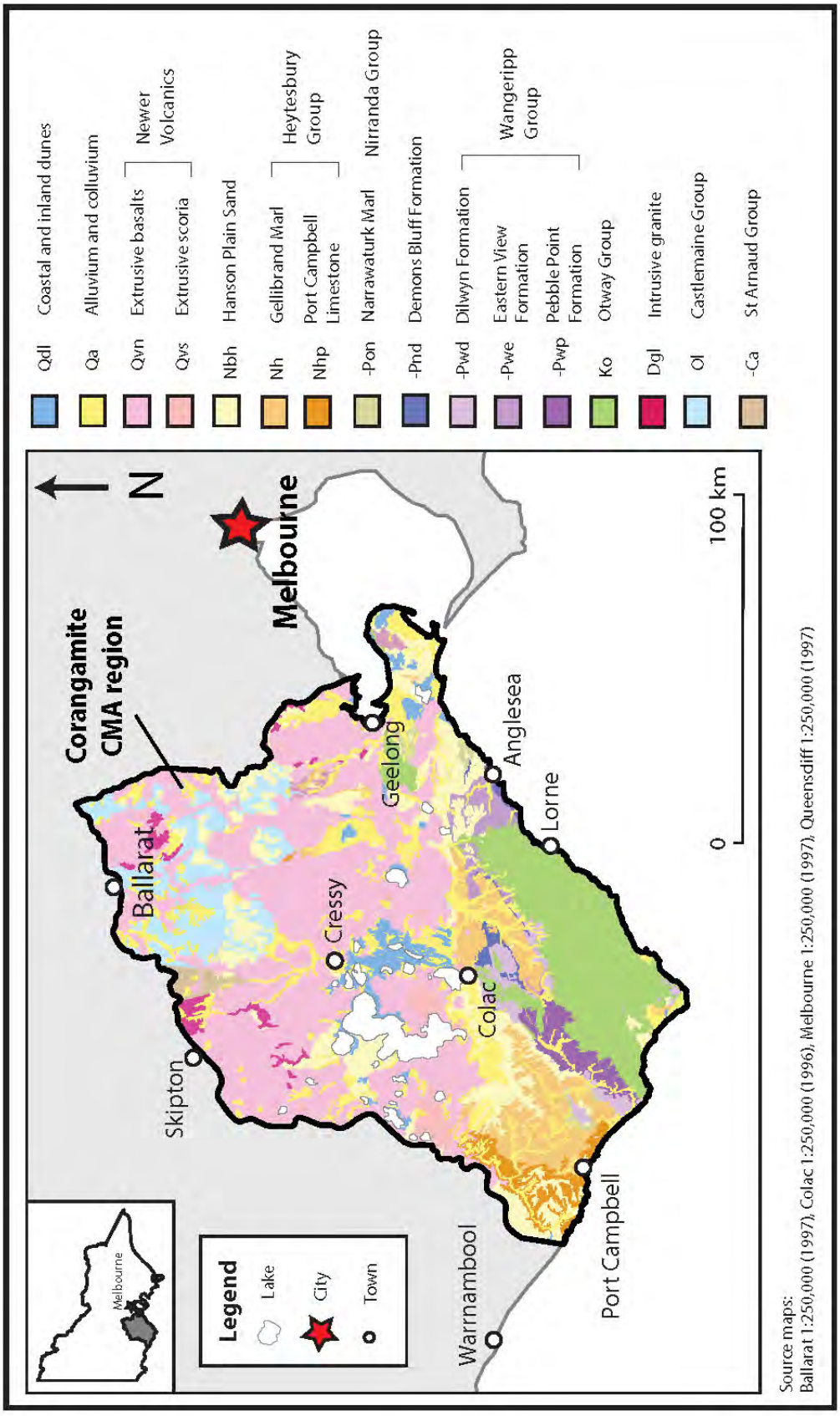

Figure 3.3 Geological map of Corangamite region

The Wangerrip Group is succeeded by the Late Palaeogene to Early-Middle Neogene dominantly open marine carbonate sediments of the Nirranda and Heytesbury Groups (Miyazaki et al. 1990; Holdgate and Gallagher 2003; Jensen-Schmidt et al. 2002). The Late Eocene to Early Oligocene Nirranda Group consists of the mixed carbonate and clastic Mepunga Formation and overlying Narrawaturk Marl (Holdgate and Gallagher 2003; Boult et al. 2002), which was deposited in low energy, mainly outer shelf conditions with terrigenous input from low energy rivers to the north (Holdgate and Gallagher 2000). To the northeast, the Nirranda Group grades laterally into the Late Eocene Demons Bluff Formation, which consists of dark brown, carbonaceous, pyritic silt to fine sand, clay and clayey sand. The Nirranda Group is disconformably overlain by the Late Oligocene to Late Miocene Heytesbury Group, consisting, in stratigraphic order, of the basal clastic carbonate Clifton Formation, the Gellibrand Marl and the Port Campbell Limestone (Holdgate and Gallagher 2003; Boult et al. 2002; Holdgate and Gallagher 2000). The basal Clifton Formation was deposited in relatively shallow water, the overlying Gellibrand Marl in deeper water and the Port Campbell Limestone in a moderately deep, middle shelf environment (Holdgate and Gallagher 2000; Nicolaides 1995).

3.2.3.2 Miocene-Pliocene Unconformity

A major break in sedimentation occurred at roughly the Miocene-Pliocene boundary, separating the Oligocene-Miocene cool-water carbonates from the Miocene-Pliocene mixed clastic-carbonate successions. This unconformity is present across all of the south-east Australian basins, including the Otway Basin (Dickinson et al. 2002; Wallace et al. 2005b). The underlying Miocene units have been deformed by gentle folding and reverse faulting, uplifted and then eroded as the result of a significant regional uplift event

corresponding to a change in plate dynamics (Dickinson et al. 2002; Wallace et al. 2005b; Singleton et al. 1976). This uplift is believed to have been largely responsible for the present topographic relief of the Otway Ranges (Dickinson et al. 2002).

3.2.3.3 Pliocene-Pleistocene Succession

The Miocene-Pliocene unconformity was followed by a marine transgression that resulted in the deposition of strandline successions (Wallace et al. 2005b; Sandiford 2003) and is characterised by a change in sedimentation to mixed clastic-carbonate facies overlain by basalt flows. The sediments range in age from very late Miocene to Pleistocene (Dickinson et al. 2002; Holdgate and Gallagher 2003). The basal quartz-rich shallow marine Whalers Bluff Formation overlies a buried karst surface formed on top of the Port Campbell Limestone (Holdgate and Gallagher 2003; Dickinson et al. 2002), and is comprised of outcrops of fossiliferous clays, oyster beds and sandy limestones (Holdgate and Gallagher 2003).

The Dorodong Sands, Grange Burn Formation, Moorabool Viaduct Formation and Hanson Plain Sand units represent a Late Neogene regressive barrier-sand sequence across the eastern Otway Basin from Hamilton to the Geelong region. The deposits range from offshore marine marls, near shore calcareous quartz sands and silts to alluvial sands and gravels (Sandiford 2003; Wallace et al. 2005b). Due to the overlying basalt which has obscured most of the strandline detail, the succession has been broken up into units from west to east according to the outcrop geology, but can be seen using detailed aeromagnetic data (Wallace et al. 2005b; Dickinson et al. 2002; Holdgate and Gallagher 2003; Sandiford 2003).

Basalt eruptions of the Newer Volcanics began in the Pliocene and ended in the Late Pleistocene (the last eruptions were about 30 ka), with extensive lava flows and pyroclastic scoria cones, maars and lava shields throughout western Victoria (Cupper et al. 2003), almost entirely covering the Late Miocene to Early Pliocene strandline sequence (Wallace et al. 2005b). Within the lava plain, individual basalt flows are hard to map, with older sequences being deeply weathered and intensively farmed (Price et al. 1997).

3.2.3.4 Quaternary sediments

Throughout the Otway Basin, Quaternary sediments form a thin veneer over the underlying units, particularly across the south-western coastal plains. The Bridgewater Group formed in shallow tidal, dune and lagoon environments during sea-level fluctuations in the Pleistocene associated with the global glaciations (Kenley 1971; Cupper et al. 2003; Kenley 1988; Orth 1988). It consists of a series of WNW-NW-trending dune and shoreline aeolianites, generally as single, continuous fore- or backshore dunes, but complex dune systems can been seen in some areas (Kenley 1971; Cupper et al. 2003; Kenley 1988).

Overlying the Bridgewater Formation in Victoria are the siliceous Pleistocene to Holocene Mallanganee Sands and the most recent volcanics, such as the Tower Hill Volcanics in the Warrnambool area (Kenley 1971; Tickell et al. 1992; Orth 1988; Cupper et al. 2003). The Mallanganee Sands are fine-grained, unconsolidated and grey to white, and most commonly form low, discontinuous sand ridges up to 5 m high parallel to the fixed dunes of the Bridgewater Group, and probably formed during a period of more arid conditions (Kenley 1988; Cupper et al. 2003).

Alluvial and swamp sediments were also deposited between dunes and along the rivers and floodplains, and low terraces developed along the Barwon River and its tributaries (Cupper et al. 2003). The Newer Volcanics have altered and dammed rivers, causing deposition of lake sediments (Cupper et al. 2003). The coastal areas have prominent headlands and active Holocene beach deposits and dune systems. The coastal carbonate dunes show karst development, and caves are present within many dune ridges of Quaternary age (Tickell et al. 1992; Cupper et al. 2003; White 1994).

3.3 Hydrogeology

Based on the model put forward by the National Land and Water Resources Audit, seventeen groundwater flow systems have been delineated in the Corangamite CMA at local, intermediate and regional scales. Water from these aquifers is pumped for irrigation, stock and domestic purposes (Dahlhaus 2002; Dahlhaus et al. 2008; Clarkson et al. 2007). The boundaries of the flow systems are based on the geological units, and have been grouped according to their hydrogeological characteristics (Dahlhaus et al. 2008). Two of these flow systems, the Basalt Plains and Otway Ranges, are relevant to this study.

3.3.1 Basalt Plains Flow System

The central part of the Corangamite CMA consists of a substantial regional groundwater flow system, the Basalt Plains. The basalts and scoria of the Newer Volcanics (section 3.2.3.3) form a fractured aquifer overlain by clay soil of variable thickness. Due to the fractures, the groundwater flows through the system at highly variable rates at both a regional and intermediate scale, and is recharged rapidly by rainfall via the scoria cones (Barton et al. 2007; Dahlhaus 2002; Bennetts et al. 2003; Raiber et al. 2009). The Basalt

Plains groundwater system is interconnected with the lakes, streams, depressions and swamps across the Basalt Plains, including saline groundwater discharge (CCMA 2003; Dahlhaus et al. 2003; De Deckker 2003; Williams 1995). Natural springs and discharge at the boundaries of lava flows often feed lakes and wetlands or contribute baseflow to adjacent streams (Barton et al. 2007; Dahlhaus 2002).

A thin veneer of gravels, sands, silts and clays were deposited over the basalts as a result of the marine regression in the Pliocene (section 3.2.3.3), and the associated flow system has a broad geographical and morphological range. Generally, the groundwater flows slowly through the partially exposed sand sheets at an intermediate scale, but local flow systems can also occur where the sand forms isolated caps on dissected ridges. Quaternary deposits of alluvium, as well as swamp and lake deposits and lunettes, are also widespread over the area, and contribute to local flow systems that develop at shallow depths below the ground surface. These deposits are recognised to be a primary source of salinisation (Barton et al. 2007; Dahlhaus 2002).

3.3.2 The Otway Ranges Flow System

The non-marine Early Cretaceous volcanogenic sedimentary sequence of the Otway Ranges contains groundwater in both intermediate and local flow systems. Groundwater flows through the fractured rocks and is recharged by the high rainfall of the area (section 3.5), with water quality being generally high. Groundwater from the flow system is also known to discharge into streams and rivers, including the Gellibrand and Barwon Rivers. While the Otway Ranges Flow System contributes water to farm and urban supplies, groundwater from the Otway foothills is a more significant source, particularly for Geelong,

and is sourced from the regional Dilwyn Flow System. The Dilwyn Flow System comprises both the Dilwyn Formation and the Eastern View Formation, which are exposed along the northern flanks and at the north-eastern end of the Otway Ranges, respectively. At depth, the flow system is confined, but has a potentiometric surface close to the land surface, which influences the overlying Gerangamete Marl Local Flow System. The major geological unit of the Gerangamete Marl Flow System is the Gellibrand Marl, with the Demons Bluff Formation and Narrawaturk Marl as minor components. These aquifers are shallow, with slow groundwater flow through the local flow systems (Barton et al. 2007; Dahlhaus 2002).

3.4 Geomorphology and Surface Drainage

Geomorphologically, the Corangamite CMA consists of highlands to the north (the Western Uplands) and south (the Southern Uplands), with a broad, flat plain (the Western Plains) in between (Figure 3.4b; Dahlhaus et al. 2006b; Hills 1975; Joyce et al. 2003b). Like the rest of Victoria, the main geomorphological divisions of the region have been directly influenced by tectonics and then further by geological structure, lithologies and the effects of past climate (Joyce et al. 2003b). These factors have also affected the surface drainage of the area (Figure 3.4a; CCMA 2003). There are approximately 19,600 km of waterways in the Corangamite CMA, and the Barwon, Moorabool, Yarrowee–Leigh, Gellibrand and Curdies Rivers are the major systems. Three important Water Supply Protection Areas (WSPA) are also located in the CMA and supply domestic and farm water to areas within and adjacent to the region (van Gameren 1997a; DSE 2011; DSE 2008; Clarkson et al. 2007).

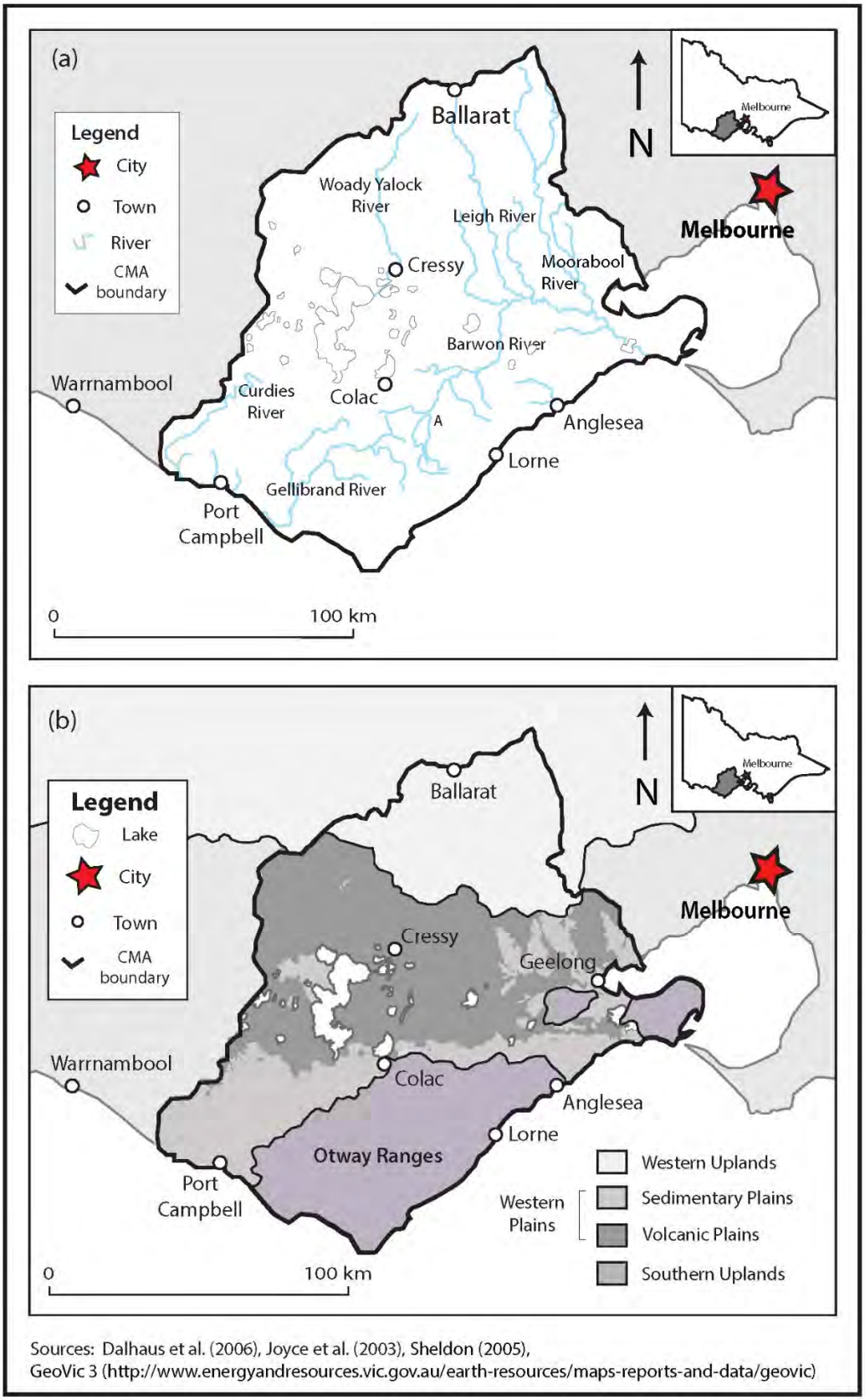

Figure 3.4a and b Study area major rivers and geomorphological regions

3.4.1 The Western Uplands

The Western Uplands to the north of the Corangamite CMA (Figure 3.4b) are part of the Victorian Highlands, a central upland axis that extends across central Victoria from east to west. The uplands extend from Kilmore Gap, north of Melbourne, to the western edge of the Dundas Tablelands (Joyce et al. 2003b; Hills 1975; Robinson et al. 2003). They are highly dissected, with rock type and structure acting as the major controls on landform (Hills 1975; Joyce et al. 2003b). The uplands also act as a hydrological divide, with rivers draining north towards the Murray River and south towards the ocean (Joyce et al. 2003b; Hills 1975; Rowan et al. 2000). The uplands do not exceed 1220 m in elevation (Hills 1975) and are characterised by undulating hills and broad valleys (Dahlhaus et al. 2006b; Dahlhaus et al. 2003) with variable, often deep, regolith, which has been produced by extended subaerial exposure and weathering of the sedimentary rocks and granite plutons (Dahlhaus et al. 2003; Joyce et al. 2003b). Alluvial deposition along valleys and on the nearby plains occurred due to the stripping of regolith by streams (Joyce et al. 2003b), which were displaced or dammed by the Newer Volcanics (section 3.2.3.3). This in turn influenced the subsequent lateral stream development (Joyce et al. 2003b; Dahlhaus et al. 2006b).

The Western Uplands are further divided into three major subregions: Dissected Uplands, the Grampians and the Tablelands (Dahlhaus et al. 2003; Joyce et al. 2003b; Dahlhaus et al. 2006b); however, only the Dissected Uplands are represented within the Corangamite region (Robinson et al. 2003).

3.4.1.1 The Dissected Uplands

The Dissected Uplands are a broad region of ridges, plateaus and hills that extend northwards from Ballarat and Gisborne to Bendigo and St Arnaud. The dominant features of the landscape are the subdued north-south trending ranges and the intervening undulating topography (Joyce et al. 2003b; Rowan et al. 2000). These landforms were preserved by substantial uplift during the Palaeogene and late Neogene (Joyce et al. 2003b; Rowan et al. 2000; Dahlhaus et al. 2003). The major ridges of the Dissected Uplands have deeply weathered slopes. Dendritic drainage patterns dissect the ridges, forming upper catchments for several of the larger river systems including the Moorabool River (Figure 3.4a), and combined with the steep angle of the slopes, have mantled the bedrock with deposits of colluvium and alluvium (Joyce et al. 2003b; Robinson et al. 2003). The southern extent of the Dissected Uplands, which falls within the Corangamite region (Figure 3.4b), and has been covered by basalt flows from the Newer Volcanics (Joyce et al. 2003b; Robinson et al. 2003).

3.4.2 The Western Plains

The Western Plains is the largest of the three geomorphological areas within the Corangamite CMA (Figure 3.4b) and comprises a large volcanic plain (known geomorphologically as the Western District Volcanic Plains) and a generally flat coastal plain (the Sedimentary Plains) to the south-west (Joyce et al. 2003b; Robinson et al. 2003).

3.4.2.1 The Volcanic Plains

The Volcanic Plains form an extensive region with an elevation generally less than 200 m AHD (Rowan et al. 2000; van Gameren 1997a; Joyce et al. 2003b). The landscape of the

plains was formed by the overlapping basalt flows, with the basalt thickness varying due to both the underlying topography and present-day surface (Robinson et al. 2003). The older basalt flows in the western region of the plains have undergone considerable weathering, with the younger flows occurring more towards the central area (Joyce et al. 2003a; Hills 1975; Robinson et al. 2003). The basalt flows are interspersed with intermittent pyroclastic deposits, while the scoria cones and stony rises form the youngest features of the landscape (Joyce et al. 2003b; Robinson et al. 2003; Dahlhaus et al. 2006b).

The surface drainage across the Basalt Plains is discontinuous and sparsely distributed (Figure 3.4a), especially compared to adjacent areas, leading to the formation of numerous lakes and swamps (Robinson et al. 2003; Rowan et al. 2000; Joyce et al. 2003b). On the volcanic plains annual evaporation exceeds rainfall, and climate has been shown to have a dominant effect on both water quality and level within most lakes and swamps (Yihdego and Webb 2013). The water quality of the lakes varies from brackish to extremely saline, depending to a large extent on the storage volume, and whether or not the lakes are connected to groundwater. The lakes can also be subject to flooding during periods of excess and sustained rainfall. Surface runoff and rainfall therefore contribute the major proportion of inflows to these lakes and swamps, however groundwater seepage can supplement the inflow. Most of the lakes and swamps on the Volcanic Plains formed in maars, depressions or from blocked drainage, and include Lake Corangamite, Lake Colac, Lake Bolac, Lake Weering, Lake Gnarpurt, Lake Coragulac, Lake Bullenmerri, Lake Purrumbete and Lough Calvert (Dahlhaus et al. 2003; Fraser 1957; Bennetts et al. 2003).

In the centre of the Corangamite CMA, a shallow basin has formed due to the uplift of the Otway Ranges and the disruption of drainage by the basalt eruptions (Robinson et al. 2003).

The volcanic eruptions blocked and diverted river courses such as the Barwon and Curdies Rivers, as the fluid basalt flowed towards the lowest points in the landscape and filled stream valleys (Joyce et al. 2003b; Robinson et al. 2003). Most of the streams and rivers within the Volcanic Plains have irregular stream flow and variable water quality. They have headwaters in the Western or Southern Uplands (Figure 3.4b), and therefore generally large catchments, but runoff is low due to the high evaporation (section 3.5). Riparian zone clearing has also had a large impact on the health of the river systems, with 51% of waterways within the Corangamite CMA rated as having moderate to poor health (Dahlhaus et al. 2003; Fraser 1957).

3.4.2.2 The Sedimentary Plains

Neogene and Quaternary marine and non-marine sediments in the south-west of the Corangamite CMA form the Sedimentary Plains (Figure 3.4b), and these sediments also appear as windows within the volcanic plains where they are not covered by basalt flows (Joyce et al. 2003b; Dahlhaus et al. 2006b; Robinson et al. 2003; Hills 1975).

3.4.3 The Southern Uplands

Across southern Victoria are several isolated, highly dissected and structurally-controlled upthrown blocks that form the Southern Uplands (Figure 3.4b; Hills 1975; Joyce et al. 2003b). Of the five geomorphic units that comprise the Southern Uplands (Rowan et al. 2000), only three are represented within the Corangamite region: the Otway Ranges, the Barrabool Hills and the Bellarine Peninsula (Robinson et al. 2003).

3.4.3.1 Otway Ranges

The Otway Ranges are a northeast-trending inverted rift sequence and consist almost completely of uplifted Lower Cretaceous sediments (Douglas 1977; Gunn 1975; Spencer-Jones et al. 1971; Tickell et al. 1992). The ranges are deeply dissected, and the fault-bounded, structurally-controlled block rises steeply from beneath the surrounding Neogene sediments. The ranges form a topographic high that separates the Otway and Port Phillip Basins and the Torquay Embayment (Figure 3.2b; Dahlhaus et al. 2006b; Dickinson et al. 2002; Douglas 1977; Gunn 1975; Spencer-Jones et al. 1971). Maximum elevation of the ranges is 670 m AHD, with the main part of the range having an average elevation of 500 m AHD (Sandiford 2003; Gunn 1975; Douglas 1977).

The Otway Ranges form the topographically highest geomorphological unit of the Southern Uplands within the Corangamite CMA. The ranges dominate the south-western margin of the CMA and are bounded by two reverse faults – the westerly dipping Torquay Fault and the easterly dipping Bambra Fault (Joyce et al. 2003b; Robinson et al. 2003). The crest of the ranges has a moderate relief, reflecting the initial flat top of the block prior to uplift, with rounded hill slopes and broad open valleys. This moderately dissected drainage divide trends north-east, paralleling the coast in the eastern Otway Ranges (Joyce et al. 2003b; Robinson et al. 2003).

On both sides of the drainage divide, a rugged, deeply dissected topography with steep valleys and interlocking spurs has developed and is strongly controlled by the geological structure (Joyce et al. 2003b; Robinson et al. 2003; Hills 1975). The dendritic drainage runs south-east and north-west where the ranges are parallel to the south-east coast, but flows north and south to the west of Mount Sabine (Robinson et al. 2003). The headwaters of

the Barwon and Gellibrand Rivers are located on the northern slope of the Otway Ranges, whereas the other major rivers within the Otways, the Gellibrand, Aire, Anglesea and Curdies Rivers, drain towards the coast (Figure 3.4a; CPA 1971; DSE 2011; Fraser 1957; van Gameren 1997a). The stream profiles are often steep and stepped over the prominent scarps of the more resistant beds of sandstone (Joyce et al. 2003b; Robinson et al. 2003; Douglas 1977). There are many permanent lakes and wetlands within the Otway Ranges due to the relatively high rainfall and low temperatures and evaporation (section 3.5). The Otway Ranges also contain several large, permanent water storages, such as the West Gellibrand Dam and the West Barwon Reservoir (Sheldon 2005).

The foothills on the flanks of the Otway Ranges are less dissected and generally form gently undulating and rounded hills, although some have broader planar crests. The low elevation hills are less defined to the east (south of the Barrabool Hills) and are transitional to the floodplains of the Barwon and Gellibrand rivers (Joyce et al. 2003b; Robinson et al. 2003; Hills 1975). Thick colluvium and landslide debris are common on many of the foothill slopes, particularly at the bases of the steep slopes on the south-eastern flanks of the ranges. Fluctuations in sea level over the last million years, combined with the uplift of the Otway Ranges, has also led to rapid erosion and numerous landslides (Joyce et al. 2003b; Robinson et al. 2003), along with deposition of alluvial fans on the surrounding plains, particularly to the north and west (Hills 1975).

3.4.3.2 The Barrabool Hills – Bellarine Peninsula

Like the Otway Ranges, the Barrabool Hills and Bellarine Peninsula represent uplifted, fault controlled blocks, but are at a lower elevation than the ranges and are less dissected

(Dahlhaus et al. 2006b; Joyce et al. 2003b). The Barrabool Hills have a maximum elevation of 200 m AHD, and consist of rounded hills separated by broad valleys drained by tributaries to the Barwon River and Waurn Ponds Creek (Joyce et al. 2003b; Robinson et al. 2003). In comparison, the Bellarine Peninsula is only weakly dissected and has an elevation of less than 150 m AHD. It consists of low hills with broad crests and gentle convex slopes. The drainage forms a radial pattern, with short, incised streams draining towards Corio Bay and longer, weakly incised valleys draining to Swan Bay. The southern margin of the Bellarine Peninsula is covered by fluvial and tidal wetlands of the Moolap lowland, including Lake Connewarre (Robinson et al. 2003; Rosengren 2009).

3.5 Climate

The Corangamite CMA has a temperate climate that is typically characterised by hot, dry summers and cool, wet winters (Figure 3.5; van Gameren 1997b). Seasonally, the temperatures within the region are highest during the summer (January and February) and lowest in July. At Ballarat and Colac, the February mean daily maximum and minimum temperatures are 25-26°C and 11°C respectively, compared to 10-12°C and 3-4°C in July (data sourced from the Bureau of Meteorology, Australia).

Annual rainfall is highly variable across the area, from approximately 600 mm on the Basalt Plains to up to 900 mm closer to the Otway Ranges (Table 3.1; Figure 3.5). Rainfall is highest between June and September, with around 40% of annual rainfall occurring during this period. Mean monthly evaporation is exceeded by rainfall from May to September, with the highest potential evaporation occurring in January and February, when temperatures are highest (data from the Bureau of Meteorology, Australia).

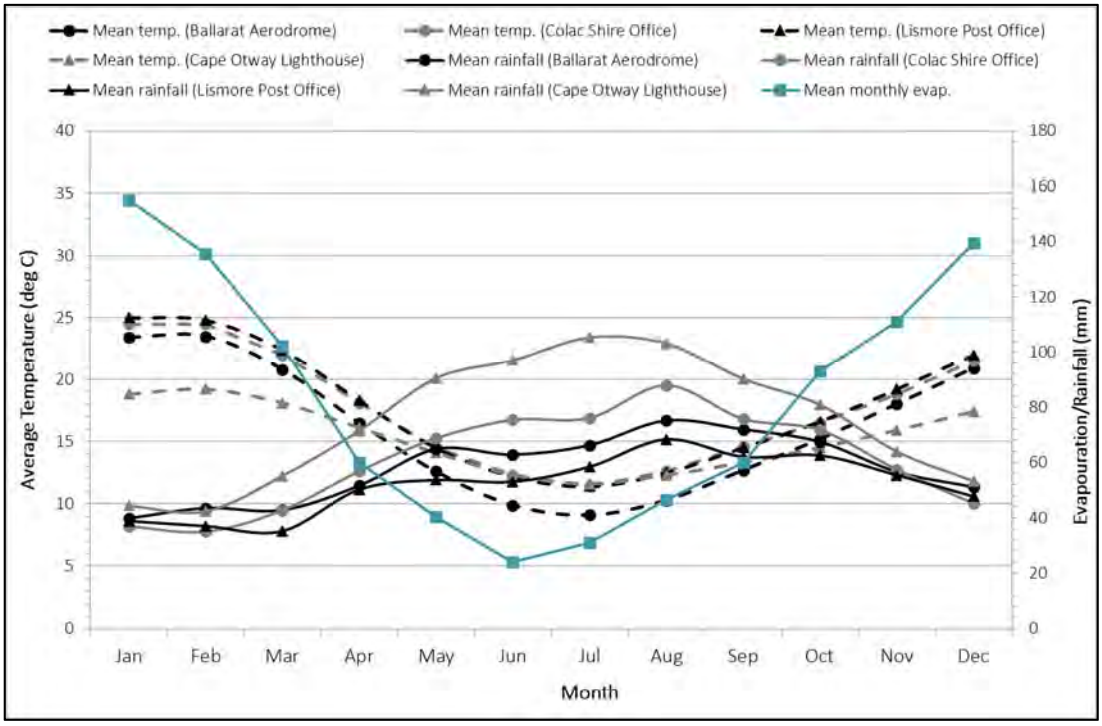

Figure 3.5 Average seasonal variation for Ballarat, Colac, Lismore and the Cape Otway Lighthouse

(Rainfall and evap. given as mean monthly values and temperatures as mean daily 3pm temperatures)

Table 3.1 Rainfall data summary for the Corangamite region (data from the Bureau of Meteorology, Australia)

Station Name	Latitude	Longitude	Elevation (m)	Measurement period	Average annual rainfall (mm)
Ballarat Aerodrome	37.51 S	143.79 E	435	1908-current	694.1
Colac Shire Office	38.34 S	143.58 E	134	1899-current	726.6
Aireys Inlet	38.46 S	144.09 E	95	1990-current	624.4
Lismore Post Office	37.95 S	143.34 E	178	1919-current	622.0
Cape Otway Lighthouse	38.86 S	143.51 E	82	1861-current	898.6

The Otway Ranges are a distinct topographic feature of the area and have a marked influence on local climate, forming one of the wettest areas in Victoria (Dwyer 1957; van Gameren 1997b). Average rainfall varies between 650-900 mm annually (Table 3.1; Figure 3.5), with some years exceeding 1200 mm. The ranges also have relatively low average temperatures, with higher altitudes averaging around 20˚C in temperature as a maximum (data from Bureau of Meteorology, Australia).

3.6 Land Use and Vegetation

3.6.1 Current Land Use

Within the Corangamite CMA, current land use is dominated by agriculture (> 60% of the CMA; Table 3.2), principally broadacre grazing for wool, sheep meat and beef, and dairy farming. Dairy farming is centred in the south-west of the region and in the Colac area, where soils are fertile and rainfall is relatively high, and contributes about 25% of Victoria's production by milk volume. The associated pasture production is predominantly dryland instead of irrigated, so milk production is seasonal (CCMA 2013b; CCMA 2013a; Clarkson et al. 2007).

Broadacre cropping of wheat, canola and barley, and horticulture production (dominated by potatoes) occurs mostly on the Basalt Plains. Plantation forestry (approximately 12% of land use) of both hardwood (blue gum) and softwood (pine) timbers occurs predominantly in the coastal fringes of the Otway Ranges (CCMA 2013b; CCMA 2013a; Dahlhaus et al. 2003). Less than 25% of the original native vegetation within the Corangamite CMA remains intact, mostly within National Parks and reserves, although some remnant vegetation also occurs on private land (Pope 2006; Parks Victoria 2002; CCMA 2005;

Clarkson et al. 2007). Only 3.5% of native vegetation still covers the Basalt Plains, while the Otway Ranges retains 81.6% of its native vegetation cover. Native grasslands and grassy woodlands have been reduced to an estimated 1% of their former extent across the Corangamite CMA (CCMA 2005).

Table 3.2 Land use within the Corangamite CMA (data sourced from Clarkson et al. 2007)

Land Use	Area (ha)	% of the CMA
Urban and peri-urban	48,000	3.60
Public Land	156,000	11.69
Forestry	164,000	12.29
Broadacre Grazing	592,000	44.38
Dairy Farming	167,400	12.55
Broadacre Cropping	94,000	7.05
Horticulture	5,000	0.37
Animal production (pigs and chickens)	645	0.05
Total Agriculture	**859,045**	**64.40**

3.6.2 Land Use Change

The Corangamite CMA has been inhabited for thousands of years, with indigenous people from the Wathaurong traditional language group, as well as smaller language groups such as the Gadubanud, Gulidjan/Kirrae Wurrung and the Djargurd Wurrung, occupying the region (CCMA 2003; CCMA 2005). These tribes used deliberate and controlled burning, sometimes several times a decade, to promote fresh vegetation growth and maintain open grassy woodlands and forest margins. This encouraged a continued supply of grazing

animals for hunting. Fire also occurred naturally within the landscape as a result of lightning strikes, and volcanic activity within the Basalt Plains is also likely to have burnt large areas of native vegetation (CCMA 2005; Lunt 1998).

After the arrival of Europeans, the Corangamite CMA was among the first regions settled within Victoria. Sealers operated along the coast from about 1800, with whaling active in the Apollo Bay area from the 1820s to 1840s (Parks Victoria 2009). Early settlers began arriving in the Port Phillip region in 1835, with the Basalt Plains being settled in the late 1830s and 1840s (CCMA 2005; Dahlhaus et al. 2003). The treeless Volcanic Plains were well suited to sheep and later cattle grazing, with the open woodlands and thick native grassland attracting settlers, who rapidly moved inland from Geelong and Portland (CCMA 2003; Lunt 1998). Introduction of hard-hoofed stock caused soil compaction within a few years of the settlers' arrival, and the intensification of grazing pressure changed the composition of the native grassland, with the more palatable grasses replaced by tough, unpalatable species. The decline of native vegetation was increased by the introduction of weeds, with gorse, boxthorn and hawthorn introduced to provide hedgerows, and cypresses and pines widely planted for stock shelter (CCMA 2005).

In the 1850s, the discovery of gold led to a massive population increase in the northern parts of the CMA, including Ballarat and the Central Highlands. As a result, large areas of forest were cleared for mine timbers, housing and firewood, as well as to provide increased agricultural production for the growing population. Riparian vegetation was also removed, leading to severe degradation of stream environments on the Basalt Plains. By the end of the 1800s, most of the original forests in the Central Highlands were either cleared or

heavily disturbed, with native flora and fauna directly impacted by the expanding settlement.

Unlike the Central Highlands, the Otway Ranges escaped broad scale clearing due to the unsuitability of the terrain for agriculture and the absence of economic mineral deposits. From the 1870s, the Colonial Government promoted settlement in the Otways, but many farms failed and the land that was cleared for farming was mostly abandoned and subsequently reclaimed by the Government, before being reforested or allowed to naturally regenerate to native forest (CCMA 2003; CCMA 2005; Parks Victoria 2009). However, from the beginning of the 20th century, settlers began clearing the Otway foothills for agriculture and dairy (farming and cropping), as well as to support timber mills supplying the house building industry in Melbourne and Geelong. The mills led to the establishment an extensive network of tram tracks for the transportation of the timber, so that the majority of the Otway Ranges was subject to timber harvesting over the last 100 years, with the area becoming one of Victoria's most productive forest regions (CCMA 2003; CCMA 2005; Parks Victoria 2009).

3.6.3 Native Vegetation

Vegetation is strongly influenced by soil and patterns of rainfall, with five bioregions occurring across the Corangamite CMA: the Central Victorian Uplands, the Otway Plain, the Otway Ranges, the Victorian Volcanic Plain, and the Warrnambool Plain (CCMA 2003; Clarkson et al. 2007). Due to the high rainfall, the Otway Ranges support dense, temperate rainforest, dominated by Myrtle Beech (*Nothofagus cunninghamii*) and Blackwood (*Acacia melanoxylon*) with an understorey of tree and ground ferns, and wet sclerophyll forest,

which grows on fertile, well-drained loamy soils and is dominated by eucalypts, particularly Mountain Ash (*Eucalyptus regnans*) (CCMA 2003; DSE 2005e; CCMA 2005). Although now mostly cleared, the foothills of the Otway Ranges were covered by shrubby lowland forests dominated by Messmate Stringybark (*Eucalyptus obliqua*), Narrow-leaf Peppermint (*Eucalyptus radiata s.l.*) and Brown Stringybark (*Eucalyptus baxteri s.l.*) (CCMA 2003; DSE 2005f; DSE 2005d). To the east and west of the Otway Ranges, heathy woodland spans a variety of underlying geology, but is generally associated with nutrient-poor soils. The heathy woodlands are also dominated by Messmate Stringybark (*Eucalyptus obliqua*) and Brown Stringybark (*Eucalyptus baxteri s.l.*), but lack a secondary tree layer and support a diverse array of shrubs, such as the Prickly Tea-Tree (*Leptospermum continentale*), the Heath Tea-Tree (*Leptospermum myrsinoides*) and various sedges (DSE 2005f; DSE 2005d).

Prior to clearing, the Basalt Plains were covered by grassy, open woodlands growing on the fertile soils, which are prone to seasonal waterlogging (CCMA 2003; CCMA 2005). Trees were either 15 m tall eucalypts (such as the Narrow-leaf Peppermint), or 10 m Sheoaks (*Allocasuarina verticillata*). Areas with over 500 mm rainfall were dominated by Kangaroo Grass (*Themeda triandra*), Common Wallaby-Grass (*Austrodanthonia caespitosa*), Common Wheat-grass (*Elymus scaber var. scaber*), and Common Bog-sedge (*Schoenus apogon*), whereas areas of lower annual rainfall (< 500 mm) were dominated by Rough Spear-grass (*Austrostipa scabra*), Knotty Spear-grass (*Austrostipa nodosa*), and Brown-back Wallaby-grass (*Austrodanthonia duttoniana*).

The higher rainfall, higher elevation Central Highlands to the north of the CMA were mostly covered by open woodland and dry forests (CCMA 2003; CCMA 2005). The woodlands are dominated by Manna Gum (*Eucalyptus viminalis*) and Swamp Gum (*Eucalyptus ovate*), with

an understory of a few sparse shrubs over a species-rich grassy and herbaceous ground layer. In contrast, the dry forests consist of low to medium height (up to 20 m) Red Stringybark (*Eucalyptus macrorhyncha*) and Messmate Stringbark (*Eucalyptus obliqua*), with a secondary tree layer of *Acacia* species, and a ground layer comprising a high diversity of drought-tolerant grasses and herbs, often including a suite of fern species (DSE 2005c).

3.6.4 Wetlands

Within the Corangamite CMA, there are approximately 1,500 widely distributed wetlands of varying sizes, covering approximately 643 km^2 (Clarkson et al. 2007), including coastal swamps, shallow seasonal meadows and marshes, stony-rise lowlands and large, permanent saline lakes. Freshwater meadows are common in the central west of the region, while saline wetlands are found across the Basalt Plains (Sheldon 2005). Significant wetland loss has occurred since European settlement, largely a result of drainage of wetlands for agriculture (Sheldon 2005).

Within the volcanic and sedimentary plains of the Corangamite CMA, freshwater wetlands are primarily grassy to sedgy-herbaceous, sometimes with scattered or fringing eucalypts or lignum shrubs. The open grassland, mostly between 0.5 to 1.0 m in height, and overlie heavy, grey-black soils (Sheldon 2005), and is dominated by grasses, such as Australian Sweet-grass (*Glyceria australis*), Brown-back Wallaby-grass (*Austrodanthonia duttoniana*), or Common Tussock-grass (*Poa labillardieri*), with sedges and herbs, such as Common Spike-rush (*Eleocharis acuta*), Joint-leaf Rush (*Juncus holoschoenus*), Prickfoot (*Eryngium vesiculosum*), and Poison Lobelia (*Lobelia pratioides*) also present. These wetlands are

often ephemeral, so the vegetation ranges between aquatic species and those tolerant of intermediate to seasonal inundation.

Across the Basalt Plains are many saline permanent to semi-permanent lakes, usually supporting aquatic herbs dominated by Hooded Water Milfoil (*Myriophyllum muelleri*), Watermats (*Lepilaena* spp.) and Seatassels (*Ruppia* spp.). The lakes are generally bordered by River Red Gum (*Eucalyptus camaldulensis*), and saltmarsh vegetation, dominated by either Spreading Saltmarshgrass (*Puccinellia stricta* var. *perlaxa*) or Samphire (*Sarcocornia quinqueflora*) (Sheldon 2005).

Tea-tree swamps are also present across the volcanic and sedimentary plains and in areas of higher elevation (such as the Otways), and are usually dominated by Woolly Tea-Tree (*Leptospermum lanigerum*), with associated vegetation consisting of Scented Paperbark (*Melaleuca squarrosa*), Tall Saw-sedge (*Gahnia clarkeii*), Blackwood (*Acacia melanoxylon*) and sedges (DSE 2005b; Department of Natural Resources and Environment 2000; Sheldon 2005). These wetlands usually occur in high rainfall areas with more sustained waterlogging and can be associated with silty peat soils (Sheldon 2005).

Chapter 4

Basalt Plains

As discussed in Chapter 3, a significant number of wetlands within the Corangamite CMA occur across the Basalt Plains (Sheldon 2005; Harding and Callister 2005). These lakes and wetlands have formed in volcanic craters and depressions, and where drainage patterns have been disrupted by lava flows. The variation in lake hydrology, as well as the type of basalt substrate and catchment to surface area ratios, mean that the lakes and wetlands have a wide range of salinities, and the Basalt Plains contain one of the most extensive areas of inland salt lakes in the world (Sheldon 2005; Hose et al. 2008).

4.1 Sample Area

Four sites on the Basalt Plains were selected for investigation, all within the Warrion Water Supply Protection Area (WSPA) (Figure 4.1). The Warrion WSPA is located north of Colac, and covers an area of 395 km^2. Under the *Water Act 1989*, the area was declared a WSPA in 2000 to protect the groundwater and surface water resources through the development of a management plan. The area is managed by Southern Rural Water (SRW) (SRW 2010). The main aquifer of the WSPA is the fractured basalt (generally less than 30 m thick) and scoria from the eruptions centred at Warrion Hill, Red Rock and Robertsons Hill (Figure 4.1), forming part of the Basalt Plains Groundwater Flow System (Chapter 3; SRW 2010; Dahlhaus 2002). This is underlain by the Pliocene Sands Flow System, which may be hydraulically connected to the basalts (SRW 2010; Thomas 1957; Dahlhaus 2002).

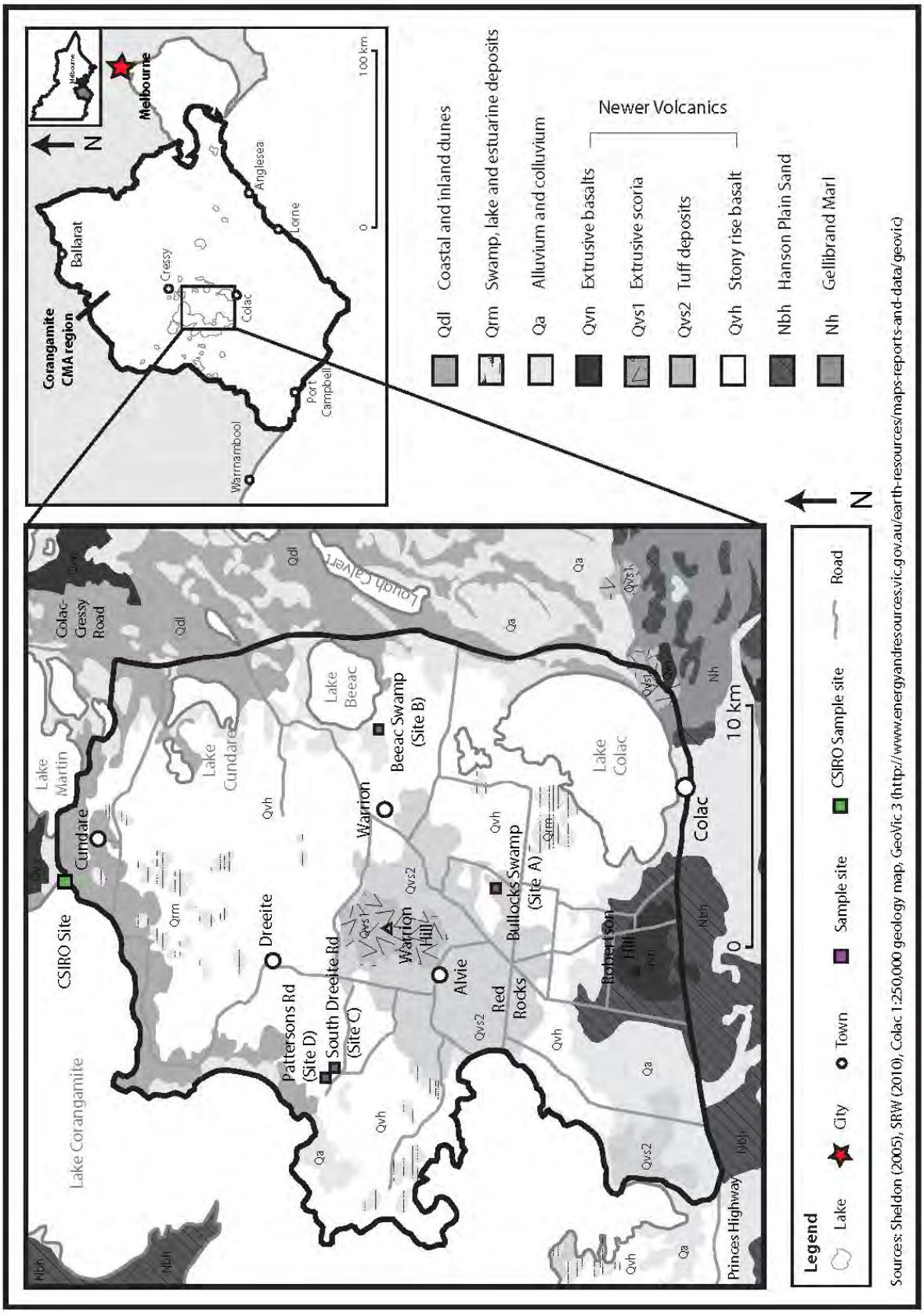

Figure 4.1 Location and geology map of Warrion WSPA

Lake Corangamite forms the western hydrogeological boundary of the Warrion WSPA, and the eastern boundary passes through an area of low groundwater flow between Lake Beeac and Lough Calvert (Figure 4.1), beyond which there is limited groundwater development in the basalt aquifer. To the south, the boundary runs along the Lake Colac shoreline and the Princes Highway, south of the ridgeline below Robertsons Hill that is an inferred groundwater divide (SRW 2010).

The climate is temperate (Chapter 3), with annual rainfall of approximately 600-700 mm (Figure 4.2). Rainfall is highest between June and September, when maximum temperatures are generally lowest (Figure 4.2). Mean monthly evaporation is exceeded by rainfall from May to September, with the highest potential evaporation occurring in January and February when temperatures are highest (data from the Bureau of Meteorology, Australia).

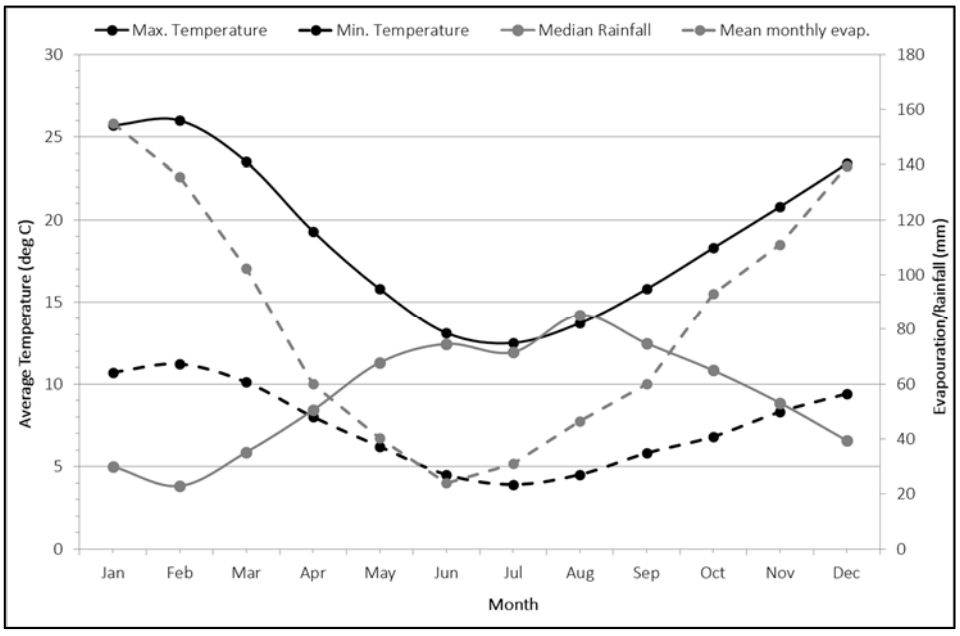

Figure 4.2 Average seasonal variation for Colac (temperature and rainfall) and mean monthly evaporation (Durdidwarrah)

(Rainfall and evap. given as mean monthly values and temperatures as mean daily 3pm temperatures)

Rainfall is the main source of recharge, and recharge rates across the area vary significantly, from up to 30% through the volcanic cones and craters and surrounding stony rises, to 5% on the Basalt Plains (SRW 2010). The variable recharge means that groundwater quality within the basalt is also highly variable. Areas of freshwater (500 mg/L TDS) are associated with areas of high recharge around volcanoes, while the groundwater along the boundary of the WSPA tends towards brackish (2000 mg/L TDS). Groundwater in the Pliocene Sands is more saline than that in the overlying basalt aquifer (SRW 2010).

The Warrion Groundwater Management Plan (2010) included a statement detailing the potential risk associated with ASS within the area. Prior to the present study, potential ASS sites had been identified by a scoping study conducted on the Corangamite CMA by the CSIRO (Fitzpatrick et al. 2007), sampling 29 sites across the Basalt Plains, but all of the sites were found to have a buffering capacity in excess of any potential acid generated via oxidation of sulfides (section 4.5).

Of the four sites sampled for this study, two were drained swamps (Bullocks Swamp (Site A) and Beeac Swamp (Site B)) and two were smaller depressions (South Dreeite Road (Site C) and Pattersons Road (Site D)), selected in order to encompass the range of locations where ASS are likely to be present.

4.2 Bullocks Swamp (Site A)

4.2.1 Site Description

Located beside Bullocks Swamp Road near Coragulac on private land (Figure 4.1), Bullocks Swamp is a wide, shallow swamp that has been drained for farming (Figure 4.3a).

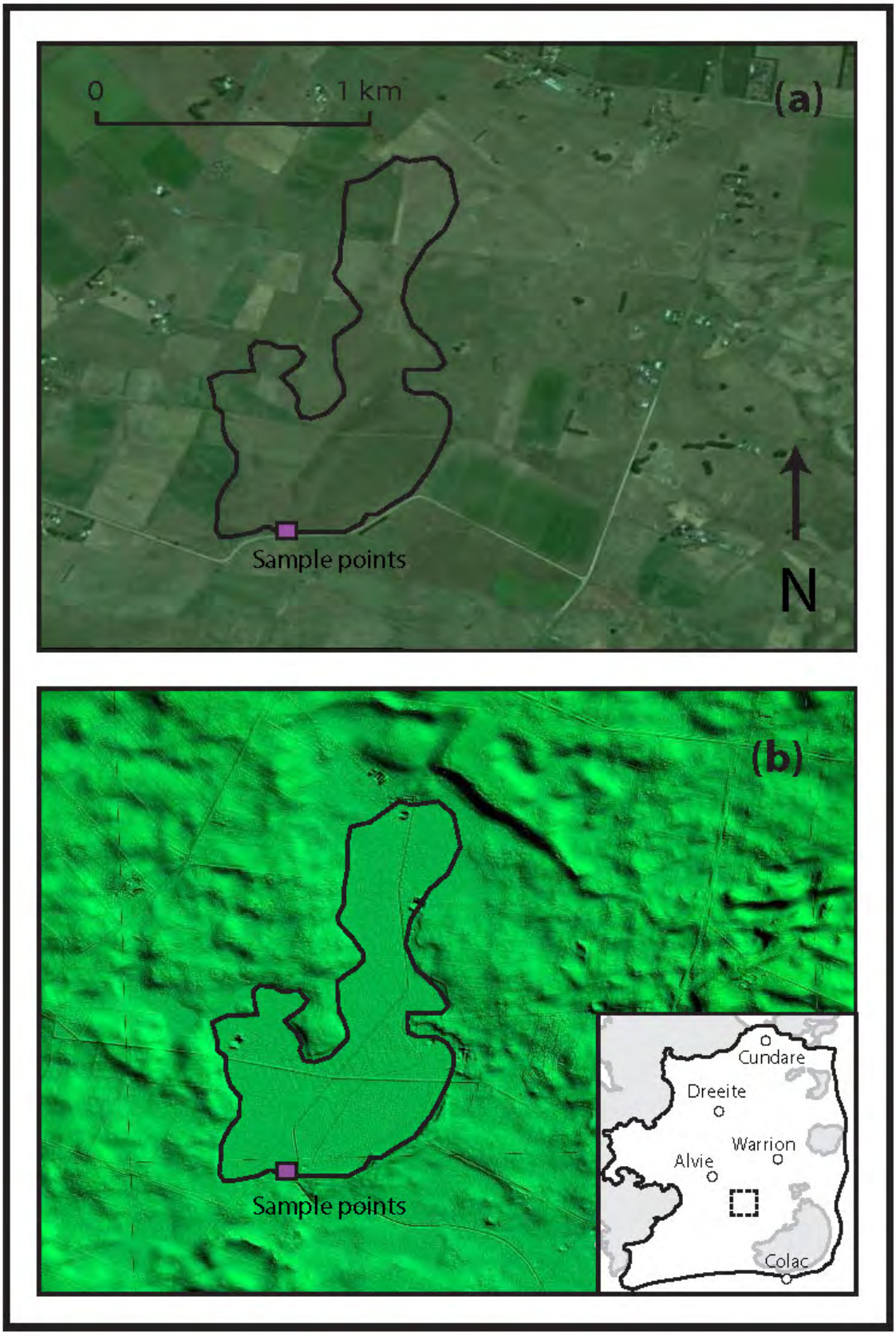

Figure 4.3a and b Google Earth and LIDAR topography of Bullocks Swamp

Figure 4.4a and b (a) Bullocks Swamp sampling area and (b) the sampled sediment profile

Anecdotally, the swamp was consistently waterlogged until approximately 10-20 years ago, when it became subject to seasonal evaporation. The swamp has an area of approximately 0.57 km^2 (Figure 4.3b), and lies approximately 2 m below the surrounding landscape. The swamp is rain fed, and is therefore subject to evaporation due to the large surface area and shallow depth.

4.2.2 Sediment characterisation

In south-eastern Australia, the weathering of younger basalt flows tends to form brown or black clays with strong swelling and shrinking properties (containing montmorillonite) (Robinson et al. 2003). Within the Corangamite CMA, these soils can vary from heavier soils with subsoil layers prone to waterlogging, to shallow, well-drained and thin soils, on the youngest basalt flows with abundant outcrop (stony rises). The Basalt Plains also contain small areas of alluvial, colluvial and swamp soils, associated with Quaternary and Pliocene sediments. Most of these soils developed with impeded drainage and include the sandy and clay loams of lake-bordering lunettes and black organic heavy clays of swamps (Clarkson et al. 2007; Robinson et al. 2003).

The sediment on the floor of Bullocks Swamp is typical of swamps on the Basalt Plains. It comprises two layers (Figure 4.4); the top layer (0-0.2 m depth) was black and rich in organic matter, while the lower layer (0.2-0.35 m, with 0.35 m being the total depth of the sediment sampled) had a finer texture as well as a lighter colour, although the colour change was not well-defined. This was confirmed by grain size analysis, which showed the upper layer of Bullocks Swamp contained almost equal amounts of fine-medium sand and

silt, with minor clay (Figure 4.5). The lower layer is also predominantly fine-medium sand and silt, but with greater amounts of clay (Figure 4.5).

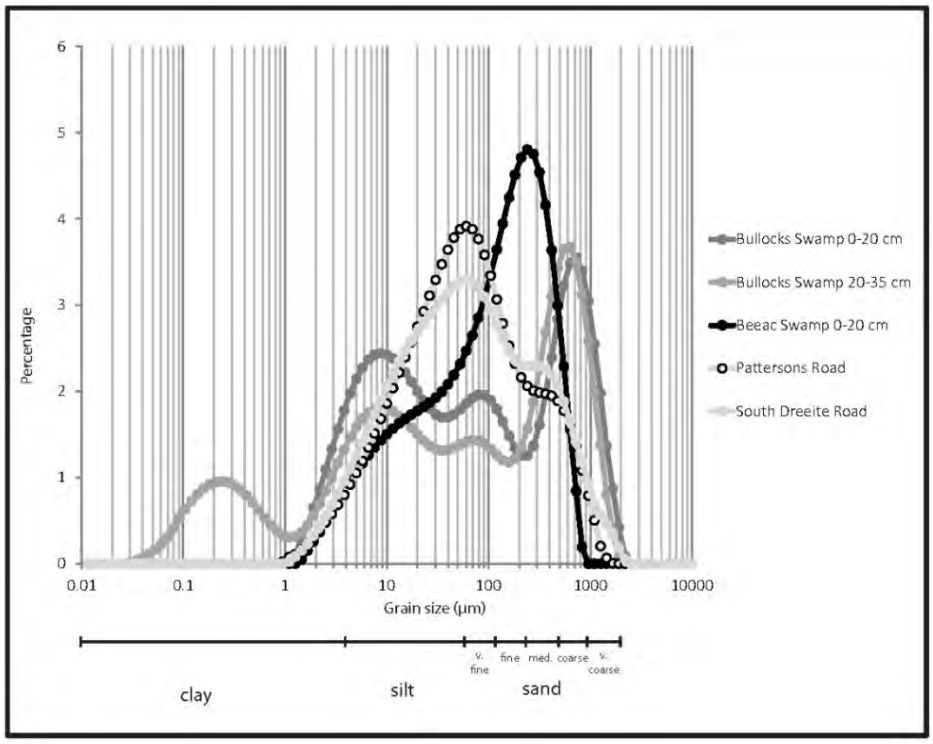

Figure 4.5 Grain size analysis on the basalt samples

X-Ray Diffraction (XRD) analysis identified quartz (SiO_2), illite, aragonite ($CaCO_3$), dolomite ($CaMg(CO_3)_2$), and small amounts of pyrite (FeS_2) and montmorillonite within the upper layer of sediment (Table 4.1). No iron monosulfide minerals (such as greigite and mackinawite) were identified; however, iron monosulfides are difficult to determine accurately via XRD, as they are amorphous or poorly crystalline (Lamontagne et al. 2004; Osterreth 1994). The basal layer showed a similar mineralogical composition of quartz, illite, dolomite and aragonite, with small amounts of montmorillonite, but lacked any identifiable sulfides (Table 4.1).

Table 4.1 Percentage mineral (wt %) composition of basalt sites

Mineral	Bullocks Swamp (0-0.2 m)	Bullocks Swamp (0.2-0.35 m)	Beeac Swamp (0-0.2 m)	South Dreeite Rd (0-0.1 m)	Pattersons Rd (0-0.1 m)
Quartz	37.1	36.8	45.8	65.4	69.3
Illite	30.0	20.4	39.5	34.6	30.7
Montmorillonite	9.60	9.70	3.9*	-	-
Aragonite	13.0	15.1	9.4	-	-
Dolomite	4.50	18.0	-	-	-
Pyrite	5.80	-	1.5*	-	-
Chi-squared value	2.42	3.32	2.75	3.92	3.72

*Values below 5% are not considered accurate

Quantitative analysis of the XRD scans (Table 4.1) show and the Bullocks Swamp sediments have abundant illite, with the major element analysis by XRF (Table 4.2) confirming the presence of clay due to the high aluminium levels. The high percentage of clay within Bullocks Swamp indicates the sediment is prone to waterlogging, providing environmental conditions that suit iron sulfide formation. The illite in the swamp sediment is probably aeolian in origin, as it is not typical of clays formed by basalt weathering. The quartz component is also of aeolian origin, with the sandy lunette soils near to Bullocks Swamps also composed of the aeolian quartz (Clarkson et al. 2007; Joyce 2003).

The levels of iron within the sediments (Table 4.2) are greater than the sulfur levels, indicating the iron is not present only as iron sulfides. Most iron in soil is found within silicate minerals (such as clays) or as iron oxides/hydroxides (Brady and Weil 2002). No iron oxide/hydroxide minerals were identified on the XRD scans, so most of the iron is likely

to be present either in the abundant clay, or as free iron oxide, which can be found in soils that form from volcanic material (Clarkson et al. 2007).

Table 4.2 Major element composition (%) of sediments from all sites

Site	Depth (m)	SiO_2	TiO_2	Al_2O_3	Fe_2O_3	MnO	MgO	CaO	Na_2O	K_2O	P_2O_5	SO_3	LOI	Total
Bullocks Swamp	0-0.2	51.0	1.49	10.1	8.49	0.10	5.09	4.37	0.33	2.17	0.29	0.09	17.0	100.5
Beeac Swamp	0-0.2	48.0	1.00	7.72	5.73	0.06	5.54	4.17	0.04	1.57	0.83	0.09	25.3	100.1
South Dreeite Rd	0-0.1	63.4	2.08	9.75	4.58	0.04	0.77	1.27	0.29	1.14	0.023	0.12	17.0	100.5
Pattersons Rd	0-0.1	64.4	1.96	8.75	5.47	0.05	1.84	1.89	0.39	1.17	0.39	0.10	14.6	101.0

The amount of pyrite found in the XRD analysis of the upper Bullocks Swamp sediments (5.8%) does not match the chromium reducible sulfur (CRS) content (0.13%), as 0.13% CRS corresponds to 0.48% pyrite (Table 4.3). The CRS levels are greater than XRF sulfur (Table 4.2); the latter are probably inaccurate due to problems with sulfur calibration on the XRF. During sample preparation, sulfur may be volatilised in samples containing sulfides, and matrix effects can be maximised (Norrish and Thompson 1990). The CRS content is in excess of the EPA trigger level for medium to heavy clays (soils with > 40% clay) of a sulfur content of > 0.1% for small disturbances (1-1000 tonnes) (EPA 2009). There was no acid volatile sulfur (AVS) found within the Bullocks Swamp sediment, suggesting that there were no iron monosulfides present and all iron sulfides are present in disulfide form (pyrite).

Table 4.3 Acidity and buffering capacity results

Site	Depth (m)	pH (1:5)	CRS (%)	AVS (%)	TAA (mol H+/t)	TSA (mol H+/t)	ANC_E (mol H+/t)	Carbon (wt%)
Bullocks Swamp	0-0.20	7.69	0.13	0.00	0.00	0.00*	3053	5.55
	0.20-0.35	8.38	0.00	0.00	0.00	0.00*	5412	4.72
Beeac Swamp	0-0.20	8.31	0.09	0.00	0.00	0.00*	1024	6.51
South Dreeite Rd	0-0.10	5.53	0.04	0.00	0.00	13.4	0.00**	6.78
Pattersons Rd	0-0.10	5.76	0.04	0.00	0.00	2.63	0.00**	5.95

*Due to large amounts of carbonate present, any acidity generated would have been obscured

**No carbonates were found and no carbonate modification step was performed

The presence of the carbonate minerals aragonite and dolomite (Table 4.1) was matched by high levels of calcium and magnesium shown in the major element analysis (Table 4.2). Carbonate minerals can precipitate within sediments prone to waterlogging, when calcium (Ca^{2+}), magnesium (Mg^{2+}) and carbonate (CO_3^{2-}) are concentrated within the groundwater by evaporation, so that the saturation indices for carbonate minerals become positive and precipitation occurs (Boettinger and Richardson 2000). As Bullocks Swamp is relatively shallow with a large surface area, the swamp is prone to high rates of evaporation in the drier months of the year, when evaporation is known to exceed rainfall (Figure 4.2).

The carbonate minerals within the sediment were present in similar levels in both layers (Table 4.1). The soil pHs are above neutral and the titratable actual acidity (TAA) is zero (Table 4.3), indicating that any iron sulfide oxidation occurring at Bullocks Swamp is being neutralised in situ by the carbonate minerals (aragonite and dolomite). Carbonate minerals

are a common buffering component in acid sulfate soils (Chapter 1; Ahern et al. 1998), and the high levels of excess acid neutralising capacity (ANC) (Table 4.3), show that the neutralising capacity of the Bullocks Swamp sediment is well in excess of any potential acidity produced by the oxidation of iron sulfide minerals. The high ANC value is matched by the substantial amount of carbon in the sediment (Table 4.3); this mainly reflects the carbon within the carbonate minerals, as the overall amount of organic matter in the sediment is relatively small, although higher levels occur in the upper layer (0-0.20 m) of the swamp (Table 4.3).

The trace element levels with the Bullocks Swamp sediments are moderate and are all within Australian background levels, except for chromium (Table 4.4).

Table 4.4 Trace element composition in mg/kg

Element	Bullocks Swamp (0-0.2 m)	Beeac Swamp (0-0.2 m)	South Dreeite Rd (0-0.1 m)	Pattersons Rd (0-0.1 m)	Australian background range*	Global background range**
Arsenic (As)	12.6	0.00	2.30	5.00	0.2-30	0.1-48
Chromium (Cr)	170	74.2	169	168	0.5-110	5-1000
Cobalt (Co)	27.4	12.1	9.80	13.1	2-170	1-40
Lead (Pb)	14.0	14.0	14.2	20.5	2-200	10-67
Molybdenum (Mo)	1.30	2.90	2.50	2.40	1-20	0.5-40
Nickel (Ni)	122	77.3	75.5	77.5	2-400	1-200
Zinc (Zn)	68.5	58.0	89.8	123	2-180	10-300

*(Australian averages from ANZECC and NHMRC 1992)

**(Global averages from Pias and Jones 1997)

Trace elements in sediments and soils are typically associated (adsorbed or precipitated) with clay and oxide mineral surfaces, or complexed by organic matter (Brady and Weil 2002; Hillel 1998). At Bullocks Swamp, the trace elements are probably predominantly held on the clay minerals, but due to the high ANC levels, they will not be mobilised by acidity accompanying sulfide oxidation.

As the ANC was considerably greater than the potential acidity (CRS) (Table 4.3), the upper layer (0-0.2 m) at Bullocks Swamp is classified, following the ASS classification scheme (Chapter 1), as a **buffered sulfidic soil (BSS)**. Due to the lack of sulfides present, the lower layer (0.2-0.35 m) is classified as a **non-sulfidic soil**.

4.3 Beeac Swamp (Site B)

4.3.1 Site Description

Beeac Swamp is a large, drained swamp, like Bullocks Swamp, located just south of Lake Beeac along Foleys Road (Figure 4.1). Part of the swamp is a nature reserve (the Beeac Swamp Lake Reserve), fenced to exclude livestock in 1994 (Carter 2010; Harris and Smith 2000), while the remainder is private farmland.

Prior to drainage for agriculture (Figure 4.6a), the site was most likely waterlogged. Spiny Peppercress (*Lepidium ascheronii*) has been identified across Beeac Swamp, indicating that the site is currently prone to waterlogging or seasonal flooding (Carter 2010; Harris and Smith 2000). The swamp was highly disturbed by the introduction of agriculture, and introduced Canary Grass (*Phalaris aquatica*), Fog grass (*Holcus lanatus*) and Perennial Rye Grass (*Lolium perenne*) have invaded the site (Carter 2010; Harris and Smith 2000).

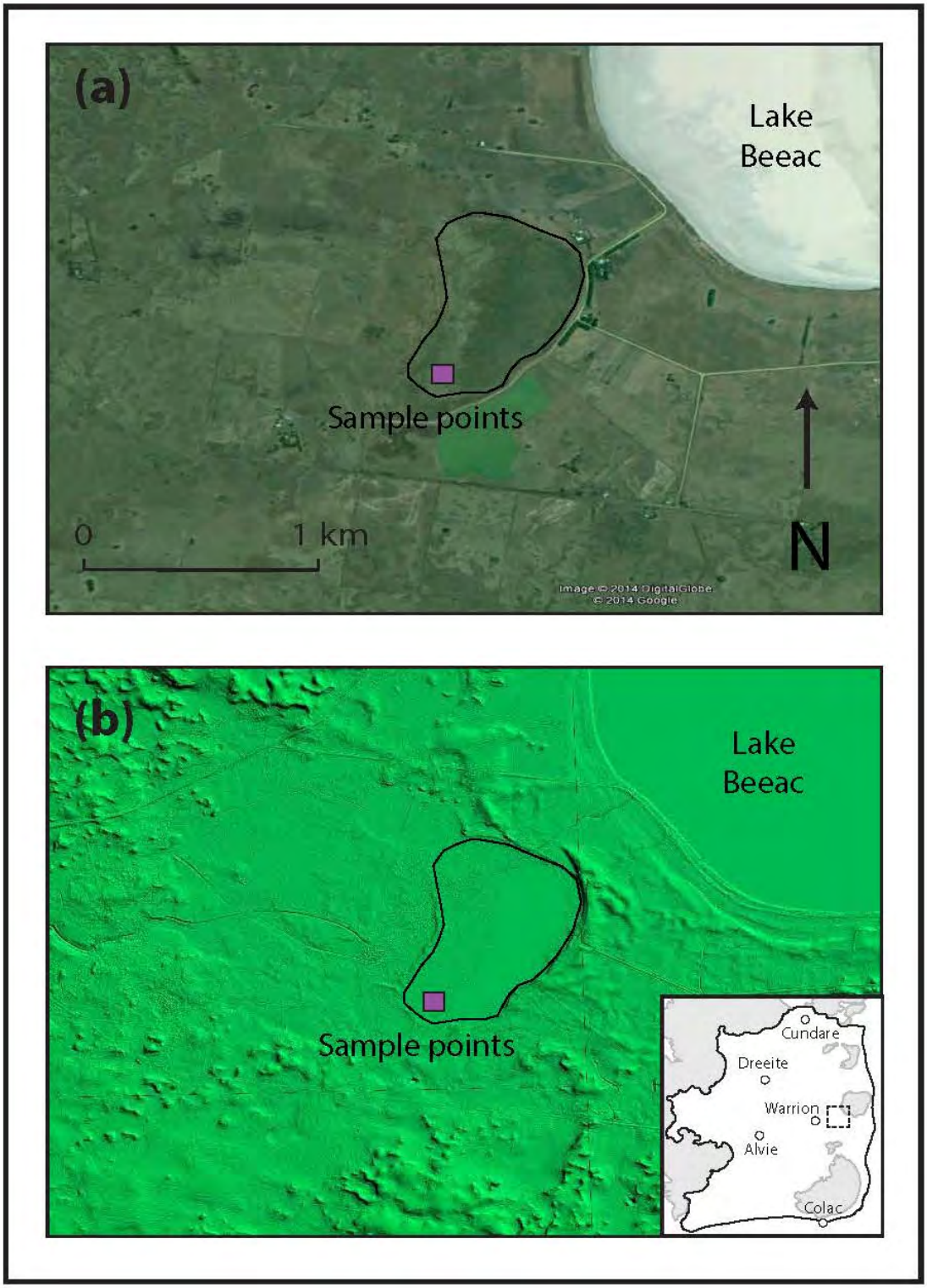

Figure 4.6a and b Google Earth and LIDAR topography of Beeac Swamp

Figure 4.7a and b (a) Beeac Swamp sampling area and (b) sampled sediment profile

Beeac Swamp has an approximate area of 0.29 km^2 (Figure 4.6 b), with its floor approximately 1 m below the surrounding landscape. The swamp is rain fed, and after the loss of consistent waterlogging due to drainage for agriculture, has been subject to seasonal evaporation.

4.3.2 Sediment characterisation

The sediment on the floor of the swamp (Figure 4.7a) comprises two layers, with the top layer (0-0.2 m depth) black and organic (Figure 4.7b), and comprising of fine-medium sand and silt, with minor clay (Figure 4.5). The lower layer (0.2-0.3 m, with 0.3 m being the total depth of the sampled sediment) had a finer texture and lighter colour, although the colour change was not well-defined. Only the upper layer of sediment was analysed due to issues during sampling.

XRD analysis identified quartz, illite, aragonite and montmorillonite (Table 4.1). A small amount of pyrite is present, but is hard to quantify because the small peaks were hard to distinguish above background. This mineralogical composition is very similar to that at Bullocks Swamp, and also represents heavy black organic clays weathered from the underlying basalt and found in swamps across the area (Clarkson et al. 2007; Robinson et al. 2003; Joyce 2003). The carbonate (aragonite) present (Table 4.1) is matched by the high level of calcium in the major element analysis (Table 4.2). Like Bullocks Swamp, Beeac Swamp sediment contains aeolian quartz and illite.

Iron and sulfur (CRS) are present in lower concentrations at Beeac Swamp than at Bullocks Swamp (Table 4.3), and the pyrite concentration is also lower (Table 4.1). The iron is most likely contained within the clay minerals, as no iron oxide/hydroxides were identified. The

CRS levels are in excess of the EPA trigger level (> 0.1% sulfur) for medium to heavy clays (soils with > 40% clay) (EPA 2009). There was no AVS content, suggesting that there were no iron monosulfides present. The carbonate levels within the sediment were reflected by the above neutral pH and TAA of zero (Table 4.3), indicating that any iron sulfide oxidation occurring at Beeac Swamp is being neutralised by the aragonite. While the ANC is about three times less than that of Bullocks Swamp, the buffering capacity is still in excess of the acidity released by oxidation of the sulfide content (Table 4.3). The trace elements present (Table 4.4) will not mobilise, because the ANC levels mean that the sediment will not become acidic. Using the classification scheme (Chapter 1), the upper layer (0-0.2 m) was determined to be a **buffered sulfidic soil (BSS)**, for the same reasons as the Bullocks Swamp sediment.

4.4 South Dreeite Road (Site C) and Pattersons Road (Site D)

4.4.1 Site Description

Unlike the larger swamps, the South Dreeite Road site (Site C) and the Pattersons Road site (Site D) were smaller depressions in the landscape. These depressions temporarily collect rainfall and runoff, leading to the waterlogging necessary for sulfide mineral formation. However, they tend to retain water for shorter times than the swamps, due to more rapid infiltration of the water (discussed further below). The landscape surrounding the depressions is undulating and characterised by shallow, dark cracking clay soils, and has been cleared for grazing (Clarkson et al. 2007; Robinson et al. 2003; DSE 2005a). The sediment on the floor of both depressions showed no obvious layering in terms of colouring

or texture, but had the same dark, organic-rich appearance as the upper layers of both Bullocks and Beeac Swamps and similar depths (approximately 0.3 m) (Figure 4.8).

4.4.2 Sediment characterisation

Grain size analysis showed both depressions (Sites C and D) were mostly fine sand and silt, with lesser medium sand and minor clay (Figure 4.5). XRD analysis identified only quartz and illite within these sediments (Table 4.1), both aeolian in origin. ANC analysis showed a lack of buffering capacity within both sediments (Table 4.3), and no carbonate minerals were identified on the XRD scans (Table 4.1), confirmed by low calcium and magnesium levels (Table 4.2). There is no existing acidity (TAA) within the sediments (Table 4.3). Slightly acidic pHs were measured at both sites and oxidation in the lab showed a small pH drop due to the small amount of iron sulfides present, as shown by the low levels of CRS, although these are substantially less than at sites A and B (Table 4.3).

The depressions on the basalt (Sites C and D) are waterlogged for shorter periods of time than the larger swamps (Sites A and B), resulting in less sulfide mineral development. Any rainfall that accumulates in the depressions infiltrates relatively quickly into the underlying watertable due to the lack of an underlying confining layer (which is present in the larger swamps), rather than being lost to evaporation.

As a result, the groundwater does not become sufficiently concentrated to precipitate carbonate minerals. The low sulfide content (0.04% CRS) is close to the EPA trigger level (%S > 0.03), so that even without buffering capacity, when combined with the small size of the sites, the soils will not release significant acidity when oxidised. Therefore, while the

sediments at both depressions would be classified (Chapter 1) as potential acid sulfate soils (PASS), they do not pose a significant risk.

Figure 4.8a and b (a) South Dreeite Road sediment and (b) Pattersons Road sediment

4.5 Comparison with other studies

As part of a study on the inland and coastal ASS in the Corangamite CMA, Fitzpatrick et al. (2007) sampled sediments from a number of lakes and swamps on the Basalt Plains. These sites included three (COR4, COR6 and COR7) at Lake Corangamite within the Warrion WSPA at Lake Corangamite (Table 4.5; Figure 4.1). Fitzpatrick et al. (2007) found that none of the soils at these sites had a pH of < 4, because despite the presence of sulfides, they all had excess neutralising capacity which prevented any acidification due to sulfide oxidation (i.e. the sulfidic layers at these sites are **buffered sulfidic soils (BSS)**; Chapter 1).

Table 4.5 Acidity and buffering capacity results (Fitzpatrick et al. 2007); see Figure 4.1 for sample sites

Site No.	Depth (m)	pH	CRS (%)	TAA (mol H+/t)	TSA (mol H+/t)	ANC (% as $CaCO_3$)
COR4	0-0.05	8.50	N/A*	0.00	N/A*	8.00
COR6	0-0.01	8.50	0.02	0.00	13.0	39.0
COR7	0.03-0.1	7.80	0.43	0.00	270	8.90

*Result was not included in report

These results match those of the present study at Bullocks Swamp and Beeac Swamp (Sites A and B), which although smaller than Lake Corangamite, are subject to the same precipitation of carbonates due to evaporation and seasonal waterlogging. The smaller depressions on the basalt which contain **potential acid sulfate soils (PASS)** were not sampled by Fitzpatrick et al. (2007).

4.6 Assessment of ASS on Basalt Plains

The surface sediments in both the swamps (Sites A and B) and the smaller depressions (Sites C and D) contain iron sulfide minerals, but none of the sites will experience a significant drop in pH and acidify if they are exposed to oxygen (Table 4.1). While all sites are fed by rainfall, the swamps are waterlogged for longer periods of time than the depressions, which drain quickly after rain. In the swamps, the lower, lighter coloured sediment below 0.2 m in depth acts as a confining layer and prevents most infiltration. The resultant waterlogging allows sufficient evaporation within the sediment at Bullocks Swamp and Beeac Swamp for the precipitation of carbonate minerals, and also allows the formation of sulfides within the upper sediment layers of the swamps. Both Bullocks Swamp and Beeac Swamp contain large amounts of carbonate minerals (aragonite and dolomite) which provide a buffering capacity well in excess of any potential acidity generating by the sulfide minerals. In comparison, the sediments in the basalt depressions contain no carbonate minerals, but have lower levels of sulfides due to faster infiltration of rainfall and less evaporation within the sediment. Therefore, while the ASS classification of the swamp and depression sediment differs (**buffered sulfidic soil** and **potential acid sulfate soil**, respectively; Chapter 1), none of the sites will undergo a large acidification event (pH drop to below 4) if the sediments are oxidised.

Chapter 5

Otways Ranges

As stated in Chapter 1, tea-tree swamps that potentially contain ASS occur in areas with sustained waterlogging, and are found across the Otway Ranges, particularly throughout the foothills to the north (Sheldon 2005). The Otway Ranges are a topographic high that separates the Otway Basin from the Port Phillip Basin (Chapter 3), with a maximum elevation of 670 m AHD, and form a drainage divide that trends north-east, parallel to the coast. From the ranges, the Barwon River system drains to the east, while the tributaries of the Gellibrand River drain the region to the west (Figure 5.1; Sheldon 2005). The foothills on the flanks of the Otway Ranges generally form gently undulating and rounded hills (Hills 1975; Joyce et al. 2003b; Robinson et al. 2003), and support the second highest number of wetlands in the Corangamite CMA region. These foothill wetlands cover approximately 51.8 km^2, and include the headwaters of the Barwon, Gellibrand and Aire Rivers, while the Otway Ranges themselves have only 2.2 km^2 of wetlands, due to the constraints of the steeper slopes. Prior to European settlement, these wetlands were highly productive and acted as a large food resource for the indigenous Gadubanud people, particularly along the Barwon River (Niewójt 2009; Sheldon 2005). Within the Otway Ranges, five wetlands were selected for investigation along the Barwon, Gellibrand and Anglesea Rivers (Figure 5.1); these will now be discussed in turn.

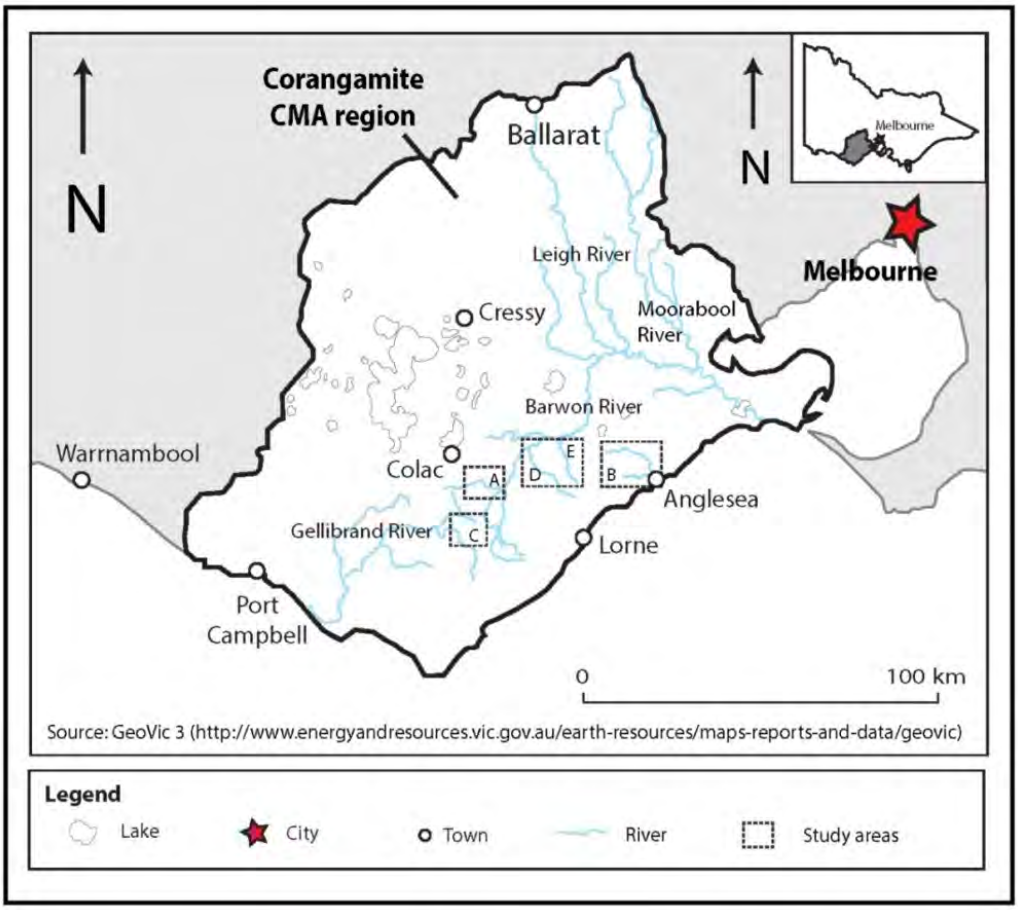

Figure 5.1 Location of Otway Ranges study areas (A: Boundary Creek, B: Anglesea River, C: Porcupine Creek, D: Pennyroyal Creek, and E: Bambra Wetlands)

5.1 Boundary Creek (Site A)

5.1.1 Site Description

Boundary Creek, a tributary of the Barwon River system, is located approximately 15 km southeast of Colac in southern Victoria (Figure 5.1). The creek drains the northern slopes of the Otway Ranges in the western part of the Barwon River catchment, before flowing into the West Barwon. To the north, basaltic lavas of the Newer Volcanics (Chapter 3; Figure 3.3) erupted around 2.31 Ma (Gibson 2007). The lavas infilled the lowest points in

the topography and dammed the Barwon River, forming extensive swamps upstream. The present course of the river has diverted along the edge of the basalt flows to the north of Birregurra (Robinson et al. 2003). The wide floodplain of the Barwon River in this area developed as a result of the rise in base level associated with the damming of the river by basalt flows, and has alluvial flats and terraces formed during the subsequent downcutting of the channel. The many swamps and wetlands throughout the Barwon River catchment were mostly drained for agriculture by the artificial deepening of the stream channels, starting in the early 1900s (Lett et al. 2007); as a result, the formerly dominant tea-tree swamp vegetation has been replaced by exotic grasses and forbs (CCMA 2006b).

The local climate is markedly influenced by the Otway Ranges (Chapter 3). The average annual rainfall at Barwon Downs is approximately 800 mm (Table 5.1), with some years exceeding 1200 mm. The ranges have relatively low average temperatures, with maximum temperatures averaging 12.5-26.0˚C at Colac (data from Bureau of Meteorology, Australia). Rainfall is highest between June and September, when maximum temperatures are generally lowest (Figure 5.2). Mean monthly evaporation is exceeded by rainfall from May to September, with the highest potential evaporation occurring in January and February, when temperatures are highest (data from the Bureau of Meteorology, Australia). As a result of this variable rainfall, Boundary Creek has a strongly seasonal flow, much like the Barwon and Leigh Rivers. Typically, the creek has natural periods of no flow in summer and autumn, with minimum flows usually occurring in the January to April period, and maximum flows usually between August and September (CCMA 2013c). Periods of low to no flow in the creek correspond to the months where evaporation exceeds rainfall, and therefore no runoff occurs.

Table 5.1 Rainfall data summary of stations near to Boundary Creek (data from the Bureau of Meteorology, Australia) (sites are shown on Figure 5.3)

Station Name	Latitude	Longitude	Elevation (m)	Measurement period	Average annual rainfall (mm)
Colac Shire Office	38.34° S	143.58° E	134	1899-current	726.6
Barwon Downs	38.47° S	143.75° E	151	1888-current	781.9
Birregurra Post Office	38.34° S	143.78° E	119	1903-current	669.5
Cape Otway Lighthouse	38.86° S	143.51° E	82	1861-current	898.6

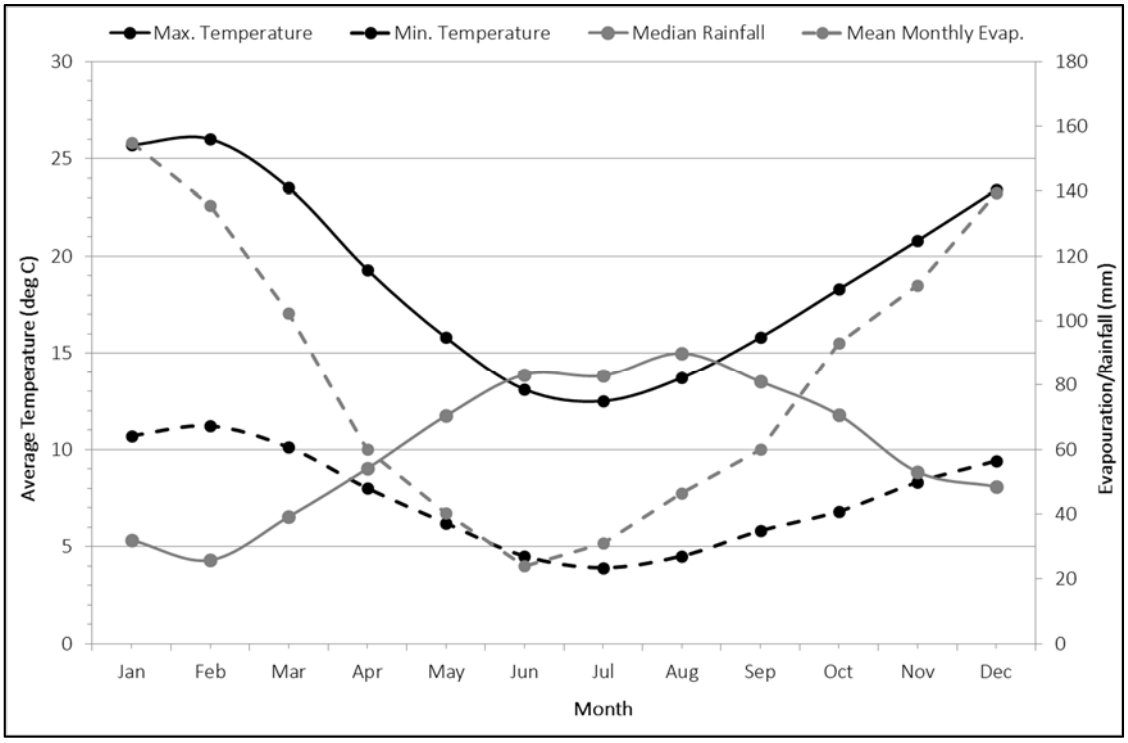

Figure 5.2 Average seasonal variation for Colac (temperature), Barwon Downs (rainfall) and mean monthly evaporation (Durdidwarrah)

(Rainfall and evap. given as mean monthly values and temperatures as mean daily 3pm temperatures)

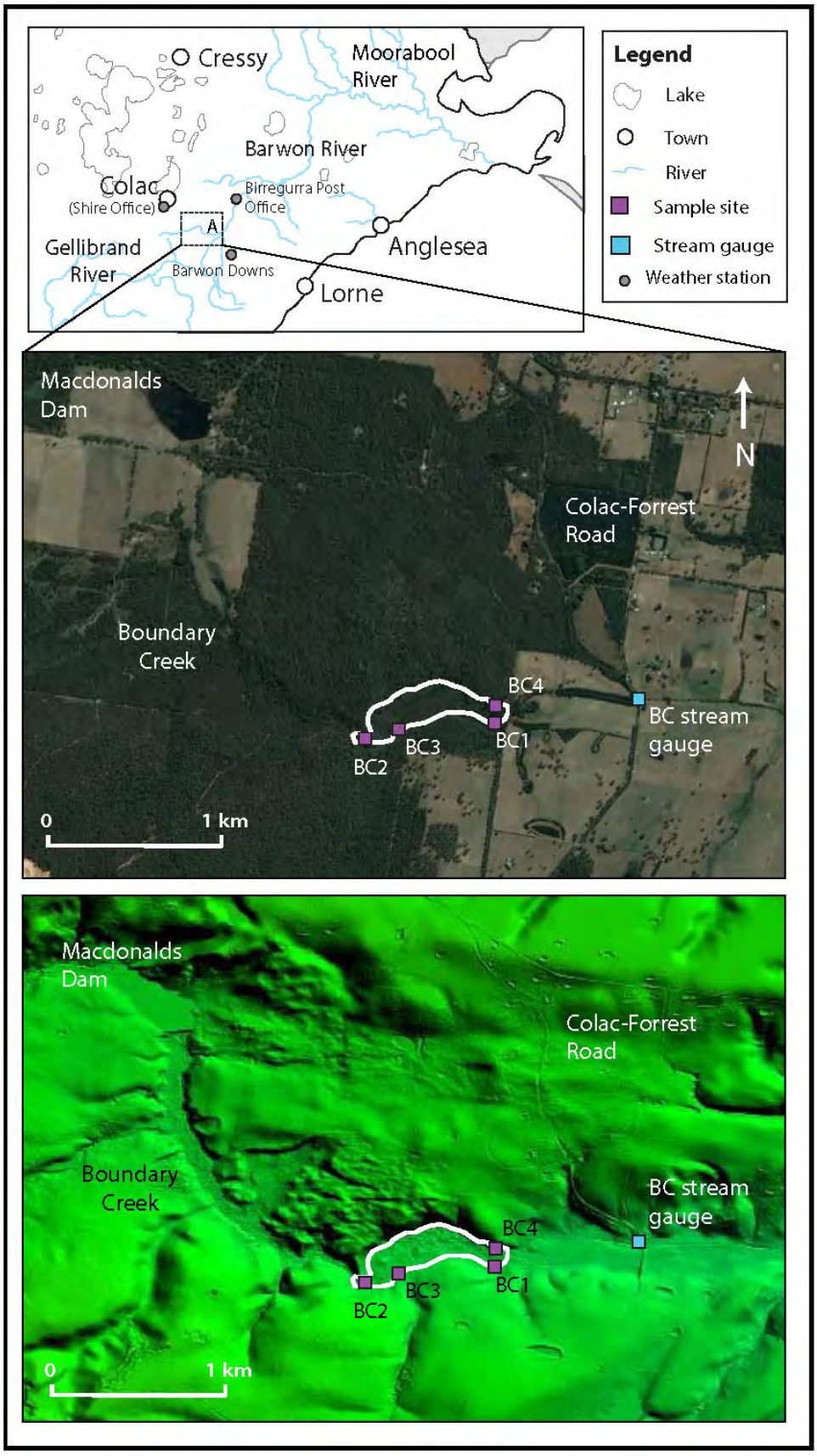

Figure 5.3 Google Earth and LIDAR images of Boundary Creek swamp

For Boundary Creek and the Barwon River, a baseflow of 1 ML/d is recommended to maintain semi-permanent aquatic habitat for small fish and macroinvertebrates, particularly in summer (CCMA 2006b). However, as the hydrology of Boundary Creek has been altered by the addition of McDonalds Dam, environmental releases were recommended for the health of the stream, with approximately 522 ML discharged into Boundary Creek during the 2012-2013 year from the dam at Yeodene (Barwon Water, 2013; CCMA 2006b).

The swamp along Boundary Creek (Figure 5.3) was partially drained when the downstream land was cleared for agriculture, leaving the surface of the eastern section of the swamp dry and allowing eucalypts to establish (Figure 5.4a). Aerial photographs taken in 1946 show drainage (through artificially deepened river channels) very similar to that in the area today. The most upstream part of the swamp was not drained, and now forms the Boundary Creek peat swamp, otherwise known as Big Swamp. The swamp itself is approximately 0.16 km^2 in area (Figure 5.3), and is fed by the water in Boundary Creek released from the dam upstream.

In the summer of 1997, the site was burnt by a bushfire that started in Yeodene, and the peat swamp smouldered subsurface between 1998 and 2010 while the swamp remained dry, before a second bushfire broke out in March 2010. Fire management at the site then became a priority, and a trench was dug between March and April 2010 along the southern and eastern sides of the site to contain the smouldering peat. This trench has since filled with low pH water and has developed iron staining (Figure 5.4b).

Figure 5.4a and b Boundary Creek swamp site (a: photo taken in the trench looking upstream, and b: photo taken where two trenches met at BC1)

The bedrock beneath the swamp is the Paleogene sediments of the Dilwyn and Demons Bluff Formations (Chapter 3; Figure 5.5), which form part of the northern foothills of the Otway Ranges. These sediments are prone to landslides on the slopes, particularly along roads on the flanks of the Otway Ranges and along waterways on the western flanks of the Barwon River Valley, south of Birregurra (Clarkson et al. 2007).

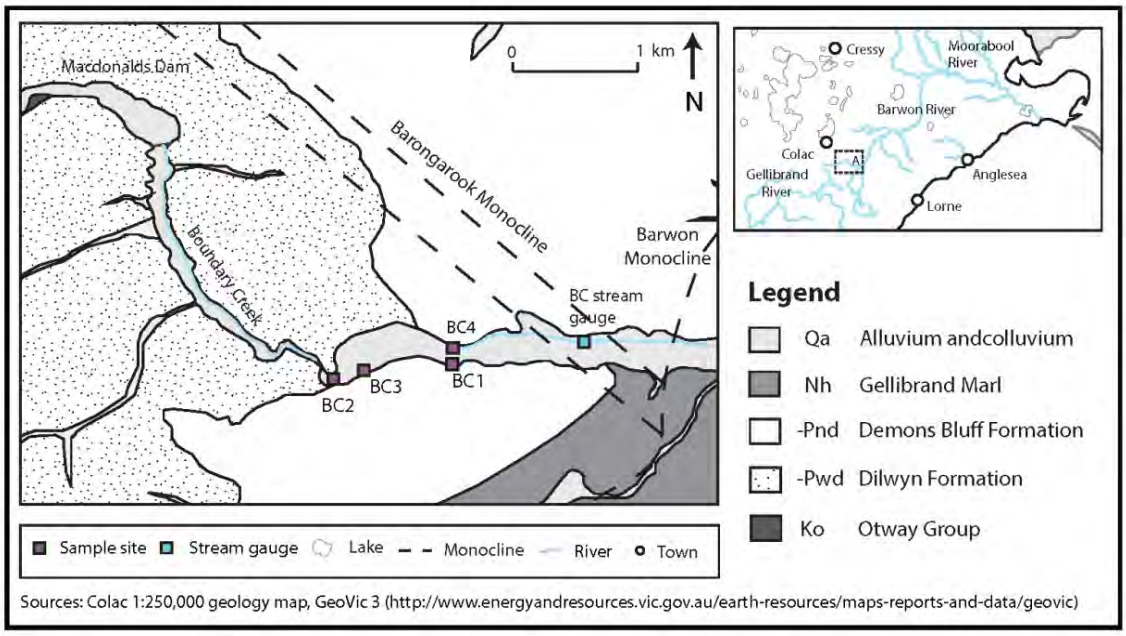

Figure 5.5 Geology map of Boundary Creek swamp site

5.1.2 Sediment characterisation

Within the swamp, three sites were selected along the previously dug trench (Figure 5.3). Grain size analysis of these samples shows that within the swamp, the inorganic fraction of the top 2.5 m is mostly fine-medium quartz sand, with lesser amounts of silt and clay (Figure 5.6). Beneath this layer, the sediment is also predominantly fine-medium sand, but with greater amounts of clay (Figure 5.7). Field oxidation pH tests on the sediments show that both layers have the potential to generate acidity (Figure 5.8).

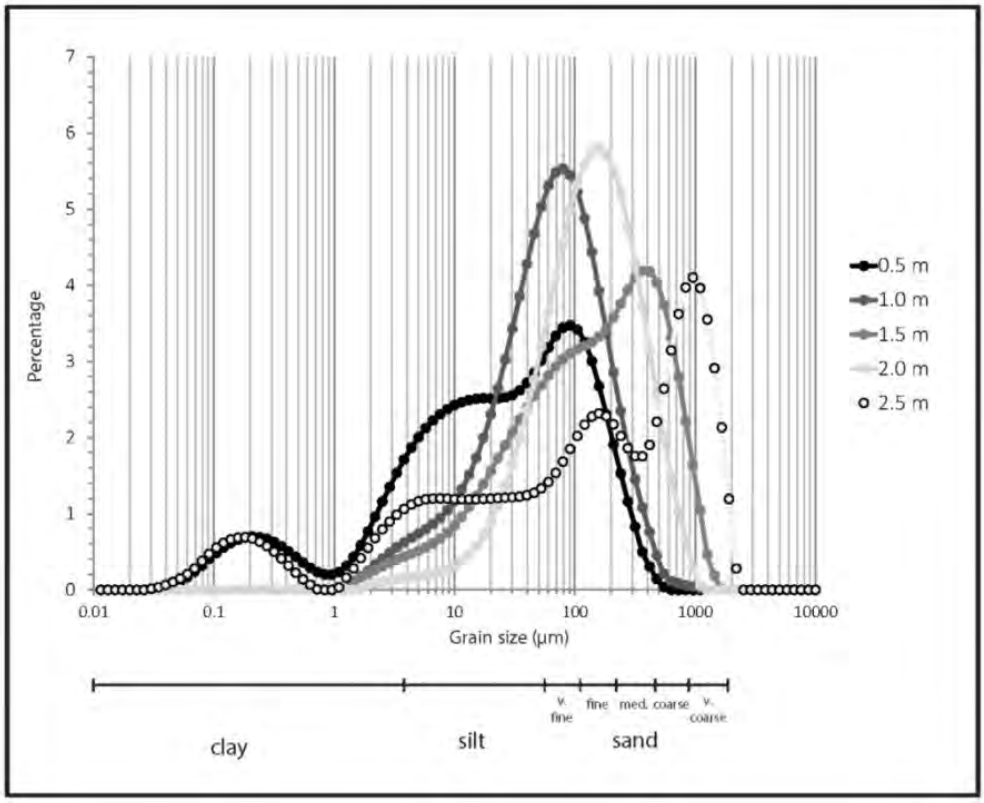

Figure 5.6 Grain size analysis for the "peat" samples

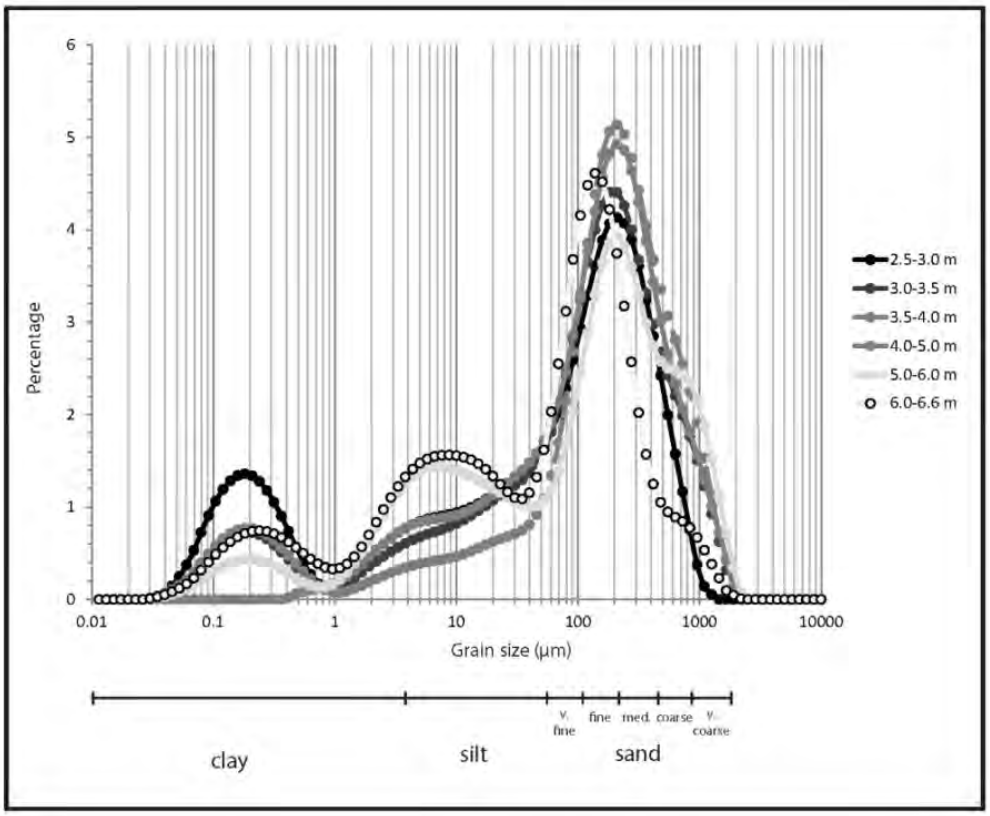

Figure 5.7 Grain size analysis for underlying sediments at BC1

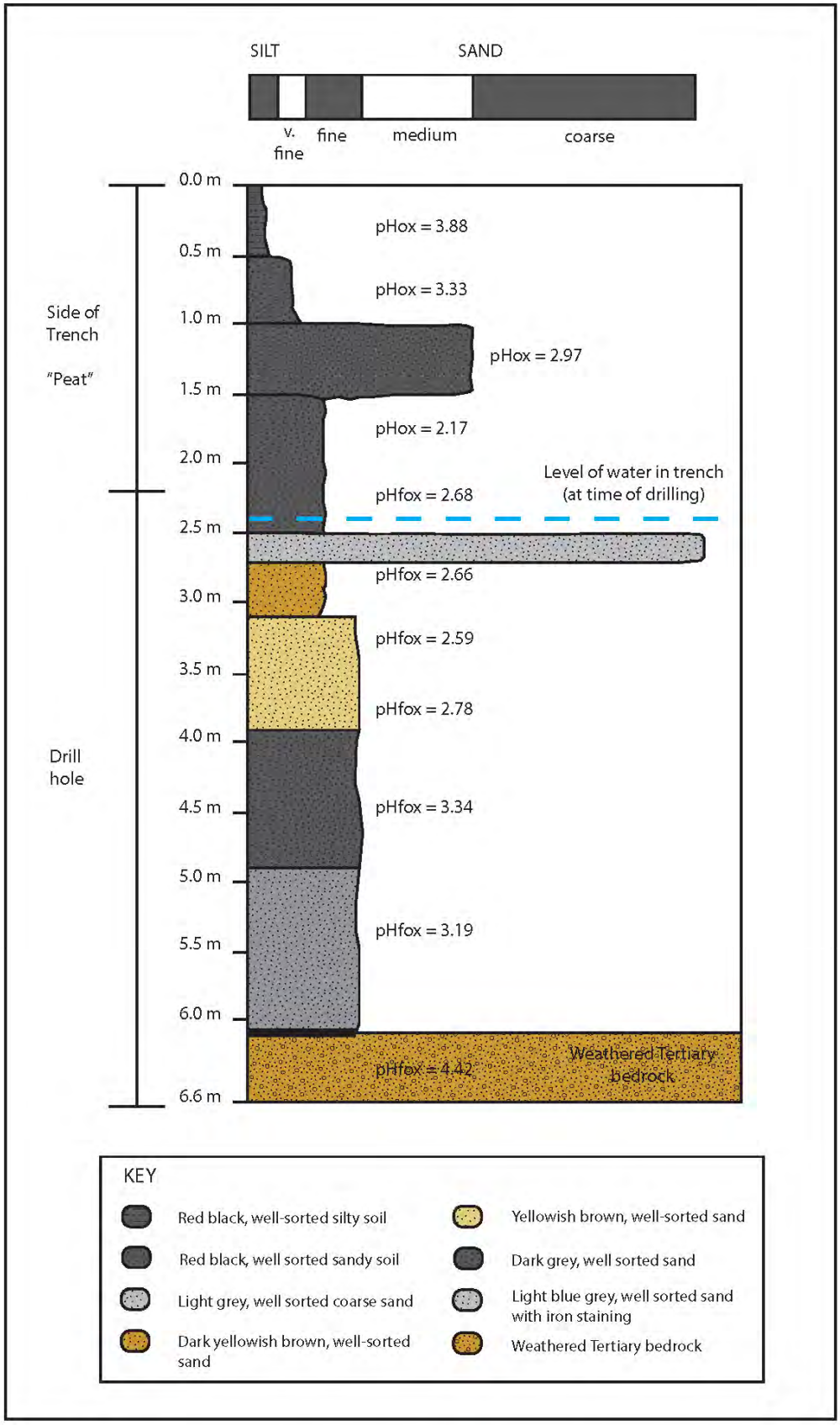

Figure 5.8 Stratigraphic column of sediments at BC1

The sediments at site BC4 are different (Figure 5.9); the upper 2.0 m thick layer is predominantly sand and contains little visible organic matter; it has a low potential for generating acidity (Figure 5.10). This layer of sediment might have originated from a small landslide that covered this part of the site, which lies close to the foothill slope on the northern side of the swamp, and is therefore not swamp sediment, accounting for the comparative lack of organic material and sulfides (as shown by the relatively high pH_{FOX}). Soils within the upper catchment of the Barwon River are known to be prone to landslides (Clarkson et al. 2007), dominantly triggered by episodes of high rainfall (Dahlhaus et al. 2006a).

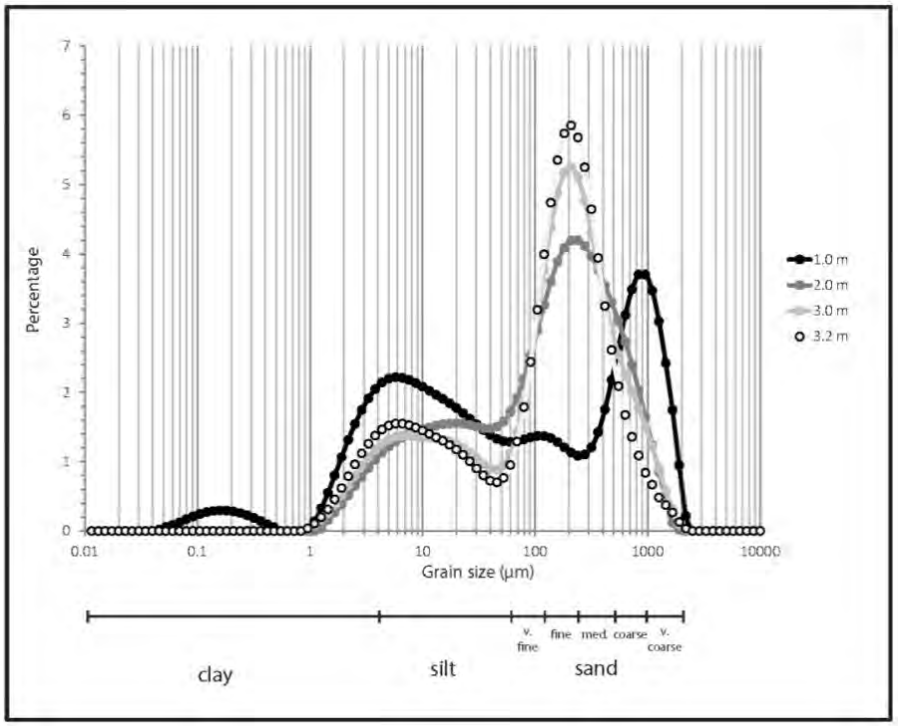

Figure 5.9 Grain size analysis for sediments at BC4

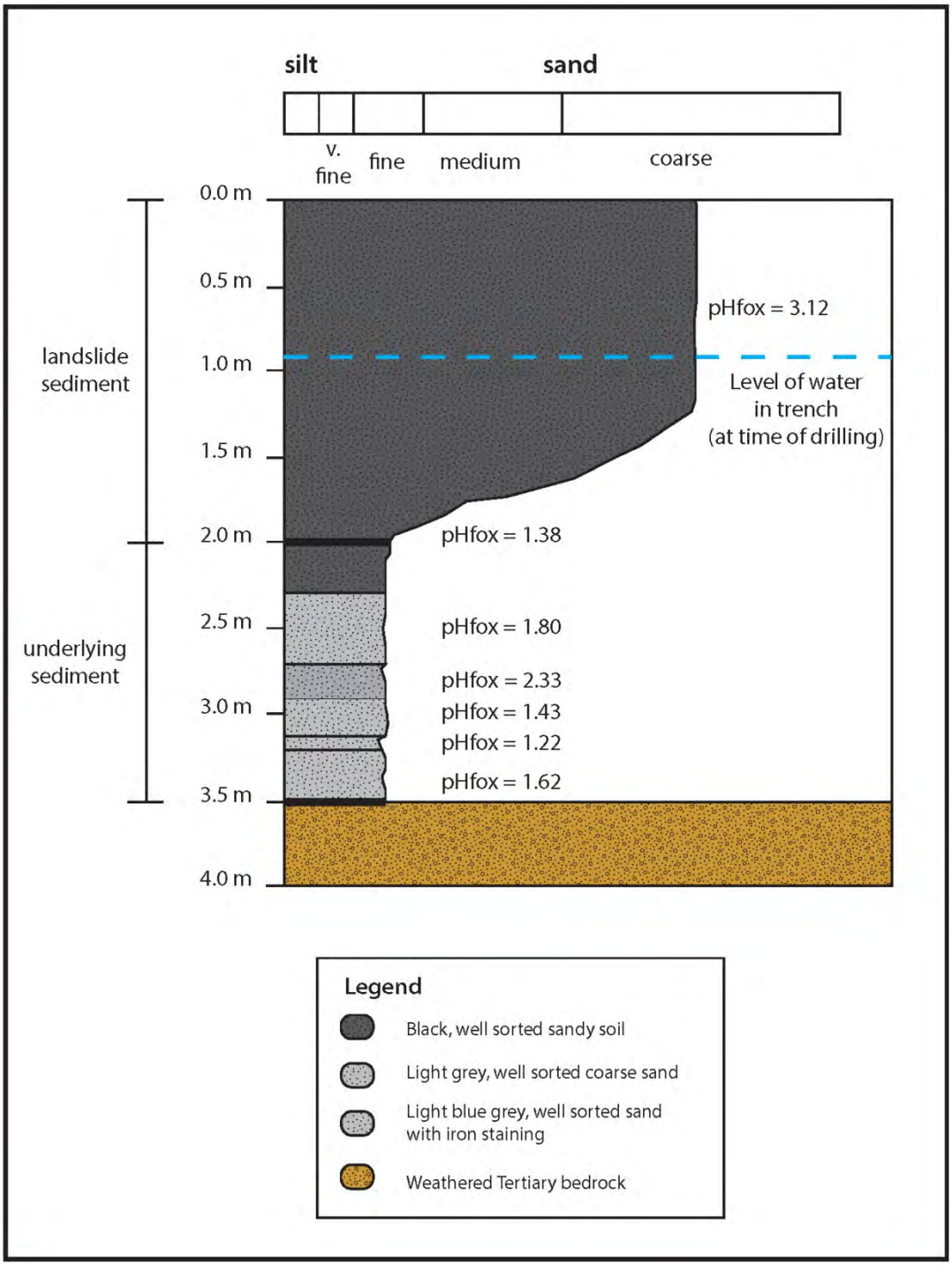

Figure 5.10 Stratigraphic column of sediments at BC4

Quantitative XRD analysis of the swamp sediment identified abundant quartz (SiO_2), kaolinite, illite, and small amounts of pyrite (FeS_2) and iron hydroxide (Table 5.2). The abundant quartz, illite and kaolinite are reflected in the high silica and aluminium levels in the XRF analyses of the sediments (Table 5.3). Composition of the sediment was very similar with depth.

Table 5.2 Mineral composition (wt %) of Boundary Creek swamp sediments

Site	Depth (m)	Quartz	Illite	Kaolinite	Pyrite	Iron hydroxide	Gypsum	Chi-squared Value
BC1	1.0	25.8	38.5	31.7	2.30*	4.00*	-	**2.32**
	2.0	19.3	34.4	34.6	2.10*	2.90*	6.70	**2.91**
BC2	1.5	24.4	23.2	27.5	-	-	6.60	**2.78**
BC3	2.0	27.8	33.7	4.50	3.90*	-	-	**2.39**

*Values below 5% are not considered accurate

Table 5.3 Major element composition (wt %) of Boundary Creek swamp sediments

Site	Depth (m)	SiO_2	TiO_2	Al_2O_3	Fe_2O_3	MnO	MgO	CaO	Na_2O	K_2O	P_2O_5	SO_3	LOI	Total
BC1	0.5	40.7	1.55	26.6	5.72	0.01	0.37	0.04	0.00	0.43	0.14	0.17	25.5	**101.2**
	1.0	43.5	1.65	28.5	3.27	0.01	0.41	0.04	0.00	0.46	0.13	0.22	23.3	**101.5**
	1.5	44.3	1.65	27.0	3.60	0.01	0.48	0.04	0.00	0.59	0.09	0.31	24.1	**102.2**
	2.0	37.6	1.29	24.2	3.66	0.01	0.40	0.04	0.00	0.53	0.12	0.41	32.1	**100.4**
BC2	1.5	54.8	1.22	19.8	1.63	0.01	0.19	0.00	0.00	0.32	0.11	0.27	22.4	**100.8**
BC3	2.0	86.2	1.17	5.20	0.63	0.01	0.02	0.00	0.00	0.12	0.04	0.13	5.69	**99.2**

Iron levels within the sediments are relatively high (Table 5.3), but only small amounts of pyrite were identified by XRD (Table 5.2), confirmed by the low levels of sulfur in the XRF analyses. The majority of the iron is probably present as iron oxides/hydroxides (Brady and Weil 2002), as identified in the upper 2.0 m of the profile at BC1 (Table 5.2). No carbonate minerals were found within the swamp sediments, matching the low levels of calcium and magnesium in the major element analysis (Table 5.3).

Table 5.4 Trace element composition in mg/kg

Site	Arsenic (As)	Chromium (Cr)	Cobalt (Co)	Lead (Pb)	Molybdenum (Mo)	Nickel (Ni)	Zinc (Zn)
Boundary Creek (BC1 2.0 m)	25.4	87.8	8.90	14.2	13.3	75.5	69.4
Australian background range*	0.2-30	0.5-110	2-170	2-200	1-20	2-400	2-180
Global background range**	0.1-48	5-1000	1-40	10-67	0.5-40	1-200	10-300

*(Australian averages from ANZECC and NHMRC 1992)

**(Global averages from Pias and Jones 1997)

The trace metals within the Boundary Creek swamp sediments are all within Australian background levels for soils (Table 5.4). These trace elements are probably adsorbed onto or precipitated with clay and iron oxide minerals, or complexed by organic matter. Trace elements on clay mineral surfaces are either adsorbed onto charged sites of the basal planes (through cation exchange) or onto specific sites around the edges of clay minerals (Brady and Weil 2002; Du Laing et al. 2009).

Organic matter is highly visible throughout the sediment profile, with carbon levels of 2.36-9.82 % (Table 5.5). To convert soil carbon to soil organic matter, it is usually assumed that carbon is 58% of organic matter (Brady and Weil 2002). However, this value generally applies to highly stabilised humus, and for most situations a value of 50% is more accurate (Brady and Weil 2002). The sediment at the Boundary Creek swamp has 4.72-19.6% organic matter (Table 5.3). Typically, peat is defined as having less than 35% mineral content or organic matter values of > 65% (Watters and Stanley 2007; Charman 2002; Clymo 1983), although in Australia peat has been defined as terrestrial sediments in which organic matter exceeds 20% dry weight and with a depth of generally greater than 0.3 m (Whinam and Hope 2005). The Boundary Creek swamp sediments do not meet the criteria of the first definition, but have an organic matter content that is very close to the limit for Australian peat (Table 5.5), and therefore, will be referred to as 'peat' for the remainder of this thesis.

Table 5.5 Carbon (wt%) analysis for Boundary Creek swamp

Site	BC1					BC2	BC3
Depth (m)	0.5	1.0	1.5	2.0	2.5	1.5	2.0
Carbon (wt%)	5.03	3.59	6.00	9.54	3.23	9.82	2.36
Calculated organic matter (%)	10.1	7.18	12.0	19.1	6.46	19.6	4.72

Reasonably high levels of acid have already been generated through the oxidation of sulfides at the Boundary Creek swamp, as determined by TAA analysis and measured soil pH (Table 5.6). However, the TSA and CRS values show there is still potential acidity at the site and the sediment has not completely oxidised (Table 5.6). The very low levels of AVS

in some samples suggest the presence of iron monosulfides in amounts too small to be identified by XRD (Table 5.2). The CRS levels confirm the presence of pyrite identified by XRD. The highest CRS value of 0.05% (Table 5.6) converts to 0.15% pyrite within the sediment, which is less than the 2.0 % indicated by the XRD analysis (Table 5.2); the difference probably reflects the variation within the sediment and difficulties in quantifying the small amount of pyrite via XRD.

Table 5.6 Acidity and buffering capacity results for Boundary Creek swamp site

Site	Depth (m)	pH (1:5)	$\%S_{CR}$ (CRS)	$\%S_{AV}$ (AVS)	TAA (mol H+/t)	TSA (mol H+/t)	ANC ($\%CaCO_3$ equivalent)
BC1	0.5	4.08	0.03	0.001	122	363	0.00*
	1.0	3.83	0.02	0.002	131	243	0.00*
	1.5	3.91	0.02	0.002	213	409	0.00*
	2.0	3.42	0.05	<0.001	259	1262	0.00*
	2.5	3.52	0.04	<0.001	209	1344	0.00*
BC2	1.5	4.63	0.02	0.002	81.2	639	0.00*
BC3	2.0	4.57	0.02	<0.001	51.2	252	0.00*

*No carbonates were found and no carbonate modification step was performed

No carbonate minerals were identified at the Boundary Creek swamp, and analysis showed an acid neutralising capacity (ANC) of zero (Table 5.6). This indicates that any alkalinity generated by the reduction of sulfate (Chapter 1) has been removed from the system, and there is no other source of buffering capacity. Therefore, neutralisation by carbonate dissolution will not occur at the site, and any generated acid will cause a drop in pH.

Davidson & Lancaster (2011) also analysed the ASS in the swamp along Boundary Creek (Table 5.7; Figure 5.11). Their sites SB14, SB15 and SB16 are within the swamp itself, while SB8, SB9, SB10 and SB11 are located downstream, within land previously drained for agriculture. For the samples taken within the swamp, the values for both TAA and CRS are, on average, higher than those analysed in this study (Table 5.6), probably because the samples analysed for this thesis were taken from the wall of the fire trench, which may have been partially oxidised prior to sampling so that some acidity has washed away, whereas Davidson & Lancaster's samples were taken from holes dug into the swamp. One sample (SB14) with extremely high TAA and CRS values (1174 moles H^+/tonne and 16.03% respectively) shows that there are small areas with very high concentrations of iron sulfide minerals within the swamp sediments.

The TAA and CRS values from the samples taken by David & Lancaster on the drained land are substantially lower, as these samples have had time to oxidise since the land was drained for agriculture; most of the acidity released has been washed from the soil by rainfall events.

Table 5.7 TAA and CRS values from Davidson & Lancaster (2011) (samples collected 1-4 March, 2010)

Site	SB8	SB9	SB10	SB11	SB14	SB15					SB16
Depth (m)	0.1	0.1	0.1	0.1	0.8	0-0.2	0.2-0.3	0.4	0.5	0.8	0.1
TAA (mol H+/t)	174	263	698	543	1174	352	276	284	265	237	499
$\%S_{CR}$ (CRS)	0.01	0.02	0.04	0.05	16.03	0.07	0.18	0.26	0.87	1.70	0.09

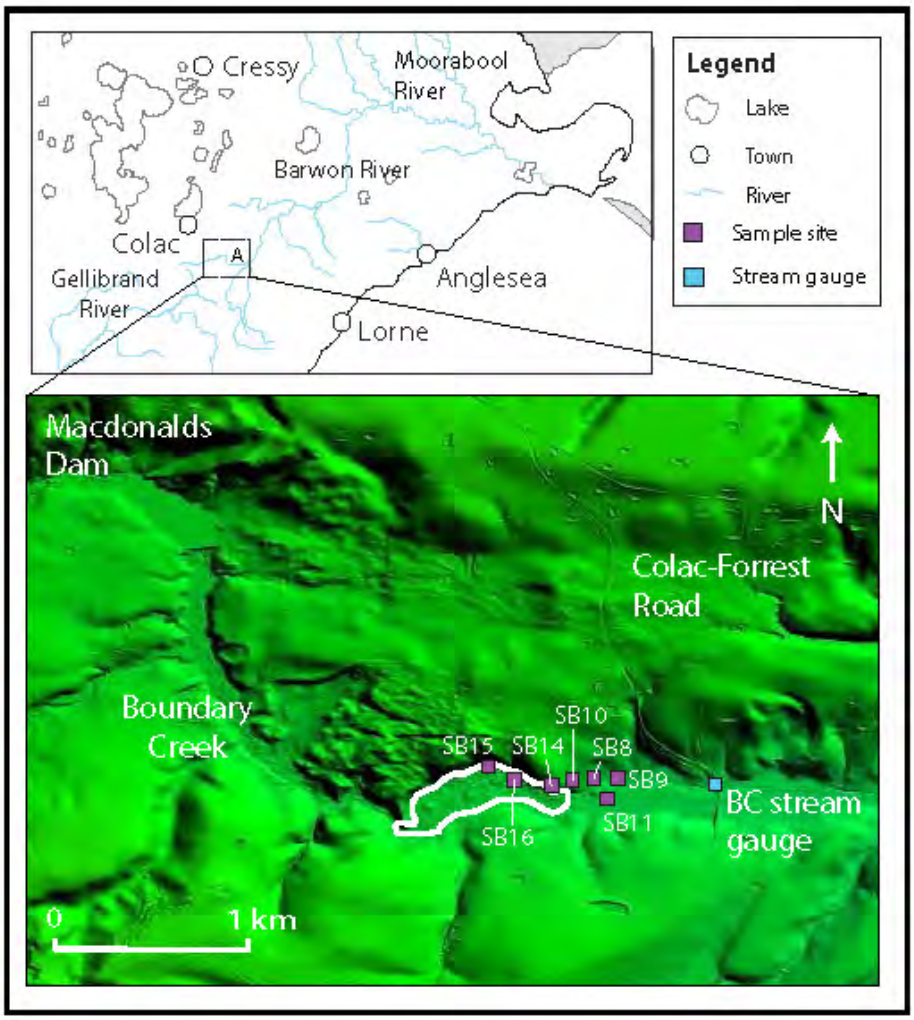

Figure 5.11 Location of sample sites from Davidson & Lancaster (2011)

For the Boundary Creek sediment, the CRS exceeds the ANC, and the TAA is above zero. As the CRS also exceeds the trigger levels, following the classification scheme (Chapter 1), the Boundary Creek swamp is an **actual acid sulfate soil (AASS)** throughout all layers of the profile to 2.5 m depth.

5.1.3 Surface water composition

Surface water analyses were conducted at several sites along Boundary Creek (Figures 5.12, 5.13 & 5.14), both upstream and downstream of the swamp. Inland ASS have

previously been linked with dryland salinity, as saline groundwater contains abundant sulfate, which is necessary for the formation of iron sulfide minerals (Wallace et al. 2005a; Wallace et al. 2008b). However, the swamp at Boundary Creek does not show this association, as the water upstream of the swamp is fresh (360-470 µS/cm), with low sulfate levels (< 10 mg/L) (Tables 5.8 and 5.9). This indicates that saline water is not a limiting factor in the development of inland ASS, and given enough time, ASS can occur in freshwater environments.

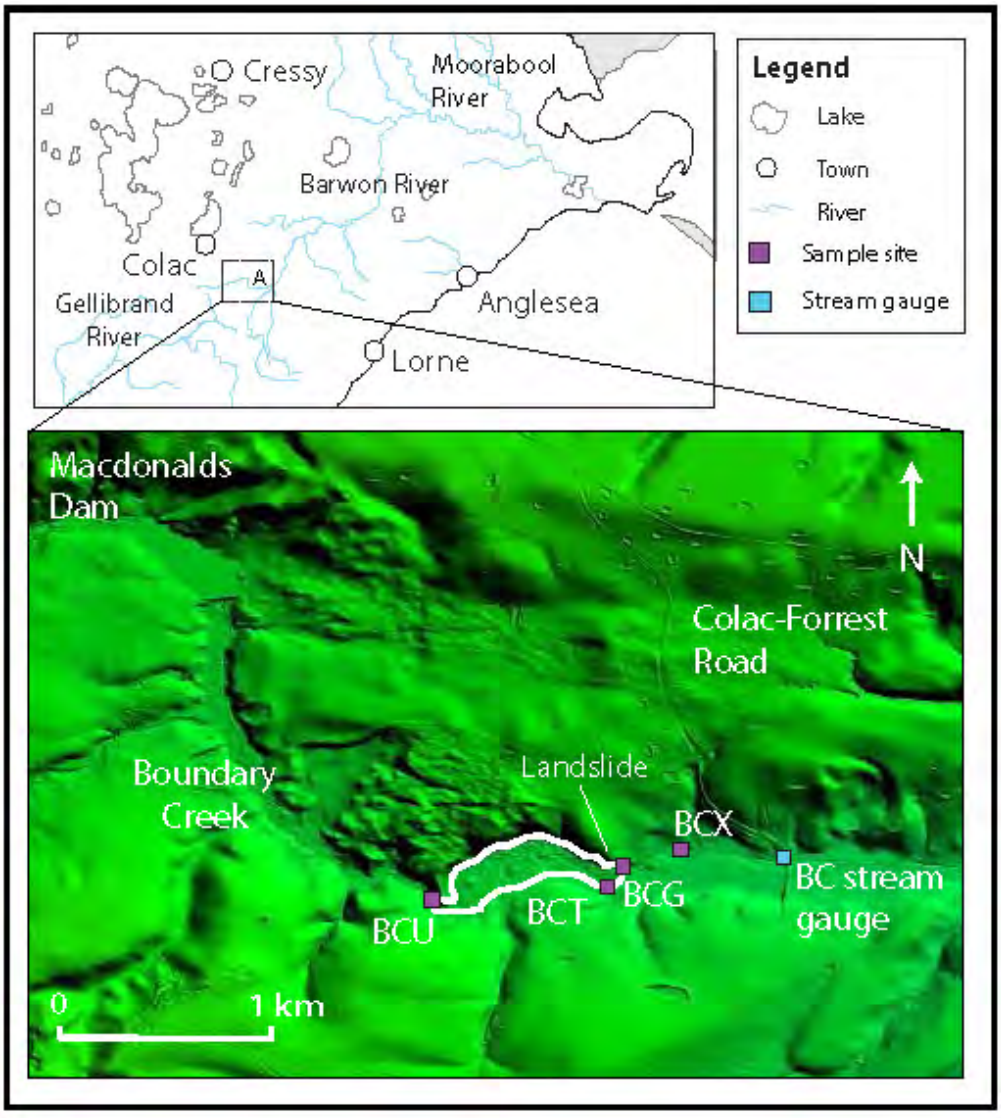

Figure 5.12 Location of water sampling locations at Boundary Creek swamp

Figure 5.13a and b (a) BCU and (b) BCG water sample points (see Figure 5.12 for locations)

Figure 5.14a and b (a) BCX and (b) BC Gauge water sample points (see Fig. 5.12 for locations)

Table 5.8 Surface water field measurements at Boundary Creek swamp site

Sample Name	Date Collected	EC (µS/cm)	Eh (mV)	pH	DO (ppm)	Temp (°C)
BCU 1	14.05.2010	360	276	5.97	N/A	11.6
BCU 2	13.10.2010	374	88.0	6.66	6.90	14.3
BCU 3	01.11.2011	470	N/A	6.16	4.10	14.5
BCT 2	13.10.2010	776	376	4.07	5.50	12.9
BCT 3	01.11.2011	970	N/A	3.09	5.40	14.7
BCG 1	14.05.2010	1710	395	3.20	N/A	11.1
BCG 2	13.10.2010	672	470	3.55	9.40	15.2
BCG 3	01.11.2011	1020	N/A	2.64	5.30	17.1
BCX 1	14.05.2010	1640	328	3.47	N/A	11.6
BCX 2	13.10.2010	430	268	4.64	8.10	13.7
BCX 3	01.11.2011	560	N/A	4.20	6.40	14.2
BC Gauge 1	14.05.2010	1490	323	3.65	N/A	14.7
BC Gauge 2	13.10.2010	613	381	4.02	6.40	12.7
BC Gauge 3	01.11.2011	650	N/A	3.24	5.10	14.9

Boundary Creek upstream of the swamp shows a pH close to neutral (6.66 to 5.97). As water moves through the Boundary Creek swamp, the pH decreases by at least two pH units before it reaches the fire trench (Table 5.8; Figure 5.4b), accompanied by a reduction in alkalinity (Table 5.9). The decrease in pH corresponds to a rise in electrical conductivity (EC), mainly as a result of the increase in sulfate due to oxidation of the iron sulfides to

sulfuric acid (Table 5.9). Downstream of the study site, the EC decreases as the pH increases along Boundary Creek, probably due to the dilution from tributary gullies; however compared to Boundary Creek upstream of the swamp site, EC remains elevated while the pH remains acidic (Table 5.8; Figure 5.15). Iron staining is present both in the trenches of the swamp site and along the immediately downstream section of Boundary Creek (Figures 5.13b & 5.14), confirming that the increased acidity and EC were released from the oxidation of the iron sulfide minerals in the swamp sediments; the iron released has precipitated as orange-brown ferric hydroxide.

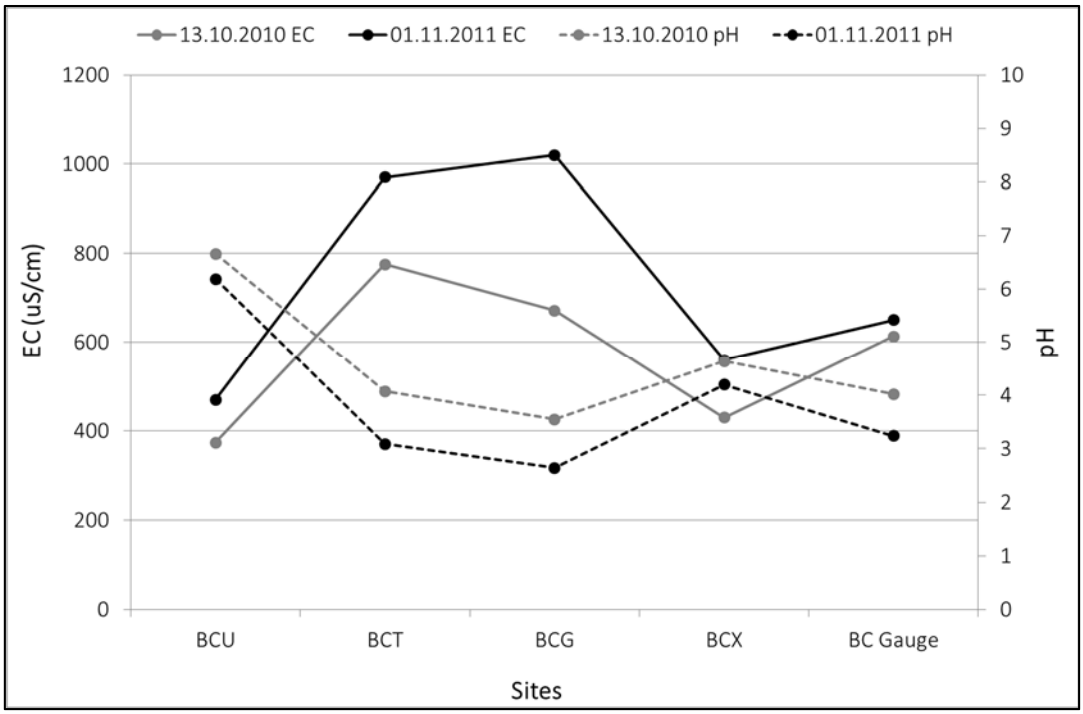

Figure 5.15 pH and EC levels at Boundary Creek swamp site

Chloride levels show a smaller increase in concentration, matched by increases in calcium, magnesium, sodium and potassium (Table 5.9). When the concentrations of all these species were standardised to chloride (Figure 5.16), they show very little difference. This

indicates that the increase is due to evapotranspiration within the swamp, which concentrates all these species equally; evaporation exceeds rainfall in the summer months (Chapter 3).

Table 5.9 Major cation and anion analysis of the surface water from Boundary Creek swamp site (see Table 5.6 for sampling dates)

Sample Name	Calcium (mg/L)	Magnesium (mg/L)	Sodium (mg/L)	Potassium (mg/L)	Chloride (mg/L)	Alkalinity (mg/L)	Sulfate (mg/L)	Aluminium (mg/L)	Iron (mg/L)
BCU 2	8.23	8.10	53.0	3.60	102	28.2	8.08	0.00	0.00
BCT 2	17.5	17.0	75.0	4.20	149	0.00	101	9.43	1.36
BCG 2	11.3	8.42	45.0	5.20	84.0	0.00	145	13.4	2.68
BCX 2	8.50	8.78	52.0	4.10	97.0	0.00	108	5.06	0.58
BC Gauge 2	15.8	11.0	60.0	4.00	120	0.00	138	7.36	1.60
BCU 3	9.57	9.10	60.0	3.10	112	29.0	9.65	0.00	0.00
BCT 3	24.3	20.1	91.0	5.70	196	0.00	57.0	12.8	1.21
BCG 3	12.0	8.70	62.0	5.40	120	0.00	109	6.89	11.4
BCX 3	8.63	8.36	59.0	3.90	113	0.00	47.0	4.32	1.55
BC Gauge 3	13.4	9.02	63.0	3.60	120	0.00	67.2	4.78	1.56

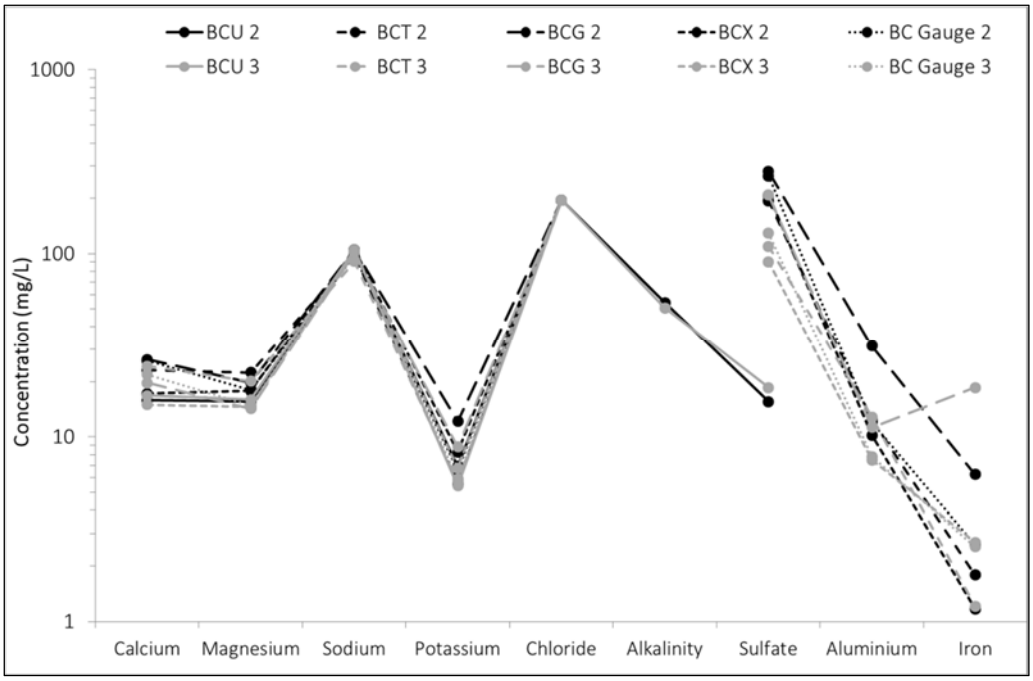

Figure 5.16 Schoeller plot of stream concentrations (standardised to chloride)

The increase in concentration of iron and aluminium in the stream downstream of the swamp (Table 5.9) is greater than the effect of evaporation alone (Figure 5.16), and reflects the solubility of these species at low pH. The aluminium is probably being released due to acid attack on the clay minerals within the sediment. High levels of both iron and aluminium are reaching the stream gauge, due to flushing into the creek from the swamp (Table 5.9). At the stream gauge, historic pH measurements fluctuate between pH 3 and 7 (Figure 5.17) according to the flow, with higher flows after rainfall events particularly in the cooler, wetter months of June to August (Chapter 3), diluting the acid washed into the creek and raising the pH, and also decreasing the EC, which is high mainly because of the sulfate released from the oxidation of the swamp sediments (Figure 5.18). The acidity and sulfate are further diluted when Boundary Creek discharges into the higher volume flow of the West Barwon.

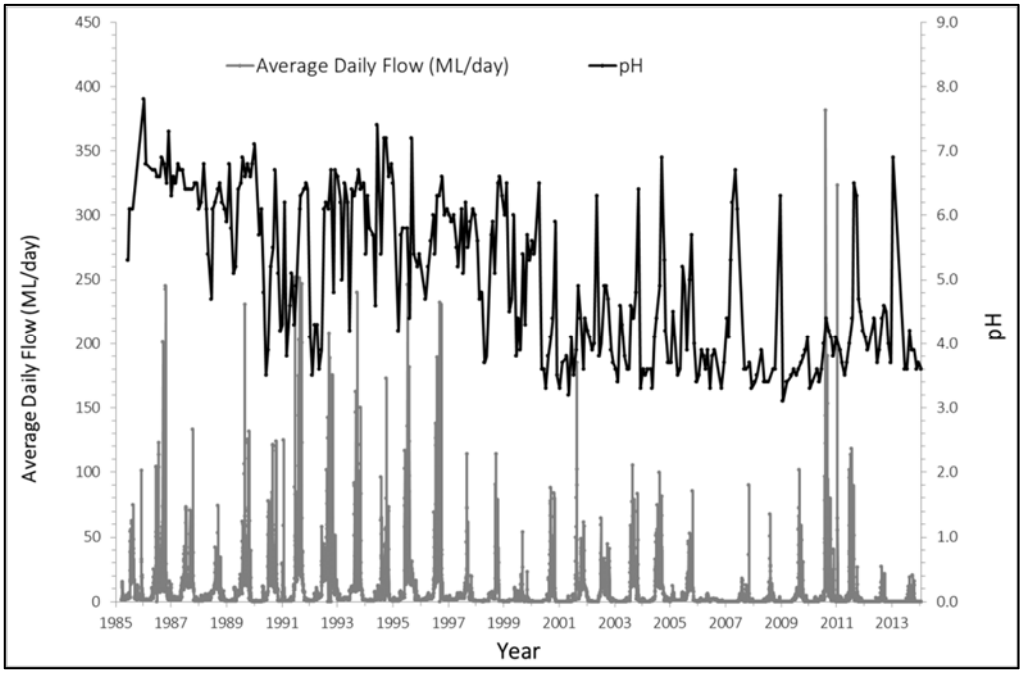

Figure 5.17 Average Daily Flow (ML/day) versus pH in Boundary Creek

(Data source: Victorian Water Resource Data Warehouse)

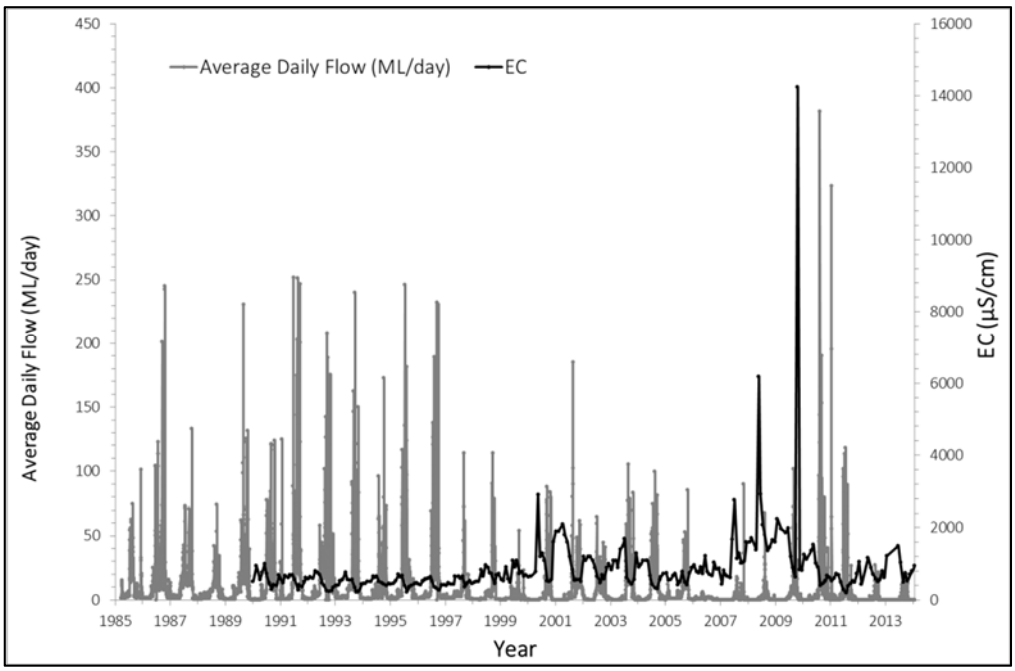

Figure 5.18 Average Daily Flow (ML/day) versus EC in Boundary Creek

(Data source: Victorian Water Resource Data Warehouse)

Trace element analysis of water samples taken at the Yeodene stream gauge and analysed by the Colac Otway Shire show that of the elements analysed (arsenic, cadmium, lead, mercury, nickel, aluminium, iron and manganese), only nickel, aluminium and manganese are present in sufficient quantities to exceed ANZECC health guidelines (Table 5.10).

Table 5.10 Water quality of Boundary Creek at Yeodene gauge (from Colac Otway Shire)

Sample taken	Nickel (mg/L)	Manganese (mg/L)	Aluminium (mg/L)	Iron (mg/L)
04/03/2009	0.110	N/A	N/A	N/A
23/04/2009	0.073	N/A	N/A	N/A
29/09/2009	0.034	N/A	N/A	N/A
28/10/2009	0.062	N/A	N/A	N/A
09/12/2009	0.088	N/A	N/A	N/A
06/01/2010	0.130	N/A	N/A	N/A
21/04/2010	0.200	N/A	N/A	N/A
22/09/2010	0.035	N/A	N/A	N/A
20/10/2010	0.040	0.074	4.7	3.9
02/02/2011	0.082	0.130	3.2	19.0
02/03/2011	0.100	0.160	3.7	24.0
ANZECC guidelines	0.02**	0.1*	0.2*	0.3*

*Values taken from ANZECC aesthetic guidelines

**Value taken from ANZECC health guidelines

The release of trace elements from soils is largely determined by how they occur (sorption/on/inclusion with minerals, organic complexes) and the pH. A decrease in pH can

lead to sufficient mobilisation of heavy metals to have an environmental impact (Brady and Weil 2002; Hillel 1998; Du Laing et al. 2009), even though the levels in the sediments are relatively low. Heavy rainfall can then leach the metals from the soil into nearby streams (Åström and Corin 2000). The nickel in Boundary Creek was probably released from oxidation of the iron sulfides, while the aluminium and manganese were leached from ASS due to cation exchange reactions and the breakdown of aluminosilicate minerals such as clays. These metals will generally remain in solution until they are reabsorbed on freshly precipitated iron hydroxides (Calmano et al. 1993) or the pH rises enough for precipitation of hydroxide minerals (Åström and Corin 2000).

5.1.4 Summary

Overall, the analysis of the Boundary Creek swamp sediment showed that the 'peat' was oxidising and producing acid at the time of sampling. A lack of carbonate minerals signifies a lack of effective acid buffering capacity (ANC), and therefore the site has no ability to neutralise the acidity produced (Table 5.7). The TSA and CRS results also indicate that there is potential for further oxidation and acid production at the site, both from the upper 'peat' layer and the underlying sands and clays. Analysis of the surface water at the site shows a low pH and lack of alkalinity within and downstream of the swamp, with substantial concentrations of iron and aluminium mobilising from the sediment.

5.2 Anglesea River (Site B)

5.2.1 Site Description

The catchment of the Anglesea River lies on the Victorian coast, approximately 110 km south-west of Melbourne (Figure 5.19). The elevation in the catchment decreases from just under 400 m AHD in the Otway Ranges to sea level at the mouth of the estuary, and the catchment is relatively small and steep compared to catchments to the east (Maher 2011; Pope 2006). The river has two tributaries, Salt Creek to the west and Marshy Creek to the north, which meet approximately 1 km above the head of the Anglesea estuary. The Anglesea River is approximately 40 m in width where the two tributaries meet, but narrows to around 15 m in width in the upper reaches. Each of the sub-catchments of the two tributaries comprise about half of the total catchment and both tributaries have a similar length (Table 5.11). The swamps along the tributaries, however, differ in size, with the swamp along Marshy Creek having an area of approximately 2.24 km^2, while Salt Creek swamp has a substantially lesser area of approximately 0.93 km^2 (Figure 5.19).

Table 5.11 Sub-catchment areas of the Anglesea Catchment (Pope 2006)

Sub-catchment	Area (km^2)	Area (%)	Length (km)
Salt Creek	51.2	41.0	15.0
Marshy Creek	65.0	52.0	17.5
Estuary	8.74	7.0	2.6

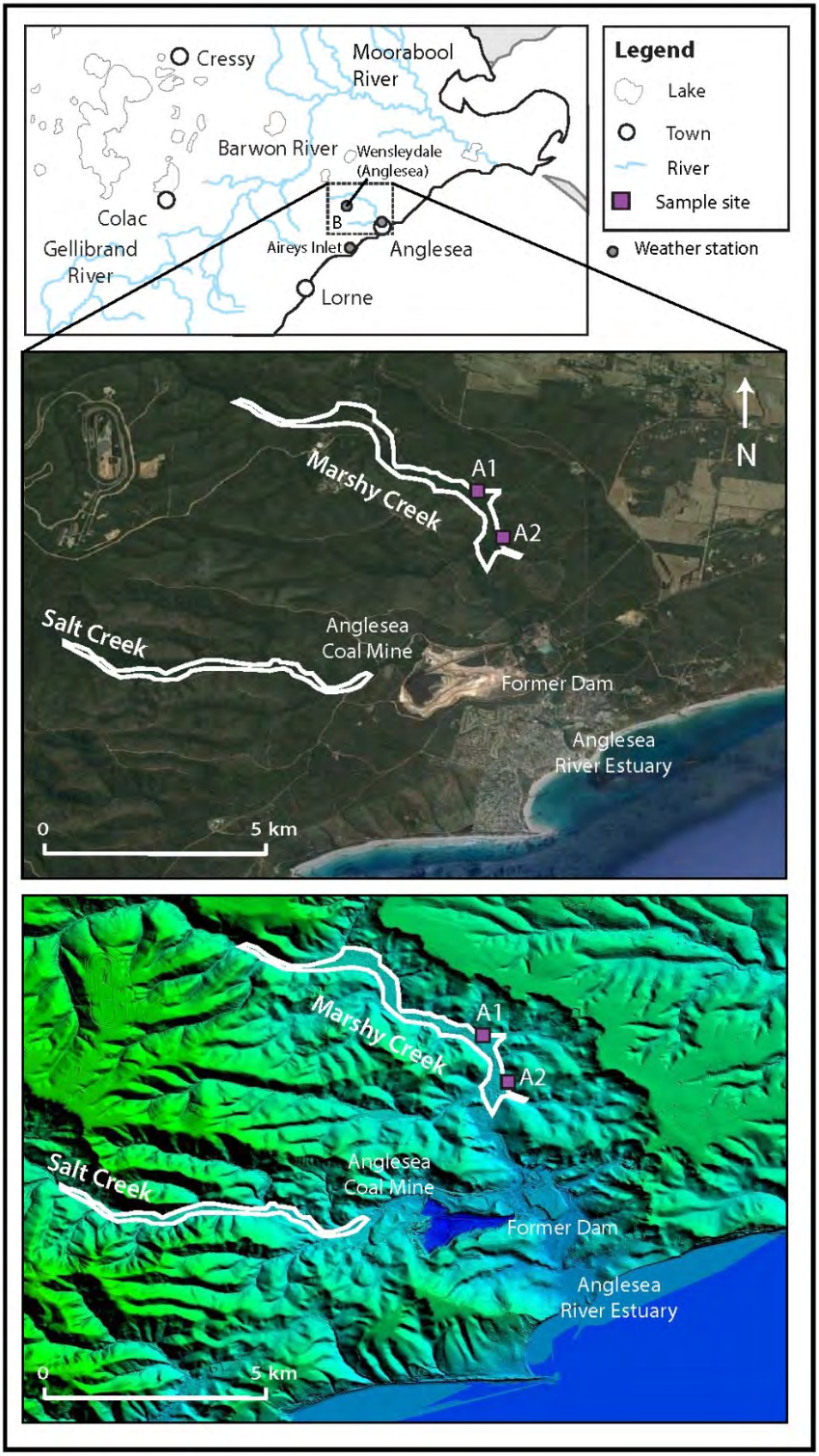

Figure 5.19 Google Earth and LIDAR images of Anglesea swamp

As at Boundary Creek, the local climate is markedly influenced by the Otway Ranges (Chapter 3). The average annual rainfall at Anglesea is approximately 650 mm (Table 5.12), with rainfall highest between August and October (Figure 5.20). The area has relatively low average temperatures, around 20˚C as a maximum (data from Bureau of Meteorology, Australia). Mean monthly evaporation is exceeded by rainfall from May to September, with the highest potential evaporation occurring in January and February, when temperatures are highest (data from the Bureau of Meteorology, Australia).

Like Boundary Creek, the Anglesea River experiences seasonal flows due to this variable rainfall. In summer and autumn, a natural period of low or no flow corresponds to the months where evaporation exceeds rainfall, and therefore no runoff occurs. This rainfall variation causes seasonal fluctuations of the underlying watertable of approximately 1 m, with the seasonal low rainfall and high evaporation leading to declines in watertable that can dry out the wetlands, although moisture is retained within the soil (Lithgow 2007). The watertable is replenished by subsurface flow as well as rainfall in the winter months (Boulton et al. 2014).

Table 5.12 Rainfall data summary of nearby stations to Anglesea (data from the Bureau of Meteorology, Australia) (sites are shown on Figure 5.19)

Station Name	Latitude	Longitude	Elevation (m)	Measurement period	Average annual rainfall (mm)
Anglesea	38.41° S	144.20° E	95 m	1926-2005	658.6
Wensleydale (Anglesea)	38.37° S	144.08° E	220 m	1965-current	814.0
Aireys Inlet	38.46° S	144.09° E	95 m	1994-current	634.9

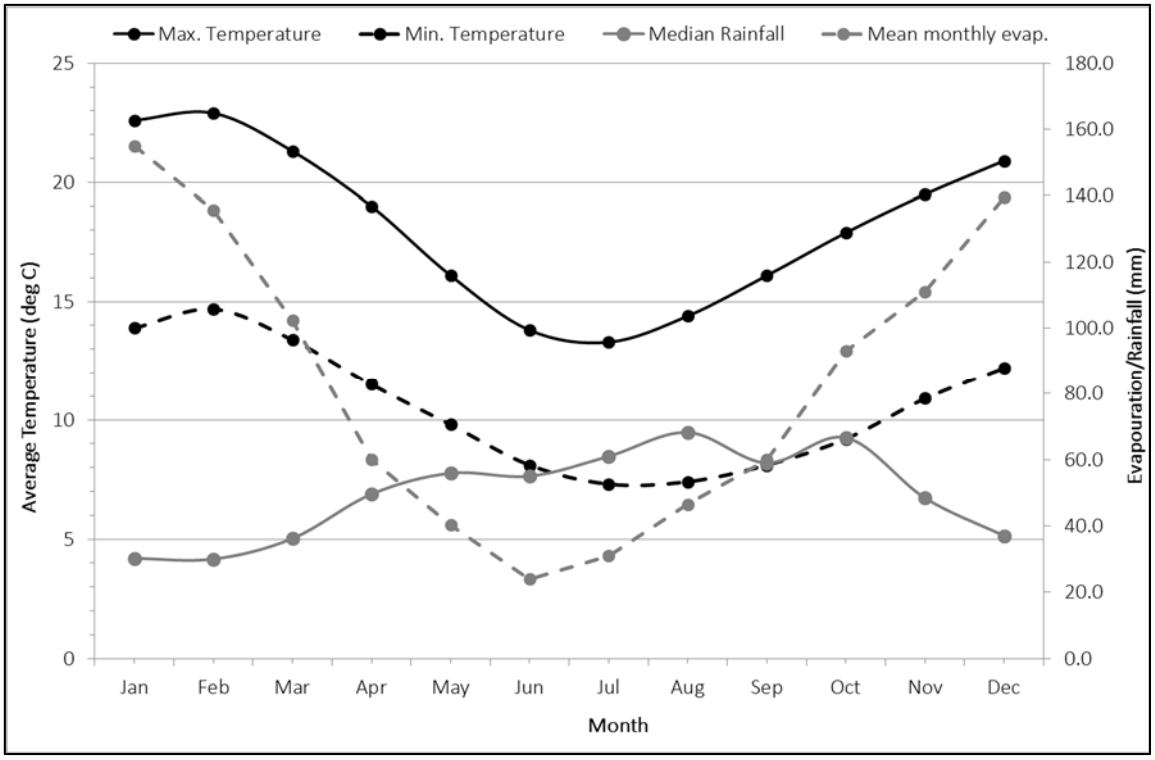

Figure 5.20 Average seasonal variation for Aireys Inlet (temperature), Anglesea (rainfall) and mean monthly evaporation (Durdidwarrah)

(Rainfall and evap. given as mean monthly values and temperatures as mean daily 3pm temperatures)

Most of the Anglesea catchment is covered by intact native vegetation, with only a small fraction of the outer areas of the catchment cleared for grazing. The vegetation surrounding the swamps along Marshy Creek (Figure 5.23a) consists of heathland and dry-sclerophyll forest, which form part of the 67.31 km^2 Anglesea Heath, located to the north of Anglesea, as well as the Angahook-Lorne State Park to the south and west, and the Anglesea Flora Reserve and the Otway State Forest to the north of the heathland (Pope 2006; Parks Victoria 2002). Marshy Creek swamp (Figure 5.23b) contains tea-trees, usually dominated by Woolly Tea-Tree (*Leptospermum lanigerum*), with associated vegetation consisting of Scented Paperbark (*Melaleuca squarrosa*), Blackwood (*Acacia melanoxylon*)

and Tall Saw-sedge (*Gahnia clarkeii*) (DSE 2005b; Deparment of Natural Resources and Environment 2000).

Settlement of the area surrounding Anglesea began in 1845, and after the discovery of lignite (brown coal), the first lignite mine near Anglesea opened in 1895. Mining closed down in 1905, and reopened close to the current Alcoa open-cut site in the 1950s. The current Alcoa lignite mine began its 50-year lease in 1961 and is located in the lower reaches of Salt Creek, which has been diverted around the open-cut pit via a concrete channel (Figure 5.19). The lignite is burnt to supply power to the Point Henry aluminium smelter; the power station is located where the tributaries merge just north of Anglesea (Figure 5.19; Pope 2006; Parks Victoria 2002). The power station releases water to the Anglesea estuary from the ash ponds, which continually overflow. Groundwater seepage from the mine pit, which is ten times smaller than the overflow from the ponds, also flows into the Anglesea estuary (Pope 2006). The lignite seam being mined is in the upper section of the Eastern View Formation, and has an average sulfur content of 3.8% (dry weight), although peaks in sulfur content of up to 5% have been recorded (Holdgate et al. 2001).

The Anglesea catchment lies within a highly dissected, low elevation plateau on the eastern flanks of the Otway Ranges (Figure 5.19). Bedrock comprises the Neogene Eastern View Formation, which is up to 500 m thick, and contains the lignite seams mined in the open cut; these sediments are folded into the Anglesea Syncline (Holdgate and Gallagher 2003). The alluvial, estuarine and swamp sediments along the river are Quaternary in age (Figure 5.21). The soils are pale grey sands with clay at depth; along the creeks are gradational soils which can be sandy and high in organic matter (Robinson et al. 2003; Clarkson et al. 2007).

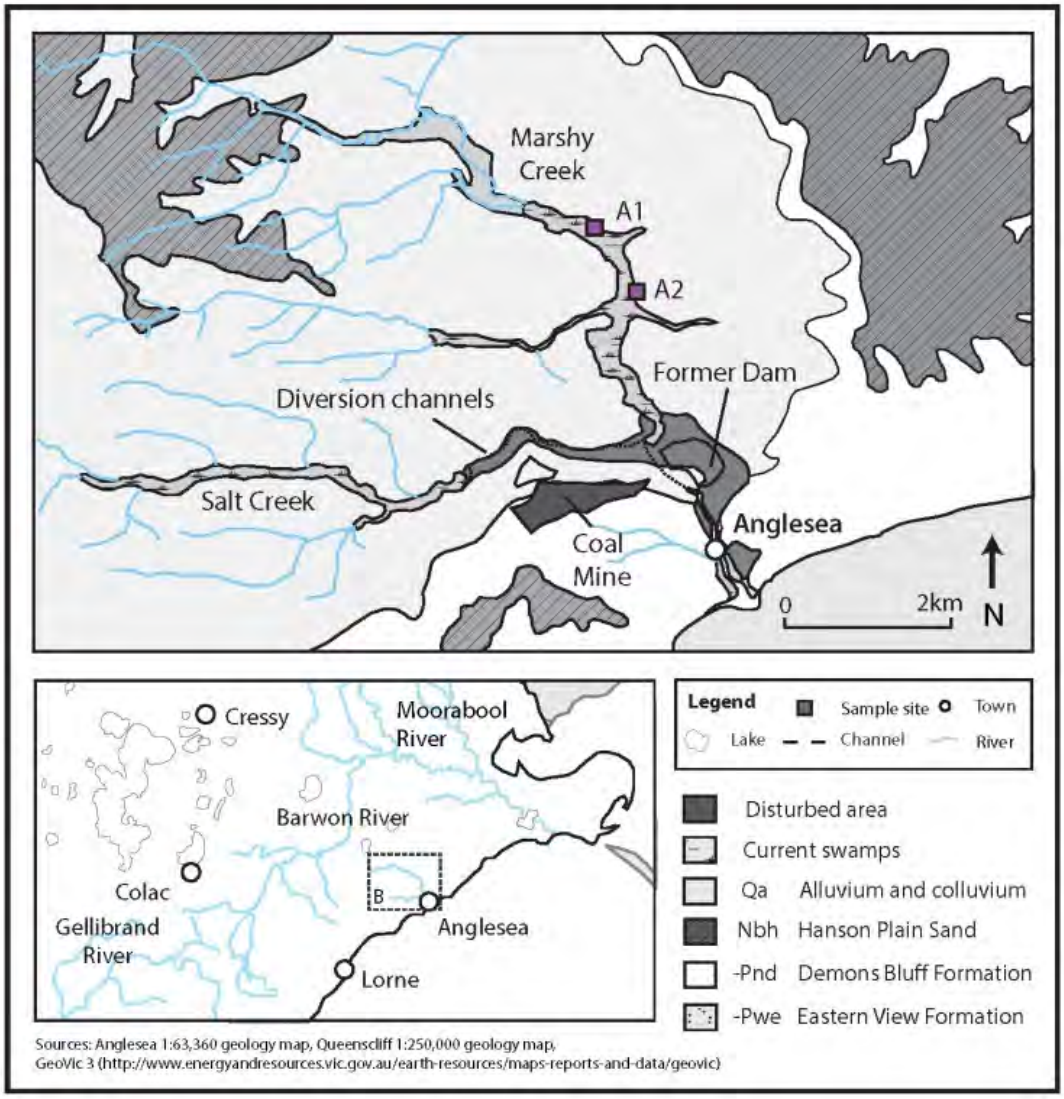

Figure 5.21 Geology map of Anglesea catchment

The swamps along the tributaries of the Anglesea River fall outside the coastal zone, as they lie above the range of tidal inundation due to the rise in slope above the estuary (Figure 5.22), and also lie above the Holocene highstand (+ 2.0 m). Therefore, the ASS of the Anglesea swamps are inland rather than coastal ASS, despite their proximity to the coast. Coastal ASS are found in estuarine systems, mangrove swamps and backswamps, and are influenced by marine processes (NRMMC 2006; Lewis et al. 2013), whereas inland

ASS are found in environments such as river and stream channels and wetlands (Fitzpatrick and Shand 2008). The proximity to the coast allows sea spray to mix with rainfall, providing a high source of sulfate to the Anglesea River swamp.

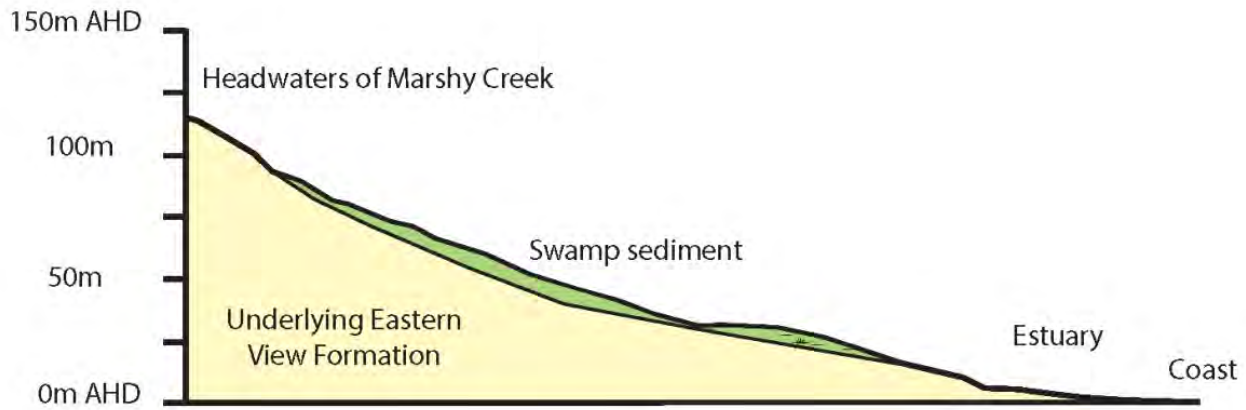

Figure 5.22 Long section of Marshy Creek

The rise in sea level after the Last Glacial Maximum (LGM) at around 20 ka allowed sediment to build up in the coastal river valleys of the Otways, forming the swamps.

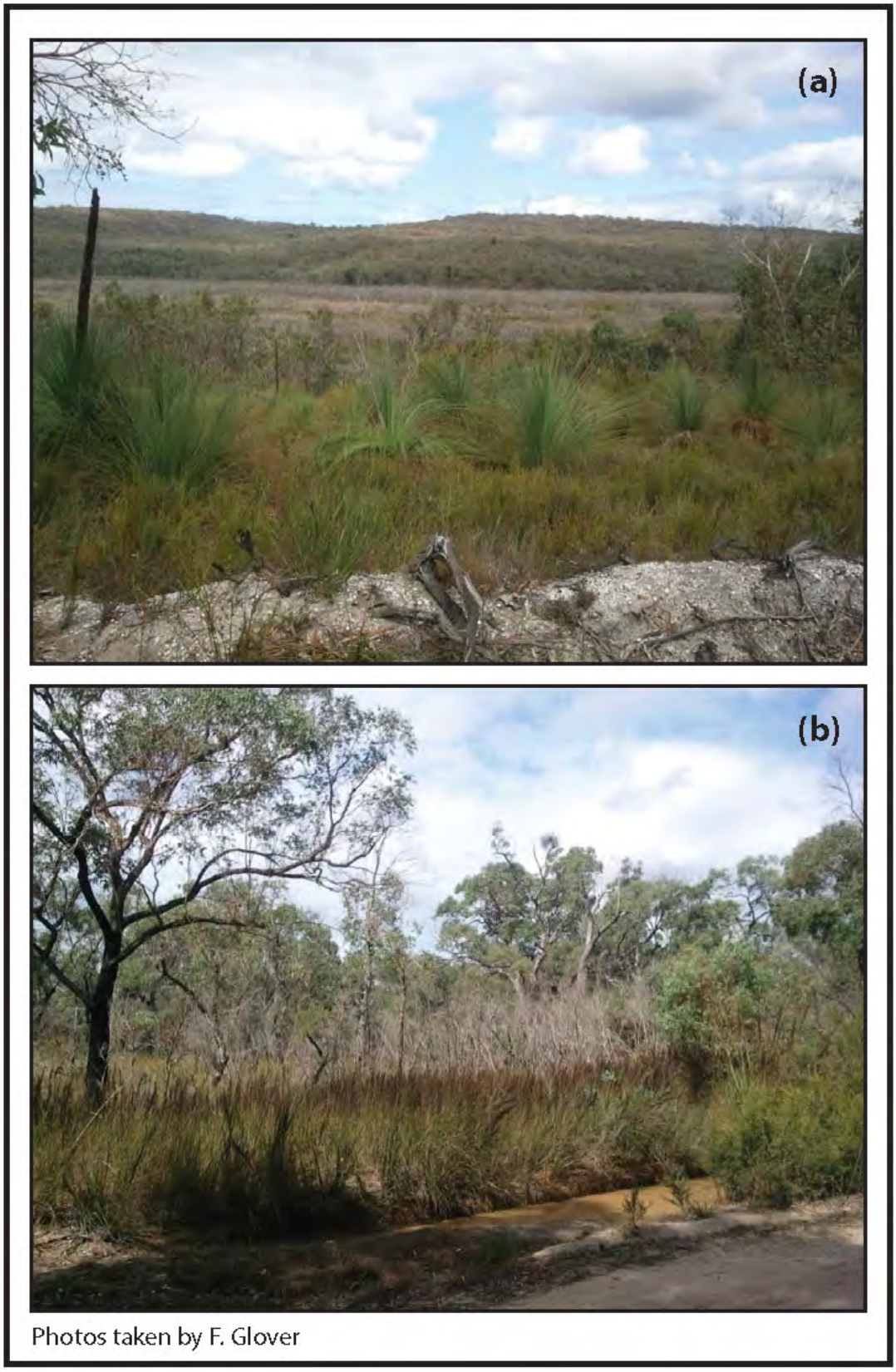

Figures 5.23a and b Anglesea Swamp site

5.2.2 Acidification Events in the Anglesea Estuary

The Anglesea River and estuary have experienced periodic low pH (pH 3-4) events, where pH was consistently low over several months, resulting in the death of fish, sea grass and invertebrates within the estuary. These events generally occurred when dry periods (typically mid-summer to autumn) were followed by a rainfall event (Maher 2011), which flushed any acidity that accumulated during the dry period down the river. Similar acid events and fish kills are seen in other rivers (such as the Richmond River in NSW and the Pocomoke Sound in Somerset County, USA) after a dry period immediately followed by rainfall (Demas et al. 2004; Sammut et al. 1996).

There is a lack of consensus as to the cause of these events (CCMA 2012; Arthur Rylah Institute 2011); the two potential sources of acidity identified are the exposed lignite-bearing sediments of the Eastern View Formation and the tea-tree swamp sediments along the upper sections of Marshy and Salt Creeks (Maher 2011). Open cut mining in the area has exposed marcasite bands within the lignite to the atmosphere, allowing them to oxidise and generate acidity, and Maher (2011) regarded this as the most likely cause of the acidification events. Potential ASS occur in the swamp sediments along Marshy and Salt Creeks, but Maher (2011) considered that these were unlikely to be a major source of acidity, as they only covered 2% of the total area of the catchment; however, no chemical analysis was conducted on the sediments prior to this study to quantify their potential acid-generating capacity.

5.2.3 Sediment characterisation

Two sites were sampled along Marshy Creek (Figure 5.19). Layering within the peat was not obvious, but a grey sandy layer was encountered beneath the peat at each site. While each of the sample cores was semi-saturated with water from a depth of approximately 0.2 m, at the time of sampling there was no obvious flow of water through the swamps. Sampling occurred in February during the mid-summer period, when there is typically no flow.

The inorganic component of the sediments within the profile is mostly fine-medium sand sized, with lesser amounts of silt and almost no clay, matching the sandy nature of the local soils. The grain size was mostly uniform down the profile, with the silt content increasing slightly with depth (Figure 5.24).

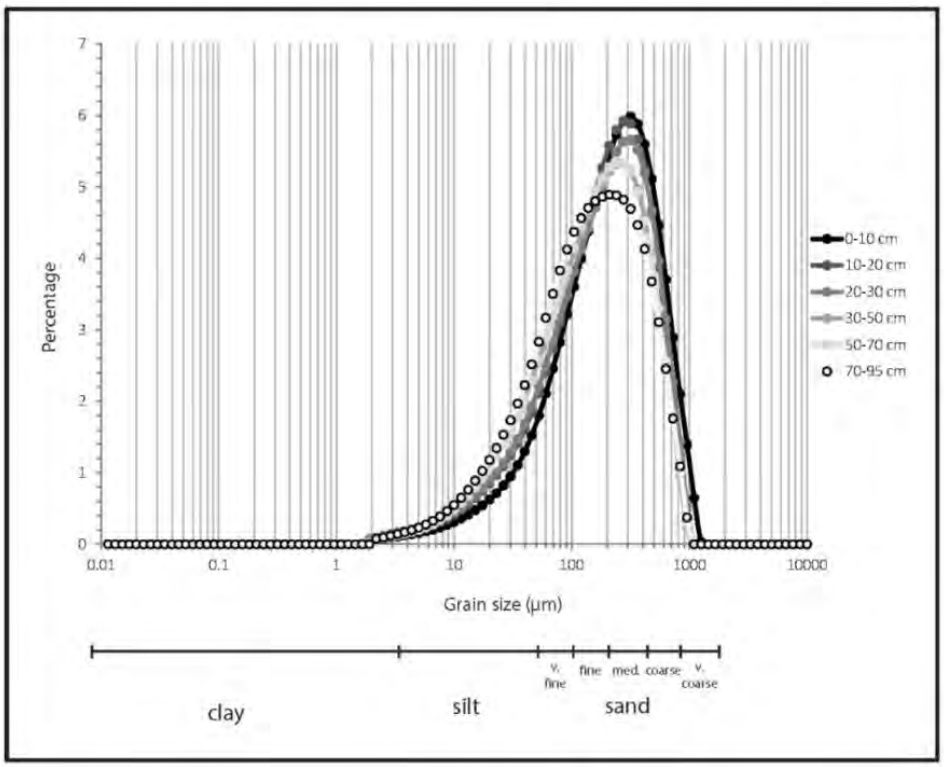

Figure 5.24 Grain size analysis for the sediment samples from A2

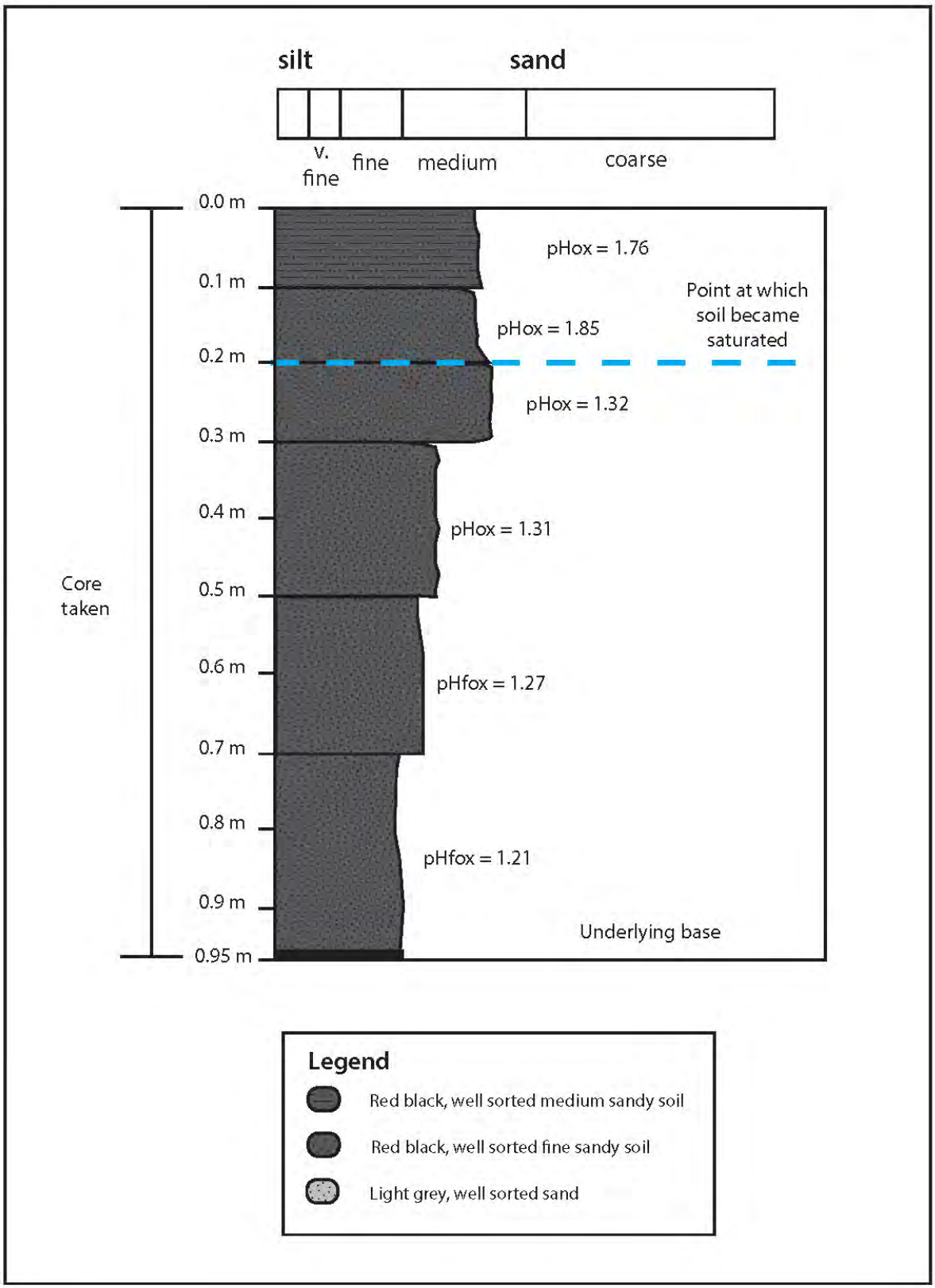

Figure 5.25 Stratigraphic column of sediment at A2

Field oxidation pH tests of samples from site A2 found the top 0.95 m of sediment contains a large potential for generating acidity (Figure 5.25), due to the accumulation of sulfide minerals in the waterlogged environment. Part of this profile was above the watertable during sampling, but Marshy Creek can rise over 1.0 m after a rainfall event (Lithgow 2007), so the sediment within the swamps is seasonally saturated, as discussed previously.

XRD analysis on the Marshy Creek sediment showed that it contains abundant quartz, with lesser amounts of kaolinite and illite, and small amounts of pyrite and iron hydroxide (Table 5.13). The silica and aluminium levels determined by XRF reflect the presence of quartz and the clay minerals (Table 5.14). The composition of the sediment varies with depth, with quartz and clay abundance inversely correlated. Quartz is the major mineral present within the basal layer, likely due to the influence of the sand immediately below (Table 5.14).

Table 5.13 Mineral composition (wt %) of Anglesea swamp sediments

Site	Depth (m)	Quartz	Illite	Kaolinite	Pyrite	Iron Hydroxide	Chi-squared value
A1	0-0.1	41.2	31.1	27.7	-	-	1.63
A2	0-0.1	69.8	18.7	9.00	1.40*	1.10*	3.02
	0.1-0.3	30.5	31.1	36.4	0.40*	1.70*	1.98
	0.5-0.7	21.3	39.6	37.2	1.90*	-	1.94
	0.7-0.95	71.7	17.8	8.00	2.50*	-	2.70

*Values below 5% are not considered accurate

Sulfur levels are not high enough for all iron within the sediment to be present as pyrite (Table 5.14), and some iron is present as iron hydroxide, as indicated by the XRD analysis (Table 5.13). No carbonate minerals were found within the sediment, and calcium and magnesium levels are low (Table 5.14).

Table 5.14 Major element composition (wt %) of Anglesea swamp

Site	Depth (m)	SiO_2	TiO_2	Al_2O_3	Fe_2O_3	MnO	MgO	CaO	Na_2O	K_2O	P_2O_5	SO_3	LOI	Total
A2	0-0.1	63.0	1.33	3.06	1.92	0.00	0.15	0.25	0.11	0.30	0.06	0.51	28.5	**99.2**
	0.3-0.5	23.0	0.56	8.87	8.39	0.00	0.44	0.64	0.26	0.38	0.10	1.21	56.5	**100.4**
	0.5-0.7	23.6	0.59	9.21	7.46	0.00	0.32	0.45	0.40	0.42	0.11	0.26	57.3	**100.1**
	0.7-0.95	73.6	1.30	3.11	1.73	0.00	0.14	0.22	0.14	0.27	0.05	0.39	20.1	**101.1**

Table 5.15 Trace element composition in mg/kg

Site	Depth (m)	Arsenic (As)	Chromium (Cr)	Cobalt (Co)	Lead (Pb)	Molybdenum (Mo)	Nickel (Ni)	Zinc (Zn)
A2	0-0.1	4.40	21.5	2.30	14.1	7.40	45.2	12.8
	0.1-0.3	11.6	47.8	0.00	14.5	17.0	48.2	19.2
	0.5-0.7	11.8	54.0	0.00	14.3	16.1	48.0	22.1
	0.7-0.95	0.00	23.7	2.20	14.0	5.50	44.9	9.70
Australian background range*		0.2-30	0.5-110	2-170	2-200	1-20	2-400	2-180
Global background range**		0.1-48	5-1000	1-40	10-67	0.5-40	1-200	10-300

*(Australian averages from ANZECC and NHMRC 1992)

**(Global averages from Pias and Jones 1997)

The swamp sediment was uniform dark-grey in colour, and contained obvious organic matter. Calculated organic matter levels (based on analysed carbon content) varied between 21.6% and 66.8% (Table 5.16). These levels place the sediment above the threshold for Australian peat, with the highest level also exceeding the more widely accepted international definition of peat (> 65%) (Watters and Stanley 2007; Whinam and Hope 2005; Charman 2002). The Marshy Creek sediment is therefore defined as a peat for this thesis.

Table 5.16 Carbon (wt%) analysis for Anglesea swamp

Site	A2					
Depth (m)	0-0.1	0.1-0.2	0.2-0.3	0.3-0.5	0.5-0.7	0.7-0.95
Carbon (wt%)	14.0	30.8	33.4	31.0	28.6	10.8
Calculated organic matter (%)	27.9	61.6	66.8	62.0	57.2	21.6

Carbon dating, conducted by Beta Analytic, of the sediment at approximately 0.5 m depth gave an age of 70 ± 30 years Before Present (BP), and the sediment at 0.7-0.95 m depth was dated as 1220 ± 30 years BP. The Holocene highstand believed to have allowed the swamp sediments to accumulate was at approximately 5-6 ka (Lewis et al. 2013); the younger age of the carbon dates may be potentially due to contamination of the sample sent for analysis by plant roots than contain younger carbon.

TAA analysis and the soil pH shows that acidity is already present within the Marshy Creek swamp (Table 5.17), and therefore oxidation of sulfides is already occurring. In addition, TSA and CRS levels show there is still potential acidity within the site, and the sediment has not completely oxidised (Table 5.17). No AVS was found above the detection limit of the

technique, so the sulfides present at the site are in disulfide (pyrite) form, as indicated by the presence of pyrite in the XRD analysis (Table 5.13). The largest CRS value (0.52%) corresponds to 1.94% pyrite within the sediment, which is similar to some of the values from the XRD analysis (Table 5.13). No carbonate minerals were identified within the Marshy Creek swamp, and analysis showed an acid neutralising capacity (ANC) of zero (Table 5.17). Therefore any alkalinity generated by pyrite formation has already been removed from the system, and if the remaining sulfides within the sediments were allowed to oxidise, neutralisation by carbonate dissolution would not occur.

Table 5.17 Acidity and buffering capacity results for Anglesea River sites

Site	Depth (m)	pH (1:5)	%S (CRS)	%S (AVS)	TAA (mol H+/t)	TSA (mol H+/t)	ANC (%CaCO3 equiv.)
A1	0-0.1	4.36	0.04	<0.001	89.6	240	0.00*
	0.1-0.3	3.78	0.03	<0.001	125	655	0.00*
	0.3-0.5	3.21	0.03	<0.001	97.8	810	0.00*
A2	0-0.1	3.45	0.05	<0.001	229	884	0.00*
	0.1-0.2	3.14	0.05	<0.001	133	1041	0.00*
	0.2-0.3	3.72	0.06	<0.001	134	2882	0.00*
	0.3-0.5	3.58	0.33	<0.001	348	1629	0.00*
	0.5-0.7	3.74	N/A	N/A	135	1764	0.00*
	0.7-0.95	3.49	0.52	<0.001	147	2041	0.00*

*No carbonates were found and no carbonate modification step was performed

Within the Marshy Creek sediment, CRS exceeds the ANC, and TAA is present. As the CRS also exceed the trigger levels, this classifies (Chapter 1) the Anglesea swamp as **actual acid sulfate soils (AASS)** throughout all layers of the profile.

Due to the level of acidity already present in the swamp sediments, it is evident that the source of acidity for the acidification events in the Anglesea River is the upstream swamp sediments, and it can be predicted that the Anglesea River will undergo further acidification events if the swamps are flushed with large enough rainfall events.

Lithgow (2007) found that cadmium, zinc, manganese and copper were leached into the Anglesea estuary after an acid event in July, 2007. While the levels of zinc, manganese and copper were below the ANZECC guidelines for aquatic environments (ANZECC 2000), cadmium levels were well in excess. The metals were released from the swamp sediment by the low pH (3.3 above the estuary); there are significant levels of zinc present within the sediment (Table 5.15).

5.2.4 Summary

The analysis of the Anglesea swamp sediment shows oxidation is already occurring and acidity is being produced. This acidity remains within the sediment profile due to the lack of effective buffering capacity (ANC), and is flushed into the creek following a rainfall event. In addition to the acidity already being produced, the TSA and CRS results indicate there is still a large potential for further oxidation and acid production within the swamp.

5.3 Porcupine Creek (Site C)

5.3.1 Site Description

Porcupine Creek is located in the upper reaches of the Gellibrand River catchment and is an important tributary of the Gellibrand River (Figure 5.26). Most of the Porcupine Creek catchment is located within the Barongarook State Forest in the southern Otway Ranges.

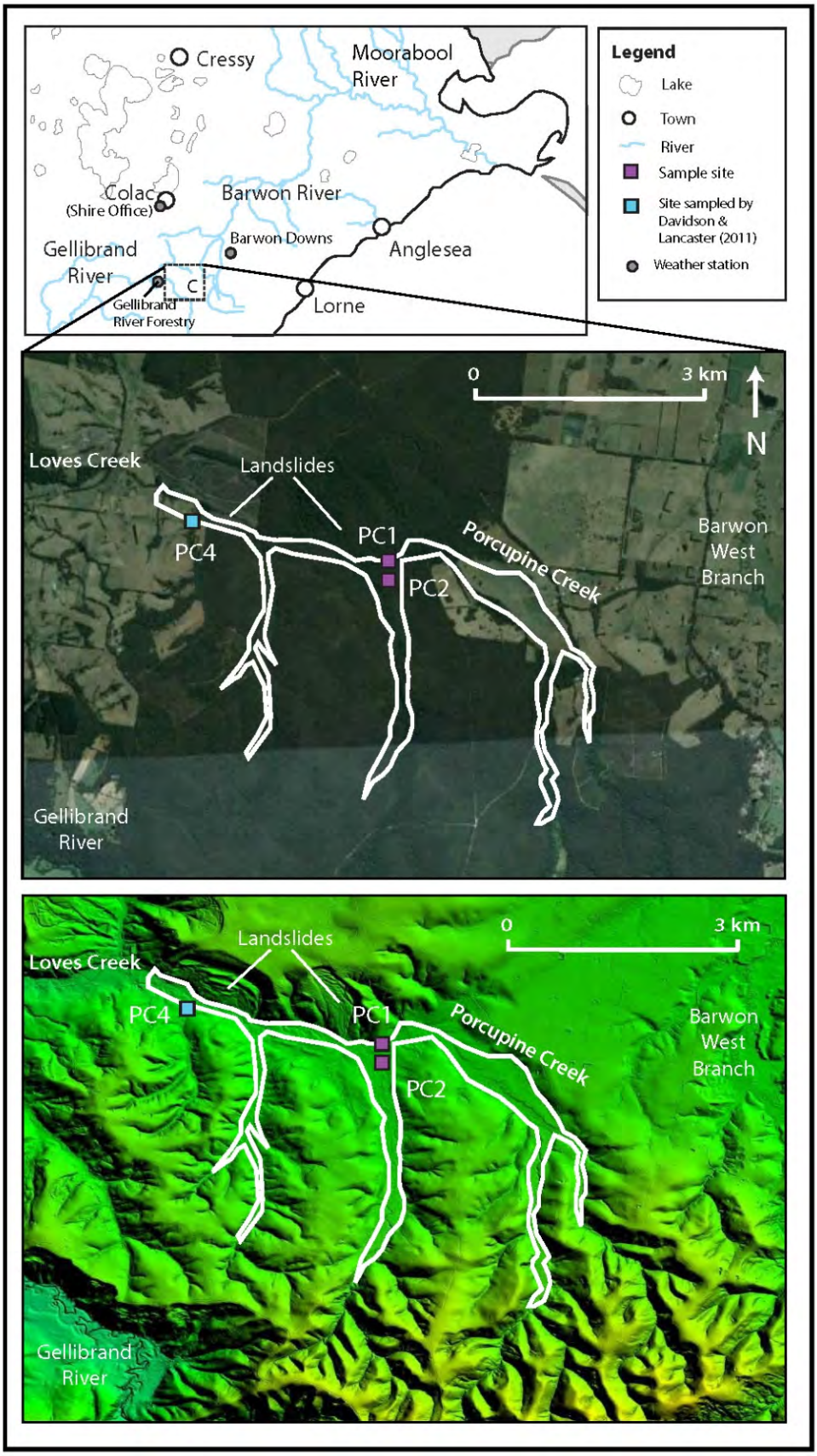

Figure 5.26 Location of Porcupine Creek swamp site

The upper catchment of the Gellibrand River is one of the wettest parts of Victoria, and is mostly covered by undisturbed wet sclerophyll forest and remnant areas of cool temperate rainforest. The Porcupine Creek catchment also contains a large wetland that, as logging was limited in the area, is relatively unaltered by European settlement (OREN 2003). The swamp lies along three unnamed tributaries of Porcupine Creek (Figure 5.26), which, from west to east, have areas of approximately 0.13 km^2, 0.27 km^2, and 0.67 km^2, respectively. The middle of the three was sampled for analysis (Figure 5.26).

The Otway Ranges have a large impact on rainfall at Gellibrand, with an average annual rainfall of 1021 mm (Table 5.18). Temperatures are generally highest in January and February (Figure 5.27), when the highest potential evaporation also occurs (data from the Bureau of Meteorology, Australia). The high rainfall in the upper catchments contributes to the mean annual regulated flow of the Gellibrand River of 315,000 ML; however, annual flows vary considerably. Flows are highest from June to November, when rainfall is highest, while the lowest flows usually occur during March (Stephenson 2005).

Table 5.18 Rainfall data summary of nearby stations to Gellibrand (data from the Bureau of Meteorology, Australia) (sites shown on Figure 5.26)

Station Name	Latitude	Longitude	Elevation (m)	Measurement period	Average annual rainfall (mm)
Colac Shire Office	38.34° S	143.58° E	134	1899-current	726.6
Barwon Downs	38.47° S	143.75° E	151	1888-current	781.9
Gellibrand River Forestry	38.53° S	143.54° E	89	1956-current	1021.3

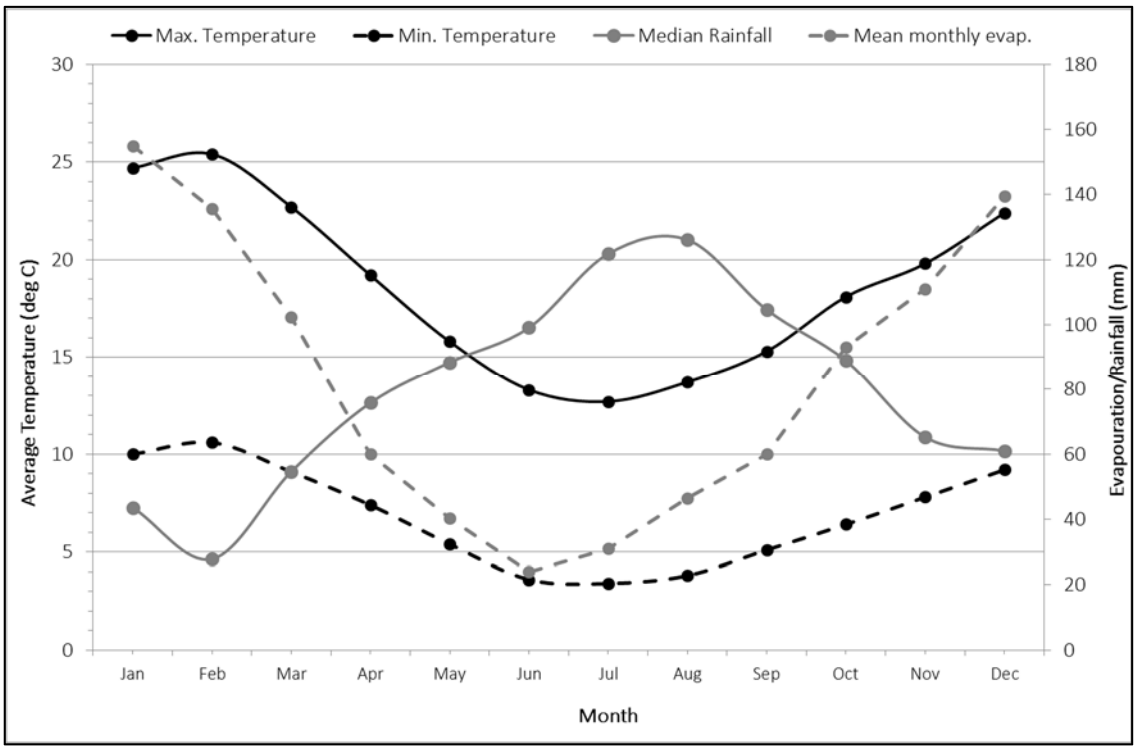

Figure 5.27 Average seasonal variation for Gellibrand (temperature and rainfall) and mean monthly evaporation (Durdidwarrah)

(Rainfall and evap. given as mean monthly values and temperatures as mean daily 3pm temperatures)

The bedrock of Porcupine Creek catchment is the Gellibrand Marl, separated by the Bambra Fault Zone from the Dilwyn Formation (Figure 5.28). Landforms in the area are characteristically rounded hills separated by broad valleys, and drainage is weakly rectilinear, favouring the south-east and north-east directions (Robinson et al. 2003). Landslides are common on the slopes along the Gellibrand River and its tributaries (Clarkson et al. 2007), and vary in size from a few square meters to more than 1.2 km^2. They are mostly triggered by prolonged and/or high intensity rainfall, and the majority occur on either Otway Group rocks or the Gellibrand Marl (Clarkson et al. 2007; Dahlhaus et al. 2006b). On the LIDAR topography there is evidence of two landslides along Porcupine

Creek (Figure 5.26); these dammed the creek, causing the valley upstream of the landslides to infill with sediment and forming the swamp, as evident by the wide areas of Quaternary sediment on the geology map along Porcupine Creek upstream of the landslides (Figure 5.28).

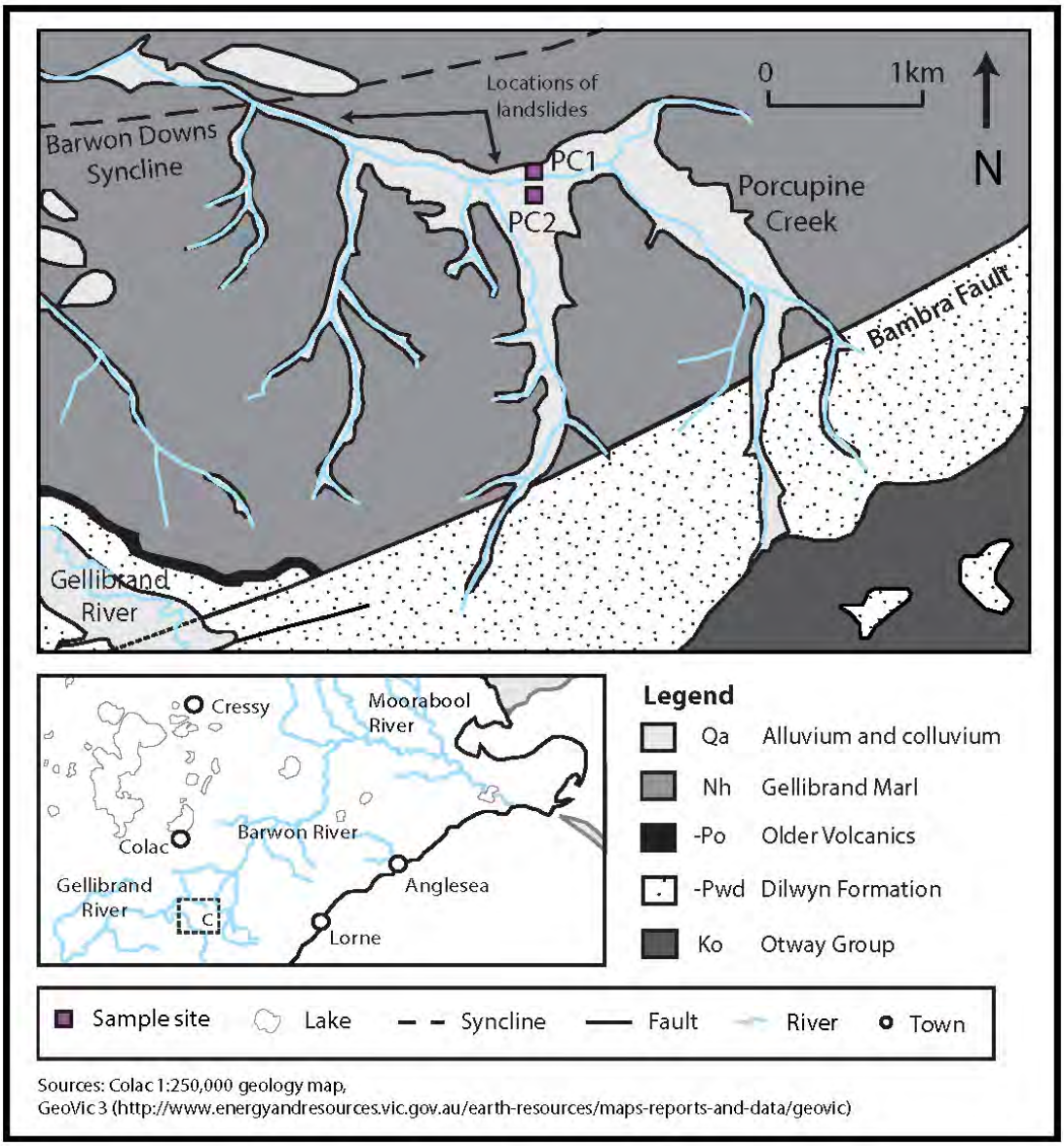

Figure 5.28 Geological map of Porcupine Creek swamp site

Figure 5.29a and b (a) sampling point at Porcupine Creek swamp site (PC2), and (b) sediment core taken from Porcupine Creek swamp site

5.3.2 Sediment characterisation

Samples were taken in only one location near where the middle tributary meets Porcupine Creek (Figure 5.29a), due to issues with access. Swamp sediments at this site were very shallow, with a total depth of 0.4 m above a confining layer of light grey, finer-textured sediment. At the time of sampling, the sediment was mostly dry (Figure 2.29b) and there was no surface water, including in nearby creek channels.

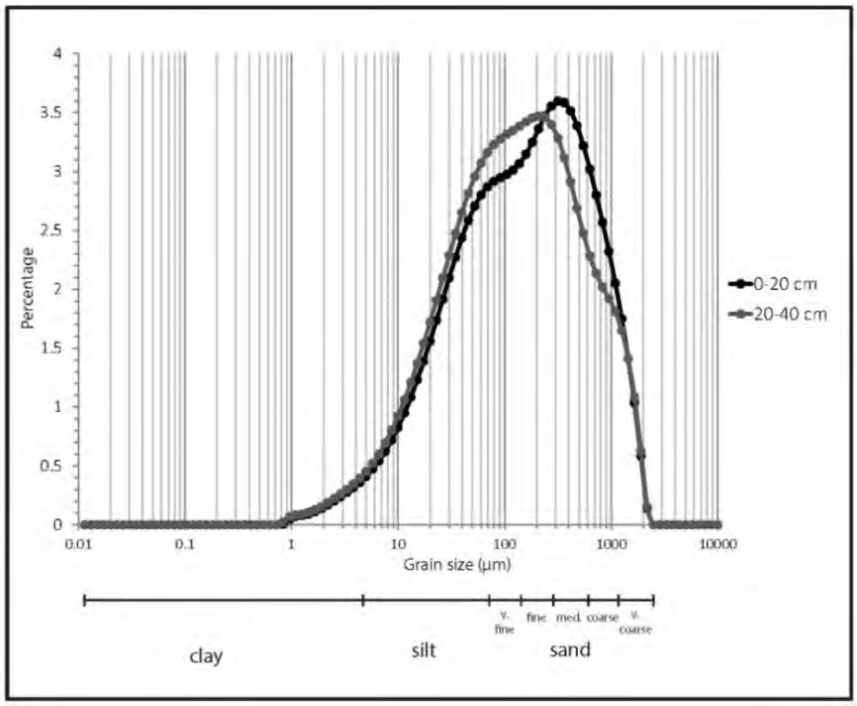

Figure 5.30 Grain size analysis for the Porcupine Creek (PC2) swamp site

The sediment at Porcupine Creek is mostly sand-sized, with lesser amounts of silt and clay (Figure 5.30). This matches the major mineral component of quartz with minor kaolinite and illite, as identified by XRD analysis (Table 5.19). Small amounts of pyrite are also present. The very high levels of silica and low levels of aluminium (Table 5.20) confirm the presence of quartz, with minor illite and kaolinite. Sulfur and iron levels were low (Table 5.20); the iron levels exceed those of sulfur, indicating that not all of the iron is present as

pyrite. No carbonate minerals were found within the sediment, with calcium and magnesium levels also low (Table 5.20).

Table 5.19 Mineral composition (wt %) of Porcupine Creek swamp

Site	Depth (m)	Quartz	Kaolinite	Illite	Pyrite	Chi-squared Value
PC2	0-0.2	81.3	4.30*	12.6	1.80*	**2.61**
	0.2-0.4	82.4	3.80*	11.9	1.80*	**2.72**

*Values below 5% are not considered accurate

Table 5.20 Major element composition (%) of Porcupine Creek swamp

Site	Depth (m)	SiO_2	TiO_2	Al_2O_3	Fe_2O_3	MnO	MgO	CaO	Na_2O	K_2O	P_2O_5	SO_3	LOI
PC2	0-0.2	80.0	1.09	4.41	0.18	0.00	0.19	0.22	0.24	0.43	0.04	0.05	11.4
	0.2-0.4	76.3	0.97	4.64	0.19	0.00	0.22	0.22	0.38	0.46	0.04	0.08	15.5

Table 5.21 Trace element composition in mg/kg of Porcupine Creek swamp

Site	Depth (m)	Arsenic (As)	Chromium (Cr)	Cobalt (Co)	Lead (Pb)	Molybdenum (Mo)	Nickel (Ni)	Zinc (Zn)
PC2	0-0.2	1.60	12.3	3.20	14.0	0.60	44.3	9.60
	0.2-0.4	2.50	18.6	3.20	14.0	0.80	44.3	10.6
Australian background range*		0.2-30	0.5-110	2-170	2-200	1-20	2-400	2-180
Global background range**		0.1-48	5-1000	1-40	10-67	0.5-40	1-200	10-300

*(Australian averages from ANZECC and NHMRC 1992)

**(Global averages from Pias and Jones 1997)

Organic matter was visible throughout the sediment, but only 7.34-9.33% is present (Table 5.22). These levels are relatively low, and therefore the sediment cannot be defined as a peat (Charman 2002; Watters and Stanley 2007; Whinam and Hope 2005). However, due to difficulties with site access, this sample may not be representative of the more waterlogged area of the site, where more peaty sediment is likely to be present.

Table 5.22 Carbon (wt %) analysis for Porcupine Creek swamp

Site	PC2	
Depth (m)	0-0.2	0.2-0.4
Carbon (wt %)	3.67	4.67
Calculated organic matter (%)	7.34	9.33

TAA analysis and soil pH show that there is only a small amount of acidity present within the sediment sampled (Table 5.23). The low TSA and CRS levels indicate there is still some potential acidity within the sediment, and it has not completely oxidised. No AVS analysis was conducted on the sediment due to its dry nature at time of sampling, and all sulfide is assumed to be pyrite. The largest CRS value (0.006%) corresponds to 0.02% pyrite within the sediment, which is substantially less than the pyrite quantified from the XRD analysis (Table 5.19). No carbonate minerals were identified within the Porcupine Creek swamp, and analysis showed an acid neutralising capacity (ANC) of zero (Table 5.23). Therefore if the sulfides within the site were allowed to oxidise, neutralisation by carbonate dissolution would not occur, and a decrease in pH of the sediment could mobilise heavy metals present in the sediment (Table 5.21). As the area is prone to high rainfall in the winter months, any

metals mobilised have the potential to be transported into the creek itself (Brady and Weil 2002; Hillel 1998; Du Laing et al. 2009).

Table 5.23 Acidity and buffering capacity results for Porcupine Creek swamp site

Site	Depth (m)	pH (1:5)	%S (CRS)*	%S (AVS)	TAA (mol H+/t)	TSA (mol H+/t)	ANC (%CaCO3 equiv.)
PC2	0-0.2	5.09	0.006	N/A	6.89	352	0.00**
	0.2-0.4	4.70	0.001	N/A	8.58	730	0.00**

*CRS measured to extra significant figure due to low levels

**No carbonates were found and no carbonate modification step was performed

For the upper layer (0-0.2 m) at PC2, the CRS and TAA are below the trigger levels, and therefore the soil layer is classified (Chapter 1) as a low-risk sulfidic soil. This is possibly due to continued oxidation of any sulfides present and rainfall events washing away any resulting acidity. However, at depth, the CRS exceeds the ANC, and due to the presence of TAA, the soil has been classified (Chapter 1) as a potential acid sulfate soil (PASS).

Davidson & Lancaster (2011) also sampled part of the Porcupine Creek swamp (PC4; Figure 5.26). The TAA and CRS results (Table 5.24) show that the sediments contain both actual and potential acidity; the values are higher than those found for this thesis, probably because the samples were collected from the wetter, more central part of the swamp. This sediment is also classified (Chapter 1) as PASS.

Table 5.24 TAA and CRS values taken from Davidson & Lancaster (2011) (samples collected 1-4 March, 2010 from PC4*)

Site	PC4/05	PC4/06	PC4/07	PC4/08	PC4/09	PC4/10
TAA (mol H+/t)	89	27	27	16	8.0	0.0
$\%S_{CR}$ (CRS)	0.03	0.07	0.07	0.16	0.13	0.02

*Individual depths of samples not given in the report, but total depth of core was 1.5 m

5.3.3 Summary

The analysis of the Porcupine Creek swamp shows that some oxidation is occurring within the sediment (Table 5.23). A lack of carbonate minerals at the site signifies a lack of effective buffering capacity (ANC) in the swamp and therefore a lack of ability to neutralise the acidity produced. The TSA and CRS results indicate there is a potential for further oxidation and acid production.

5.4 Pennyroyal Creek and Bambra Wetlands (Sites D and E)

5.4.1 Site Description

Both Pennyroyal Creek and the Bambra Wetlands sites lie along tributaries of the Barwon River (Pennyroyal and Retreat Creeks respectively), and are found within the upper Barwon catchment on the northern foothills of the Otway Ranges, about 20 km east of Colac (Figure 5.31). The many swamps and wetlands along these tributaries have been drained by the artificial deepening of the stream channels, and the land has been converted to agriculture (mainly grazing of dairy and beef cattle or sheep). Most of the native vegetation has been cleared, including the swamps along the creeks (Rothols and Rowe 1961; CCMA 2013a).

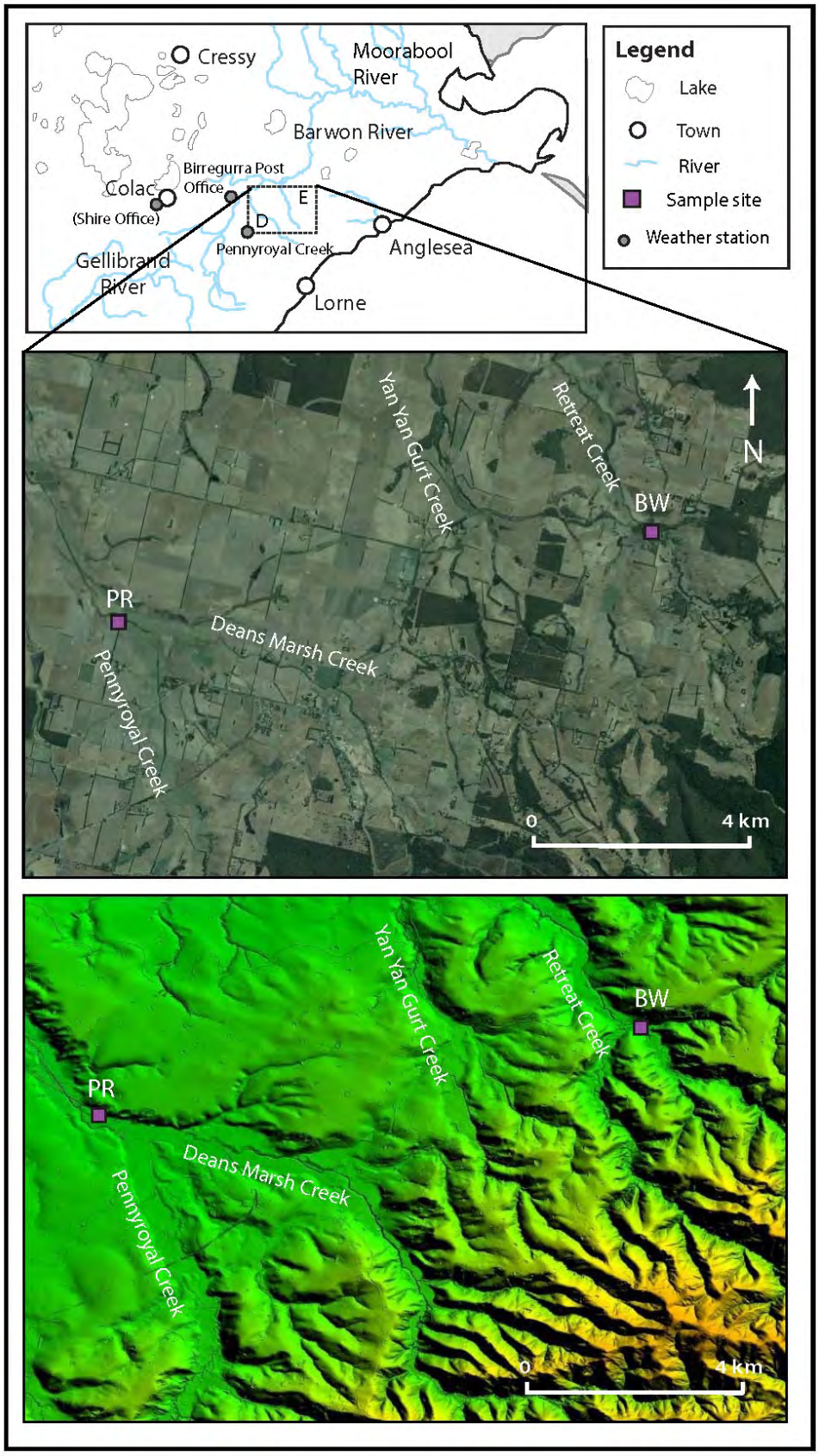

Figure 5.31 Location of Pennyroyal Creek (PR) and Bambra Wetlands (BW) sites

The average annual rainfall in the area is approximately 650-800 mm (Table 5.25), with rainfall highest between July and September (Figure 5.32). Mean monthly evaporation is exceeded by rainfall from May to October, with the highest potential evaporation occurring in January and February, when temperatures are highest (data from the Bureau of Meteorology, Australia).

Table 5.25 Rainfall data summary of stations near Pennyroyal Creek and the Bambra Wetlands (data from the Bureau of Meteorology, Australia) (sites are shown on Figure 5.31)

Station Name	Latitude	Longitude	Elevation (m)	Measurement period	Average annual rainfall (mm)
Colac Shire Office	38.34° S	143.58° E	134	1899-current	726.6
Pennyroyal Creek	38.42° S	143.83° E	160	1881-current	794.8
Birregurra Post Office	38.34° S	143.78° E	119	1903-current	669.5

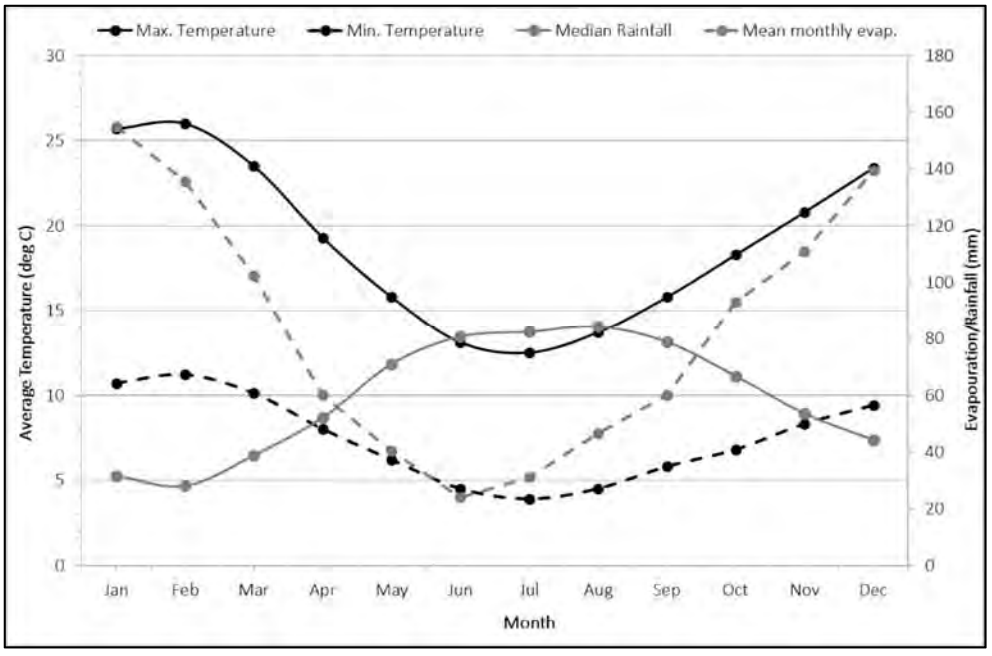

Figure 5.32 Average seasonal variation for Gellibrand (temperature), Pennyroyal Creek (rainfall) and mean monthly evaporation (Durdidwarrah)

(Rainfall and evap. given as mean monthly values and temperatures as mean daily 3pm temperatures)

Pennyroyal and Retreat Creeks flow from the uplifted Cretaceous Otway Group across the easterly dipping Bambra Fault onto the Miocene Gellibrand Marl and Palaeogene Dilwyn Formation (Chapter 3; Figure 5.33; Joyce et al. 2003b; Robinson et al. 2003). The upper parts of the catchments consist mainly of steep hills, becoming lower and rounded downstream, with broad planar crests (Robinson et al. 2003; Rothols and Rowe 1961). Both river channels flow over Quaternary alluvial sediment, which has formed grey gradational soils in the river valleys (Clarkson et al. 2007; Robinson et al. 2003).

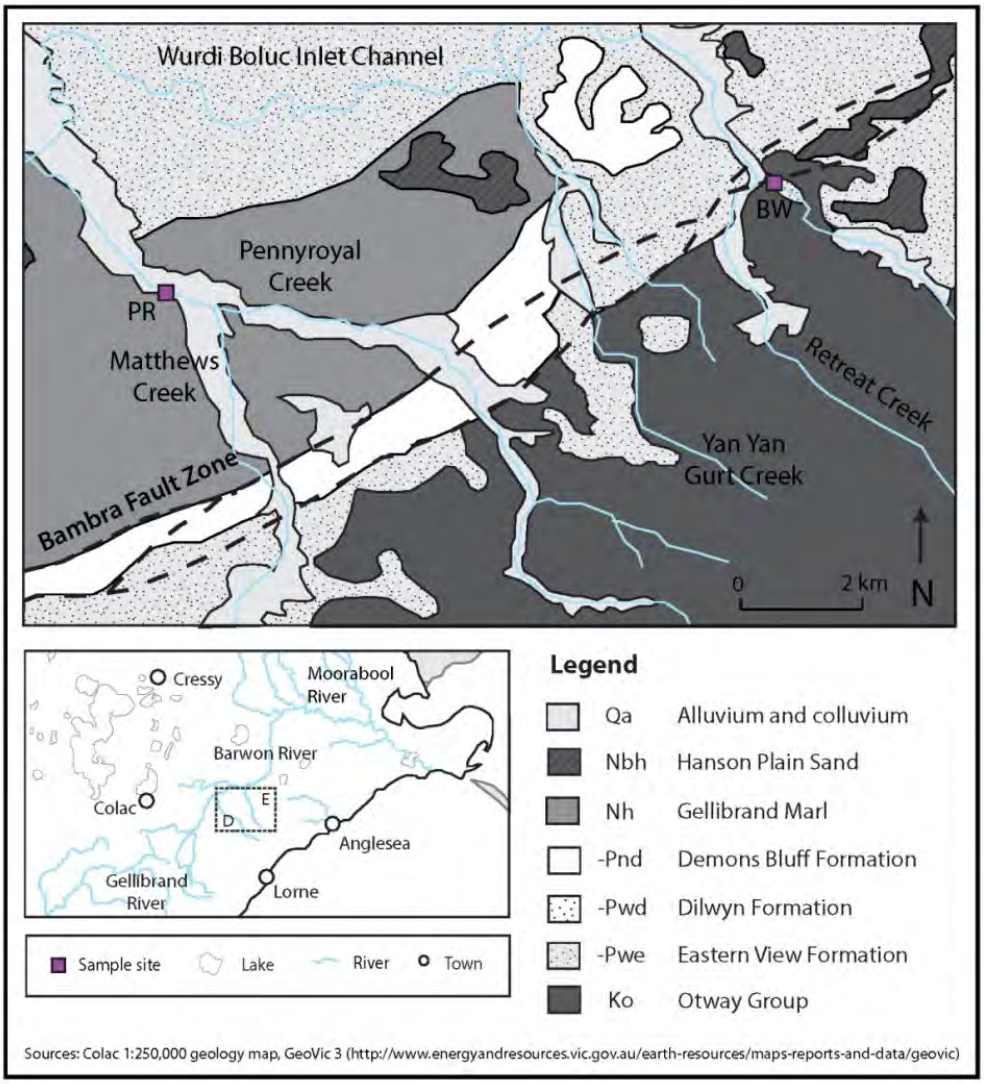

Figure 5.33 Geology map of Pennyroyal Creek and Bambra Wetlands sites

5.4.2 Pennyroyal Creek

Most of the Pennyroyal Creek floodplain has been drained and cleared for agriculture, and is highly altered from its original state (Figure 5.34). As a result, the creek suffers from bank erosion and instability, the presence of exotic flora, channel modifications (deepening of the channel) and degraded riparian vegetation (CCMA 2006a).

Figure 5.34 Pennyroyal Creek site

5.4.2.1 Sediment characterisation

Samples were taken from a small swamp along Pennyroyal Creek that appears to have been drained during the conversion of the surrounding land to agriculture and the building of the nearby road (Figure 5.31). Samples were taken to a depth of 0.4 m before a confining layer was encountered. At the time of sampling, the sediment was completely dry, with no sign of nearby surface water and a little iron staining visible within the sediment. Grain size analysis found that the sediments were both mostly fine-medium sand-sized, with lesser

amounts of silt and clay (Figure 5.35). This matches the gradational soils in the area, which have a sandy component, particularly in the upper part of the profile (Robinson et al. 2003).

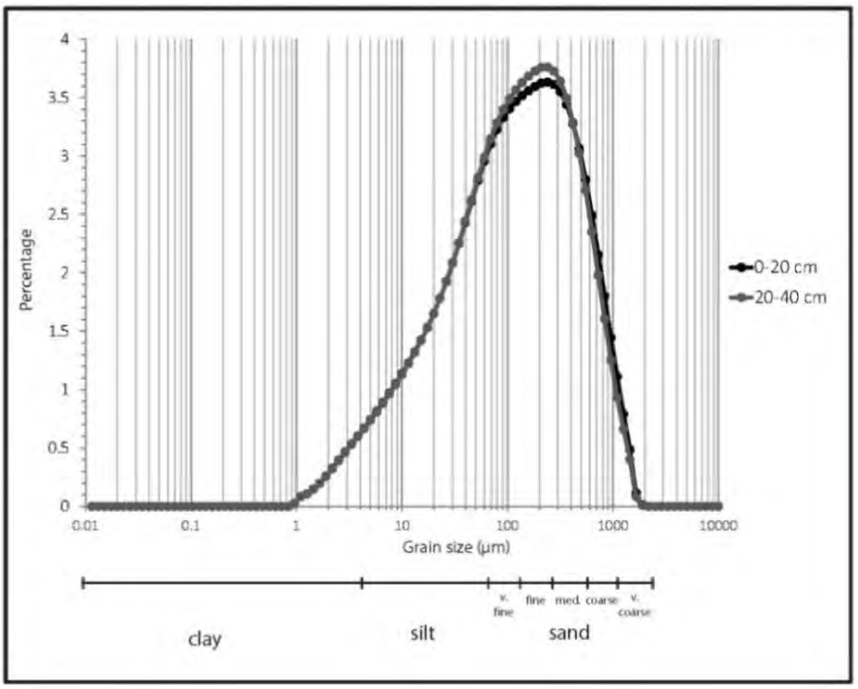

Figure 5.35 Grain size analysis for the Pennyroyal Creek site

XRD analysis on the sediment shows that quartz and illite are the major components, with a small amount of hematite (Table 5.26). XRF analysis showing high levels of silica (Table 5.27) confirms the presence of abundant quartz, with the reasonably high levels of aluminium confirming the presence of clay (illite). Sulfur levels were low, as were iron levels (Table 5.27); no sulfide minerals were found, so it can be assumed that the iron present is mostly as hematite. No carbonate minerals were found within the sediment, with calcium and magnesium levels also low (Table 5.27).

Table 5.26 Mineral composition (wt %) of Pennyroyal Creek and Bambra Wetlands sites

Site	Depth (m)	Quartz	Illite	Kaolinite	Hematite	Goethite	Chi-squared Value
PR	0-0.2	71.3	26.5	-	2.2*	-	**2.63**
BW	0-0.1	63.4	26.4	7.20	1.90*	1.10*	**2.80**
	0.1-0.3	66.2	24.7	6.30	1.90*	0.90*	**2.85**

*Values below 5% are not considered accurate

Table 5.27 Major element composition (%) of Pennyroyal Creek and Bambra Wetlands sites

Site	Depth (m)	SiO_2	TiO_2	Al_2O_3	Fe_2O_3	MnO	MgO	CaO	Na_2O	K_2O	P_2O_5	SO_3	LOI
PR	0-0.2	68.5	1.13	9.88	3.87	0.10	0.64	0.59	0.58	0.66	0.16	0.15	13.8
BW	0-0.1	64.6	0.82	10.9	2.67	0.01	0.74	0.40	1.85	1.47	0.17	0.15	13.5
	0.1-0.3	66.9	0.86	11.6	2.83	0.00	0.74	0.40	1.93	1.45	0.11	0.13	8.43

Table 5.28 Trace element composition in mg/kg of Pennyroyal Creek and Bambra Wetlands

Site	Depth (m)	Arsenic (As)	Chromium (Cr)	Cobalt (Co)	Lead (Pb)	Molybdenum (Mo)	Nickel (Ni)	Zinc (Zn)
PR	0-0.2	8.70	52.9	12.6	14.2	1.60	49.9	52.8
BW	0-0.1	1.50	20.2	6.20	14.1	1.50	49.3	54.6
	0.1-0.3	0.00	27.4	6.80	14.2	0.70	49.9	51.9
Australian background range*		0.2-30	0.5-110	2-170	2-200	1-20	2-400	2-180
Global background range**		0.1-48	5-1000	1-40	10-67	0.5-40	1-200	10-300

*(Australian averages from ANZECC and NHMRC 1992)

**(Global averages from Pias and Jones 1997)

Organic matter was visible throughout the sediment, but calculated levels were only between 4.13% and 9.21% (Table 5.29). This level is well below the threshold for peat, and therefore the sediment cannot be defined as peat (Charman 2002; Whinam and Hope 2005).

Table 5.29 Carbon (wt%) analysis for Pennyroyal Creek and Bambra Wetlands sites

Site	PR		BW		
Depth (m)	0-0.2	0.2-0.4	0-0.1	0.1-0.3	0.3-0.6
Carbon (wt%)	4.61	2.07	5.43	2.69	1.89
Calculated organic matter (%)	9.21	4.13	10.9	5.37	3.77

Table 5.30 Acidity and buffering capacity results for the Bambra Wetlands and Pennyroyal Creek

Site	Depth (m)	pH (1:5)	$\%S_{CR}$ (CRS)	$\%S_{AV}$ (AVS)	TAA (mol H+/t)	TSA (mol H+/t)	ANC ($\%CaCO_3$ equivalent)
BW	0-0.1	4.81	0.005	N/A	8.46	449	0.00*
	0.1-0.3	4.46	0.003	N/A	6.80	155	0.00*
	0.3-0.6	4.67	0.006	N/A	4.30	123	0.00*
PR	0-0.2	7.31	0.002	N/A	0.00**	533	0.00*
	0.2-0.4	6.86	0.002	N/A	0.00**	48.1	0.00*

*No carbonates were found and no carbonate modification step was performed

**TAA is zero, because pH of sediment is above end point of titration

TAA results showed no acidity within the soil (Table 5.30), so no oxidation is currently occurring at the site. The TSA and CRS values show that there is a very small amount of sulfides present (Table 5.30), too small to register in the XRD analysis. AVS analysis was not conducted due to the low CRS values.

As Pennyroyal Creek has previously been drained, any sulfide minerals that built up within the sediment profile due to previous waterlogging have been oxidised and the acidity leached from the sediment. The iron oxide minerals present could be products of this ASS oxidation (Table 5.26). No carbonate minerals were found and analysis showed a lack of acid neutralising capacity (ANC) (Table 5.27). The site is unlikely to undergo acidification as the potential acidity is low, and the trace elements found within the sediment (Table 5.28) will not mobilise. Due to the low levels of CRS, combined with the lack of TAA and ANC and the presence of iron oxides, Pennyroyal Creek is classified (Chapter 1) as a **post-active sulfidic soil** for both layers within the sediment profile.

5.4.3 The Bambra Wetlands

The Bambra Wetlands lie along Retreat Creek, and cover an area of approximately 0.16 km^2 (Figure 5.31). The Bambra Wetlands Reserve is a community project that is revegetating crown land, managed by the East Otway Landcare Group (EOLG) (Figure 5.36a). The wetlands suffer from similar concerns to the Pennyroyal Creek floodplain (erosion, wetland protection and weed control). Landslides and gully erosion are common, with the instability intrinsically linked to past drainage of the original swamps and wetlands (CCMA 2006a).

Figure 5.36a and b (a) the Bambra Wetlands site and (b) the sediment sampled from the Bambra Wetlands

5.4.3.1 Sediment characterisation

The Bambra Wetlands were sampled to a depth of 0.6 m, before a denser confining layer was encountered. The core was then divided into smaller intervals for analysis, even though no distinct layering was seen (Figure 5.36b). At the time of sampling, the Bambra Wetland sample sites were saturated with water, but there was no obvious flow of water through the area.

Grain size analysis found that, like Pennyroyal Creek, the sediments were mostly sand-sized, although with a broader spread of grain sizes than at Pennyroyal Creek; lesser amounts of silt and clay are present (Figures 5.37), matching the alluvial soils known to exist in the area (Robinson et al. 2003).

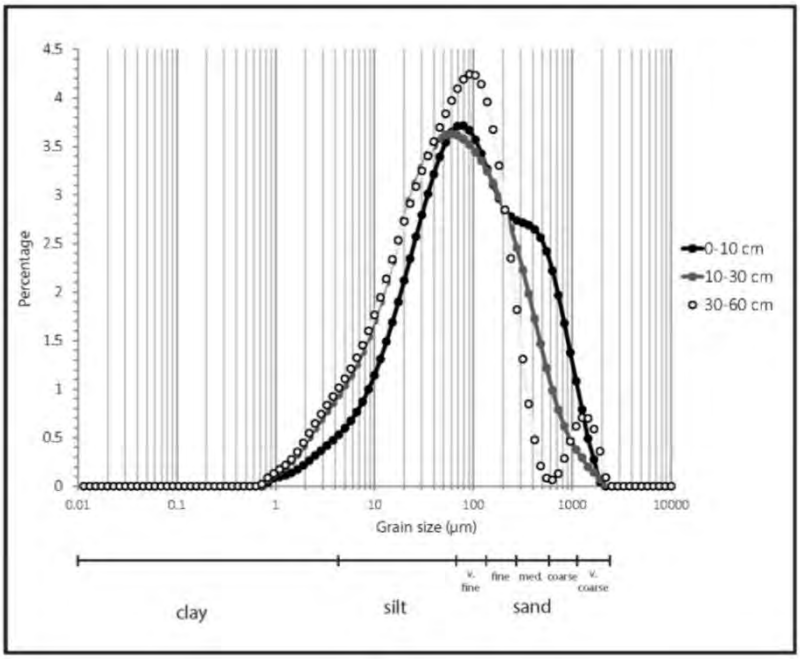

Figure 5.37 Grain size analysis for the Bambra Wetlands site

The Bambra Wetlands sediment consists of quartz, illite, and small amounts of hematite, along with kaolinite and minor goethite (Table 5.27). This was confirmed by the high levels of silica and reasonably high levels of aluminium shown in the XRF analysis (Table 5.28). Like Pennyroyal Creek, no sulfide minerals were identified and therefore the iron can be assumed to mainly be present as iron oxide minerals.

Organic matter was visible throughout the sediment, with calculated levels of 3.77-10.9% (Table 5.29). Like Pennyroyal Creek, this level is well below the threshold for peat, and therefore the sediment cannot be defined as peat (Charman 2002; Whinam and Hope 2005).

The TAA levels at the Bambra Wetland were low (Table 5.30), indicating that only a very small amount of acidity is being produced. The TSA and CRS results were moderate (Table 5.30), suggesting that the sulfides within the sediment have not completely oxidised. This may be due to the re-flooding, which has reintroduced a waterlogged environment to the site, and therefore allowed the continued formation of sulfide minerals. As a CRS value of 0.006% corresponds to only around 0.02% pyrite, the levels of pyrite are too small to accurately identify using XRD analysis. Like Pennyroyal Creek, AVS analysis was not conducted due to the low CRS values. The history of drainage at the Bambra Wetlands (prior to the re-flooding) allowed oxidation of sulfide minerals to occur before waterlogging was reintroduced, and this could be the source of the iron oxide minerals found at the site (Table 5.26). No carbonate minerals were found and analysis showed a lack of acid neutralising capacity (ANC) (Table 5.30). Due to the low levels of sulfide present at the site and the current waterlogging, it is unlikely the wetland will undergo a large acid event, and therefore the trace elements found within the sediment (Table 5.28) are unlikely to

mobilise. Due to the low levels of CRS, combined with the lack of TAA and ANC and the presence of iron oxides, the Bambra Wetlands are classified (Chapter 1) as a **post-active sulfidic soil** for both layers within the profile.

5.5 Comparison of CRS and TSA measurements

When the CRS and TSA analysis of the samples from ASS sites within this study were compared (as moles H^+ per tonne; Chapter 2; Table 5.31), obvious differences were observed. The TSA values are often an order of magnitude or more greater than the CRS values. Peroxide digestion (the TSA method) is known to be vulnerable to inaccuracies due to the release of additional sources of acidity (Ward 2004; McElnea et al. 2002), particularly the oxidation of the organic sulfur fraction The formation of organic acids through the oxidation by peroxide of the organic matter can also cause overestimates of acidity (Ward et al. 2002; Clark et al. 1996). Similar reactions to the oxidation of organic matter by hydrogen peroxide occur under natural conditions, but reaction rates are very slow compared to the laboratory procedure (Clark et al. 1996). The oxidation of chelated ferrous iron and manganese within organic matter can also lead to overestimates of acidity (Brady and Weil 2002; Clark et al. 1996); the oxidation of manganese from Mn^{2+} to Mn^{4+} releases twice as much acidity as the oxidation of Fe^{2+} to Fe^{3+} (Clark et al. 1996). A soil containing ferrous iron but negligible sulfide will give elevated TSA values that would be considered indicative of an ASS (Clark et al. 1996).

Clark et al. (1996) found that TSA is correlated with the percentage of organic carbon in a soil, increasing by approximately 0.09 mol/kg/% organic carbon (Figure 5.38). The analysis of soil samples in the study area showed a similar correlation between organic matter and

TSA (Figure 5.39), with a gradient of 0.07% mol H^+/kg/% organic carbon, so that the affect is greater at the sites with the higher carbon levels (Anglesea and Boundary Creek swamps).

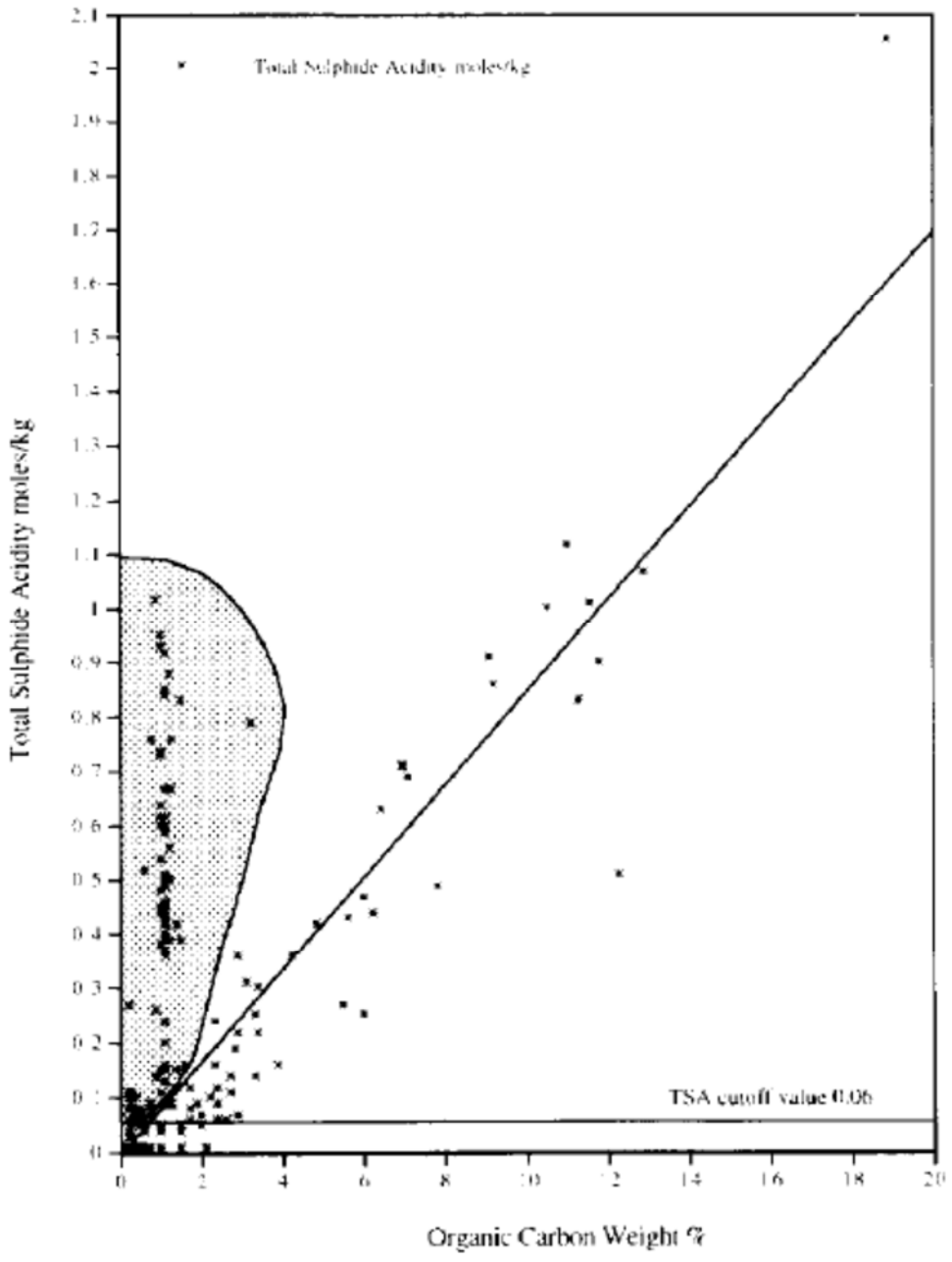

Figure 5.38 Plot of organic carbon content against measured TSA (Clark et al. 1996)

(The shaded area shows that for soils that actually contain iron sulfides, TSA is independent of the organic carbon content of the soil. The other soils show a strong relationship between the measured TSA and organic carbon content.)

Table 5.31 Comparisons of acidity generated by CRS, TSA and organic carbon (wt%)

Site	Depth (m)	CRS (mol H+/t)	TSA (mol H+/t)	Organic carbon (wt%)	Acidity contributed by organic matter (mol H+/t)*
BC1	0.5	18.7	363	5.03	337
	1.0	12.5	243	3.59	240
	1.5	12.5	409	6.00	402
	2.0	31.2	1262	9.54	639
	2.5	24.9	1344	3.23	216
BC2	1.5	12.5	639	9.82	658
BC3	2.0	12.5	252	2.36	158
A2	0-0.1	31.2	884	14.0	936
	0.1-0.2	31.2	1041	30.8	2064
	0.2-0.3	37.4	2882	33.4	2236
	0.3-0.5	206	1629	31.0	2076
	0.5-0.7	N/A	1764	28.6	1916
	0.95	324	2041	10.8	724
PC2	0.2	3.74	352	3.67	246
	0.4	0.62	730	4.67	313
BW	0.1	3.12	449	5.43	364
	0.3	1.87	155	2.69	180
	0.6	3.74	123	1.89	126
PR	0.2	1.25	533	4.61	309
	0.4	1.25	48.1	2.07	138

*Values calculated using the 0.068 mol H+/kg value from graph

** N/A = result not available

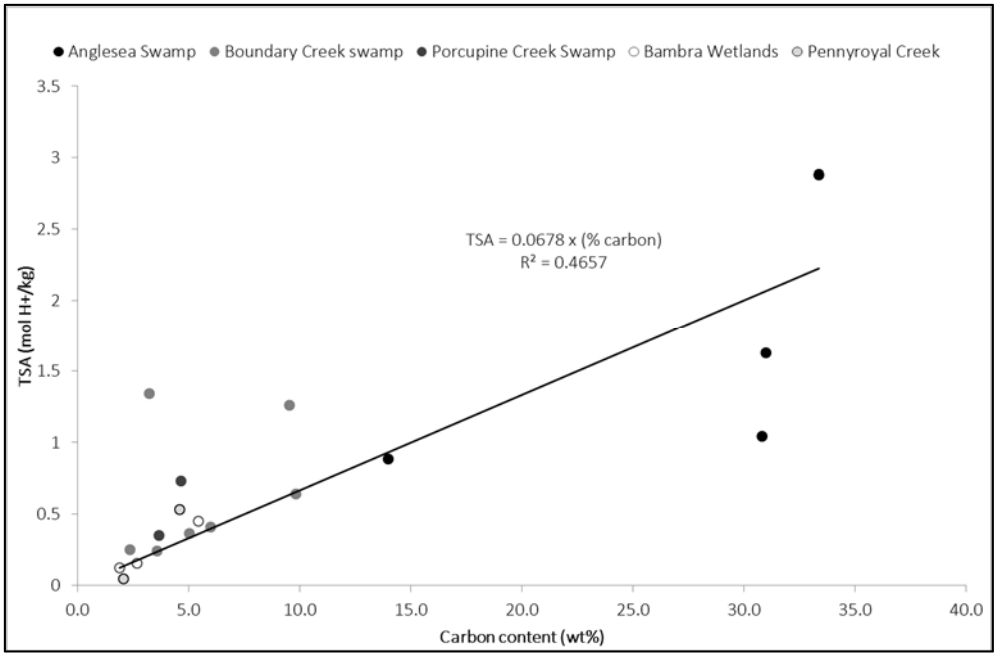

Figure 5.39 Plot of organic carbon content against the measured TSA for samples from the study area

From Figure 5.39, the acidity contributed by the oxidation of organic matter can be estimated (Table 5.31). Subtracting this from the measured TSA values gives levels that are close to the measured CRS values, confirming that the discrepancy between measured TSA and CRS values is due to the oxidation of organic matter and any chelated reduced iron and manganese.

5.6 Comparison of sites

5.6.1 Sediment composition

Of the five sites sampled within the Otway Ranges, the sediments at three contain sufficiently high levels of organic matter to be defined as 'peat' by the Australian definition (> 20% dry weight) (Whinam and Hope 2005). Each of these sites (Boundary Creek (Site A),

Anglesea River (Site B) and Porcupine Creek (Site C)) have differing levels of organic matter (Tables 5.5, 5.16 and 5.22), due to the differences in history of waterlogging (section 5.6.4), as well as differences in size of the swamps and their surrounding vegetation, and the location of sampling points.

All three sites are similar in a number of ways. They are fed by freshwater creeks that undergo seasonal variation in flow, with little or no flow from mid-summer to autumn and higher flows during winter and spring. The inorganic content of the swamp sediment is mostly sand-sized quartz, with lesser amounts of quartz silt and clay (kaolinite and illite) (Figures 5.6, 5.9, 5.24 and 5.30). The swamp sediments contain small amounts of pyrite, verified by the low CRS levels. The sulfur levels are exceeded by the iron levels (Tables 5.3, 5.14 and 5.20); much of the iron is present as iron oxides/hydroxides at Boundary Creek and Anglesea. No carbonate minerals were found within any of these swamp sediments, matching the low levels of calcium and magnesium found at all sites (Tables 5.3, 5.14 and 5.20). The trace metal levels within the 'peat' sediments, which are all within Australian background levels for soils (Tables 5.4, 5.15 and 5.21), could be mobilised by a decrease in pH of the sediment due to oxidation of sulfides, and could then be transported into the nearby waterways by high rainfall events in the winter months within the Otway Ranges.

The other two sites sampled within the Otways, Pennyroyal Creek (Site D) and the Bambra Wetlands (Site E) occur in areas of the floodplain of the Barwon River that have been drained and cleared for agriculture, although the Bambra Wetlands have since been re-flooded. Organic matter levels were too low for the sediments to be classified as peat (Charman 2002; Watters and Stanley 2007; Whinam and Hope 2005), but otherwise the sediments were similar to those at the other sites found within the Otway Ranges (mostly

sand-sized quartz with some clay (kaolinite and illite)) (Table 5.26). At these sites there are higher amounts of iron oxide minerals than at the 'peat' sites, and a lack of pyrite, reflecting the oxidation of these sediments when they were drained (see discussion in 5.6.5). No carbonate minerals are present (Table 5.26).

5.6.2 Cause of swamp development

The three 'peat' swamps, Boundary Creek (Site A), the Anglesea River (Site B) and Porcupine Creek (Site C), formed in different ways. The Boundary Creek swamp formed when the Barwon River was dammed by the eruption of the Newer Volcanics to the north at approximately 2.31 Ma (Robinson et al. 2003; Gibson 2007). The damming caused the deposition of sediment through the loss of energy in the river and its tributaries, catching sediment washed into the swamp by upland runoff and aeolian transport (Petersen et al. 2014).

Porcupine Creek was dammed by two landslides, clearly visible on the LIDAR topography (Figure 5.26). Soils within the upper catchment of the Barwon River are known to be prone to landslides (Clarkson et al. 2007), which are dominantly triggered by rainfall (Dahlhaus et al. 2006a). The valley of Porcupine Creek upstream of the landslides has been infilled by swamp sediments, evident as wide areas of Quaternary sediment on the geology map (Figure 5.28).

The Anglesea River swamps formed as a result of the rise in sea level after the Last Glacial Maximum (LGM), culminating in the Holocene highstand (+ 2.0 m) at ~5-6 ka (Lewis et al. 2013). During the LGM, streams flowing to the sea incised deep river valleys in response to the substantial lowering of the base level (sea level) associated with the glaciation. The

following rise in sea level progressively decreased the stream gradient, and therefore decreased the energy of the stream flow, allowing the valleys to fill with sediment (Lewis et al. 2013; Petersen et al. 2014).

5.6.3 Effect of near-coast location

The proximity of the coast has had an impact on the development of ASS at the Anglesea River swamp, even though the swamp is above the range of tidal inundation. The input of sea spray to rainfall gives the swamp a higher source of sulfate than sites further inland, as seawater contains high levels of sulfate (Powell and Ahern 1999; Rabenhorst et al. 2006). The relatively high input of sulfate to the Anglesea swamp allowed sulfide formation (Chapter 1), and this is reflected in the much higher CRS values at Anglesea than at the other sites, particularly at depth (Table 5.17).

5.6.4 Causes of drying and oxidation of surface layers at some sites

Oxidation of sulfides begins with the introduction of oxygen, generally due to the drying out of previously waterlogged sediment (Chapter 1). Seasonal fluctuations in the watertable, due to variability in rainfall and temperature, mean that the upper part of the wetland is often prone to seasonal drying. The resultant loss of anaerobic conditions does not always extend uniformly down the profile. The subsequent rise in watertable due to subsurface flow as well as rainfall in the winter months can re-establish anaerobic conditions (Boulton et al. 2014).

At Anglesea (Site B), the watertable fluctuates over 1 m, although the drained soil does not completely dry out (Lithgow 2007). This seasonal drying allows partial oxidation of the sulfides in the top 0.3 m of the sediment, reflected in the lower CRS values (Table 5.17).

Sampling at Anglesea occurred during the drier months, and the generated acidity has remained within the sediment profile, but could be flushed into the Anglesea River by winter rainfall. The sediment profile sampled was entirely within the range of the seasonal watertable fluctuation; the sediment below the limit of watertable fluctuation probably remains under anaerobic conditions.

The sediment profile at Porcupine Creek (Site C) is prone to periodic drying and oxidation, and was not saturated when sampled, indicating the samples were taken above the seasonal lowering of the watertable. The CRS and TAA values are relatively similar down the profile (Table 5.23), as were the values recorded by Davidson & Lancaster (2011) for the same site, so there is no clear indication of surface layer oxidation.

The downstream part of the Boundary Creek swamp (Site A) has partially dried out due to the draining of nearby land for agriculture, resulting in removal of the formerly dominant tea-tree swamp vegetation (CCMA 2006b), and allowing eucalypts to establish (Figure 5.4a; section 5.6.5). The upper layer of sediment in this part of the swamp shows evidence of seasonal drying. The top 1.5 m has lower CRS values and higher amounts of iron hydroxide than deeper in the profile (Table 5.6), also seen in Davidson & Lancaster's (2011) analyses at Boundary Creek (Table 5.7). Due to the trenches dug recently at the site, partial drying has extended to the base of the trench (approx. 2 m); however, the effect has been minimised, as the trenches fill with water, particularly during the wetter months.

5.6.5 Effect of draining swamps on ASS

Permanent drying of the sediment profile has been caused by the draining of the swamps for agriculture. The digging of drainage channels, such as those in the West Barwon, which

are 0.5 – 2 m in depth, permanently lowered the watertable by this amount and removed even seasonal waterlogging. As a result, the top 2 m of the profile was exposed to oxygen, and any sulfides have undergone at least partial oxidation across the entire floodplain. However, the resulting acidity has largely been washed from the sediment by rainfall, due to the substantial period of time since the drainage channels were dug (> 70 years). This removal of sulfides has occurred at both Pennyroyal Creek (Site D) and the Bambra Wetlands (Site E), as shown by the low CRS values and presence of iron hydroxide in the sediment. Both profiles are less than 2 m in depth; deeper sediment that remains waterlogged will still contain sulfides.

To the east of the Boundary Creek swamp is an area of farmland on the Boundary Creek floodplain that has been drained by artificial deepening of the drainage channels. Davidson & Lancaster (2011) found that CRS levels in samples taken in the drained part of the floodplain were lower than in the undrained part of the swamp (Table 5.7), but still significant.

Therefore, any additional lowering of the watertable on the West Barwon floodplain, such as through further deepening of the drainage channels or excavation for pipelines or other development, will expose this waterlogged sediment to oxygen. Any sulfides present will oxidise, producing acidity, which can be transported into the nearby streams by rainfall, potentially leading to an acidification event. This has management implications for any development on the floodplain.

Chapter 6

ASS Mapping

Within Australia, ASS are an important environmental concern (Chapter 1), particularly to surface and groundwater management (SRW 2010; CCMA 2012; CCMA 2006a). Mapping of ASS across the Corangamite CMA is therefore important in determining areas potentially at risk, aiding in the management of these sites and avoiding potential disturbance. There has been some previous mapping of ASS in Australia, especially in coastal areas (Chapter 1; Rampant et al. 2003; Naylor et al. 1998; Fitzpatrick et al. 2011); however, from a national perspective, large gaps still remain, particularly for inland ASS. The Corangamite CMA was highlighted as one such gap (Fitzpatrick and Shand 2008), although broad scale mapping through ASRIS identified some areas of potential ASS (Fitzpatrick et al. 2011). The purpose of the mapping in this study was to provide the location of areas likely to contain inland ASS within the Corangamite CMA, based on the environments where these ASS are found. This information can then be used by land managers to assess when further investigation and analysis is needed before land disturbance. The geochemical and sedimentary analyses of this study have shown that inland ASS exist within both the Basalt Plains (Chapter 4) and the Otway Ranges (Chapter 5). However, due to the large excess buffering capacity within the Basalt Plains sites (and therefore the lack of acidification if these sites were disturbed), the Basalt Plains were excluded from the mapping process.

6.1 Initial methodology

Initially, GIS analysis and mapping was conducted using the software programs Global Mapper (version 13.2), ENVI (version 4.2) and ArcGIS (version 10.0). A compilation of data was used, including Landsat 7 satellite images (downloaded from the USGS), LIDAR topographic information provided by the DSE and CCMA, geological and geomorphological information (Robinson et al. 2003; Tickell et al. 1992; Tickell 1990; Tickell et al. 1991), and wetland maps (Sheldon 2005). Using the known characteristics for the formation of ASS (Chapter 1), a conceptual mapping methodology was developed for the Otway Ranges (Figure 6.1).

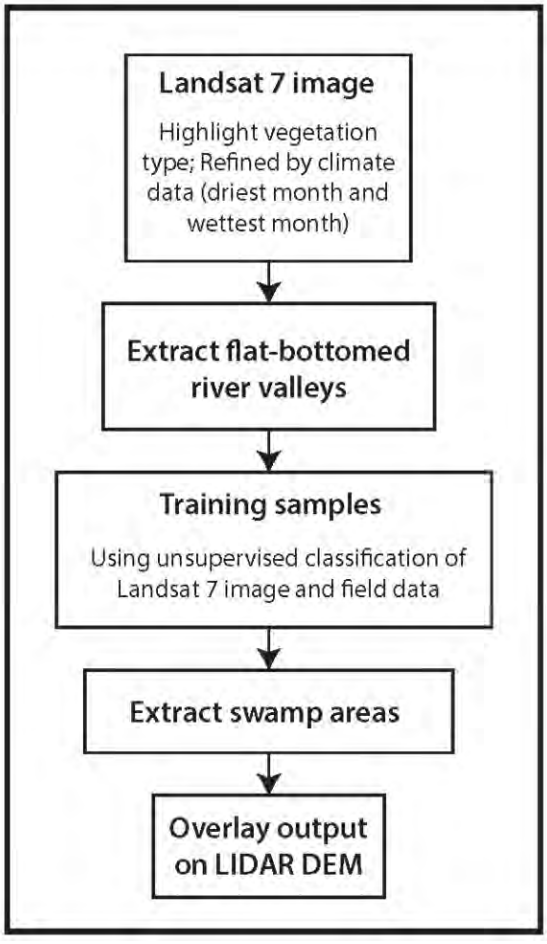

Figure 6.1 Conceptual model of initial methodology

The Landsat 7 data was processed using ENVI to highlight vegetation type, in particular to isolate areas covered by native and waterlogged vegetation. In an effort to increase the accuracy of the analysis, Landsat images from the driest and wettest parts of a selected year were compared, constrained by selecting images with a lack of cloud cover. The processed images were then combined with topographic (through slope analysis; section 6.2) and geomorphic information to isolate the swamp areas (Figure 6.1).

In the Otway Ranges, swamps are confined to flat-bottomed river valleys. These river valleys have been dammed to allow infilling by alluvial sediment, either by the eruption of the Newer Volcanics (Chapter 1), or by the landslides known to be a large risk to areas of the Corangamite CMA region, such as the Gellibrand River and its tributaries (Clarkson et al. 2007; Robinson et al. 2003), or by the rise in sea level associated with the Holocene highstand (+ 2.0 m) (Lewis et al. 2013). This alteration of landscape has resulted in river valleys with a characteristic flat bottom that indicates the location of a waterlogged environment, as well as the development of alluvial terraces and floodplains (Joyce et al. 2003b).

However, there were difficulties in distinguishing vegetation types on the analysed images, particularly native vegetation and partially drained areas, and the Landsat 7 images are too low resolution (30 m pixel size) to accurately map the comparatively small size of the swamps (0.13 – 0.96 km^2). Therefore, the satellite vegetation analysis was replaced by pre-existing Ecological Vegetation Class (EVC) mapping, both the 2005 map layer and the modelled 1750 vegetation map (section 6.3).

6.2 Slope Analysis

To make the process as automated as possible, and therefore more widely applicable to other areas, slope analysis to identify flat areas likely to be swamps was conducted on the LIDAR topography using the Global Mapper software. To extract a specific range of slopes, the LIDAR data was exported as elevation grid (in float/grid file format) with the slope values exported in place of the elevation values. However, due to the very high resolution of the LIDAR data (with up to 18 hours processing time prior to extraction), the elevation data was resampled at 5 m spacing to reduce processing time while still retaining as much detailed information as possible. Once the LIDAR topography had been processed in this way, the files could then be loaded back into the Global Mapper software and a specific range of slope angles chosen. For this analysis, the range of 0-4° slope was used (Figure 6.2).

Some areas of the Corangamite CMA were omitted from this analysis due to a lack of LIDAR data (Figure 6.2), but these areas fall within the Basalt Plains, which were previously excluded from the mapping (as stated above). The slope analysis overestimated the area of potential waterlogging, because it identified low slopes of the basalt plains and the northern foothills of the Otway Ranges, as well as extensive flat ridge-tops (Figure 6.2; Joyce et al. 2003b); these are areas where PASS do not occur. Therefore, an additional method was needed to constrain which areas of low slopes are likely to be waterlogged and contain PASS.

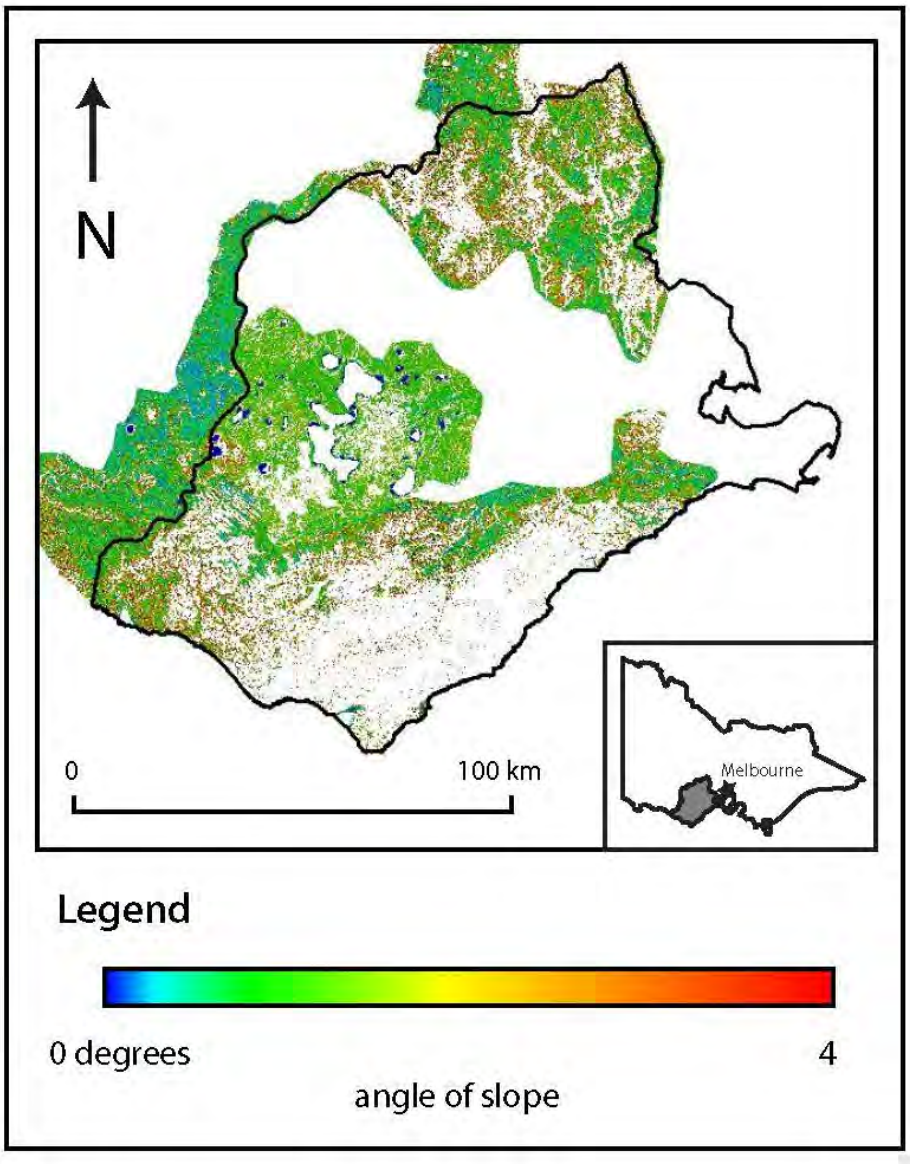

Figure 6.2 Automated slope analysis of the Corangamite CMA

6.3 LIDAR and EVC method

Ecological Vegetation Classes (EVCs) are a native vegetation classification system that uses a combination of floristics, vegetation structure, landscape features and ecological characteristics to define distinct vegetation types (DSE 2004; CCMA 2005; Sheldon 2005). Each EVC represents one or more floristic communities that are associated with a

recognisable environmental niche. EVCs are the basic mapping units for vegetation management and conservation, and can be used at a landscape level, as they provide a finer level of detail than bioregion classifications (CCMA 2005; Sheldon 2005; DSE 2004).

EVC mapping of the study area, derived from analysis of floristic data for 2005, was conducted by the Department of Sustainability and Environment (DSE) at 1:25 000 scale (DSE 2004). Pre-1750 EVC mapping is also available, which is a modelled estimate of the extent of vegetation at EVC level prior to European settlement, based on field data, spatial data (such as soils, rainfall and topography) and historical records, such as Parish plans. This dataset was modelled at a scale of 1:100,000 (DSE 2004). The pre-1750 EVC mapping is particularly useful in areas that now have highly fragmented landscapes, with only small patches of extant native vegetation (CCMA 2005).

Within the Otway Ranges, all inland ASS sites are or were waterlogged/swampy areas within in-filled valleys, so to refine the areas highlighted by the slope analysis, the 1:100,000 EVC mapping (both 2005 and the modelled 1750) was overlaid on the LIDAR and slope analysis, so valley floors with a very low slope and waterlogged and/or swampy vegetation could be selected. Thus, using the EVC mapping, the initial methodology was refined (Figure 6.3). High resolution satellite images from Google Earth were used in conjunction with the EVC mapping to accurately map the extent of the swamps, based on the visible changes in vegetation.

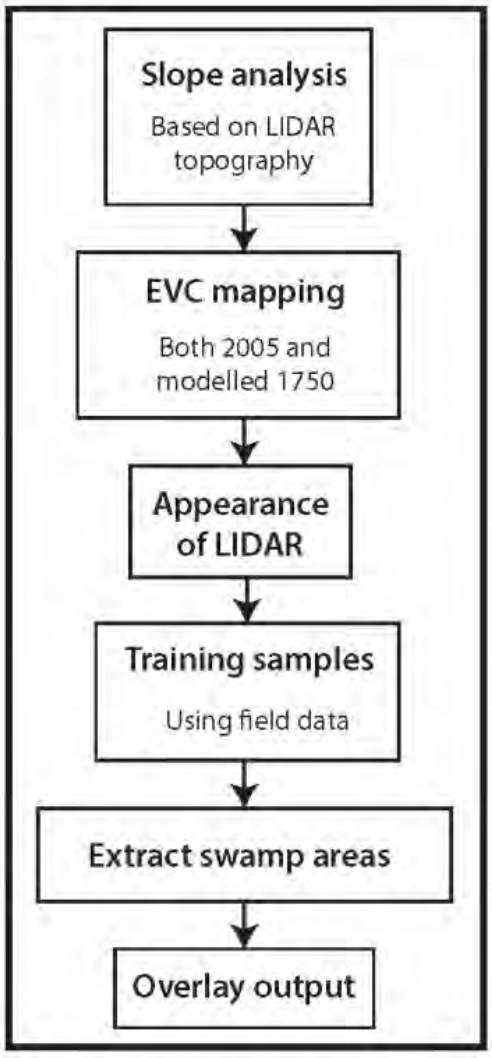

Figure 6.3 Refined conceptual of mapping methodology

6.4 Mapped ASS classes

Based on the mapping, four classes of ASS could be distinguished: two within uncleared areas, and two on cleared land. ASS within the uncleared areas of remnant native vegetation (forestry areas, national parks and protected heathland) were divided (Table 6.1) into Type 1, which show a lack of visible surface drainage and a distinctive hummocky texture on the LIDAR topography (Figure 6.7), and Type 2, which have visible natural

channels <0.5 m in depth (Figure 6.7). The presence of channels in Type 2 ASS indicates the watertable depth may be 0.5 m below the surface, so that the top 0.5 m of sediment in these areas has probably undergone drying and oxidation. Both Type 1 and 2 ASS lie within the valley floors and show swampy and/or waterlogged vegetation classes for both the 1750 and 2005 EVC mapping.

Within the Corangamite CMA, the land cleared for agriculture has a history of disturbance and had to be classified differently to the uncleared areas. The cleared land has also been divided into two types, both occurring within flat-bottomed (in-filled) valleys where the 1750 modelled EVC mapping showed swampy and/or waterlogged vegetation prior to clearing. **Type 3** ASS (Figure 6.5) show visible and often man-made drainage channels (0.5-2.0 m in depth), whereas **Type 4** ASS (Figure 6.8) lack drainage channels, and show current signs of waterlogging (either on the 2005 EVC mapping or Google Earth images) (Table 6.1).

The Type 3 cleared areas have been drained, so the upper part of these ASS would have already undergone drying and oxidation (probably to at least 0.5-2.0 m depth); however, there would still be ASS present beneath the watertable and any disturbance below the watertable depth could cause acidification. Type 4 ASS are currently waterlogged, but have probably been periodically affected by lower watertables in the past in the surrounding cleared areas, causing some near surface oxidation. However, they still have the potential to release acidity from the upper sections of the soil profile due to the current waterlogging.

Type 5 ASS (Table 6.1) are areas of Victorian coastal ASS that were mapped to a 1:100 000 scale as part of a project undertaken by the DSE for the purpose of land management and

environmental planning. Type 5 ASS is the extent of probable ASS based on formation processes, height above current sea level, geological mapping, soil mapping and site assessment (Rampant et al. 2003).

Table 6.1 ASS Classifications and consequences of disturbance

Land Type	Classification Type	Colour on map	Characteristics	Consequences of Disturbance
Uncleared	1	Purple	• Flat-bottomed valley • Waterlogged and/or swampy vegetation (as shown by 2005 EVC maps) • Evidence of hummocky ground surface (LIDAR) • No obvious drainage channels	• If disturbed, acid will be produced and released
	2	Blue	• Flat-bottomed valley • Waterlogged and/or swampy vegetation (as shown by 2005 EVC maps) • Obvious drainage channels (< 0.5m deep)	• If disturbed below level of water table, acidification will occur
Cleared	3	Orange	• Flat-bottomed valley • Waterlogged and/or swampy vegetation in the past (as shown by 1750 EVC maps) • Obvious drainage channels (0.5-2.0 m)	• If disturbed below level of water table, acidification will occur
	4	Yellow	• Flat-bottomed valley • Waterlogged and/or swampy vegetation in the past (as shown by 1750 EVC maps) • Evidence of current waterlogging (as shown by 2005 EVC mapping and/or Google Earth images)	• If disturbed, acid will be produced and released
Coastal	5	Silver	• Coastal area • As defined in DSE coastal ASS mapping	• See DSE coastal mapping report (Rampant et al. 2003)

6.5 Verification of ASS mapping

Three areas of known inland ASS in the Otway Ranges (Chapter 5) were used to check the validity of the mapping process using the slope, LIDAR and EVC analysis (Figure 6.3): the West Barwon Valley (mostly Type 3), Anglesea (Types 1, 2 and 5), and Porcupine Creek (mostly Types 1 and 2) (Figure 6.4).

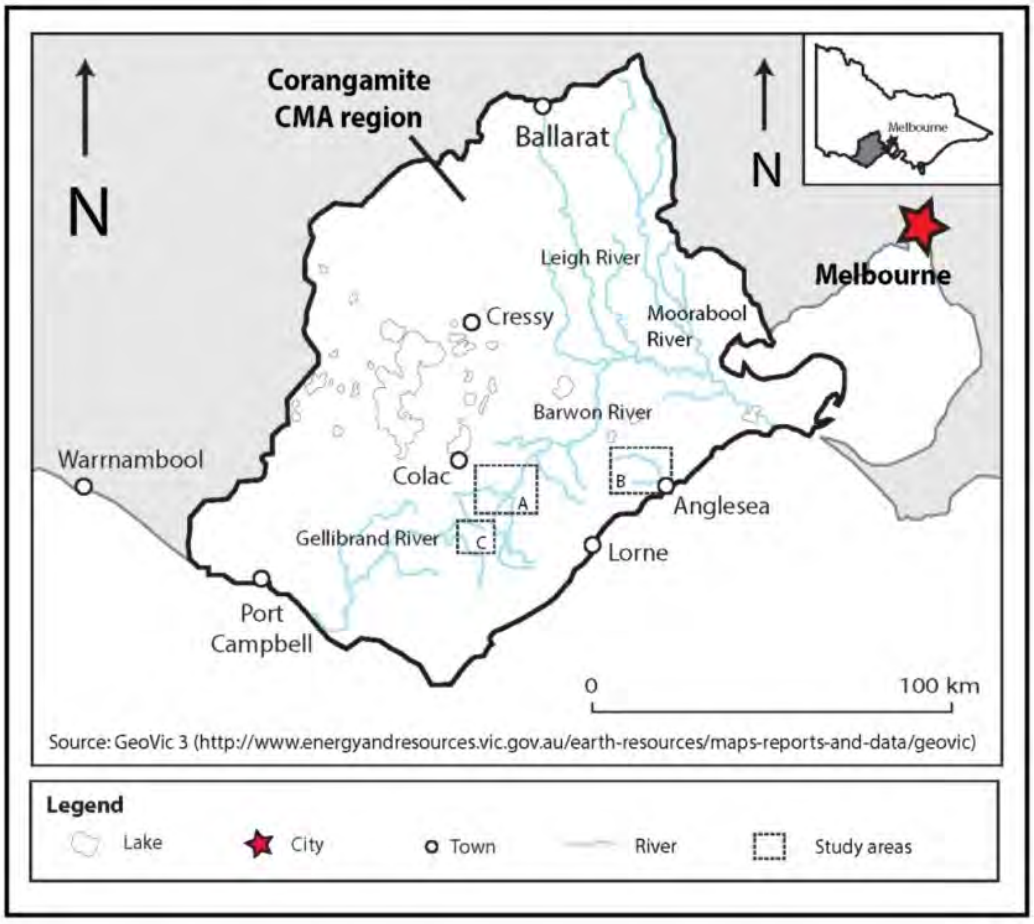

Figure 6.4 Location of mapped ASS examples (A: West Barwon Valley, B: Anglesea River and C: Porcupine Creek)

6.5.1 West Barwon River valley (Site A)

The West Barwon valley occupies a wide area to the south-east of Colac in the northern foothills of the Otway Ranges (Figure 6.4). Two of the tributaries of the West Barwon River

are Boundary Creek, along which is a 'peat' swamp, and Pennyroyal Creek (Chapter 5; Figure 6.5).

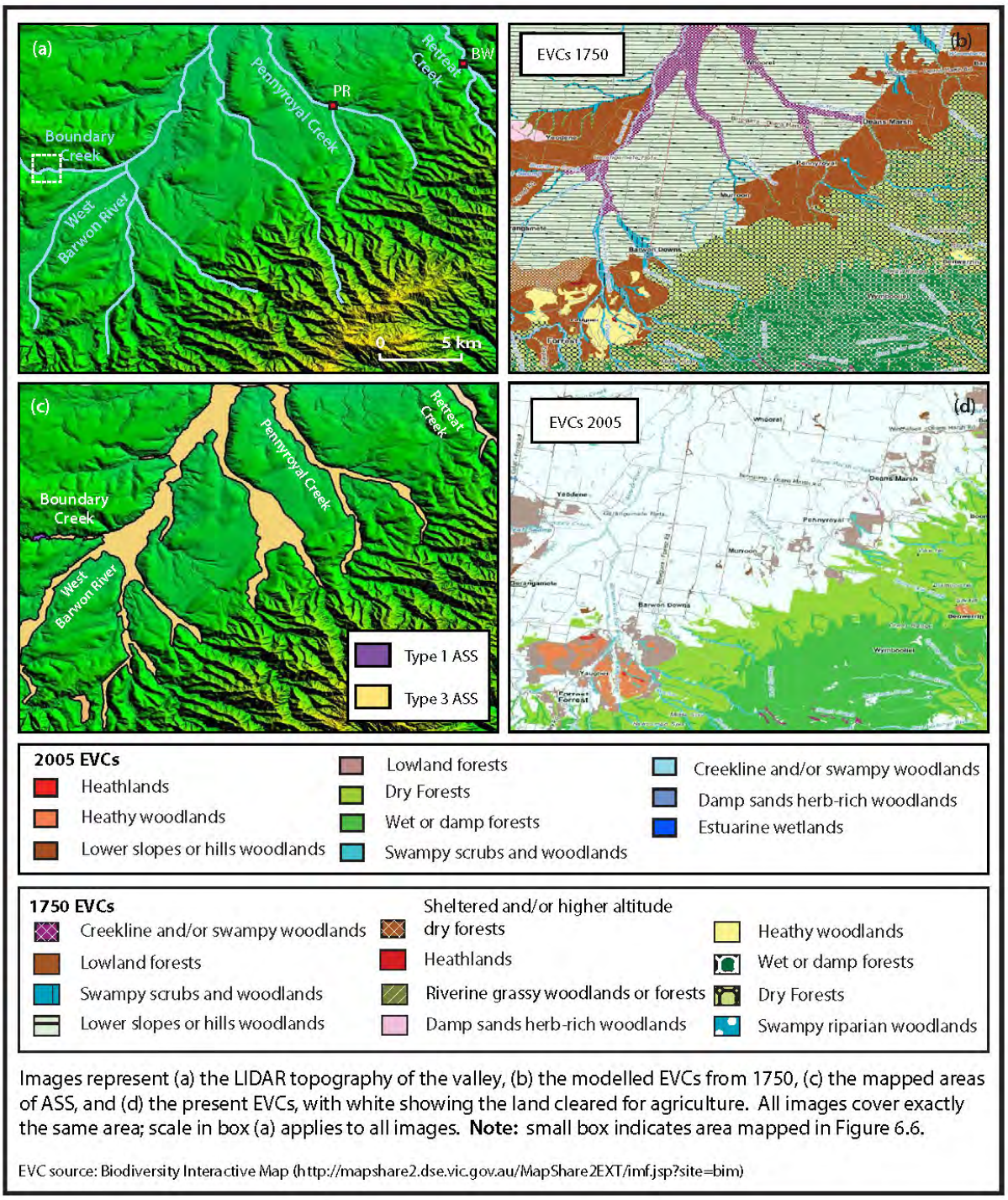

Images represent (a) the LIDAR topography of the valley, (b) the modelled EVCs from 1750, (c) the mapped areas of ASS, and (d) the present EVCs, with white showing the land cleared for agriculture. All images cover exactly the same area; scale in box (a) applies to all images. **Note:** small box indicates area mapped in Figure 6.6.

EVC source: Biodiversity Interactive Map (http://mapshare2.dse.vic.gov.au/MapShare2EXT/imf.jsp?site=bim)

Figure 6.5 Mapped ASS of the West Barwon River valley

The wide floodplain of the West Barwon River developed due to damming by the Newer Volcanics and the increase of the base level of the river system in response (Chapter 3). As a result, alluvial flats and terraces with extensive swamps have formed on the wide valley floors, providing ideal environments for the development of inland ASS (Robinson et al. 2003). The majority of the swamps in this area have been cleared and drained using channels in order to make the area suitable for farming, so the main type of ASS present is Type 3 (Figure 6.5).

The man-made drainage channels (Chapter 5) removed the waterlogging, and allowed the top section of the soil to oxidise (through exposure to oxygen). It is assumed any acidity was flushed from the soil soon after draining, as the upper sediment shows little or no acidification at present. Field analysis of Pennyroyal Creek (Chapter 5), where an original swamp has been largely drained for farmland, showed that there are low levels of sulfidic acidity in the sediment, and the sediment was classified as post-active acid sulfate soil. Field analysis of the Bambra Wetlands (Chapter 5), which lie along Retreat Cree and where the originally drained swamp has been recently revegetated, showed similar low levels of sulfidic acidity in the sediment. The sediment was classified as post-active acid sulfate soil, although there is potential for more sulfides to develop within the Bambra Wetlands if it is kept waterlogged and anaerobic.

However, at both sites, sulfide minerals, and therefore potential acidity, probably still exist below the watertable. The Type 3 ASS over most of the area, including Pennyroyal Creek and Retreat Creek, would only produce significant acid if the soil below the water table was disturbed.

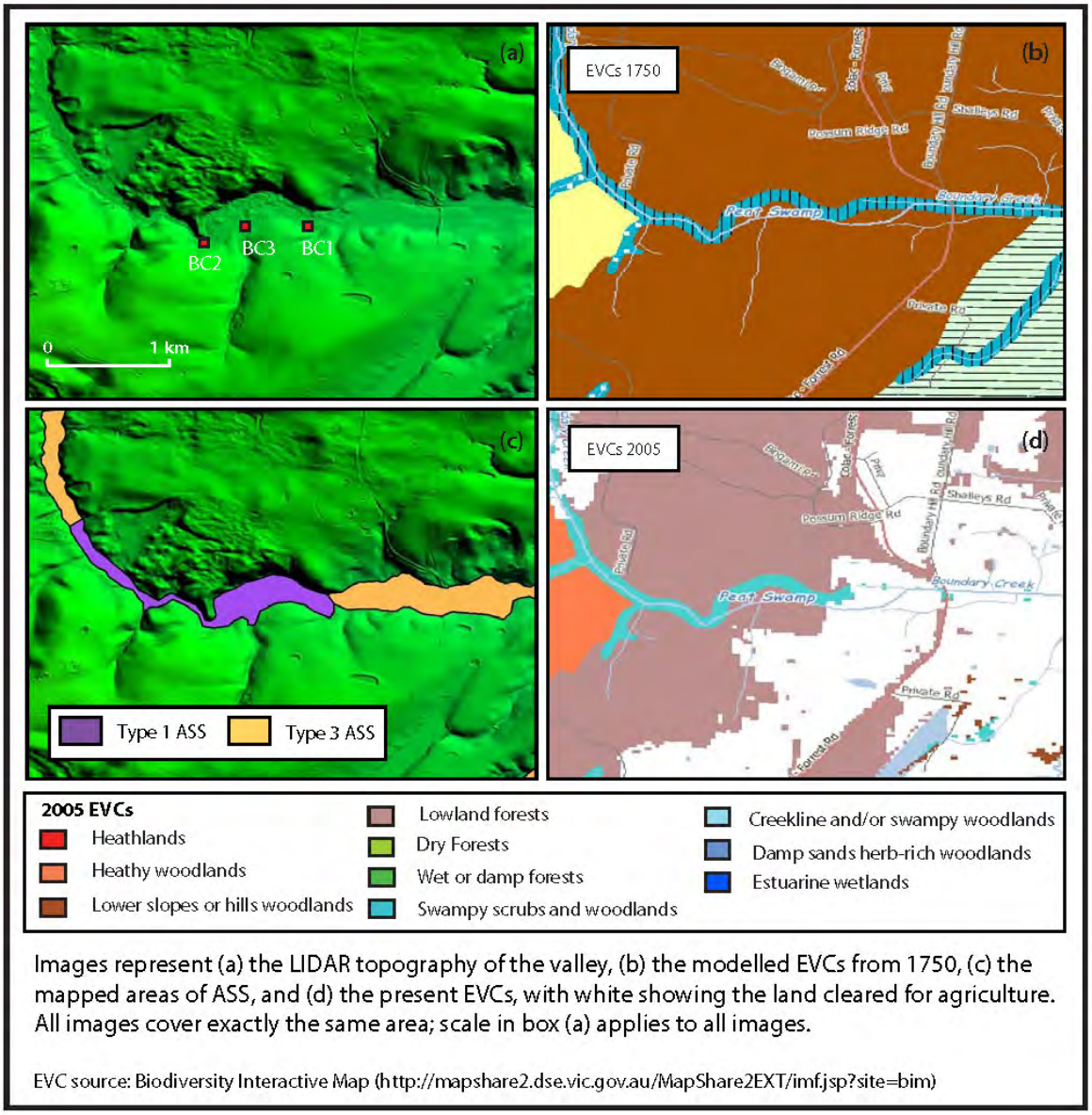

Images represent (a) the LIDAR topography of the valley, (b) the modelled EVCs from 1750, (c) the mapped areas of ASS, and (d) the present EVCs, with white showing the land cleared for agriculture. All images cover exactly the same area; scale in box (a) applies to all images.

EVC source: Biodiversity Interactive Map (http://mapshare2.dse.vic.gov.au/MapShare2EXT/imf.jsp?site=bim)

Figure 6.6 Mapped ASS of Boundary Creek

Two areas of Type 1 ASS are present in the West Barwon valley along Boundary Creek (Figure 6.6), and these represent an acidification risk if disturbed. Field analysis found the swamp along Boundary Creek to be an **actual acid sulfate soil (AASS)** (Chapter 5; Figure 6.6), indicating acidity has already been generated through the oxidation of sulfides. However, there is still potential acidity within these areas, as the sulfides within the sediment have

not been completely oxidised. As there are no carbonate minerals present, neutralisation by carbonate dissolution will not occur at this site, and any generated acid will cause a drop in pH. Any further loss of anaerobic conditions, due to lowering of the watertable through human activity such as excavation, drainage or disturbance, would lead to further acidification (Bowman 1993; Dent 1986; Fitzpatrick and Shand 2008; Sammut et al. 1996; Simpson et al. 2008). Oxidising ASS are in rapid flux, whereby the acid forming from oxidation during one year can leach from the system and a similar quantity reform in the following year, so that the sediments can have a similar low pH from one year to the next, despite the reserves of potential acidity decreasing (Brinkman and Pons 1973).

6.5.2 The Anglesea River (Site B)

Anglesea lies on the Victorian coast, approximately 110 km south-west of Melbourne (Figure 6.4) on the Great Ocean Road. The Anglesea River flows to the sea through the town; above Anglesea the river splits into two tributaries, Salt Creek to the west and Marshy Creek to the north. This is a coastal area, and most of the estuary and lower tidal reaches of the Anglesea River are identified as coastal ASS (Type 5) (Figure 6.7).

However, above the range of tidal inundation, the tea-tree swamps are freshwater environments and were therefore classified as inland ASS. The upper sections of both tributaries (above the zone of anthropogenic disturbance associated with the lignite mine and the power plant) show Type 1 ASS, with no clear drainage channels and the hummocky topography that matches the peat swamp on Boundary Creek (Figure 6.7). Sections of Marshy Creek show drainage channels within uncleared heathland (Type 2 ASS).

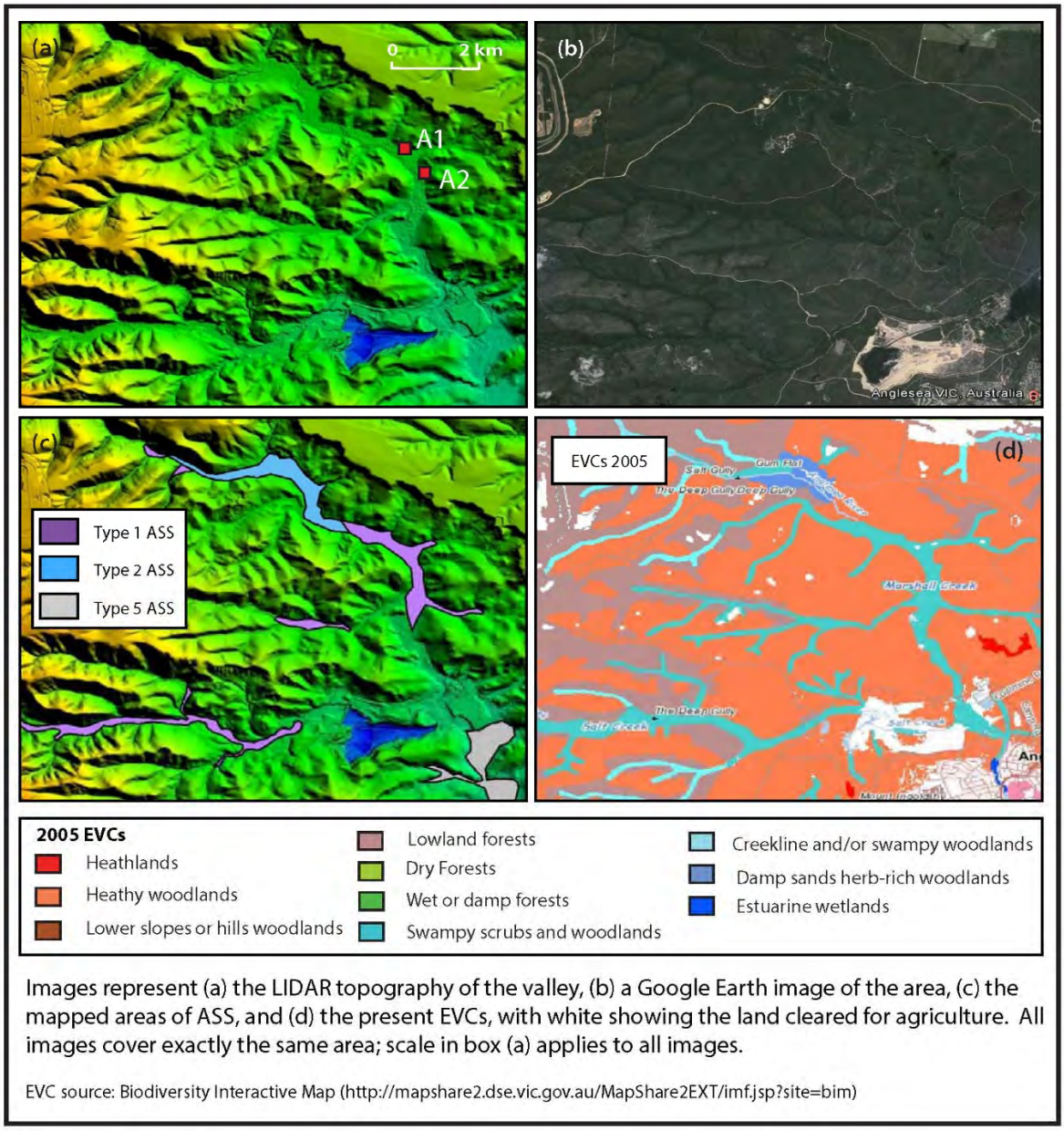

Figure 6.7 Mapped ASS of the Anglesea River

Analysis of the sediment along Marshy Creek (Chapter 5) showed the sediment was an **actual acid sulfate soil (AASS)** throughout all layers of the profile, and has a potential to generate further acidity (Chapter 5; Glover and Webb 2013), confirming the identification as Type 1 ASS.

6.5.3 Porcupine Creek (Site C)

Porcupine Creek lies south of Colac within a forestry area (Figure 6.8). Most of the upper reaches of Porcupine Creek are covered with uncleared forest, but there are also sections of farmland, and as a result, all four of the inland ASS types occur here (Figure 6.8). The infilling of the valley appears to have occurred due to several landslides damming the creek, causing swamps to form along several of the tributaries feeding into Porcupine Creek; these developed Type 1 ASS (like the peat swamp along Boundary Creek; Figure 6.6).

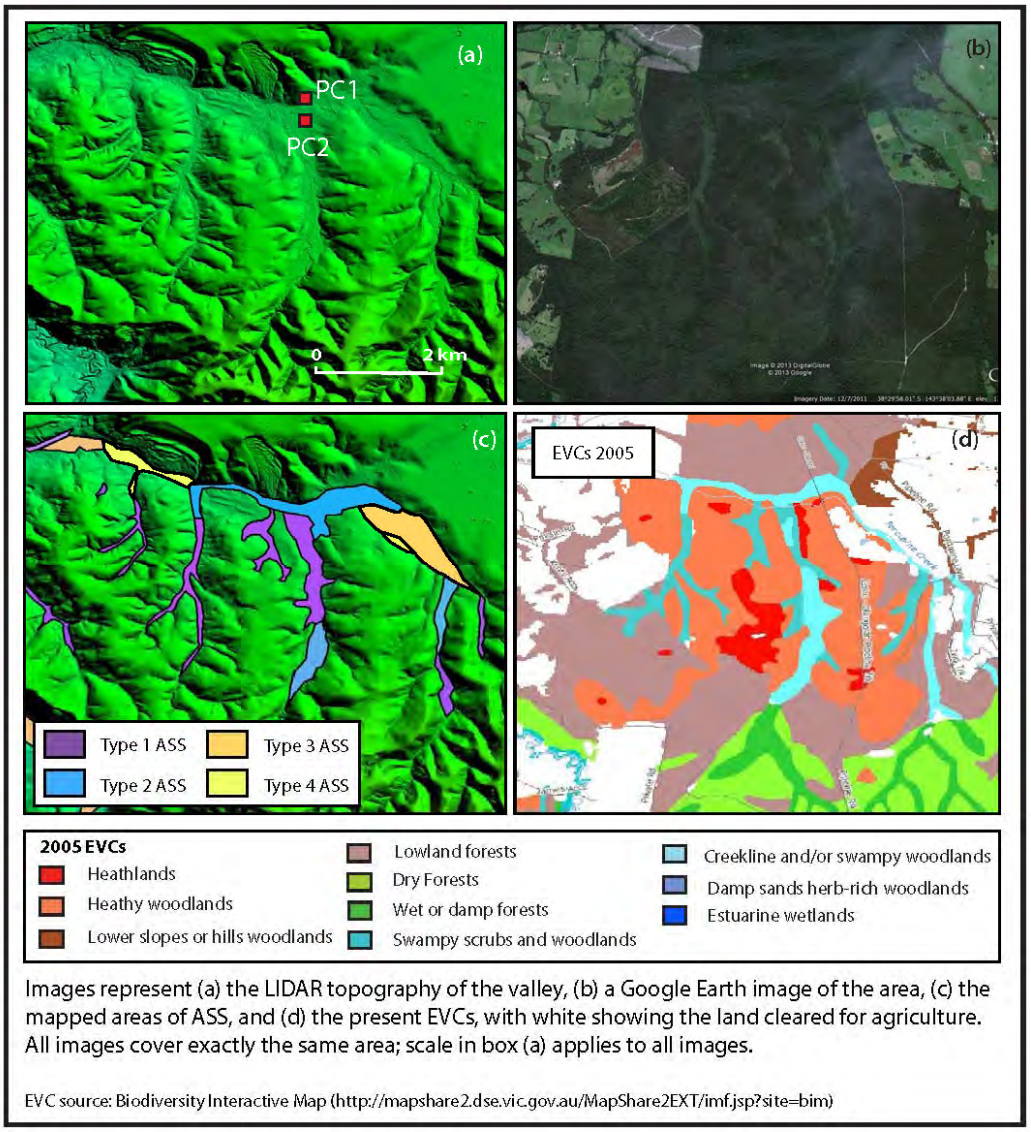

Figure 6.8 Mapped ASS along Porcupine Creek

Porcupine Creek itself has an obvious drainage channel for most of its length (Type 2 and 3 ASS). Analysis of the sediment (Chapter 5) classified the upper layer as a low-risk sulfidic soil, probably due to the continued oxidation as a result of seasonal lowering of the watertable, followed by rainfall events washing away the acidity released. However, below 0.2 m, the sediment is classified as a potential acid sulfate soil (PASS), which confirms the identification of Type 1 and 2 ASS from the mapping. Sections of cleared land along Porcupine Creek to east and west of the forested area show signs of waterlogging where the surface drainage becomes less clear (Type 4), so there are large sections of this cleared land that will probably acidify if disturbed.

6.6 Conclusions

Acid sulfate soils (ASS) are an important environmental concern across the Corangamite CMA. The generation of acidity from these sediments once they are disturbed can be washed into waterways following large rainfall events, and as such have the potential to export low pH water downstream with large environmental effects. Mapping of ASS across the CMA is therefore important in determining areas potentially at risk. Mapping was conducted using the software programs Global Mapper (version 13.2), ENVI (version 4.2) and ArcGIS (version 10.0), and the following data: Landsat 7 satellite images (analysed to highlight vegetation and water content), LIDAR topography, geology and vegetation maps (EVCs). Areas with slope angles of 0-4° extracted from the LIDAR overestimated the potential areas of ASS, because the broad, flat tops of ridges and the gently sloping foothills of the Otway Ranges are not subject to waterlogging due to their elevation and slope respectively, and the sediments on then very flat Basalt Plains either have a very low sulfide

content or sufficient carbonate mineral content to neutralise any acidity released. Furthermore, the vegetation and water content analysis using Landsat 7 images was at too low a resolution for the areas being mapped. Therefore, the automated slope and vegetation analysis was constrained by using the pre-existing Ecological Vegetation Class (EVC) mapping, both the 2005 map layer and the modelled 1750 vegetation map, overlaid on the LIDAR topography and slope analysis. Areas that had a very low slope and waterlogged and/or swampy vegetation were selected, and these were ground-truthed in three areas: West Barwon valley (including Boundary Creek), Porcupine Creek and Anglesea. The GIS mapping matched known ASS sites, indicating that the method developed for mapping these areas remotely is accurate.

Chapter 7

Conclusions

7.1 Assessment of ASS on Basalt Plains

The Basalt Plains lie in the north of the Corangamite CMA, and contain a significant number of wetlands, which have formed in volcanic craters and depressions, and where drainage patterns have been disrupted by lava flows (Sheldon 2005; Harding and Callister 2005). Of the four sites sampled for the study, two were drained swamps, Bullocks Swamp (Site A) and Beeac Swamp (Site B), and two were smaller depressions (Sites C and D). Both swamps (Sites A and B) had sediment occurring in two layers: an upper layer rich in organic matter, and a lower layer of finer texture. The swamp sediments were mainly composed of quartz, illite and aragonite (Table 4.1), with small amounts of pyrite and montmorillonite. The illite and quartz in the swamp sediment are aeolian in origin, as illite is not typical of clays formed by basalt weathering, and the sandy lunette soils near Bullocks Swamp also contain aeolian quartz. The smaller depressions (Sites C and D) showed no obvious layering of the sediment in terms of colouring or texture, but had a similar mineralogical composition, with quartz and illite as the main minerals present (Table 4.1), both aeolian in origin. No carbonate minerals were identified (Table 4.1), confirmed by low calcium and magnesium levels (Table 4.2).

In the drained swamps, the confining lower layer limits infiltration, leading to waterlogging and allowing the formation of iron sulfides. The greater evaporation within the two swamps also allowed sufficient concentration of water in the swamp for the precipitation

of carbonate minerals, providing buffering capacity well in excess of any potential acidity. Using the classification scheme (Chapter 1), the sediments within both swamp sites were determined to be **buffered sulfidic soils (BSS)** above the confining layer, while the confining layer itself was classified as a **non-sulfidic soil**. In comparison, the smaller depressions (Sites C and D) contain no carbonate minerals, as any rainfall infiltrates relatively quickly into the underlying watertable, and the surface water does not become sufficiently concentrated for carbonate precipitation. The depressions showed no existing acidity (TAA) despite the lack of buffering capacity (Table 4.3), and oxidation in the lab showed only a small drop in pH. This was confirmed by the low levels of CRS (Table 4.3). The classification (Chapter 1) identifies the sediments in both smaller depressions as **potential acid sulfate soils (PASS)** as the sulfide content (0.04% CRS) is close to the EPA trigger level (%S > 0.03). However, even without buffering capacity, when combined with the small size of the sites, the soils will not release significant acidity when oxidised.

Therefore, the ASS classification of the swamp and depression sediments (**buffered sulfidic soil** and low level **potential acid sulfate soils (PASS)**, respectively), indicates that none of the sites are likely to undergo a large acidification event (pH drop to below 4) if the sediments are oxidised. As a result, the Basalt Plains are regarded as a low risk area for ASS.

7.2 Assessment of ASS in the Otway Ranges

The Otway Ranges contain a number of wetlands, including freshwater, poorly drained tea-tree peat swamps. Of the sites sampled within the Otways, three were defined as 'peat' swamps: Boundary Creek (Site A), the Anglesea River (Site B), and Porcupine Creek (Site C).

The two remaining sites were on the drained floodplain of the Barwon River: Pennyroyal Creek (Site D) and the Bambra Wetlands (Site E).

All three 'peat' sites formed through the infilling of river valleys, although each has a different cause of damming, and all have similar mineralogical compositions of predominantly quartz, kaolinite and illite, with smaller amounts of pyrite. Iron oxides are present at Boundary Creek and Anglesea, but not at Porcupine Creek (Tables 5.2, 5.13 and 5.19). No carbonate minerals were found within any of the swamp sediments. The two sites on the altered floodplain of the Barwon River (Sites D and E) also contained quartz and clay (kaolinite and illite) (Table 5.26), and had higher amounts of iron oxide minerals than the 'peat' sites; no pyrite was identifiable on the XRD scans despite CRS levels showing disulfide was present (Table 5.26).

The three 'peat' sites show not only that oxidation of sulfides is already occurring, but that there is still potential for further oxidation (due to the CRS levels present). No carbonate minerals were identified, so the swamps have no in situ buffering capacity, and any generated acidity will remain within the sediment until flushed by a rainfall event. Due to the lack of ANC, and both the present and potential acidity, all three sites contain **actual acid sulfate soils (AASS)**, although the swamp margin sediments sampled at Porcupine Creek (Site C) have lowered TAA and CRS values and are classified as a **potential acid sulfate soil (PASS)** at depth. The upper layer at Porcupine Creek was classified (Chapter 1) as a **low-risk sulfidic soil**, due to the continued oxidation of sulfides and the subsequent washing away of the generated acidity by rainfall events.

Due to the draining of the swamps originally present at Pennyroyal Creek (Site D) and the Bambra Wetlands (Site E), any sulfides that had built up within the sediments due to previous waterlogging have been oxidised and the acidity leached from the sites. The low levels of CRS and TAA classify Pennyroyal Creek and the Bambra Wetlands as **post-active sulfidic soils** throughout both layers of each profile.

Surface water analyses upstream and downstream of the Boundary Creek swamp showed that the water upstream is fresh (360-470 μS/cm) (Table 5.8), demonstrating that iron sulfide formation in inland ASS does not have to be linked with dryland salinity (Wallace et al. 2005a). The downstream analyses showed that although acidity and metals are being leached from the site, seasonal dilution by winter rainfall events and mixing with the higher volume flow of the West Barwon mean that the downstream water quality meets ANZECC guidelines.

7.3 Assessment of ASS Mapping

To determine the overall distribution of ASS in the Otways, so that areas potentially at risk of acidification events can be managed appropriately, ASS mapping was carried out using LIDAR topography, geology, Google Earth satellite images and Ecological Vegetation Class (EVC) mapping, both the 2005 map layer and the modelled 1750 vegetation map. The results were verified against known ASS sites, indicating that the method developed for mapping these areas remotely is accurate.

The mapping showed that relatively undisturbed swamps partially or completely covered by native vegetation and containing ASS with high CRS levels are uncommon in the Otways, but present a high risk of acidification if they are disturbed. In contrast, drained floodplains

originally covered by swamp vegetation are common, particularly along the West Barwon River. The drying of the upper part of the sediment profile due to the draining of the floodplains has resulted in oxidation of the sulfides and flushing of the generated acidity, but the underlying ASS below the watertable remain under anaerobic conditions and still contain high CRS levels. Therefore, any additional lowering of the watertable will expose this waterlogged sediment to oxygen and the sulfides present will oxidise, producing acidity, which can be transported into the nearby streams by a rainfall event. This means that these sediments need to be carefully managed; development or excavation of the floodplain could potentially lead to an acidification event.

References

Ahern, C, Blunden, B & Stone, Y 1998. Acid Sulfate Soil Laboratory Methods Guidelines. Wollongbar, NSW.

Ahern, C & McElnea, A. Reactions of acid sulfate soils. *In:* Hey, KM, Ahern, CR, Eldershaw, VJ, Anorov, JM & Watling, KM, eds. Acid sulfate soils and their management in coastal Queensland: forum and technical papers, 1999 Indooroopilly, Queensland. Department of Natural Resources, 1-5.

Ahern, C, McElnea, A, Hicks, W & Baker, D. A combined routine peroxide method for analysing acid sulphate soils. *In:* Smith, R, ed. second national acid sulphate soil conference, September, 1996 1996 Coffs Harbour. Wollongbar, NSW: Acid Sulfate Management Advisory Committee, 82-85.

Ahern, C, McElnea, A & Sullivan, L 2004. Acid Sulfate Soils Laboratory Methods Guidelines, version 2.1. Indooroopilly, Queensland: Queensland Department of Natural Resources, Mines and Energy.

Aller, R 1980. Diagenic processes near the sediment-water interface of Long Island Sound: II Fe and Mn. *Advances in Geophysics,* 22**,** 351-415.

Andriesse, W & van Mensvoort, M 2006. Acid Sulfate Soils: distribution and extent. *In:* Lal, R (ed.) *Encyclopedia of Soil Science.* second ed. Boca Raton, FL: CRC Press, Taylor & Francis Group.

ANZECC 2000. Australian and New Zealand guidelines for fresh and marine water quality.

ANZECC & NHMRC 1992. Australian and New Zealand guidelines for the assessment and management of contaminated sites. Australia: Australian and New Zealand Environment Conservation Council (ANZECC) and National Health and Medical Research Council (NHMRC).

Arkensteyn, G 1980. Pyrite oxidation in acid sulphate soil: the role of microorganisms. *Plant and Soil,* 54**,** 119-134.

Åström, M & Corin, N 2000. Abundance, sources and speciation of trace elements in humus-rich Streams affected by acid sulphate soils. *Aquatic Geochemistry,* 6**,** 367-383.

Baker, B & Banfield, J 2003. Microbial communities in acid mine drainage. *FEMS Microbiology Ecology,* 44**,** 139-152.

Baldwin, D, Hall, K, Rees, G & Richardson, A 2007. Development of a protocol for recognizing sulfidic sediments (potential acid sulfate soils) in freshwater wetlands. *Ecological Management and Restoration,* 8**,** 56-60.

Barton, A, Cox, J, Dahlhaus, P & Herczeg, A 2006. Groudnwater flow and groundwater-surface water interactions in the Corangamite CMA region. *In:* Fitzpatrick, RW & Shand, P (eds.) *Regolith 2006 - consolidation and dispersion of ideas: proceedings of the CRC LEME regolith symposium.* CRC LEME.

Barton, A, Herczeg, A, Dahlhaus, P & Cox, J 2007. A geochemical approach to determining the hydrological regime of wetlands in a volcanic plain, south–eastern Australia. *Groundwater and Ecosystems. XXXV IAH Congress.* Lisbon, Portugal.

Barwon 2013. Gerangamete Groundwater Management Area 2012-2013 report. *In:* Water, Barwon (ed.). Geelong, Victoria: Barwon Water.

Bennetts, D, Webb, J & Gray, C 2003. Distribution of Plio-Pleistocene basalts and regolith around Hamilton, western Victoria, and their relationship to groundwater recharge and discharge. *In:* Roach, IC (ed.) *Advances in Regolith.* CRC LEME.

Berner, R 1970. Sedimentary pyrite formation. *American Journal of Science,* 268.

Berner, R 1984. Sedimentary pyrite formation: An update. *Geochimica et Cosmochimica Acta,* 48**,** 605-615.

Bibi, I, Singh, B & Silvester, E 2011. Akaganeite (b-FeOOH) precipitation in inland acid sulfate soils of south-western New South Wales (NSW), Australia. *Geochimica et Cosmochimica Acta,* 75**,** 6429-6438.

Boettinger, J & Richardson, J 2000. Chapter 18: Saline and wet soils of wetlands in dry climates. *In:* Richardson, JL & Vepraskas, MJ (eds.) *Wetland Soils: Genesis, Hydrology, Landscapes, and Classification.* United States of America: CRC Press LLC.

Boult, P, White, M, Pollock, R, Morton, J, Alexander, A & Hill, A 2002. Chapter 6: lithostratigraphy and environments of deposition. *The petroleum geology of South Australia, vol. 1: Otway Basin, 2nd edition.* South Australia: Department of Primary Industries and Resources.

Boulton, A, Brock, M, Robson, B, Ryder, D, Chambers, J & Davis, J 2014. *Australian freshwater ecology: processes and management*.

Bowman, G 1993. Case studies of acid sulphate soil management. *In:* Bush, R (ed.) *Proceedings: national conference on acid sulphate soils, 24-25 June 1993.* Orange, NSW: NSW Agriculture.

Brady, N & Weil, R 2002. *The nature and properties of soil,* New Jersey, Prentice Hall.

Brinkman, R & Pons, L. Recognition and prediction of acid sulphate soil conditions. *In:* Dost, H, ed. Proceedings of the International Symposium on Acid Sulphate Soils, 1973 Wageningen. International Insitute for Land Reclaimation and Improvement, 169-203.

Bryan, S, Constantine, A, Stephens, C, Ewart, A, Shön, R & Parianos, J 1997. Early Cretaceous volcano-sedimentary successions along the eastern Australian continental margin: Implications for the break-up of eastern Gondwana. *Earth and Planetary Science Letters,* 153**,** 85-102.

Burton, E, Bush, R & Sullivan, L 2006. Acid-volatile sulfide oxidation in coastal flood plain drains: iron-sulfur cycling and effects on water quality. *Environmental Science and Technology,* 40**,** 1217-1222.

Burton, E, Sullivan, L, Bush, R & Johnston, SK, AF 2008. A simple and inexpensive chromium-reducible sulfur method for acid-sulfate soils. *Applied Geochemistry,* 23**,** 2759-2766.

Bush, R, Fyfe, D & Sullivan, L 2004a. Occurance and abundance of monosulfidic black ooze in coastal acid sulfate soil landscapes. *Australian Journal of Soil Research,* 42**,** 609-616.

Bush, R, McGrath, R & Sullivan, L 2004b. Occurence of marcasite in organic-rich Holocene estuarine mud. *Australian Journal of Soil Research,* 42**,** 617-621.

Calmano, W, Hong, J & Förstner, U 1993. Binding and mobilization of heavy metals in contaminated sediments affected by pH and redox potential. *Water Science and Technology,* 28**,** 223-235.

Campbell, E 1983. Chapter 5: mires of Australasia. *In:* Gore, AJP (ed.) *Mires: swamp, bog, fen and moor.* Oxford, New York: Elsevier Scientific Publishing Company.

Canfield, D, Raiswell, R, Westrich, J, Reaves, C & Berner, R 1986. The use of chromium reduction in the analysis of reduced organic sulfur in sediments and shales. *Chemical Geology,* 54**,** 149-155.

Carter, O 2010. National Recovery Plan for the Spiny Peppercress *Lepidium aschersonii*. Melbourne, Victoria: Victorian Government Department of Sustainability and Environment (DSE).

Cayley, R & McDonald, P 1995. Beaufort 1:100 000 geological map report. *Geological Survey of Victoria Report.*

CCMA 2003. Corangamite Regional Catchment Strategy 2003-2008. Colac, Victoria: Corangamite Catchment Management Authority (CCMA).

CCMA 2005. Corangamite Native Vegetation Plan 2003-2008. Colac, Victoria: Corangamite Catchment Management Authority (CCMA).

CCMA 2006a. Corangamite River Health Strategy 2006-2011. Colac, Victoria.

CCMA 2006b. Environmental flow determination for the Barwon River: final report - flow recommendations. Colac, Victoria: Corangamite Catchment Management Authority.

CCMA 2012. Draft Anglesea River Estuary Management Plan 2012-2020. Corangamite Catchment Management Authority (CCMA).

CCMA 2013a. Corangamite Catchment Management Authority Annual Report 2012-2013. Colac, Victoria: Corangamite Catchment Management Authority (CCMA).

CCMA 2013b. Corangamite Regional Catchment Strategy 2013-2019. Colac, Victoria: Corangamite Catchment Management Authority (CCMA).

CCMA 2013c. Seasonal Watering Proposal for the Lower Barwon Wetlands 2013 – 2014. Colac, Victoria.

Charman, D 2002. *Peatlands and Environmental Change,* UK, John Wiley & Sons.

Clark, M, Lancaster, G & McConchie, D 1996. Total sulphide acidity for the definition and quantitative assessment of the acid sulphate hazard: a simple solution of a suite of new problems. *The Science of the Total Environment,* 183**,** 249-254.

Clarkson, T, Crook, I & Dahlhaus, P 2007. Corangamite Soil Health Strategy 2006-2012. Colac, Victoria: Department of Primary Industries on behalf of the Corangamite Catchment Management Authority.

Clymo, R 1983. Chapter 4: Peat. *In:* Gore, AJP (ed.) *Mires: swamp, bog, fen and moor.* Oxford, New York: Elsevier Scientific Publishing Company.

Constantine, A 2001. Section C: Otway Basin. *Petroleum Atlas of Victoria, Australia.* Victoria: Victorian Department of Primary Industries.

Cooper, G 1995. Seismic structure and extensional development of the eastern Otway Basin-Torquay Embayment. *Australian Petroleum Exploration Association Journal,* 35, 436-450.

CPA 1971. Water resources and utilisation. *In:* Committee, Central Planning Authority in collaboration with the Barwon Regional (ed.) *Resources Survey: Barwon Region.* Melbourne: C.H. Rixon, Government Printer.

Crawford, A, Cayley, R, Taylor, D, Morand, V, Gray, C, Kemp, A, Wohlt, K, VandenBerg, A, Moore, D, Maher, S, Direen, N, Edwards, J, Donaghy, A, Anderson, J & Black, L 2003. Chapter 3: Neoproterozoic and Cambrian - continental rifting, continent-arc collision and post-collisional magmatism. *In:* Birch, WD (ed.) *Geology of Victoria.* 3rd ed.: Geological Society of Australia (Victorian Division).

CSIRO 2012. Contributing to the Australian Soil Resource Information System (ASRIS): guidelines for the inclusion of your soil data and information. *In:* CSIRO (ed.). Canberra, Australia: CSIRO.

Cupper, M, White, S & Neilson, J 2003. Chapter 11: Quaternary: ice ages - environments of change. *In:* Birch, WD (ed.) *Geology of Victoria.* 3rd ed.: Geological Society of Australia (Victoria Division).

Dahlhaus, P 2002. Groundwater Flow Systems of the Corangamite Catchment Management Authority region. *CCMA reports.* Dahlhaus Environmental Geology Pty Ltd.

Dahlhaus, P, Cox, J, Macewan, R & Codd, P 2003. Victorian Volcanic Plains Scoping Study Final Report. CSIRO Land and Water.

Dahlhaus, P, Cox, J, Simmons, C & Smitt, C 2008. Beyond hydrogeologic evidence: challenging the current assumptions about salinity processes in the Corangamite region, Australia. *Hydrogeology Journal,* 16**,** 1283-1298.

Dahlhaus, P, Miner, A, Feltham, W & Clarkson, T 2006a. The impact of landslides and erosion in the Corangamite region, Victoria, Australia. *In:* Culshaw, M, Reeves, H, Spink, T & Jefferson, I (eds.) *10th IAEG International Congress.* Nottingham, United Kingdom The Geological Society of London.

Dahlhaus, P, Miner, A, Feltham, W & Clarkson, T. The impact of landslides and erosion in the Corangamite region, Victoria, Australia. The 10th IAEG International Congress, 6-10 September 2006b Nottigham, United Kingdom. IAEG, pp. 10.

Davidson, N & Lancaster, G 2011. Preliminary inland acid sulfate soil assessment report: investigation of wetland habitats (Barongarook Creek catchment, Boundary Creek catchment, Loves Creek catchment), Otway Ranges, south of Colac, Victoria, prepared for Land and Water Resources Otway Catchment (LAWROC). EAL Consulting Service (Southern Cross University).

De Deckker, P 2003. Saline playa-groundwater interactions in the Western District of Victoria. *In:* Roach, IC (ed.) *Advances in Regolith.* CRCLEME.

Dear, S, Moore, N, Dobos, S, Watling, K & Ahern, C 2002. *Queensland acid sulfate soil technical manual: soil management guidelines, version 3.8,* Indooroopilly, Queensland, Department of Natural Resources and Mines.

Degens, B, Fitzpatrick, R & Hicks, W 2008. Chapter 11: Avon Bason, WA wheat belt - acidification and formation of inland ASS matieral in salt lakes by acid drainage and regional groundwater discharge. *In:* Fitzpatrick, R & Shand, P (eds.) *Inland acid sulfate soil systems across Australia.* Perth, Australia: CRC LEME.

Demas, S, Hall, A, Fanning, D, Rabenhorst, M & Dzantor, E 2004. Acid sulfate soils in dredged materials from tidal Pocomoke Sound in Somerset County, MD, USA. *Australian Journal of Soil Research,* 42**,** 537-545.

Dent, D 1986. *Acid sulphate soils: a baseline for research and development,* Wageningen, International Institute for Land Reclamation and Improvement (IILRI).

Dent, D & Bowman, G 1993. Definition and quantitative assessment of the acid sulphate hazard for planning and environmental management. *In:* Bush, R (ed.) *Proceedings: national conference on acid sulphate soils, 24-25 June 1993.* Orange, NSW: NSW Agriculture.

Dent, D & Bowman, G 1996. Quick quantitative assessment of the acid sulfate hazard. *Divisional Report.* Illustrated ed.: CSIRO Division of Soils.

Dent, D & Pons, L. Acid and muddy thoughts. *In:* Bush, R, ed. Proceedings: national conference on acid sulphate soils, 24-25 June 1993, 1993 Orange, NSW. NSW Agriculture, 1-18.

Department of Agriculture, FaFD 1999. Mineral Assessment Report. *In:* Committee, Commonwealth and Victorian Regional Forest Agreement (RFA) Steering (ed.).

Dickinson, J, Wallace, M, Holdgate, G, Gallagher, S & Thomas, L 2002. Origin and timing of the Miocene-Pliocene unconformity in southeast Australia. *Journal of Sedimentary Research,* 72**,** 288-303.

Douglas, J 1977. The geology of the Otway region, southern Victoria. *Proceedings of the Royal Society of Victoria,* 89**,** 19–24.

DSE 2004. Vegetation quality assessment manual: guidelines for applying the habitat hectares scoring method, version 1.3. Melbourne, Victoria: Victorian Government Department of Sustainability and Environment (DSE).

DSE 2005a. Dreeite Nature Conservation Reserve Management Statement. Melbourne, Victoria: Department of Sustainability and Environment.

DSE 2005b. EVC/Bioregion benchmark for vegetation quality assessment EVC 53: swamp scrub. Victoria: Department of Sustainability and Environment.

DSE 2005c. EVC/Bioregion Benchmark for Vegetation Quality Assessment: Central Victorian Uplands bioregion. *In:* (DSE), Department of Sustainability and Environment (ed.). Melbourne, Victoria: Department of Sustainability and Environment (DSE).

DSE 2005d. EVC/Bioregion Benchmark for Vegetation Quality Assessment: Otway Plain bioregion. *In:* (DSE), Department of Sustainability and Environment (ed.). Melbourne, Victoria: Department of Sustainability and Environment (DSE).

DSE 2005e. EVC/Bioregion Benchmark for Vegetation Quality Assessment: Otway Ranges bioregion. *In:* (DSE), Department of Sustainability and Environment (ed.). Melbourne, Victoria: Department of Sustainability and Environment (DSE).

DSE 2005f. EVC/Bioregion Benchmark for Vegetation Quality Assessment: Warrnambool Plain bioregion. *In:* (DSE), Department of Sustainability and Environment (ed.). Melbourne, Victoria: Department of Sustainability and Environment (DSE).

DSE 2008. Climate change in the Corangamite region. Melbourne: Department of Sustainability and Environment.

DSE 2009. Victorian coastal acid sulfate soil strategy. *In:* (DSE), Department of Sustainability and Environment (ed.). Melbourne, Victoria: Department of Sustainability and Environment.

DSE 2011. Western Region Sustainable Water Strategy.

Du Laing, G, Rinklebe, J, Vandecasteele, E, Meers, E & Tack, F 2009. Trace metal behaviour in estuarine and riverine floodplain soils and sediments: A review. *Science of the Total Environment,* 407**,** 3972-3985.

Duddy, I 2003a. Chapter 9: Mesozoic - a time of change in tectonic regime. *In:* Birch, WD (ed.) *Geology of Victoria.* 3rd ed. Victoria: Geological Society of Australia (Victorian Division).

Duddy, I 2003b. Chapter 9: Mesozoic - a time of change in tectonic regime. *Geology of Victoria.* Victoria: Geological Society of Australia, Victorian Division.

Dwyer, L 1957. Climate. *In:* Committee, Central Planning Authority in collaboration with the Corangamite Regional (ed.) *Resources Survey: Corangamite Region.* Melbourne: A.C. Brooks, Government Printer.

Environment, DoNRa 2000. Biodiversity assessment report: Victorian West RFA region. Department of Natural Resources and Environment.

EPA 2009. Information bulletin: acid sulfate soil and rock, publication 655.1. Victoria: Evironmental Protection Agency.

Evangelou, V & Zhang, Y 1995. A review: pyrite oxidation mechanisms and acid mine drainage prevention. *Critical Reviews in Environmental Science and Technology,* 25**,** 141-199.

Evans, C, Fanning, D & Short, J 2000. Human-influenced soils. *In:* Brown, RB, Huddleston, JH & Anderson, JL (eds.) *Mangaing soils in an urban environment.* Madison, Wisconsin: American Society of Agronomy.

Fanning, D 1993. Salinity problems in acid sulfate soils. *In:* Lieth, H & Al Masoom, A (eds.) *Towards the rational use of high salinity tolerant plants.* Kluwer Academic Publishers.

Fanning, D 2006. Acid sulfate soils. *In:* Lal, R (ed.) *Encyclopedia of Soil Science.* second ed.: CRC Press.

Fanning, D, Coppock, C, Orndorff, Z, Daniels, W & Rabenhorst, M 2004. Upland active acid sulfate soils from construction of new Stafford County, Virginia, USA, ariport. *Australian Journal of Soil Research,* 42**,** 527-536.

Fanning, D & Fanning, M 1989. *Soil morphology, genesis and classification,* New York, John Wiley and Sons.

Fanning, D & Muckel, G 2004. Acid sulfate soils. *In:* Muckel, GB (ed.) *Understanding soil risks and hazards: using soil survey to identify areas with risks and hazards to human life and property.* Lincoln, Nebraska: United States Department of Agriculture (USDA).

Fanning, D, Rabenhorst, M, Balduff, D, Wagner, D, Orr, R & Zurheide, P 2010. An acid sulfate perspective on landscape/seascape soil mineralogy in the U.S. Mid-Atlantic region. *Geoderma,* 154**,** 457-464.

Fanning, D, Rabenhorst, M, Wagner, D, Lowery, D & James, B 2012. Rethinking sulfidization and the role of hydrogen sulfide. *In:* Österholm, P, Yli-Halla, M & Edén, P (eds.) *7th International Acid Sulfate Soil Conference.* Vaasa, Finland.

Fawcett, J, Fitzpatrick, R & Norton, R 2008. Chapter 18: Inland acid sulfate soils of the spring zones across the eastern Dundas Tableland, south eastern Australia. *In:* Fitzpatrick, R & Shand, P (eds.) *Inland acid sulfate soil systems across Australia.* Perth, Australia: CRC LEME.

Fergusson, C 2003. Ordovician–Silurian accretion tectonics of the Lachlan Fold Belt, southeastern Australia. *Australian Journal of Earth Sciences,* 50**,** 475-490.

Fitzpatrick, R, Fritsch, E & Self, P 1996. Interpretation of soil features produced by ancient and modern processes in degraded landscapes: V development of saline sulfidic features in non-tidal seepage areas. *Geoderma,* 69**,** 1-29.

Fitzpatrick, R, Hicks, W, Marvanek, S, Raven, M, Dahlhaus, P & Cox, J 2007. Scoping study of coastal and inland acid sulfate soils in the Corangamite CMA.

Fitzpatrick, R, Marvanek, S, Shand, P, Merry, R & Thomas, M 2008a. Acid Sulfate Soil Maps of the River Murray below Blanchetown (Lock 1) and Lakes Alexandrina and Albert when water levels were at pre- drought and current drought conditions. *CSIRO Land and Water Science Report.* South Australia: CSIRO Land and Water.

Fitzpatrick, R, Powell, B & Marvanek, S 2008b. Chapter 2: Atlas of Australian Acid Sulfate Soils. *In:* Fitzpatrick, R & Shand, P (eds.) *Inland Acid Sulfate Soil Systems Across Australia.* Perth, Australia: CRC LEME.

Fitzpatrick, R, Powell, B & Marvanek, S 2011. Atlas of Australian Acid Sulphate Soils. v2. *In:* CSIRO (ed.).

Fitzpatrick, R & Shand, P 2008. Chapter 1: Inland acid sulfate soils - overview and conceptual models. *In:* Fitzpatrick, R & Shand, P (eds.) *Inland acid sulfate soil systems across Australia.* Perth, Australia: CRC LEME.

Foster, D & Gray, D 2000. Evolution and structure of the Lachlan Fold Belt (Orogen) of eastern Australia. *Annu. Rev. Earth Planet. Sci,* 28**,** 47-80.

Fraser, I 1957. Water resources and utilisation. *In:* Committee, Central Planning Authority in collaboration with the Corangamite Regional (ed.) *Resources Survey: Corangamite Region.* Melbourne: A.C. Brooks, Government Printer.

Gardner, E, Rayment, G & Cook, F 2000. Distribution, behaviour and management of acid sulfate soils. *Environmental short course for sustainable sugar production: course manual.* Townsville: Cooperative Research Centre (CRC) for Sustainable Sugar Production.

Gibson, D 2007. Potassium-Argon ages of Late Mesozoic and Cainozoic Igneous rocks of eastern Australia, CRC LEME open file report 193. Bentley, WA: CRC LEME.

Glover, F. 2008. *Inland acid sulfate soils: a study of three wetlands along the Murray River, Australia.* Honours, La Trobe University.

Glover, F & Webb, J 2013. Report on Anglesea River Acid Sulfate Soils. La Trobe University: La Trobe University.

Glover, FW, KL, Kappen, P, Baldwin, D, Rees, G, Webb, J & Silvester, E 2011. Acidification and buffering mechanisms in acid sulfate soil wetlands of the Murray-Darling Basin, Australia. *Environmental Science and Technology,* 45**,** 2591–2597.

Gray, D & Foster, D 1997. Orogenic concepts - application and definition: Lachlan Fold Belt, eastern Australia. *American Journal of Science,* 297**,** 859-891.

Grover, S, McKenzie, B, Baldock, J & Papst, W 2005. Chemical characterisation of bog peat and dried peat of the Australian Alps. *Australian Journal of Soil Research,* 43**,** 963-971.

GSV 1995. The stratigraphy, structure, geophysics and hydrocarbon potential of the Eastern Otway Basin. *In:* (GSV), Geological Survey of Victoria (ed.) *Geological Survey of Victoria reports.* Melbourne.

Gunn, P 1975. Mesozoic-Cainozoic tectonics and igneous activity: southeastern Australia. *Australian Journal of Earth Sciences,* 22**,** 215-221.

Hall, K, Baldwin, D, Rees, G & Richardson, A 2006. Distribution of inland wetlands with sulfidic sediments in the Murray-Darling Basin, Australia. *Science of the Total Environment,* 370**,** 235-244.

Harding, C & Callister, K 2005. Corangamite Wetland Inventory. Ballarat, Victoria: Prepared for the Corangamite Catchment Management Authority by the Centre for Environmental Management, Univeristy of Ballarat.

Harris, S & Smith, S 2000. Flora and Fauna Guarantee Action Statement No 111: Spiny Pepper-cress *Lepidium aschersonii*. Melbourne, Victoria: Department of Natural Resources and Environment.

Hart, M 1963. Observations in the source of acid empoldered mangrove soils II: oxidation of polysulphides. *Plant and Soil,* 19**,** 106-114.

Hicks, W, Bowman, G & Fitzpatrick, R 1999. East Trinity acid sulfate soil, part one: environmental hazards, technical report 14/99. Urrbrae, SA: CSIRO Land and Water.

Hill, K, Cooper, G, Richardson, M & Lavin, C 1994. Structural framework of the eastern Otway Basin: inversion and interaction between two major structureal provinces. 25.

Hill, P, Meixner, A, Moore, A & Exon, N 1997. Structure and development of the west Tasmanian offshore sedimentary basins: Results of recent marine and aeromagnetic surveys. *Australian Journal of Earth Sciences,* 44**,** 579-596.

Hillel, D 1998. *Environmental soil physics,* San Diego, Academic Press.

Hills, E 1975. *Physiography of Victoria: an introduction to geomorphology,* Australia, New Zealand, London, Whitcombe & Tombs Pty. Ltd.

Holdgate, G & Gallagher, S 2000. The palaeogeographic and palaeoenvironmental evolution of a Palaeogene mixed carbonate–siliciclastic cool-water succession in the Otway Basin, Southeast Australia. *Palaeogeography, Palaeoclimatology, Palaeoecology,* 156**,** 19-50.

Holdgate, G & Gallagher, S 2003. Chapter 10: Tertiary - a period of transition to marine basin environments. *In:* Birch, WD (ed.) *Geology of Victoria.* 3rd ed.: Geological Society of Australia (Victoria Division).

Holdgate, G, Smith, T, Gallagher, S & Wallace, M 2001. Geology of coal-bearing Palaeogene sediments, onshore Torquay Basin, Victoria. *Australian Journal of Earth Sciences,* 48**,** 657–679.

Hose, K, Mitchell, B & Gwyther, J 2008. Investigation and reporting of past and present ecological characteristics of seven saline lakes in the Corangamite Catchment Management Area. Geelong, Australia: Deakin University.

House, M, Farley, K & Kohn, B 1999. An empirical test of helium diffusion in apatite: borehole data from the Otway Basin, Australia. *Earth and Planetary Science Letters,* 170, 463-474.

Ingram, H 1983. Chapter 3: Hydrology. *In:* Gore, AJP (ed.) *Mires: swamp, bog, fen and moor.* New York: Elsiever Publishing Company.

Institute 2011. Documenting fish assemblages in the Anglesea River estuary following acidification events. The Arthur Rylah Institute.

Janzen, H & Ellert, B 1998. Chapter 2: sulfur dynamics in temperate agroecosystems. *In:* Maynard, DG (ed.) *Sulfur in the environment.* New York: Marcel Dekker Inc.

Jensen-Schmidt, B, Cockshell, C & Boult, P 2002. Chapter 5: structural and tectonic setting. *The petroleum geology of South Australia, vol. 1: Otway Basin, 2nd edition.* South Australia: Department of Primary Industries and Resources.

Joyce, E 2003. Western volcanic plains Victoria. *In:* Anand, RR & de Broekert, P (eds.) *Regolith Landscape Evolution Across Australia.* Bentley: Cooperative Research Centre for Landscape Environments and Mineral Exploration.

Joyce, E, Webb, J, Dahlhaus, P, Grimes, K, Hill, S, Kotsonis, A, Martin, J, Mitchell, M, Neilson, J, Orr, M, Peterson, J, Rosengren, N, Rowan, J, Rowe, R, Sargeant, I, Stone, T, Smith, B, White, S & Jenkin, J 2003a. Chapter 18: Geomorphology - the evolution of Victorian landscapes. *In:* Birch, WD (ed.) *Geology of Victoria.* Geological Society of Australia (Victoria Division).

Joyce, E, Webb, J, Dahlhaus, P, Grimes, K, Hill, S, Kotsonis, A, Martin, J, Mitchell, MN, JL

Orr, ML, Peterson, J, Rosengren, N, Rowan, J, Rowe, R, Sargeant, I, Stone, T, Smith, B, White, S & Jenkin, J 2003b. Chapter 18: Geomorphology - the evolution of Victorian landscapes. *In:* Birch, WD (ed.) *Geology of Victoria.* Geological Society of Australia (Victoria Division).

Kenley, P 1971. Cainozoic geology of the eastern part of the Gambier Embayment, Southwestern Victoria. *In:* Wopfner, H & Douglas, JG (eds.) *The Otway Basin of southeastern Australia. Special Bulletin.* Adelaide: Geological Surveys of South Australia and Victoria.

Kenley, P 1988. Quaternary - Southwestern Victoria. *In:* Douglas, JG & Ferguson, JA (eds.) *Geology of Victoria.* Melbourne: Geological Society of Australia, Victorian Division.

Konhauser, K 2007. Introduction to geomicrobiology. United Kingdom: Blackwell Publishing.

Korsch, R, Barton, T, Gray, D, Owen, A & Foster, D 2002. Geological interpretation of a deep seismic-reflection transect across the boundary between the Delamerian and Lachlan Orogens, in the vicinity of the Grampians, western Victoria. *Australian Journal of Earth Sciences,* 49**,** 1057-1075.

Lamontagne, S, Hicks, W, Fitzpatrick, R & Rogers, S 2003. Sulfidic materials: an emerging issue for the management of saline areas, the River Murray floodplain. *Advances in Regolith.* Canberra: Cooperative Research Centre for Landscape Environments and Mineral Exploration (CRC LEME).

Lamontagne, S, Hicks, W, Fitzpatrick, R & Rogers, S 2004. Survey and description of sulfidic materials in wetlands of the Lower River Murray floodplains: implications for floodplain salinity management, CRC LEME open file report 165. South Australia: CSIRO.

Lamontagne, S, Hicks, W, Fitzpatrick, R & Rogers, S 2006. Sulfidic materials in dryland river wetlands. *Marine and Freshwater Research,* 57**,** 775-788.

Lavin, C 1997. The Maasstrichtian breakup of the Otway Basin margin - a model developed by intergrating seismic interpretation, sequence stratigraphy and thermochronological studies. *Exploration Geophysics,* 28**,** 252-259.

Lennie, A, Redfern, S, Champness, P, Stoddart, C, Schofield, P & Vaughan, D 1997. Transformation of mackinawite to greigite: An in situ X-ray powder diffraction and transmission electron microscope study. *American Mineralogist,* 82**,** 302-309.

Lett, R, Abernathy, B & H, C. Are all river reaches created equal? Identifying erosion hotspots for catchment management. *In:* Wilson, AL, Dehaan, RL, Watts, RJ, Page, KJ, Bowmer, KH & Curtis, A, eds. Proceedings of the 5th Australian Stream Management Conference. Australian rivers: making a difference. , 2007 Charles Sturt University, Thurgoona, New South Wales. 6.

Lewis, S, Sloss, C, Murray-Wallace, C, Woodroffe, C & Smithers, S 2013. Post-glacial sea-level changes around the Australian margin: a review. *Quaternary Science Reviews,* 74**,** 115-138.

Lithgow, S. 2007. *The source of acid run events in the Anglesea River and its tributaries.* Honours, Deakin University.

Lunt, I 1998. Two Hundred Years of Land Use and Vegetation Change in a Remnant Coastal Woodland in Southern Australia. *Australian Journal of Botany,* 46**,** 629-647.

Madigan, M & Martinko, J 2006. *Brock biology of microorganisms,* USA, Pearson Prentice Hall.

Maher, W. 2011. Anglesea River Water Quality Independant Review. Available: http://www.water.vic.gov.au/environment/rivers/river-health/anglesea-river-water-quality-review [Accessed 28/02/2012].

McElnea, A, Ahern, C & Menzies, N 2002. The measurement of actual acidity in acid sulfate soils and the determination of sulfidic acidity in suspension after peroxide oxidation. *Australian Journal of Soil Research,* 40**,** 1133-1157.

McElnea, A, Ahern, C & Menzies, N 2002a. Improvements to peroxide oxidation methods for analysing sulfur in acid sulfate soils. *Australian Journal of Soil Research,* 40**,** 1115-1132.

McElnea, A, Ahern, C & Menzies, N 2002b. The measurement of actual acidity in acid sulfate soils and the determination of sulfidic acidity in suspension after peroxide oxidation. *Australian Journal of Soil Research,* 40**,** 1133-1157.

Melville, M, White, I & Lin, C. The origins of acid sulphate soils. *In:* Bush, R, ed. Proceedings: national conference on acid sulphate soils, 24-25 June 1993, 1993 Orange, NSW. NSW Agriculture, 19-25.

Miller, J, Norvick, M & Wilson, C 2002a. Basement controls on rifting and the associated formation of ocean transform faults-Cretaceous continental extension of the southern margin of Australia 359.

Miller, J, Norvick, M & Wilson, C 2002b. Basement controls on rifting and the associated formation of ocean transform faults - Cretaceous continental extension of the southern margin of Australia. *Tectonophysics,* 359**,** 131-155.

Miyazaki, S, Lavering, I & Stephenson, A 1990. Australian petroleum report 6: Otway Basin, South Australia, Victoria and Tasmania. Canberra: Australian Government Publishing Service.

Morand, V, Ramsay, W, Hughes, M & Stanley, J 1995. The southern Avoca fault zone: Site of a newly identified 'greenstone' belt in western Victoria. *Australian Journal of Earth Sciences,* 42**,** 133-143.

Morse, J & Cornwell, J 1987. Analysis and distribution of iron sulfide minerals in recent anoxic marine sediments. *Marine Chemistry,* 22**,** 55-69.

Moses, C & Herman, J 1991. l?yrite oxidation at chumneutral pH. *Geochimica et Cosmochimica Acta,* 55**,** 471-482.

Moses, C, Nordstrom, D, Herman, J & Mills, A 1987. Aqueous pyrite oxidation by dissolved oxygen and by ferric iron. *Geochimica et Cosmochimica Acta,* 51**,** 1561-1571.

Naylor, S, Chapman, G, Atkinson, G, Murphy, C, Tulau, M, Flewin, T, Milford, H & Morand, D 1998. Guidelines for the Use of Acid Sulfate Soil Risk Maps. 2nd ed. Sydney, NSW.

Nicholson, C, Dahlhaus, P, Anderson, G, Kelliher, C & Stephens, M 2006. Corangamite Salinity Action Plan 2005-2008. 1st ed. Colac, Victoria.

Nicolaides, S 1995. Cementation in Oligo-Miocene non-tropical shelf limestones, Otway Basin, Australia. *Sedimentary Geology,* 95**,** 97-121.

Niewójt, L 2009. Gadubanud society in the Otway Ranges, Victoria: an environmental history. *In:* Read, P (ed.) *Aboriginal History Volume 33.* ANU E Press and Aboriginal History Incorporated.

Norrish, K & Thompson, G 1990. XRS analysis of sulphides by fusion methods. *X-ray Spectrometry,* 19**,** 67-71.

NRMMC 2006. National cooperative approach to coastal intergrated management: framework and implementation plan. Canberra: Department of Environment and Heritage.

OREN 2003. Angahook – Otway Investigation. Submission regarding discussion paper and Otway National Park boundaries *In:* (OREN), Otway Ranges Environment Network (ed.). Otway Ranges Environment Network (OREN).

Orndorff, Z, Daniels, W & Fanning, D 2008. Reclamation of acid sulfate soils using lime-stabilized biosolids. *Journal of Environmental Quality,* 37**,** 1447-1455.

Orth, K 1988. Geology of the Warrnambool 1:50,000 mapsheet. Report 86.: Geological Survey of Victoria.

Osterreth, M 1994. Iron sulfides and pedogenesis in alluvial soils of the late Holocene in the coastal area of Buenos Aires, Argentina. *Trans. 15th World Congress of Soil Science,* 6b**,** 129-130.

Petersen, J, Sack, D & Gabler, R 2014. Chapter 14: fluvial processes and landforms. *Fundamentals of Physical Geography.* second ed. USA: Cengage Learning.

Petrides, B & Cartwright, I 2006. The hydrogeology and hydrogeochemistry of the Barwon Downs Graben aquifer, southwestern Victoria, Australia. *Hydrogeology Journal,* 14**,** 809-826.

Pias, I & Jones, J 1997. *The handbook of trace elements,* Florida, St. Lucie Press.

Pons, L, van Breeman, N & Driessen, P 1982. Chapter 1: Physiography of coastal sediments and the development of potential soil acidity. *In:* Kittrick, JA, Fanning, DS & Hossner, RL (eds.) *Acid Sulfate Weathering.* Madison, Wisconsin: Soil Science Society of America.

Pope, A. 2006. *Freshwater influences on the hydrology and seagrass dynamics of intermittent estuaries.* PhD, Deakin University.

Powell, B & Ahern, C. Nature, origin and distribution of acid sulfate soils: issues for Queensland. *In:* Hey, KM, Ahern, CR, Eldershaw, VJ, Anorov, JM & Watling, KM, eds. Acid sulfate soils and their management in coastal Queensland: forum and technical papers, 1999 Indooroopilly, Queensland. Department of Natural Resources, 1-11.

Price, R, Gray, C & Frey, F 1997. Strontium isotopic and trace element heterogeneity in the plains basalts of the Newer Volcanic Province, Victoria, Australia. *Geochimica et Cosmochimica Acta,* 61**,** 171-192.

Pyper, W & Davidson, S 2001. Bubble, bubble: uncovering the true nature and severity of acid sulfate soil in inland Australia. *Ecos,* 106**,** 28-31.

Rabenhorst, M & Fanning, D 2006. Acid sulfate soils: problems. *In:* Lal, R (ed.) *Encyclopedia of Soil Science.* CRC Press.

Rabenhorst, M, Fanning, D & Burch, S 2006. Acid sulfate soils: formation. *In:* Lal, R (ed.) *Encyclopedia of Soil Science.* second ed.: CRC Press.

Raiber, M, Webb, J & Bennetts, D 2009. Strontium isotopes as tracers to delineate aquifer interactions and the influence of rainfall in the basalt plains of southeastern Australia. *Journal of Hydrology,* 367**,** 188-199.

Rampant, P, Brown, A & Croatto, G 2003. Acid sulfate soil mazard maps: guidelines for coastal Victoria. Department of Primary Industries (DPI).

Rayment, G & Higginson, F 1992. *Australian Laboratory Handbook of Soil and Water Chemical Methods,* Melbourne, Australia, Inkata Press.

Rickard, D 1995. Kinetics of FeS precipitation, part I: competing reaction mechanisms. *Geochimica et Cosmochimica Acta,* 59**,** 4367-4379.

Rickard, D 2006. The solubility of FeS. *Geochimica et Cosmochimica Acta,* 70**,** 5779–5789.

Rickard, D 2012. *Sulfidic sediments and sedimentary rocks,* Amsterdam, The Netherlands, Elsevier.

Robinson, N, Rees, D, Reynard, K, Macewan, R, Dahlhaus, P & Baxter, N 2003. A land resource assessment of the Corangamite region. Bendigo: Department of Primary Industries.

Rosengren, N 2009. Murtnaghurt Lagoon, Bellarine Peninsula and related landforms: nature, origin and geoscience significance. Melbourne: La Trobe University and Environmental GeoSurveys Pty Ltd.

Rothols, W & Rowe, R 1961. Report on the upper Barwon water supply catchment. Soil Conservation Authority.

Rowan, J, Ransome, S, Russell, L & Rees, D 2000. Land systems of Victoria, technical report no. 56. *In:* Rees, DB (ed.) 3 ed. Victoria: Centre for Land Protection Research.

Sammut, J 2000. *An introduction to acid sulphate soils,* Canberra, Environment Australia.

Sammut, J, White, I & Melville, M 1996. Acidification of an estuarine tributary in eastern Australia due to drainage of acid sulfate soils. *Journal of Marine and Freshwater Research,* 47**,** 669-684.

Sandiford, M 2003. Geomorphic constraints on the Late Neogene tectonics of the Otway Range, Victoria. *Australian Journal of Earth Sciences,* 50**,** 69-80.

Santomartino, S. 2000. *Comparison of methods for acid sulphate soil analysis.* Honours, La Trobe University.

Schoonen, M & Barnes, H 1991. Reactions forming pyrite and marcasite from solution: II. Via FeS precursors below 100˚C. *Geochimica et Cosmochimica Acta,* 55**,** 1505-1514.

Sheldon, R 2005. Corangamite Wetland Strategy 2006 - 2011. *In:* (CCMA), Corangamite Catchment Management Authority (ed.). Colac.

Simpson, S, Fitzpatrick, R, Shand, P, Angel, B, Spadaro, D, Merry, R & Thomas, M 2008. Chapter 3: Acid and metal mobilisation following rewetting of acid sulfate soils from the River Murray, South Australia - a rapid laboratory method. *In:* Fitzpatrick, R & Shand, P (eds.) *Inland Acid Sulfate Soil Systems Across Australia.* Perth, Australia: CRC LEME.

Singer, P & Stumm, W 1970. Acid mine drainage: the rate-determining step. *Science,* 167**,** 1121-1123.

Singleton, O, McDougall, I & Mallett, C 1976. The Pliocene-Pleistocene boundary in southeastern Australia. *Australian Journal of Earth Sciences,* 23**,** 299-311.

Smith, J 2004. Chemical changes during oxidation of iron monosulfide-rich sediments. *Australian Journal of Soil Research,* 42**,** 659-666.

Smith, J, van Oploo, P, Marston, H, Melville, M & Macdonald, B 2003. Spatial distribution and management of total actual acidity in an acid sulphate soil environment, McLeod's Creek, north-eastern NSW, Australia. *CATENA,* 51**,** 61-79.

Spencer-Jones, D, Kenley, P, Rochow, K & Wopfner, H 1971. Chapter 1: area and regional setting. *In:* Douglas, JG & Wopfner, H (eds.) *The Otway Basin of southeastern Australia. Special Bulletin.* Adelaide: Geological Surveys of South Australia and Victoria.

SRW 2010. Groundwater Management Plan: Warrion Water Supply Protection Area. Southern Rural Water.

Stephenson, C 2005. Environmental flow determination for the Gellibrand River: site paper. EarthTech.

Struckmeyer, H & Felton, E 1990. The use of organic fades for refining palaeoenvironmental interpretations: a case study from the Otway Basin, Australia. 37.

Sullivan, L, Bush, R, McConchie, D, Lancaster, G, Haskins, P & Clark, M 1999. Comparison of peroxide-oxidisable sulfur and chromium-reducible sulfur methods for determination of reduced inorganic sulfur in soil. *Australian Journal of Soil Research,* 37**,** 255-265.

Sullivan, L, Fitzpatrick, R, Bush, R, Burton, ES, P & Ward, N 2010. The classification of acid sulfate soil materials: further modifications. *Southern Cross Geosciences Technical Report.*

Thomas, D 1957. Physiography, geology and mineral resources. *In:* Committee, Central Planning Authority in collaboration with the Corangamite Regional (ed.) *Resources Survey: Corangamite Region.* Melbourne: A.C. Brooks, Government Printer.

Tickell, S, Edwards, J & Abele, C 1992. Geology of the Port Campbell 1:100,000 mapsheet. Report 95. Geological Survey of Victoria.

Tickell, SJ. 1990. *Colac and part of Beech Forest 1:50 000 geological map*. Department of Manufacturing and Industry Development.

Tickell, SJ, Cummings, S, Leonard, IG & Withers, JA 1991. Colac 1:50 000 map geological report. Geological Survey of Victoria Report 89.: Geological Survey of Victoria.

Tosolini, A, McLoughlin, S & Drinnan, A 2002. Early Cretaceous megaspore assemblages from southeastern Australia 23.

van Gameren, M 1997a. Water Watch Education Kit, Corangamite Region, part 2. 2 ed. Victoria.

van Gameren, M 1997b. Water Watch Education Kit, Corangamite Region, part 3. 2 ed. Victoria.

Victoria, P 2002. Anglesea Heath Management Plan November 2002. *In:* Victoria, Parks (ed.). Parks Victoria.

Victoria, P 2009. Caring for Country — The Otways and You. Great Otway National Park and Otway Forest Park Management Plan. Melbourne, Victoria: The Department of Sustainability and Environment and Parks Victoria.

Vile, M & Novak, M 2006. Chapter 12: sulfur cycling in boreal peatlands: from acid rain to global climate change. *In:* Wieder, RK & Vitt, DH (eds.) *Boreal Peatland Ecosystems.* Germany: Springer-Verlag.

Vitolins, M & Swaby, R 1969. Activity of sulphur-oxidising microorganisms in some Australian soils. *Australian Journal of Soil Research,* 7**,** 171-183.

Wallace, L, McPhail, B, Fitzpatrick, R, Welch, S, Kirste, D, Beavis, S & Lamontagne, S 2008a. Chapter 15: spatial variability in the storage of sulfur, carbon and acid generation potential in an inland saline sulfidic wetland, Lower Murray Floodplains, South Australia. *In:* Fitzpatrick, R & Shand, P (eds.) *Inland acid sulfate soil systems across Australia.* Perth, Australia: CRC LEME.

Wallace, L, McPhail, B, Fitzpatrick, R, Welch, S, Kirste, D, Beavis, S & Lamontagne, S 2008b. Chapter 16: sulfur and carbonate mobility during changes in water regime in an inland sulfidic wetland, Lower Murray floodplains, South Australia. *In:* Fitzpatrick, R & Shand, P (eds.) *Inland acid sulfate soil systems across Australia.* Perth, Australia: CRC LEME.

Wallace, L, Welch, S, Kirste, D, Beavis, S & McPhail, D 2005a. Characteristics of inland acid sulfate soils of the Lower Murray Floodplains, South Australia. *In:* Roach, IC (ed.) *Regolith 2005 – Ten Years of CRC LEME.* CRC LEME.

Wallace, M, Dickinson, J, Moore, D & Sandiford, M 2005b. Late Neogene strandlines of southern Victoria: a unique record of eustasy and tectonics in southeast Australia. *Australian Journal of Earth Sciences,* 52**,** 279-297.

Warburton, J, Holden, J & Mills, A 2004. Hydrological controls of surficial mass movements in peat. *Earth-Science Reviews,* 67**,** 139-156.

Ward, N 2004. Sulfide oxidation in some acid sulfate soil material, thesis. Southern Cross University.

Ward, N, Sullivan, L, Bush, R & Lin, C 2002. Assessment of peroxide oxidation for acid sulfate soil analysis: 1. Reduced inorganic sulfur. *Australian Journal of Soil Research,* 40**,** 433-442.

Watkinson, J & Bolan, N 1998. Chapter 5: modelling the rate of elemental sulfur oxidation in soils. *Sulfur in the environment.* New York: Marcel Dekker Inc.

Watters, J & Stanley, E 2007. Stream channels in peatlands: the role of biological processes in controlling channel form. *Geomorphology,* 89**,** 97-110.

Whinam, J & Hope, G 2005. The peatlands of the Australiasian region. *In:* Steiner, GM (ed.) *Mires: from Siberia to Teirra del Feugo.* Linz, Austria: Stafia 85.

White, I, Melville, M, Wilson, B & Sammut, J 1997. Reducing acidic discharge from coastal wetlands in eastern Australia. *Wetlands Ecology and Management,* 5**,** 55-72.

White, S 1994. Speleogenesis in aeolian calcarenite: a case study in western Victoria. *Environmental Geology,* 23**,** 248-255.

Wilkin, R & Barnes, H 1997. Formation processes of framboidal pyrite. *Geochimica et Cosmochimica Acta,* 61**,** 323-339.

Williams, W 1995. Lake Corangamite, Australia, a permanent saline lake: conservation and management issues. *Lakes & Reservoirs: Research and Management,* 1**,** 55-64.

Wolthers, M, Charlet, L, van der Linde, P, Rickard, D & van der Weijden, C 2005. Surface chemistry of disordered mackinawite (FeS). *Geochimica et Cosmochimica Acta,* 69**,** 3469-3481.

Yihdego, Y & Webb, J 2013. An empirical water budget model as a tool to identify the impact of land-use change in stream flow in southeastern Australia. *Water Resources Management,* 27**,** 4941-4958.

Zhabina, N & Volkov, I 1978. A method of determination of various sulfur compounds in sea sediments and rocks. *In:* Seiler, W & Krumbein, WE (eds.) *Environmental Biogeochemisty and Geomicrobiology.* Ann Arbor, Michigan: Ann Arbor Science Publications.

Appendix I: Basalt Plains XRD Scans

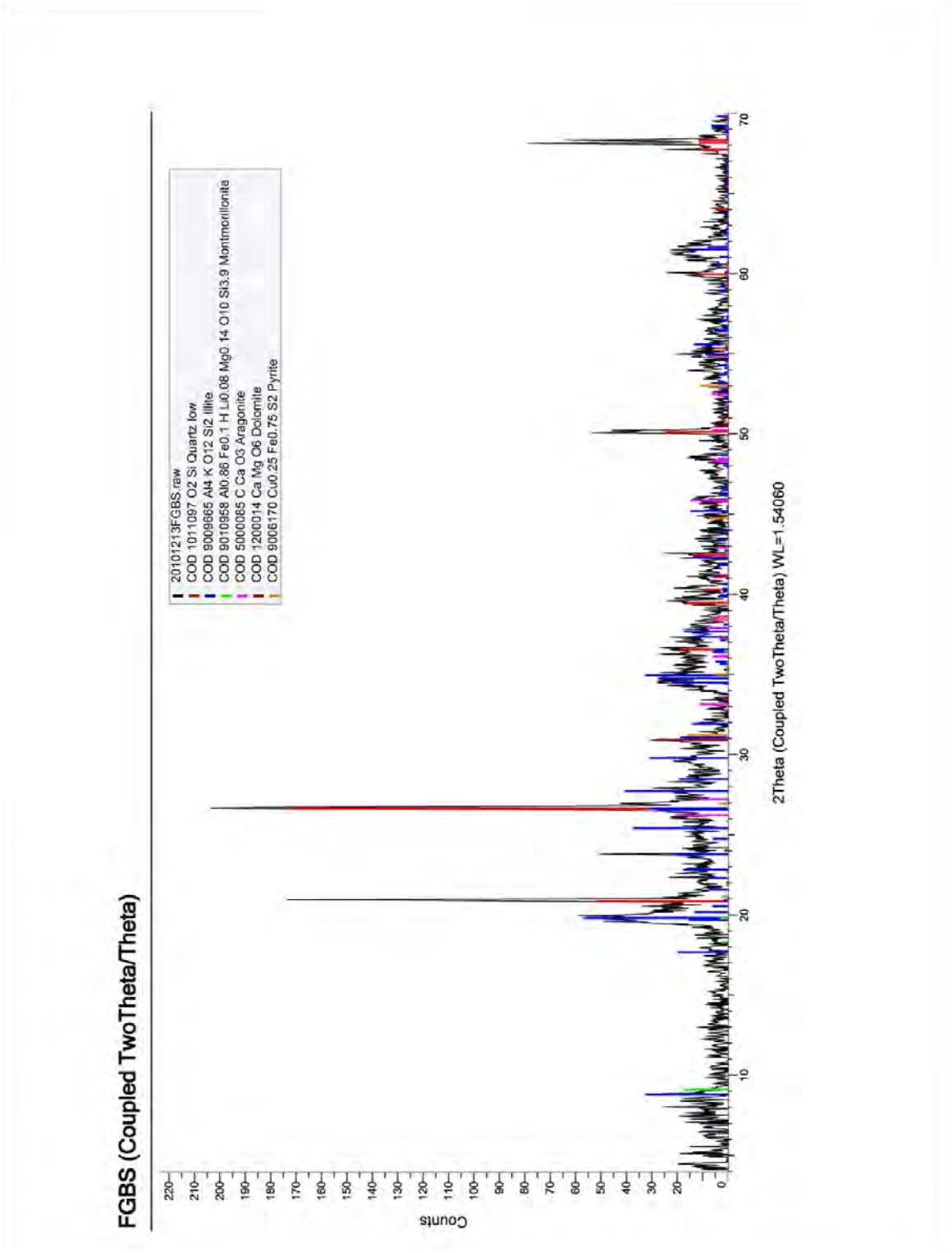

Figure AI-1 Bullocks Swamp (Site A) 0-0.2 m depth

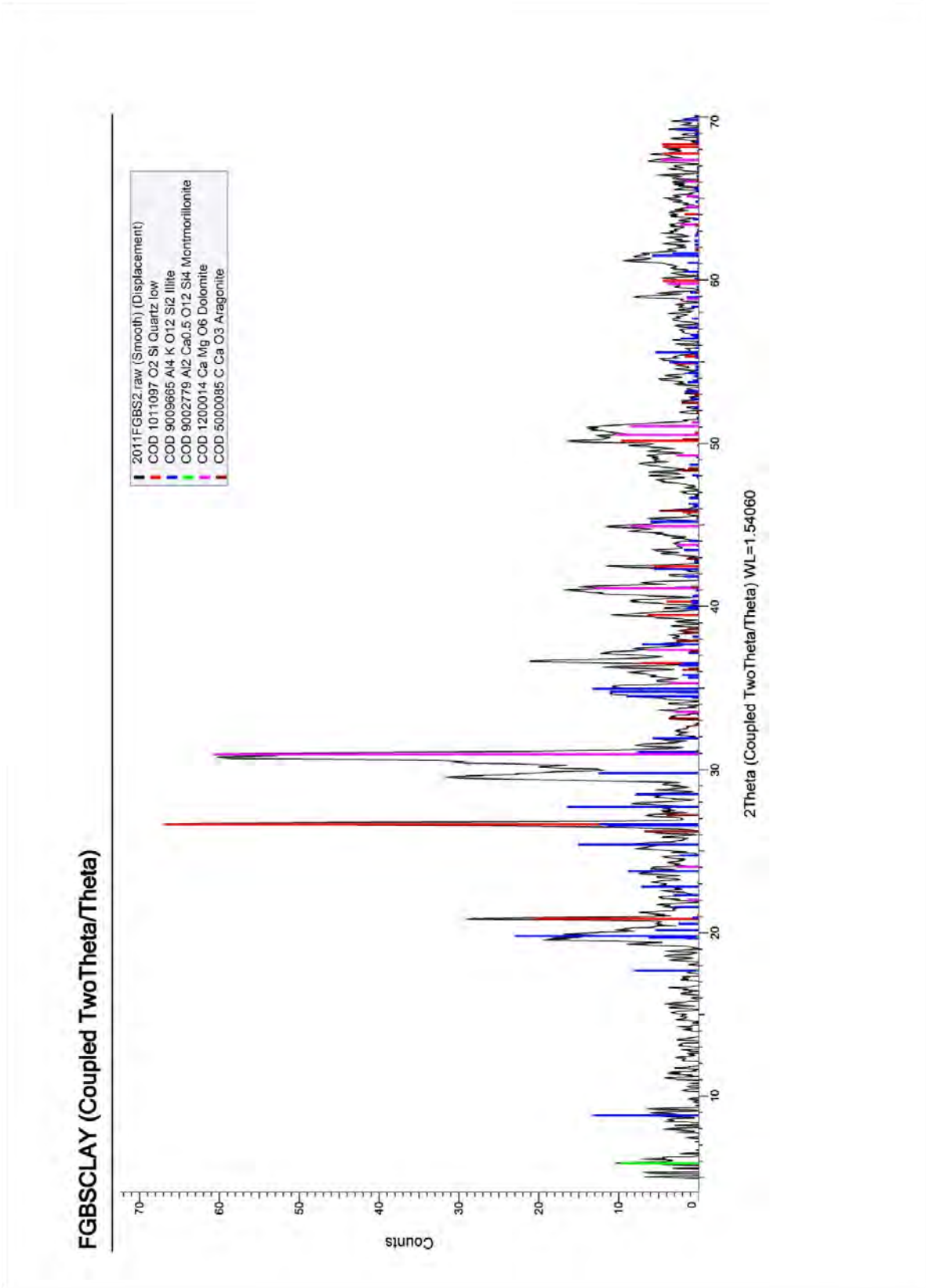

Figure AI-2 Bullocks Swamp (Site A) 0.2-0.3 m depth

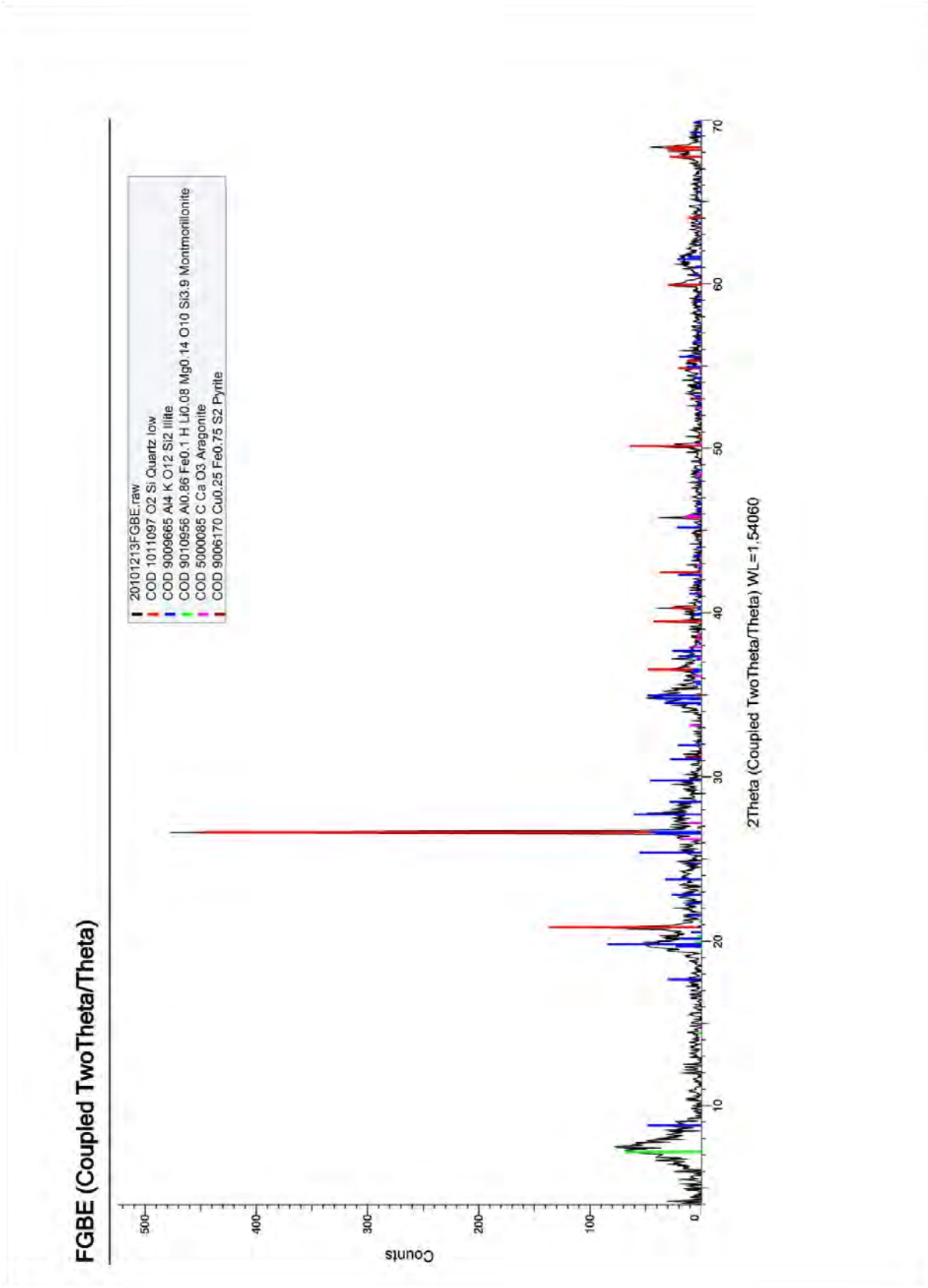

Figure AI-3 Beeac Swamp (Site B) 0-0.2 m depth

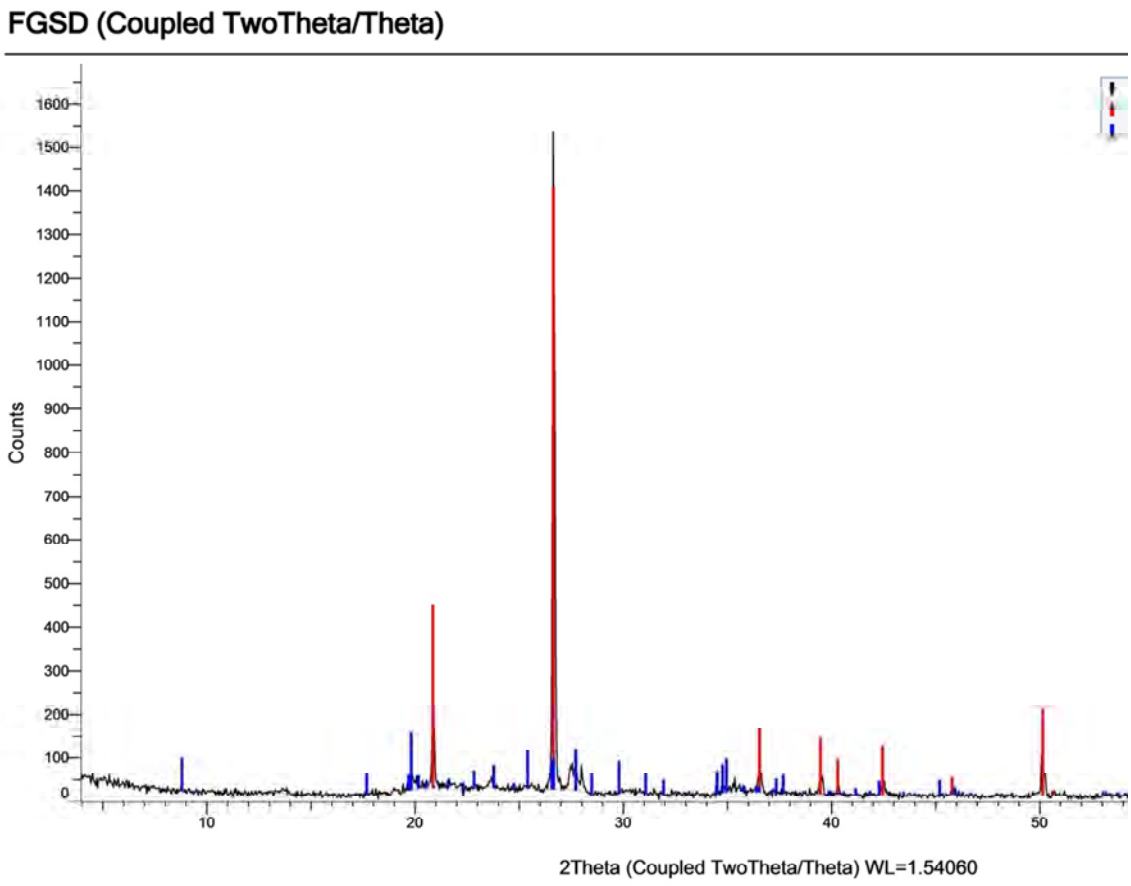

Figure AI-4 South Dreeite Road (Site C) 0-0.1 m depth

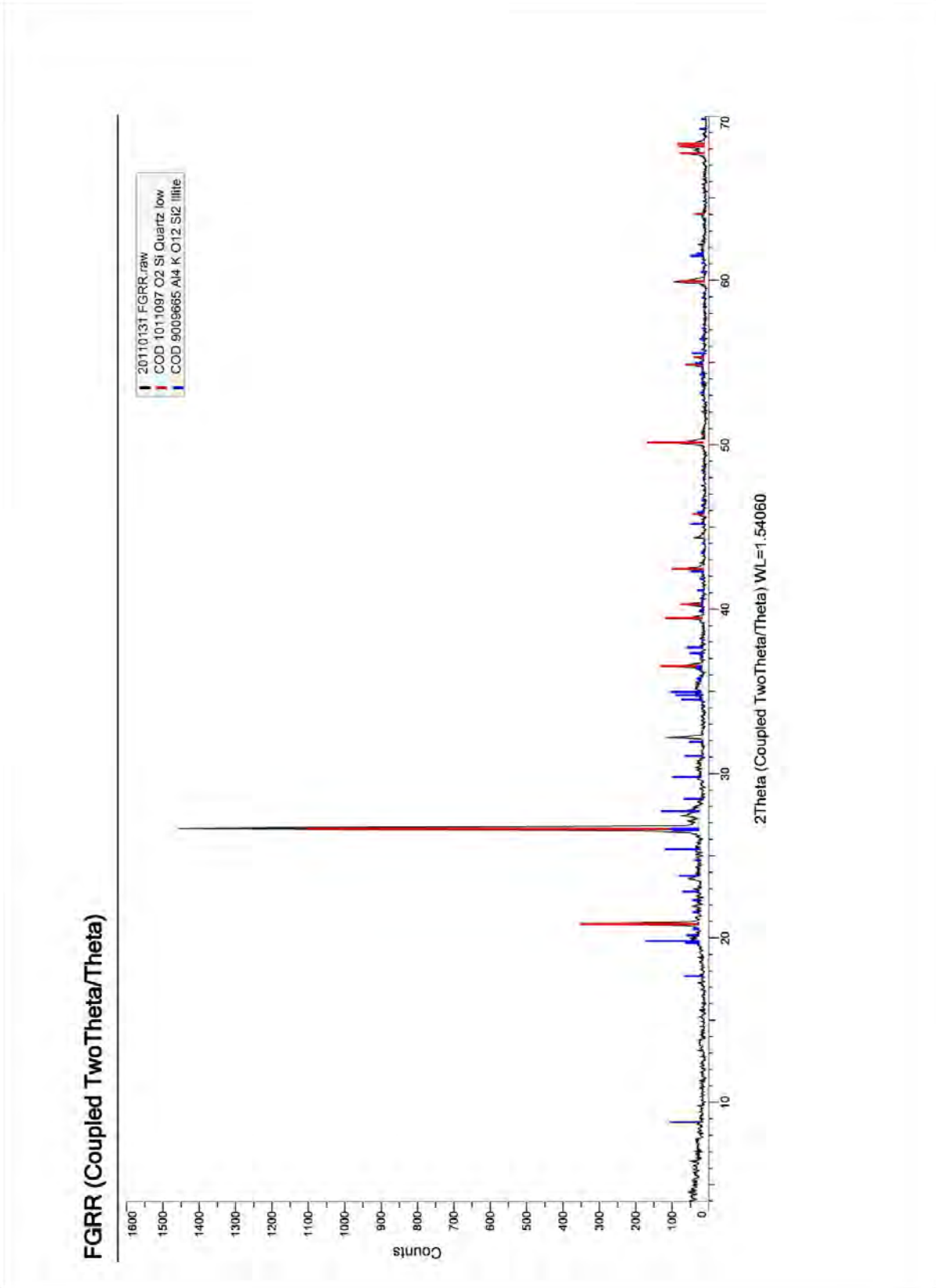

Figure AI-5 Patterns Road (Site D) 0-0.1 m depth

Appendix II: Otway Ranges XRD Scans

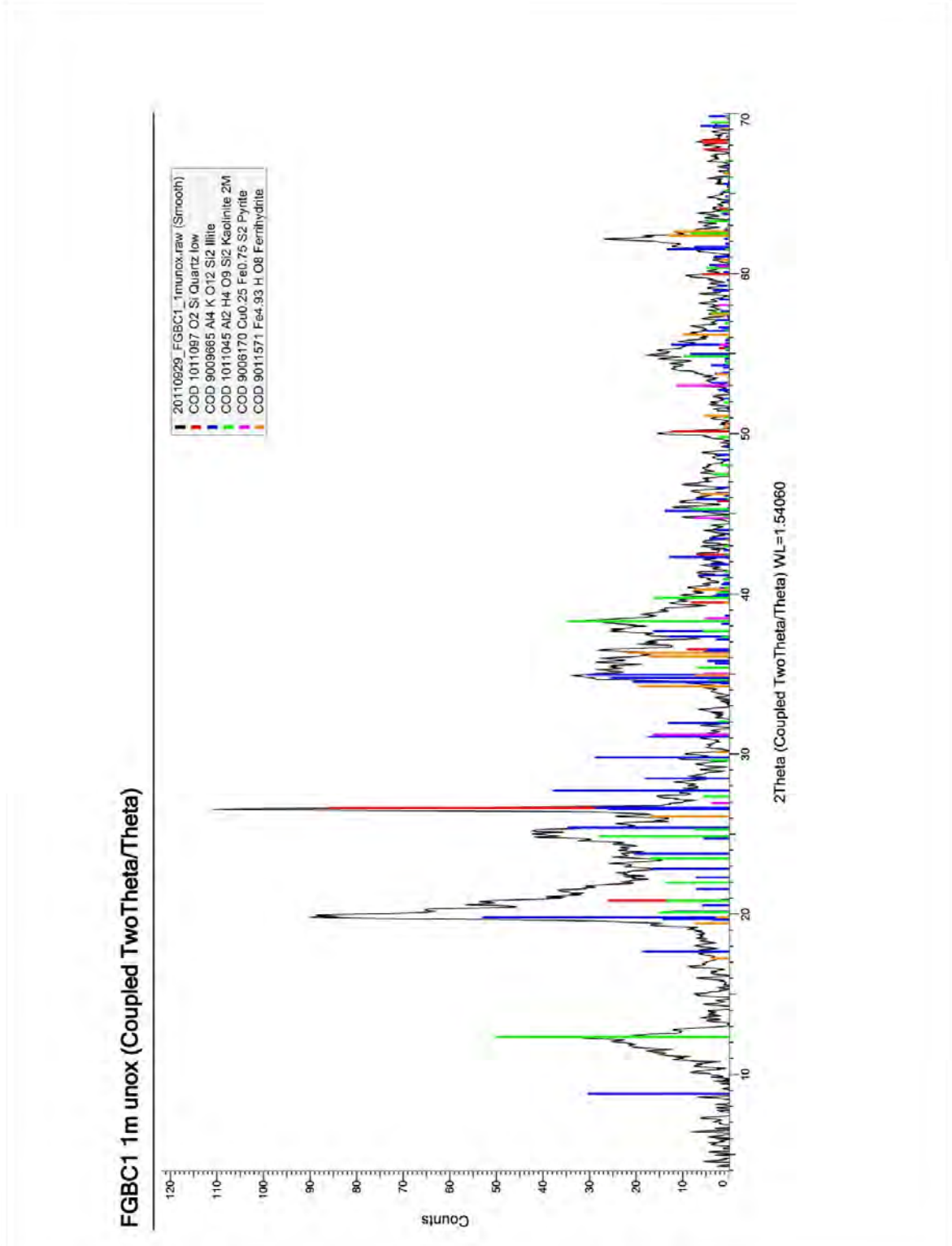

Figure AII-1 Boundary Creek swamp (Site A) BC1 1.0 m depth

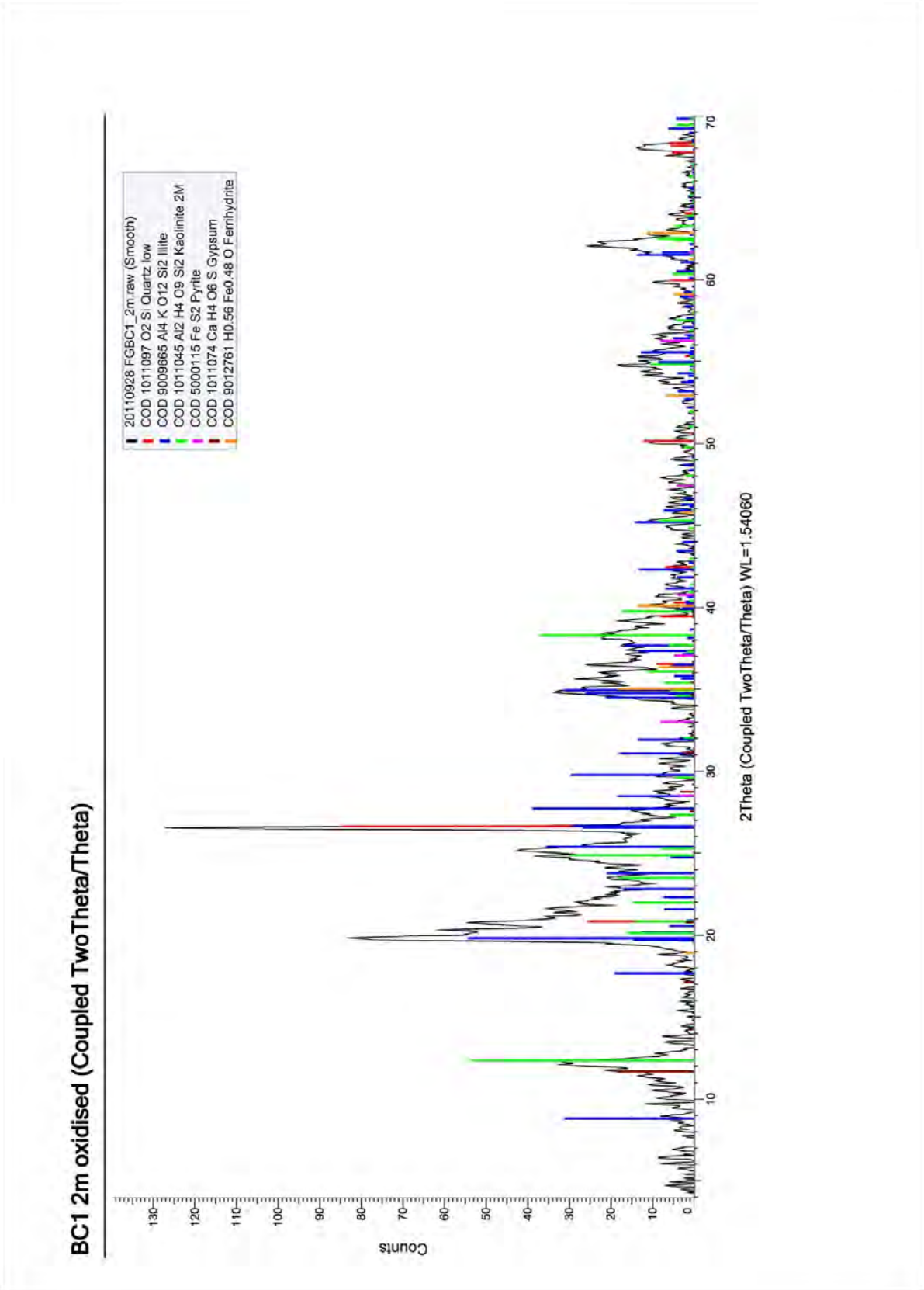

Figure AII-2 Boundary Creek Swamp (Site A) BC1 2.0 m depth

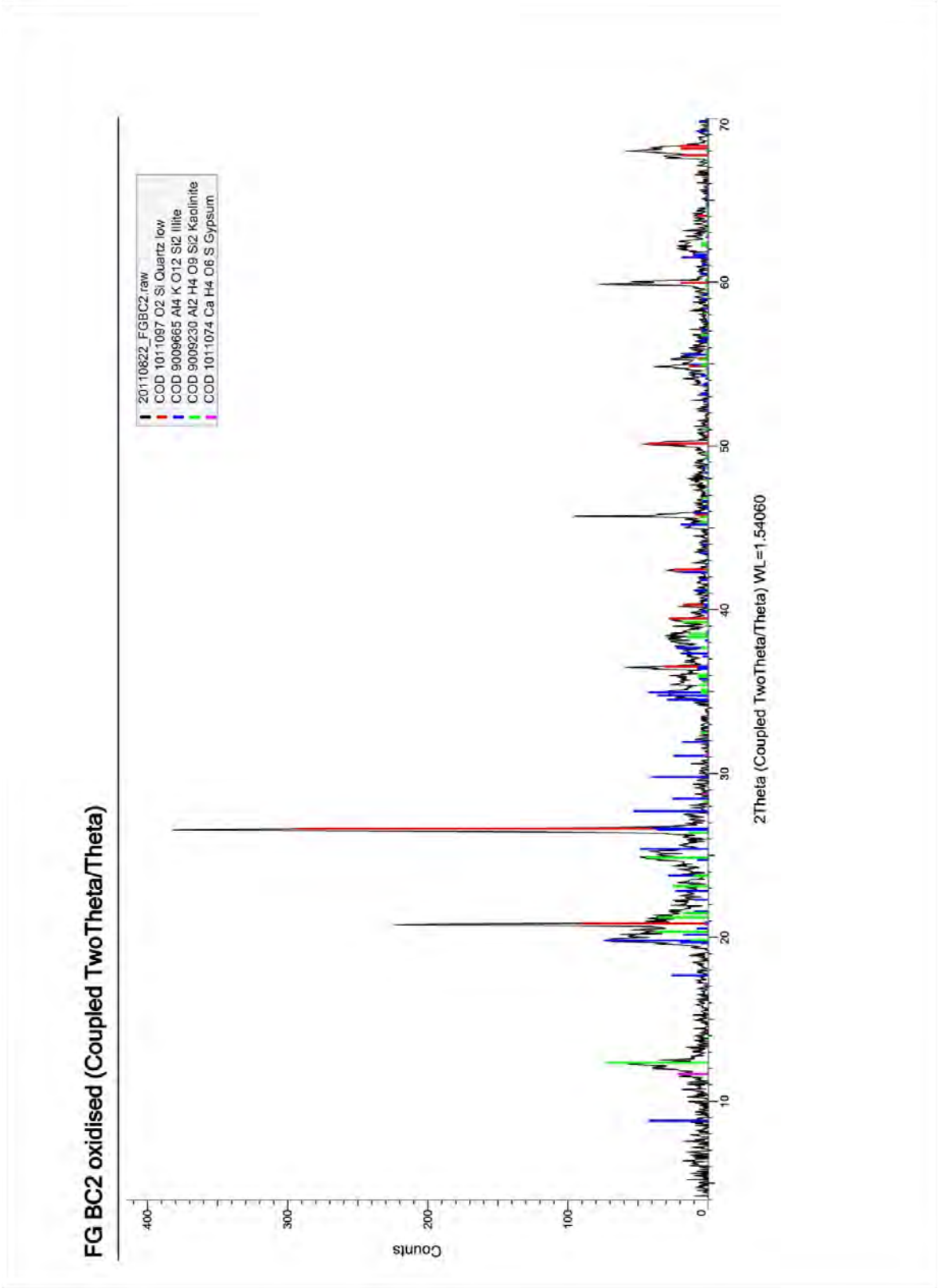

Figure AII-3 Boundary Creek Swamp (Site A) BC2 1.5 m depth

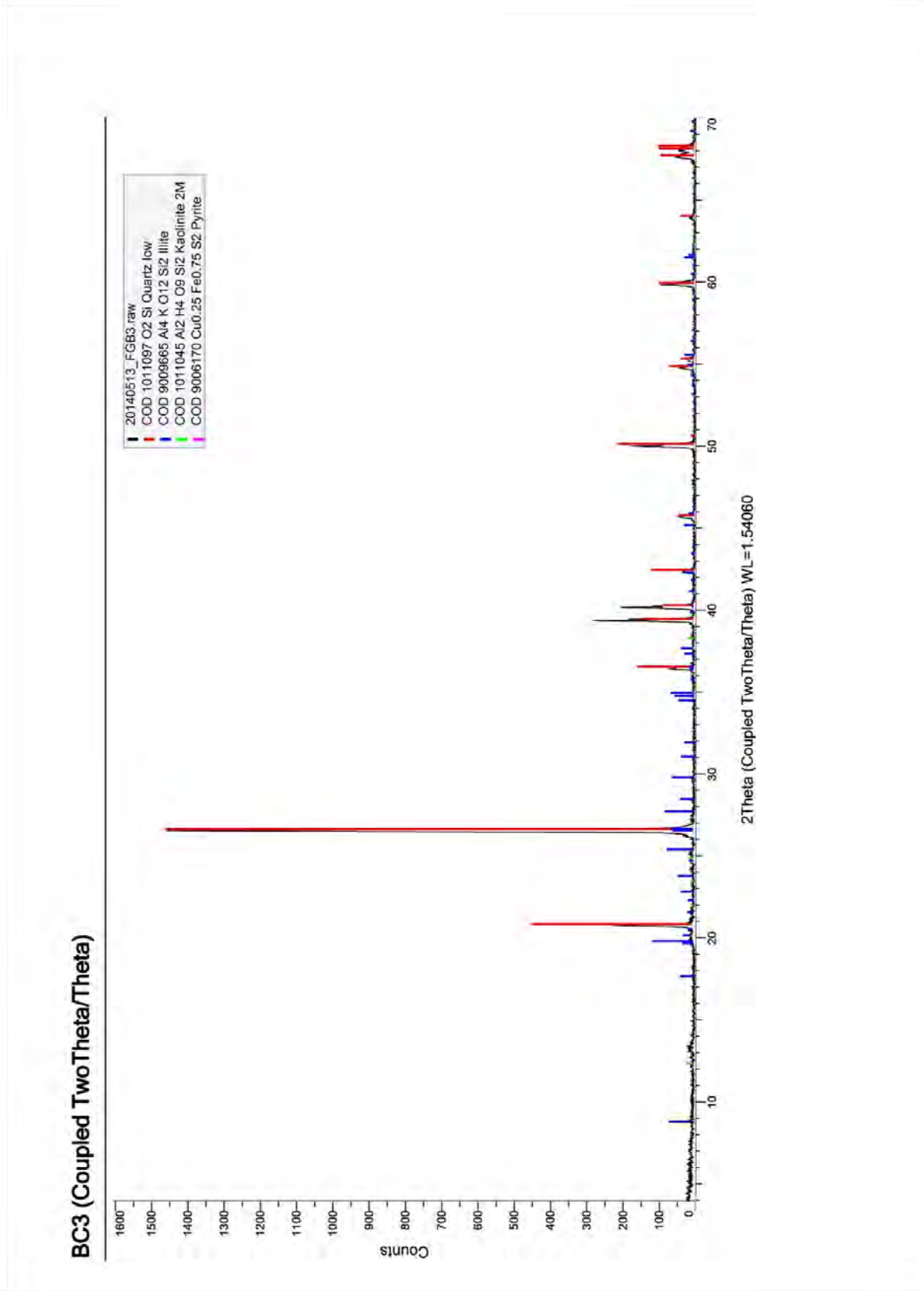

Figure AII-4 Boundary Creek Swamp (Site A) BC3 2.0 m depth

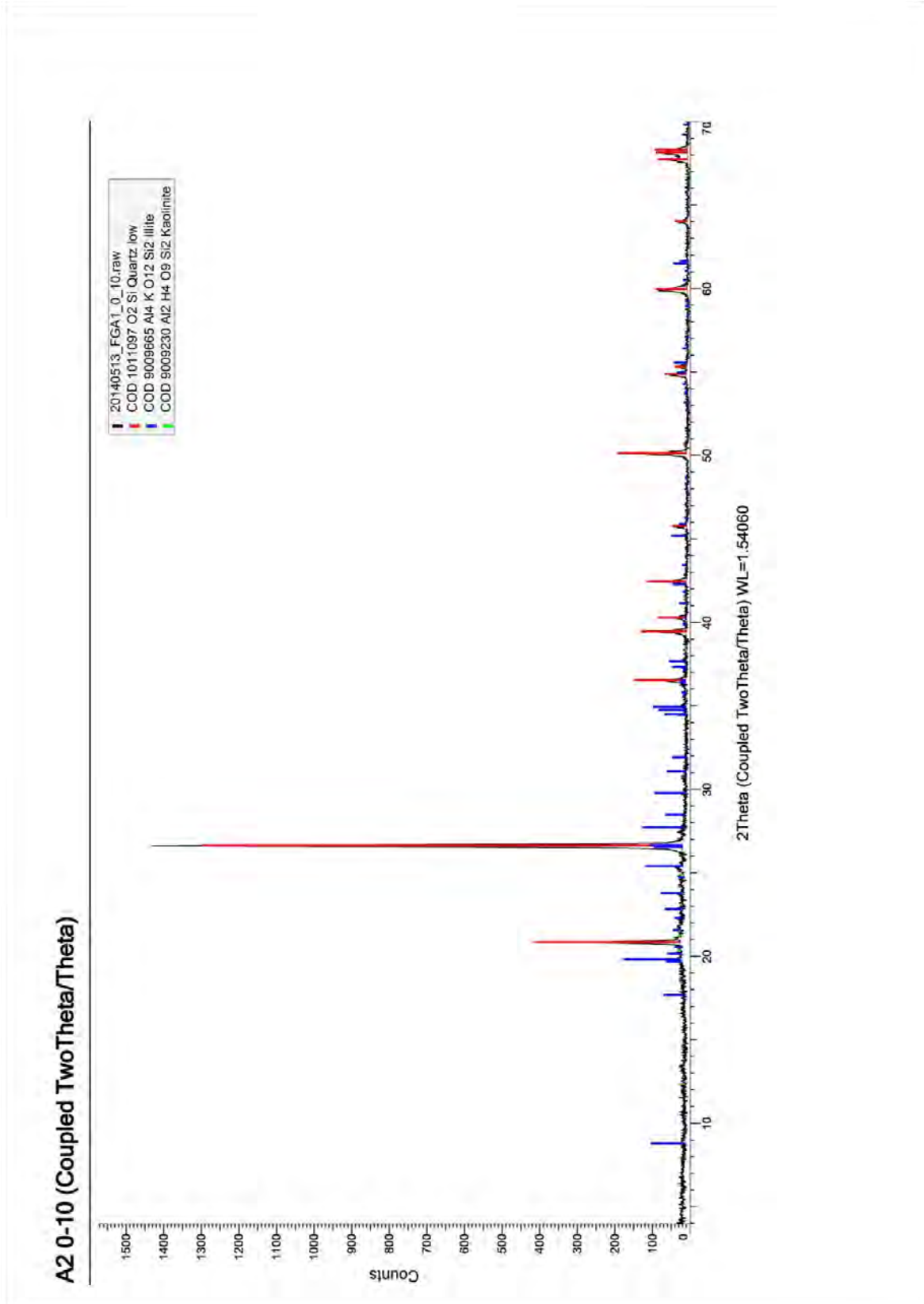

Figure AII-5 Anglesea swamp (Site B) A1 0-0.1 m depth

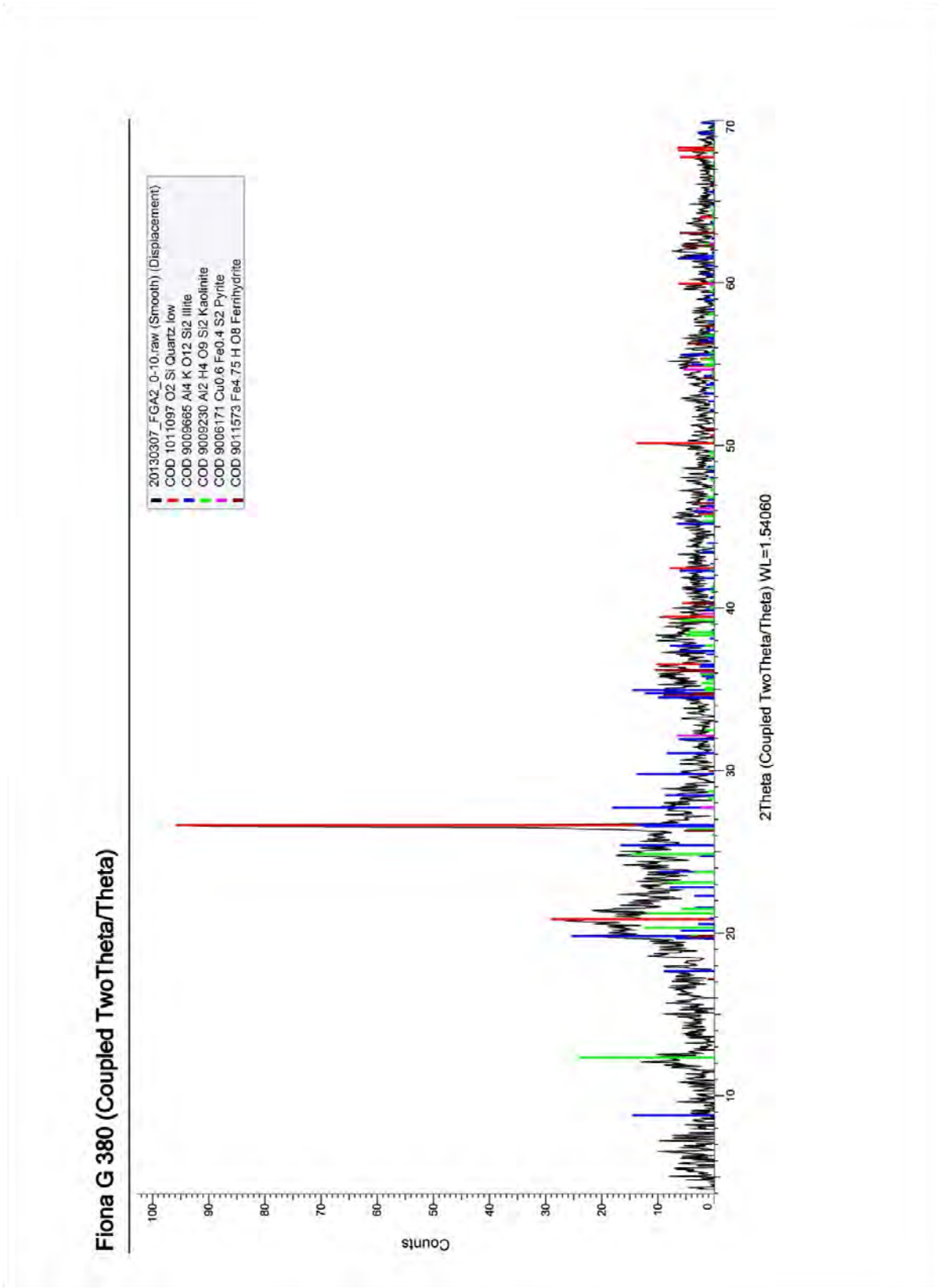

Figure AII-6 Anglesea swamp (Site B) A2 0-0.1 m depth

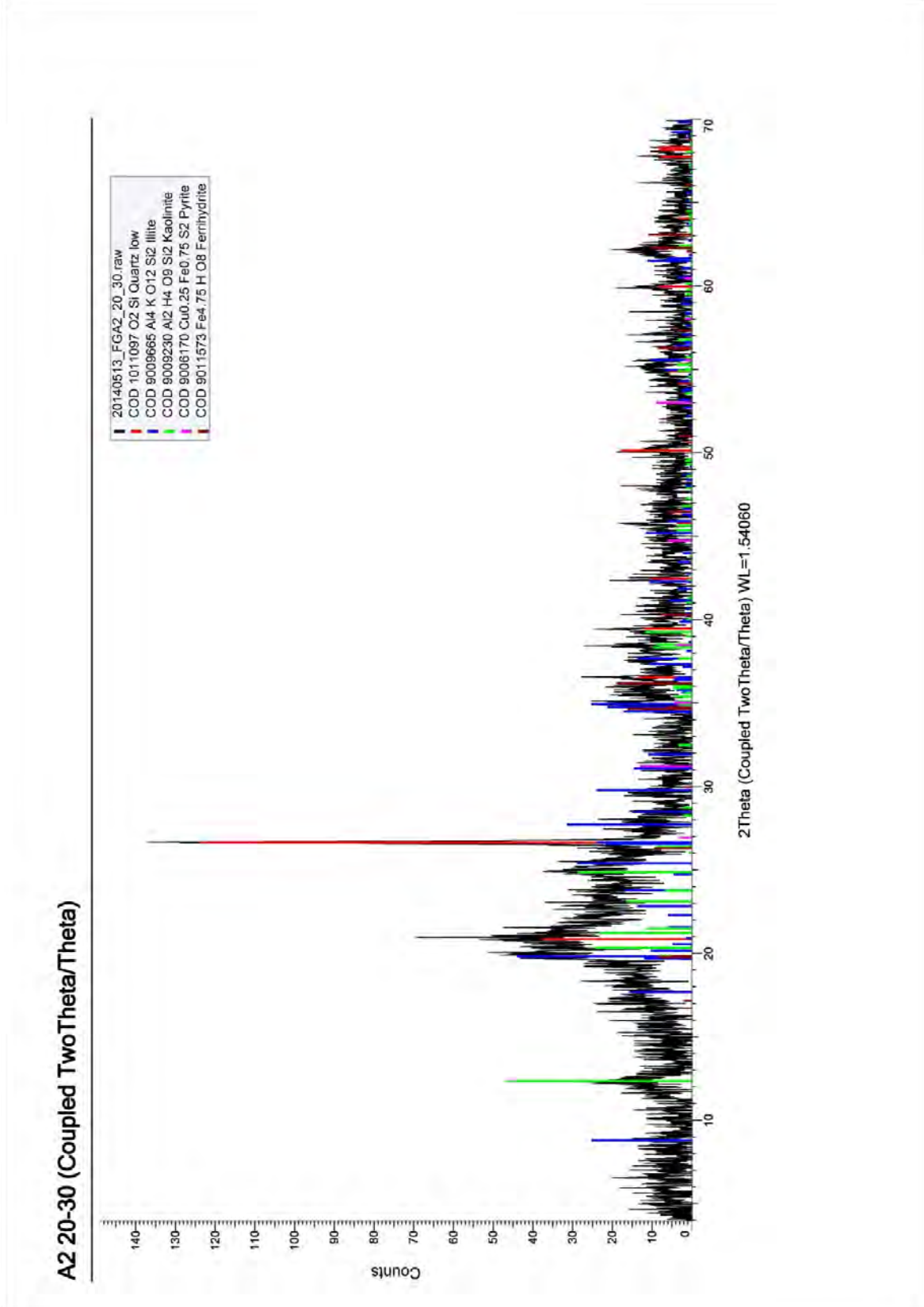

Figure AII-7 Anglesea swamp (Site B) A2 0.1-0.3 m depth

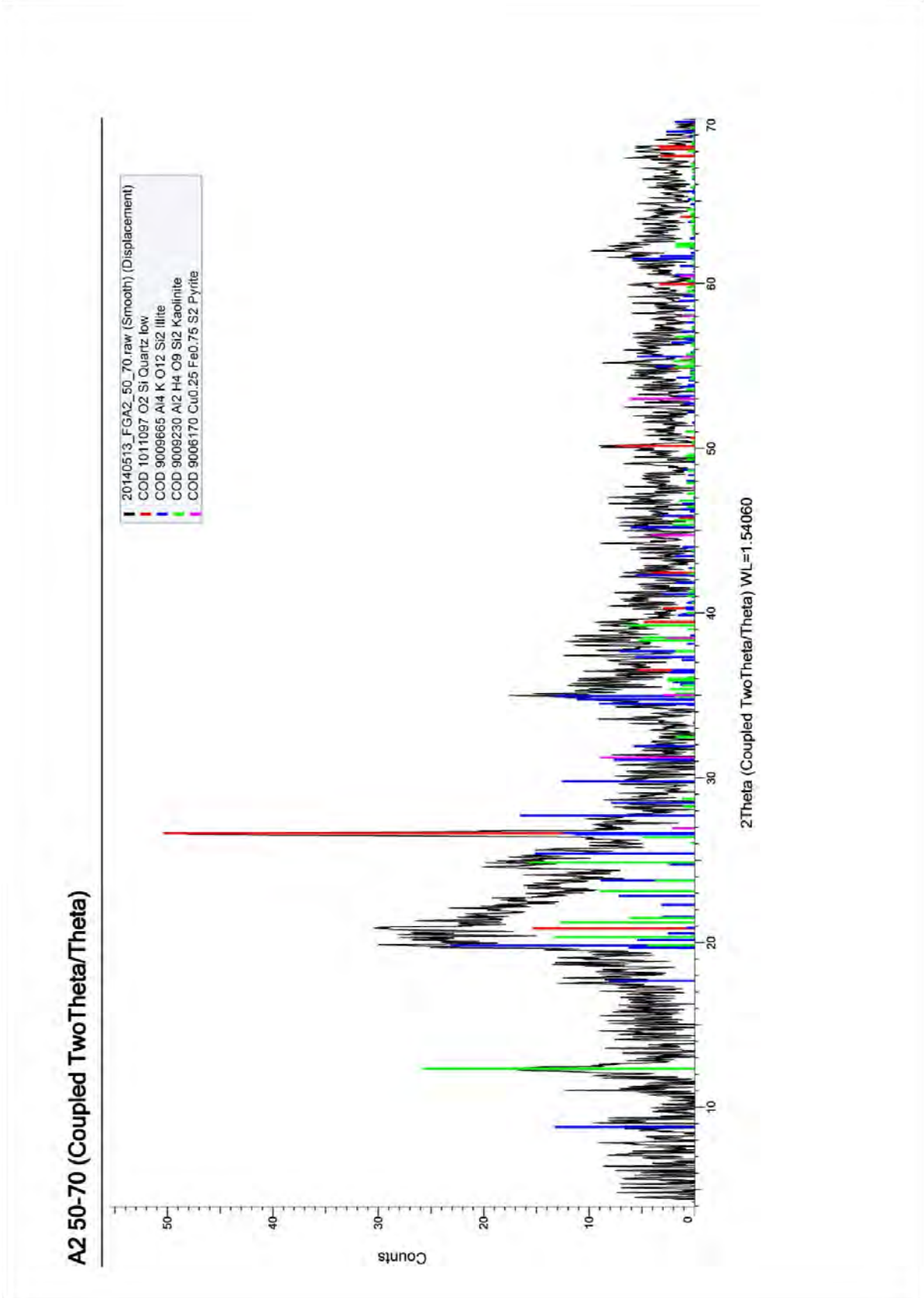

Figure AII-8 Anglesea swamp (Site B) A2 0.5-0.7 m depth

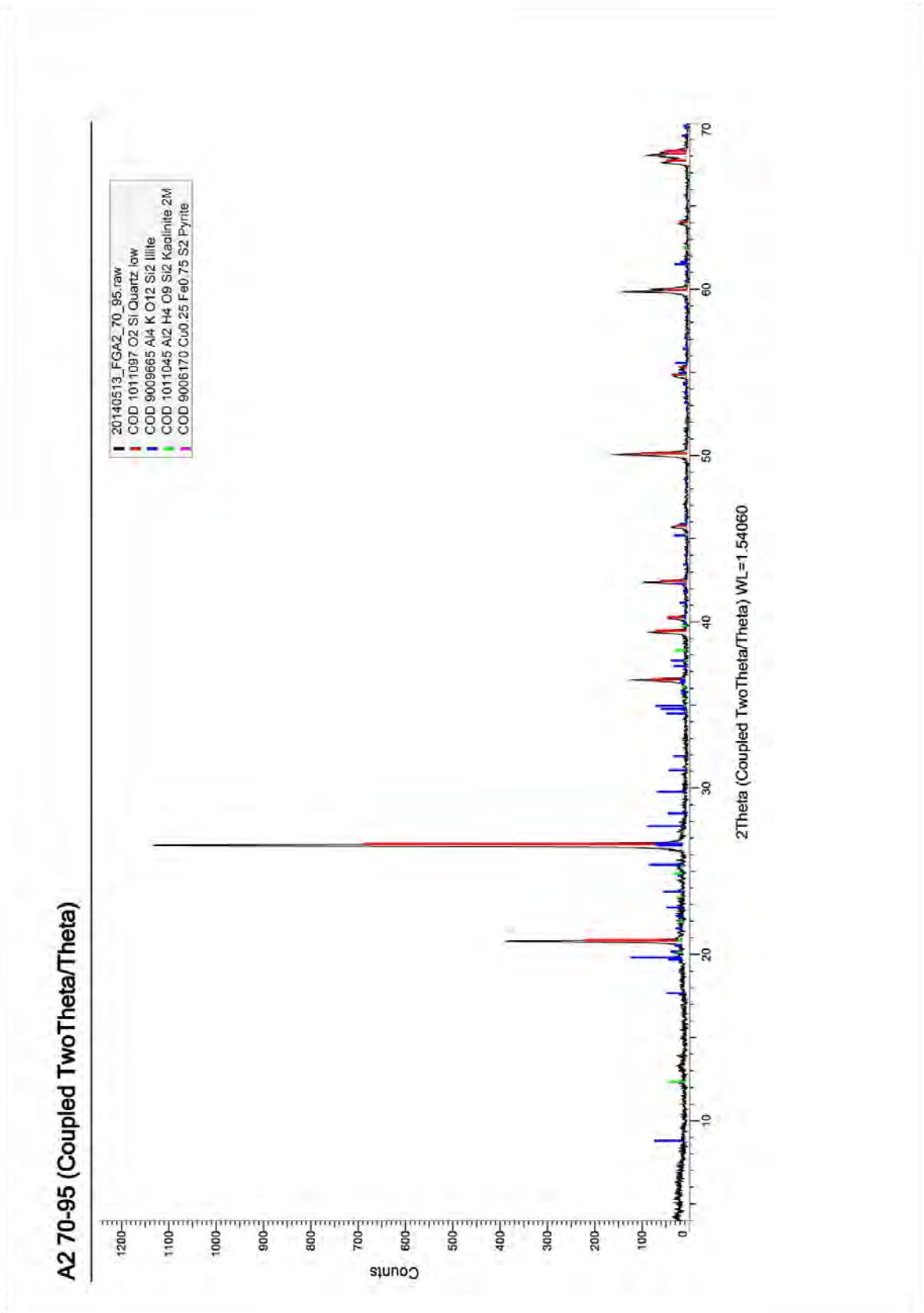

Figure AII-9 Anglesea swamp (Site B) A2 0.7-0.95 m depth

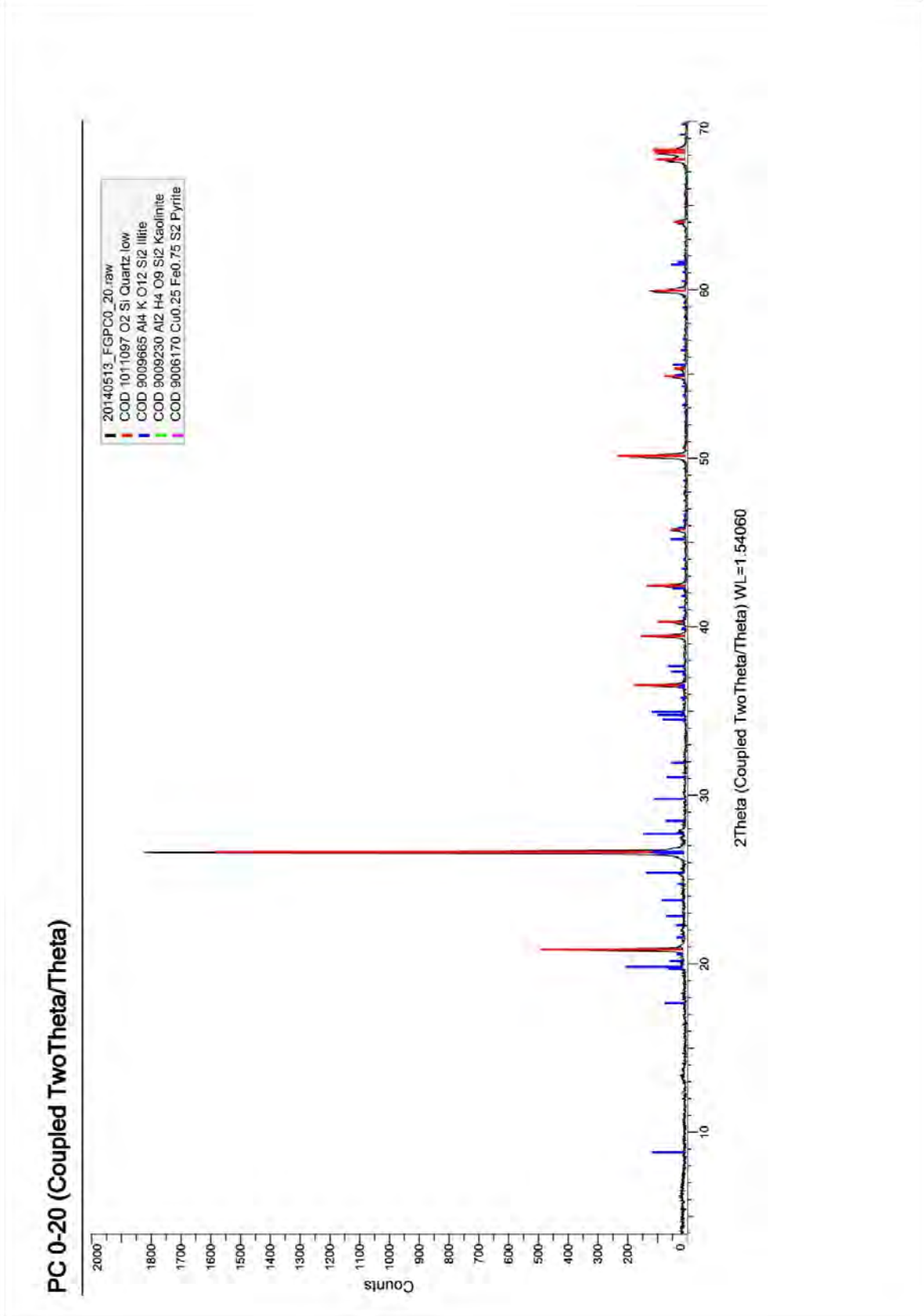

Figure AII-10 Porcupine Creek swamp (Site C) PC2 0-0.2 m depth

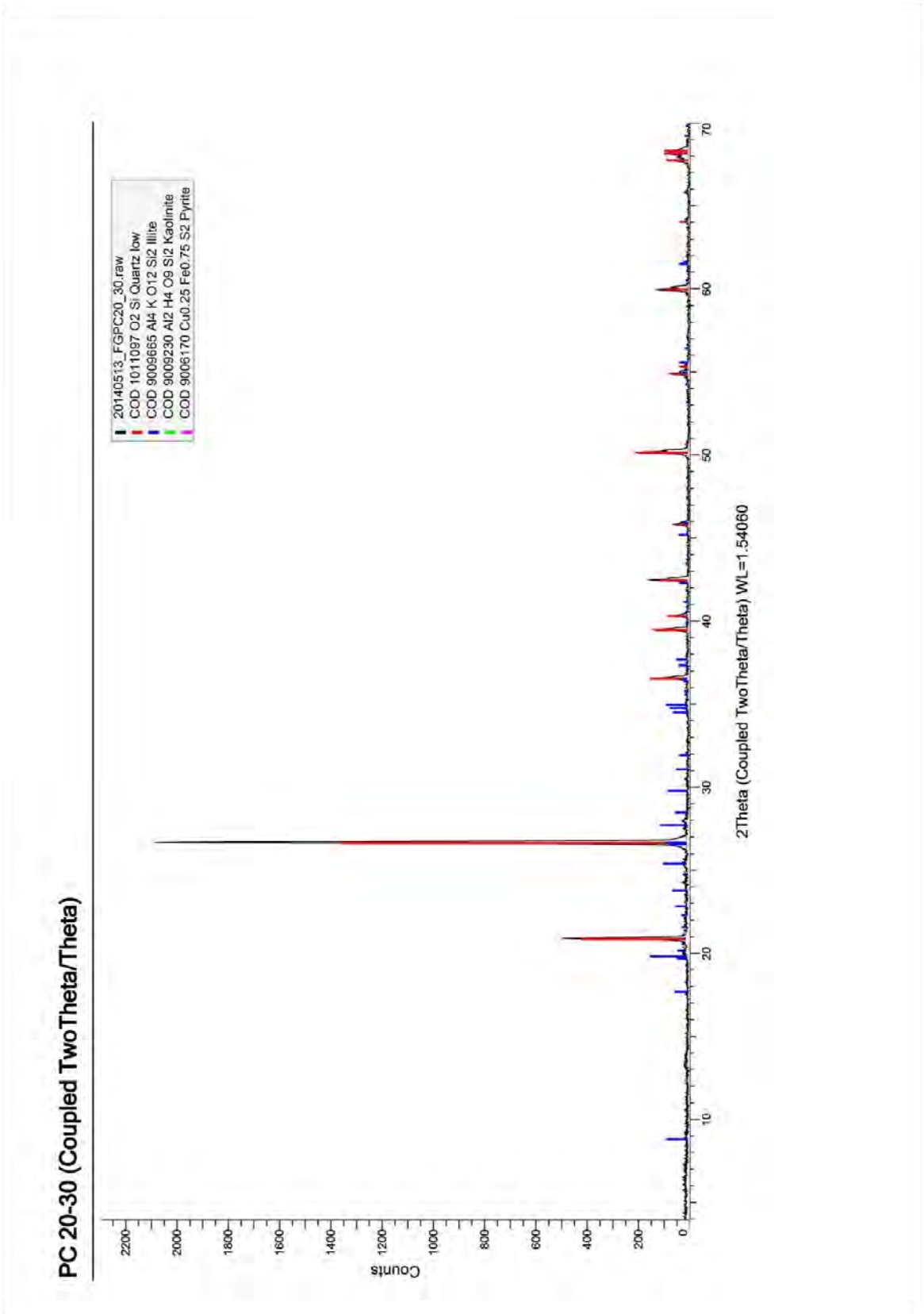

Figure AII-11 Porcupine Creek swamp (Site C) PC2 0.2-0.4 m depth

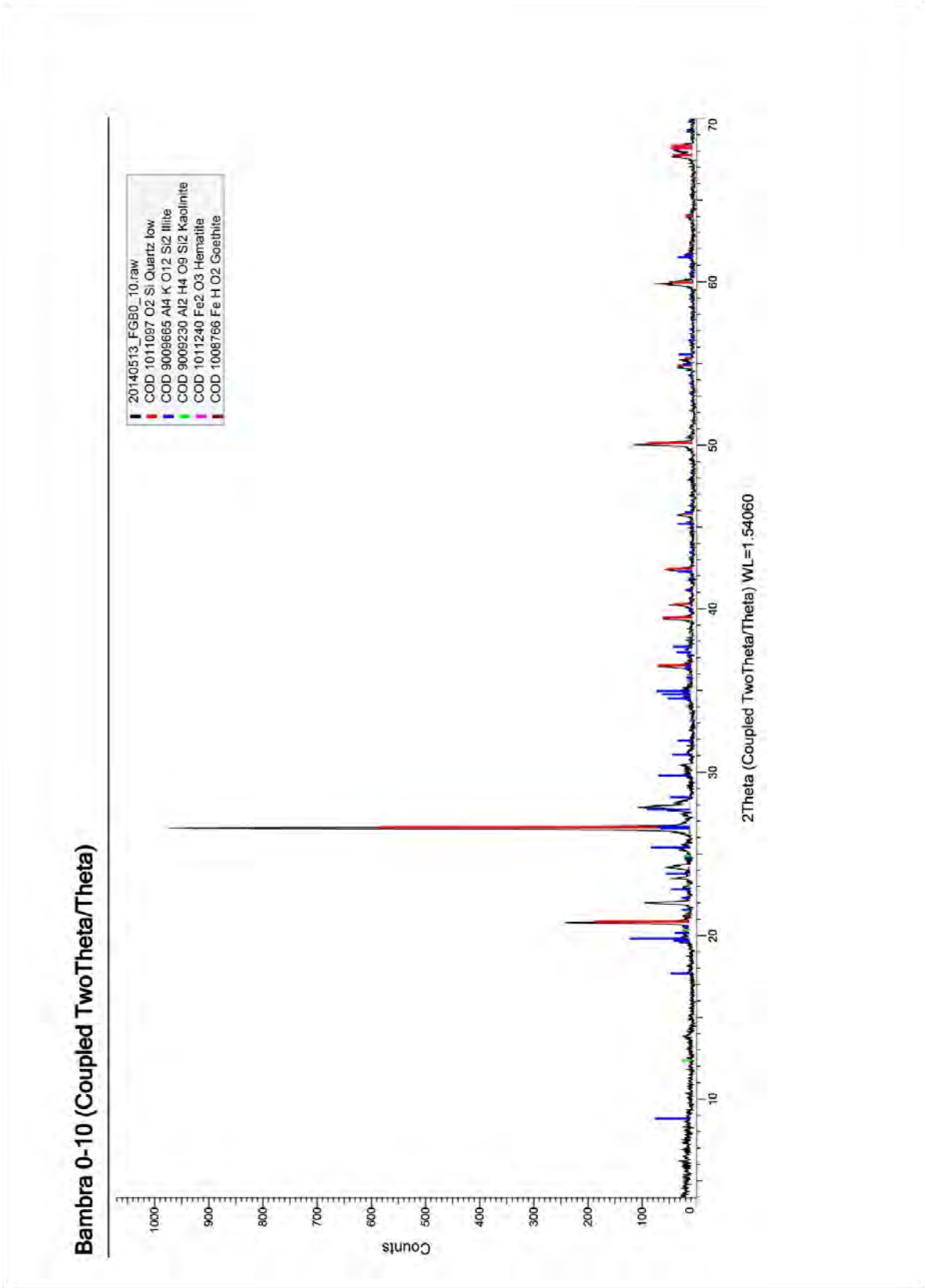

Figure AII-12 Bambra Wetlands (Site D) 0-0.1 m depth

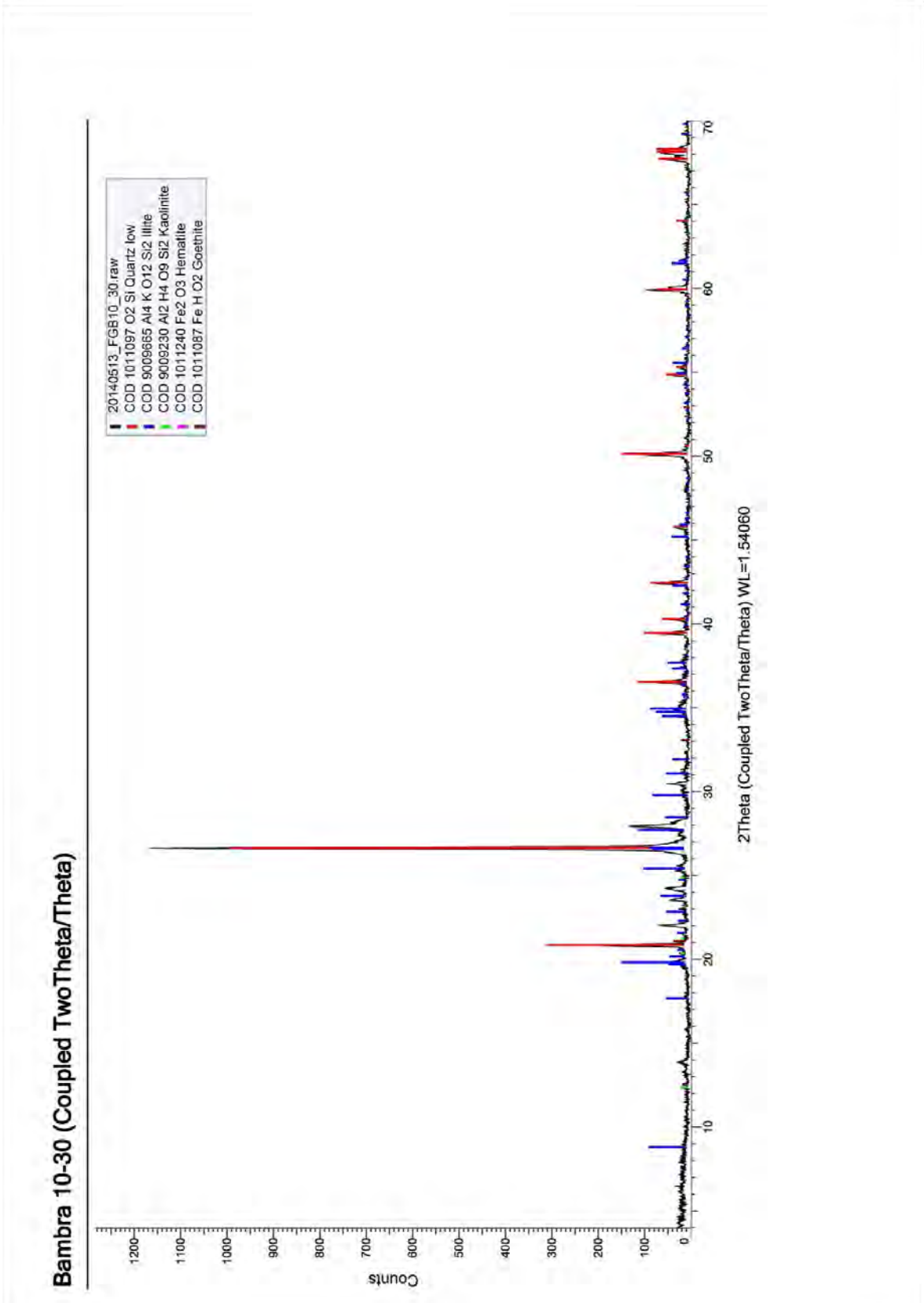

Figure AII-13 Bambra Wetlands (Site D) 0.1-0.3 m depth

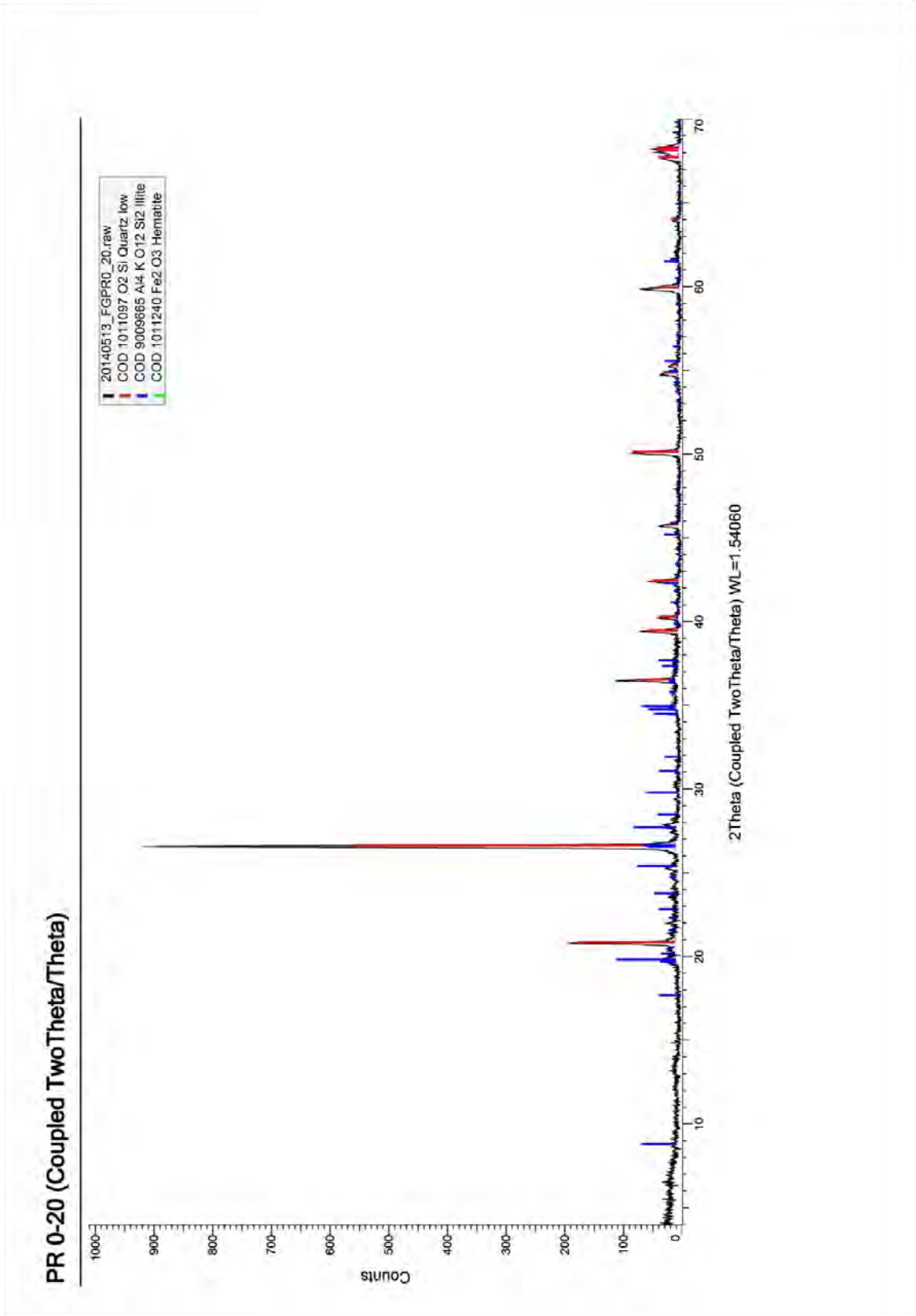

Figure AII-14 Pennyroyal Creek (Site E) 0-0.2 m depth

Appendix III: Beta Analytic Report

BETA ANALYTIC INC.
DR. M.A. TAMERS and MR. D.G. HOOD
4985 S.W. 74 COURT
MIAMI, FLORIDA, USA 33155
PH: 305-667-5167 FAX:305-663-0964
beta@radiocarbon.com

REPORT OF RADIOCARBON DATING ANALYSES

Dr. Fiona Glover — Report Date: 8/12/2013

La Trobe University — Material Received: 7/24/2013

Sample Data	Measured Radiocarbon Age	13C/12C Ratio	Conventional Radiocarbon Age(*)
Beta - 354965	120 +/- 30 BP	-28.1 o/oo	70 +/- 30 BP
SAMPLE : FGloverMarsh01_50cm			
ANALYSIS : AMS-Standard delivery			
MATERIAL/PRETREATMENT : (organic sediment): acid washes			
2 SIGMA CALIBRATION :	Cal AD 1690 to 1730 (Cal BP 260 to 220) AND Cal AD 1810 to 1920 (Cal BP 140 to 30) Cal AD Post 1950		
Beta - 354966	1250 +/- 30 BP	-26.7 o/oo	1220 +/- 30 BP
SAMPLE : FGloverMarsh02_70-95cm			
ANALYSIS : AMS-Standard delivery			
MATERIAL/PRETREATMENT : (organic sediment): acid washes			
2 SIGMA CALIBRATION :	Cal AD 690 to 750 (Cal BP 1260 to 1200) AND Cal AD 760 to 890 (Cal BP 1190 to 1060)		

Dates are reported as RCYBP (radiocarbon years before present, "present" = AD 1950). By international convention, the modern reference standard was 95% the 14C activity of the National Institute of Standards and Technology (NIST) Oxalic Acid (SRM 4990C) and calculated using the Libby 14C half-life (5568 years). Quoted errors represent 1 relative standard deviation statistics (68% probability) counting errors based on the combined measurements of the sample, background, and modern reference standards. Measured 13C/12C ratios (delta 13C) were calculated relative to the PDB-1 standard.

The Conventional Radiocarbon Age represents the Measured Radiocarbon Age corrected for isotopic fractionation, calculated using the delta 13C. On rare occasion where the Conventional Radiocarbon Age was calculated using an assumed delta 13C, the ratio and the Conventional Radiocarbon Age will be followed by "*". The Conventional Radiocarbon Age is not calendar calibrated. When available, the Calendar Calibrated result is calculated from the Conventional Radiocarbon Age and is listed as the "Two Sigma Calibrated Result" for each sample.

CALIBRATION OF RADIOCARBON AGE TO CALENDAR YEARS

(Variables: C13/C12=-28.1:lab. mult=1)

Laboratory number: **Beta-354965**

Conventional radiocarbon age: **70±30 BP**

2 Sigma calibrated results: **Cal AD 1690 to 1730 (Cal BP 260 to 220) and**
(95% probability) **Cal AD 1810 to 1920 (Cal BP 140 to 30) and**
Cal AD Post 1950

Intercept data

Intercepts of radiocarbon age with calibration curve: Cal AD 1900 (Cal BP 50) and
Cal AD 1900 (Cal BP 50) and
Cal AD Post 1950

1 Sigma calibrated results: Cal AD 1710 to 1720 (Cal BP 240 to 230) and
(68% probability) Cal AD 1830 to 1830 (Cal BP 120 to 120) and
Cal AD 1890 to 1910 (Cal BP 60 to 40) and
Cal AD Post 1950

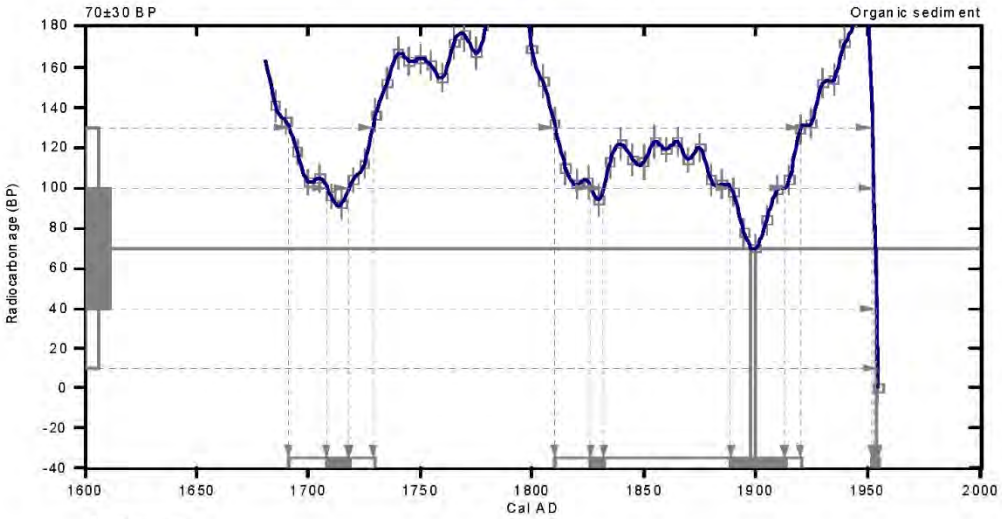

References:

Database used

INTCAL09

References to INTCAL09 database

Heaton,et al.,2009, Radiocarbon 51(4):1151-1164, Reimer,et al, 2009, Radiocarbon 51(4):1111-1150, Stuiver,et.al,1993, Radiocarbon 35(1):1-244, Oeschger,et.al.,1975,Tellus 27:168-192

Mathematics used for calibration scenario

A Simplified Approach to Calibrating C14 Dates
Talma, A. S., Vogel, J. C., 1993, Radiocarbon 35(2):317-322

Beta Analytic Radiocarbon Dating Laboratory

4985 S.W. 74th Court, Miami, Florida 33155 • Tel: (305)667-5167 • Fax: (305)663-0964 • E-Mail: beta@radiocarbon.com

CALIBRATION OF RADIOCARBON AGE TO CALENDAR YEARS

(Variables: C13/C12=-26.7:lab. mult=1)

Laboratory number: **Beta-354966**

Conventional radiocarbon age: **1220±30 BP**

2 Sigma calibrated results: **Cal AD 690 to 750 (Cal BP 1260 to 1200) and**
(95% probability) **Cal AD 760 to 890 (Cal BP 1190 to 1060)**

Intercept data

Intercept of radiocarbon age with calibration curve: Cal AD 780 (Cal BP 1170)

1 Sigma calibrated results: Cal AD 730 to 740 (Cal BP 1220 to 1210) and
(68% probability) Cal AD 770 to 830 (Cal BP 1180 to 1120) and
Cal AD 840 to 870 (Cal BP 1110 to 1080)

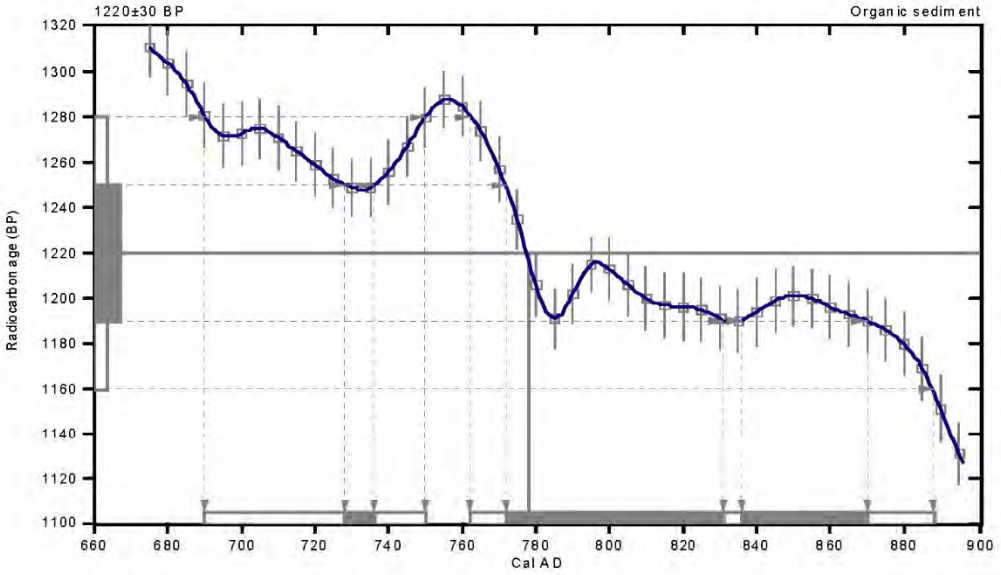

References:

Database used

INTCAL09

References to INTCAL09 database

Heaton,et al.,2009, Radiocarbon 51(4):1151-1164, Reimer,et al, 2009, Radiocarbon 51(4):1111-1150, Stuiver,et.al,1993, Radiocarbon 35(1):1-244, Oeschger,et.al.,1975,Tellus 27:168-192

Mathematics used for calibration scenario

A Simplified Approach to Calibrating C14 Dates
Talma, A. S., Vogel, J. C., 1993, Radiocarbon 35(2):317-322

Beta Analytic Radiocarbon Dating Laboratory

4985 S.W. 74th Court, Miami, Florida 33155 • Tel: (305)667-5167 • Fax: (305)663-0964 • E-Mail: beta@radiocarbon.com

Appendix IV: EAL Report

RESULTS OF ACID SULFATE SOIL ANALYSIS

10 samples supplied by Latrobe University on the 29th January, 2014 - Lab. Job No. D1266
Analysis requested by Fiona Glover.

Sample Site	EAL lab code	TEXTURE (note 7)	MOISTURE CONTENT		REDUCED INORGANIC SULFUR (% chromium reducible S)	
			(% moisture of total wet weight)	(g moisture / g of oven dry soil)	(%Scr)	(mole H^+/tonne)
Method Info.					*(POTENTIAL ACIDITY-Method 22B)*	
BE#1 0-20cm	*D1266/1*	Fine	42.9	0.8	0.003	2
BS#1 0-20cm	*D1266/2*	Fine	37.6	0.6	0.003	2
BS#1 20-35cm	*D1266/3*	Fine	36.7	0.6	0.007	4
PR#1 0-20cm	*D1266/4*	Fine	34.7	0.5	0.002	1
PR#1 20-40cm	*D1266/5*	Fine	26.9	0.4	0.002	1
PC#1 0-20cm	*D1266/6*	Fine	15.4	0.2	0.006	4
PC#1 20-40cm	*D1266/7*	Fine	3.2	0.0	0.001	1
RC#1 1-10cm	*D1266/8*	Fine	44.1	0.8	0.005	3
RC#1 10-30cm	*D1266/9*	Fine	32.6	0.5	0.003	2
RC#1 30-60cm	*D1266/10*	Fine	23.1	0.3	0.006	4

NOTE:
1 - All analysis is Dry Weight (DW) - samples dried and ground immediately upon arrival (unless supplied dried and ground)
2 - Samples analysed by SPOCAS method 23 (ie Suspension Peroxide Oxidation Combined Acidity & sulfate) and 'Chromium Reducible Sulfur' technique (Scr - Method 22B)
3 - Methods from Ahern, CR, McElnea AE , Sullivan LA (2004). ***Acid Sulfate Soils Laboratory Methods Guidelines.*** QLD DNRME.
4 - Bulk Density is required for liming rate calculations per soil volume. Lab. Bulk Density is no longer applicable - field bulk density rings can be used and dried/ weighed in th
5 - **ABA Equation: Net Acidity = Potential Sulfidic Acidity (ie. Scrs or Sox) + Actual Acidity + Retained Acidity - measured ANC/FF (with FF currently defaulted to 1.5)**
6 - The neutralising requirement, lime calculation, includes a 1.5 safety margin for acid neutralisation (an increased safety factor may be required in some cases)
7 - For Texture: coarse = sands to loamy sands; medium = sandy loams to light clays; fine = medium to heavy clays and silty clays
8 - .. denotes not requested or required. '0' is used for ANC and Snag calcs if TAA pH <6.5 or >4.5
9 - SCREENING, CRS, TAA and ANC are NATA accredited but other SPOCAS segments are currently not NATA accredited
10- Results at or below detection limits are replaced with '0' for calculation purposes.
11 - Projects that disturb >1000 tonnes of soil, the ≥0.03% S classification guideline would apply (refer to acid sulfate management guidelines).
12 - Results refer to samples as received at the laboratory. This report is not to be reproduced except in full.

(Classification of potential acid sulfate material if: coarse Scr≥0.03%S or 19mole H^+/t: medium Scr≥0.06%S or 37mole H^+/t: fine Scr≥0.1%S or 62mole H^+/

Environmental Analysis Laboratory, Southern Cross University,
Tel. 02 6620 3678, website: scu.edu.au/eal

Appendix V: ASS Mapping Report

LA TROBE UNIVERSITY

Inland Acid Sulfate Soil Mapping Layers

Produced by Fiona Glover and Dr John Webb
La Trobe University
Environmental Geosciences
Department of Agriculture

Mapping includes:

4 mapping layers (shapefile format):
- Type 1 ASS.shp
- Type 2 ASS.shp
- Type 3 ASS.shp
- Type 4 ASS.shp

Note: See Table 1 for description of each layer

Projection: Geographic Latitude/Longitude

Datum: Geocentric Datum of Australia 1994 (GDA 94)

LA TROBE UNIVERSITY

Table 1 ASS Classifications and Consequences of disturbance

Land Type	Classification Type	Colour on map	Characteristics	Consequences of Disturbance
Uncleared	1	Purple	• Flat-bottomed valley • Waterlogged and/or swampy vegetation (as shown by 2005 EVC maps) • Evidence of textured ground surface (LIDAR) • No obvious drainage channels	• If disturbed, acid will be produced and released
	2	Blue	• Flat-bottomed valley • Waterlogged and/or swampy vegetation (as shown by 2005 EVC maps) • Obvious drainage channels (< 0.5m)	• If disturbed below level of water table, acidification will occur
Cleared	3	Orange	• Flat-bottomed valley • Waterlogged and/or swampy vegetation (as shown by 1750 EVC maps) • Obvious drainage channels (0.5-1 m)	• If disturbed below level of water table, acidification will occur
	4	Yellow	• Flat-bottomed valley • Waterlogged and/or swampy vegetation (as shown by 1750 EVC maps) • Evidence of current waterlogging (as shown by 2005 EVC mapping and/or Google Earth images)	• Acidification will occur if disturbed below water table
Coastal	5	Silver	• Coastal area • As defined in DSE coastal ASS mapping	• See DSE coastal mapping report

Note: The coastal mapping has not been including as a layer